

Copyright is owned by the Author of the thesis. Permission is given for a copy to be downloaded by an individual for the purpose of research and private study only. The thesis may not be reproduced elsewhere without the permission of the Author.

The Synthesis and Chemistry of [2.2]Paracyclophane Amino Acid Derivatives

*A thesis presented in partial fulfillment of the
requirements for the degree of*

Doctor of Philosophy

in

Chemistry

*at Massey University, Manawatū,
New Zealand.*

Leonie Ruth ETHERIDGE

2020

Declaration of Authorship

I, Leonie Ruth ETHERIDGE, declare that this thesis titled, "The Synthesis and Chemistry of [2.2]Paracyclophane Amino Acid Derivatives" and the work presented in it are my own. I confirm that:

- This work was done wholly or mainly while in candidature for a research degree at this University.
- Where any part of this thesis has previously been submitted for a degree or any other qualification at this University or any other institution, this has been clearly stated.
- Where I have consulted the published work of others, this is always clearly attributed.
- Where I have quoted from the work of others, the source is always given. With the exception of such quotations, this thesis is entirely my own work.
- I have acknowledged all main sources of help.
- Where the thesis is based on work done by myself jointly with others, I have made clear exactly what was done by others and what I have contributed myself.

Signed:

Date:

“Nothing in life is to be feared, it is only to be understood. Now is the time to understand more, so that we may fear less.”

Marie Curie

Abstract

Due to the ever-growing requirement for chiral compounds, new conditions for stereoselective synthesis are in constant development. Asymmetric organocatalysis is well-studied, with peptide catalysts popular due to their modular and highly-functionalizable nature. One such example of their utility is in the Michael reaction, a well-studied carbon-carbon bond forming reaction.

[2.2]Paracyclophane is an aromatic industrial precursor compound with remarkable structural and electronic properties. Its conformational bulk and rigidity make it an attractive target for integration into sterically-hindered unnatural amino acids for incorporation into peptides that may be effective organocatalysts.

An updated route to 4-amino-13-[2.2]paracyclophane-carboxylic acid (*Pca*) was developed and optimised. The synthetic route comprises four steps with an overall yield of 50%. This compares with previous routes which had yields between 7 and 48% for 6 - 7 steps. Peptide coupling conditions for the poorly-reactive *Pca* were developed with some success; including devising a route for direct synthesis of a glycine residue on *Pca*'s aniline. Four new *Pca*-containing peptides were described. The above work sets the stage for development of interesting new planar chiral peptide compounds with diverse chemistry.

Three *Pca*-containing peptides were studied as asymmetric organocatalysts in Michael addition between *trans*- β -nitrostyrene and hexanal and were compared to proline, a known catalyst for this reaction. These tests were performed to probe the relationship between relative conformation between the carboxylic acid and amine moieties of the catalyst, and the catalyst's stereoselectivity. The *Pca*-containing catalysts showed an interesting trend to reversal of the prevailing *syn* product configuration.

Acknowledgements

I must first acknowledge Massey University for funding my study through a Vice Chancellor's Doctoral Scholarship.

I wish to express my sincere gratitude to my supervisor, Gareth Rowlands, for his guidance and encouragement. His enthusiasm for organic chemistry, immense knowledge, and writing and design finesse have been inspiring. I am also grateful to Paul Plieger, my co-supervisor, for his support and valuable advice. Thank you both.

Many colleagues contributed to my research. Thank you to David Lun for his practical instruction and running countless mass spectra and HPLCs; to Pat Edwards for assistance with technical and theoretical aspects of NMR spectroscopy; to Martyn Coles for X-ray crystallography; to Tyson Dais for molecular modelling; and to Krishanthi Jayasundera, Graham Freeman, and members of the Rowlands and Plieger research groups, for all manner of practical help.

My studies were enriched by members of the Rowlands and Plieger groups past and present. Their advice and support has been invaluable. A special mention to Ben Munro, David Nixon, Sidney Woodhouse, Sam Brooke, Suraj Patel, and Tyson Dais, who helped me solve many problems over a gin or two. Thank you also to the wider SFS staff and students.

A special thank you belongs to my family and friends: to Mum and Dad & Linda, without whom none of this would have been possible. Thank you to my brother, Kingsley, who taught me the value of curiosity; to my grandparents, for backing my every endeavour; and to my step-siblings for being constantly uplifting. My friends who saw me through my study and will probably never read this thesis deserve acknowledgement nonetheless: cheers - Graeme, Mia, Greg & Sara, Jack & James, Gordon, and Catly.

This work has been realised thanks to the support of Thomas Bell, whose patience is second to none.

Contents

Declaration of Authorship	iii
Abstract	vii
Acknowledgements	ix
1 Introduction	1
1.1 [2.2]Paracyclophane: a peculiar pro-planar chiral compound	1
1.1.1 [2.2]Paracyclophane structure	2
1.1.2 Synthesis of [2.2]paracyclophane	5
1.1.3 Planar chirality	6
1.1.4 Resolution	12
Kinetic resolution	13
Chromatography	14
Recrystallisation	15
1.1.5 [2.2]Paracyclophane in asymmetric catalysis	15
1.2 Unnatural amino acids	19
1.2.1 Terminology	19
1.2.2 Unnatural cyclic amino acids	20
1-Aminocyclohexanecarboxylic acid	21
1.2.3 Ferrocene-centred amino acid	22
Synthesis of ferrocene amino acid	24
Ferrocene amino acid peptides	27
1.2.4 Adamantane-centred amino acids	30
Synthesis of aminoadamantanecarboxylic acid	30
Adamantane amino acid peptides	33

1.3	Asymmetric organocatalysis	33
1.3.1	Early asymmetric organocatalysis	35
	Brønsted acid catalysis	35
	Lewis base catalysis	36
1.3.2	Enamine catalysis	40
1.3.3	Iminium catalysis	40
1.3.4	Proline in enamine mechanism of catalysis	42
1.3.5	<i>Trans</i> -4,5-methano-L-proline in iminium mechanism of catalysis	43
1.4	Peptide organocatalysis	43
1.4.1	Miller's peptide organocatalysts	46
1.4.2	Wennemers' peptide organocatalysts	50
1.4.3	Reymond's aryl peptide dendrimers	51
1.4.4	Schreiner's peptide organocatalysts	53
	Dakin-West reaction	53
	Peptide multicatalysts	56
1.4.5	Prolinamide BINAM derivative organocatalyst	60
1.5	Michael addition	61
1.6	Conclusion	67
2	Synthesis of 4-amino[2.2]paracyclophane-13-carboxylic acid	69
2.1	Project scope	70
2.2	Literature syntheses of [2.2]paracyclophane-centred pseudoamino acids	72
2.2.1	Pseudo- <i>ortho</i> [2.2]paracyclophane amino acid synthesis	73
2.2.2	Pseudo- <i>geminal</i> [2.2]paracyclophane amino acid synthesis	73
2.3	Syntheses of 4-amino[2.2]paracyclophane-13-carboxylic acid in this work	78
2.3.1	Chiral resolution	78
2.3.2	Oxime methodology	78
	Friedel-Crafts acylation	78
	Reiche formylation	82
	Oximation	85
	Oxime rearrangement to amine	85

	Ester hydrolysis	90
2.3.3	The nitro group methodology	91
	Nitration	92
	Formylation	94
	Resolution of 4-nitro-13-carboxy[2.2]paracyclophane	95
	Aldehyde oxidation to carboxylic acid	97
	Resolution of 4-toluenesulfonylamido[2.2]paracyclophane-13- carboxylic acid	102
	Resolution of 4-nitro[2.2]paracyclophane-13-carboxylic acid	104
	Nitro reduction to amine	105
	Methyl ester protection of the carboxylic acid	108
2.4	Conclusion	109
3	Synthesis of 4-amino[2.2]paracyclophane-13-carboxylic acid pseudopeptides	111
3.1	Pseudopeptide design rationale	111
3.2	Coupling studies with [2.2]paracyclophane analogues	113
3.2.1	Reactions of <i>o</i> -toluidine	115
3.2.2	Coupling reagent: carbodiimides	116
3.2.3	Reactions of anthranilic acid	118
3.2.4	Reactions of 2,6-diaminotoluene	119
3.2.5	Coupling reagent: aminium-uronium salts	122
3.3	Coupling amino acids with 4-amino[2.2]paracyclophane-13-carboxylic acid	124
3.3.1	Synthesis of Pca-Phe	124
	Coupling L-phenylalanine with 4-nitro[2.2]paracyclophane-13- carboxylic acid 3.24	124
	Resolution of diastereomers of Pca-peptides	126
	Resolution of 4-nitro[2.2]paracyclophan-13-(amido-Phe)	127
	Nitro reduction to give Pca-Phe	128
	Coupling to the N-terminus of Pca-Phe	129
	Coupling reagent: chloroformates	130
3.3.2	Peptide coupling to the N-terminus of Pca	131

3.3.3	Attempted synthesis of Pro-Pca	133
	Coupling Boc-L-proline to Pca-OMe	133
	Coupling reagent: imidazoles	136
	Coupling reagent: acyl chlorides	137
	Coupling reagent: <i>N</i> -hydroxysuccinimide in the synthesis of Pro-Pca	138
3.3.4	Attempted synthesis of 4-methylamino[2.2]paracyclophane-13- -carboxylic acid	142
3.3.5	Attempted coupling of Boc-proline derivatives to Pca	143
	Reductive amination	143
	Substitution with prolinol derivatives	146
3.3.6	Deprotection of and attempted peptide coupling to Boc-Pro- Pca-OMe	147
	Ester hydrolysis of the Boc-Pro-Pca-OMe dipeptide	147
	Coupling attempts to Boc-Pro-Pca's C-terminus	147
	Boc cleavage of Boc-Pro-Pca	148
	Resolution of Pro-Pca	148
	Synthesis of the mono-substituted 4-prolinamido[2.2]paracy- clophane	150
3.3.7	Synthesis of Pro-Gly-Pca	150
	Synthesis of bromide 3.35	151
	Synthesis of azide 3.36	153
	Synthesis of amine 3.37	153
	Attempted resolution of Gly-Pca	154
	Coupling of Pro to Gly-Pca	155
	Deprotection of the Boc-Pro-Gly-Pca-OMe tripeptide	156
	Coupling attempts to Boc-Pro-Gly-Pca's C-terminus	158
	Boc cleavage of Boc-Pro-Gly-Pca	161
	Resolution of Pro-Gly-Pca	163
	Synthesis of the mono-substituted 4-Pro-glycinamido[2.2]para- cyclophane	163
	Attempted synthesis of the glycine residue on Pca-Phe	163

3.4	Outcome of peptide syntheses	165
4	Asymmetric organocatalysed Michael addition with planar chiral amine derivatives	167
4.1	Michael addition between <i>trans</i> - β -nitrostyrene and hexanal	168
4.1.1	Initial reaction condition screening	169
4.2	Catalysis screening results	171
4.2.1	Proline 4.1 and 4.2	173
4.2.2	Tests for importance of stereochemical resolution of catalysts	173
4.2.3	Tests for effect of time and temperature	174
4.2.4	Pca 4.3	175
4.2.5	Pro-NH-22PC 4.4	176
4.2.6	Pro-Gly-NH-22PC 4.5	176
4.2.7	Pro-Gly-Pca 4.6	177
4.2.8	Pro-Pca 4.7	179
4.3	Conclusion	180
4.4	Future directions	182
4.4.1	R group functionalisation	182
4.4.2	<i>N</i> -alkylation	182
4.4.3	Synthesis of further peptides	182
4.4.4	Acyl fluoride activation	183
4.4.5	Resolution of catalysts	183
4.4.6	Potential thioether catalyst	184
5	Methods and Materials	187
5.1	General information	187
5.2	Synthetic methods	190
5.2.1	Synthesis of Pca, oxime methodology	190
	[2.2]Paracyclophane-4-carboxylic acid 2.12	190
	Methyl [2.2]paracyclophane-4-carboxylate 2.13	191
	Methyl 13-formyl[2.2]paracyclophane]-4-carboxylate 2.19	191
	Methyl 13-hydroxyimino[2.2]paracyclophane-4-carboxylate 2.20	192
	Hydroxyl(tosyloxy)iodobenzene 2.31	193

	Methyl 4-(<i>N</i> -hydroxyamido)[2.2]paracyclophane-13-carboxylate 2.34	193
	Methyl 13-amino[2.2]paracyclophane-4-carboxylate 2.21	194
	4-Carboxyl[2.2]paracyclophane 5.1	195
	4-Hydroxyimino[2.2]paracyclophane 5.2	196
	4-Amino[2.2]paracyclophane 5.3	196
5.2.2	Synthesis of Pca, nitrate methodology	197
	4-Nitro[2.2]paracyclophane 2.38	197
	4-Amino[2.2]paracyclophane 5.3	198
	4-Nitro-13-formyl[2.2]paracyclophane 2.39	198
	4-Nitro-13-[<i>N</i> -(1-phenylethyl)][2.2]paracyclophanyl methanimine 2.45	199
	4-Nitro-13-formyl[2.2]paracyclophane (resolved) 2.39	200
	4-Nitro[2.2]paracyclophane-13-carboxylic acid 2.40	200
	Resolution of 4-(<i>p</i> -Toluenesulfonamido)[2.2]paracyclophane-13-carboxylic acid	201
	2.50	201
	2.48	202
	Methyl 4-nitro[2.2]paracyclophane-13-carboxylate 2.41	203
	4-Amino[2.2]paracyclophane-13-carboxylic acid 2.3	203
	Methyl 4-amino[2.2]paracyclophane-13-carboxylate 2.21	204
	4-Amino[2.2]paracyclophane-13-carboxylic acid, ester hydrolysis 2.3	205
5.2.3	Synthesis of Gly-Pca	205
	Methyl 4-[(2-bromo-1-oxoethyl)amino][2.2]paracyclophane-13-carboxylate 3.35	205
	Methyl 4-[(2-azido-1-oxoethyl)amino][2.2]paracyclophane-13-carboxylate 3.36	206
	Methyl 4-[(2-amino-1-oxoethyl)amino][2.2]paracyclophane-13-carboxylate 3.37	207
	4-[(2-Amino-1-oxoethyl)amino][2.2]paracyclophane-13-carboxylic acid 3.38	207

5.2.4	Peptide couplings & transformations	208
	Pivaloyl-L-valine 5.4	208
	2-(Boc-prolinamido)-6-aminotoluene 5.5	209
	2-(Pivaloyl-L-valinamido)-6-aminotoluene 3.23	209
	2-(Pivaloyl-L-valinamido)toluene 3.13	210
	4-Nitro[2.2]paracyclophan-13-(amido-Phe) 3.25	211
	Pca-Phe 3.26	212
	Fmoc-L-proline 5.6	213
	4-Pivalamido[2.2]paracyclophane-13-carboxylic acid 5.7	214
	Boc-Pro-Gly-Pca-OMe 3.39	215
	Boc-Pro-Gly-Pca 3.40	216
	Pro-Gly-Pca 3.41	217
	L-Phenylalanine, methyl ester hydrochloride 5.8	217
	(4- <i>N</i> -Boc-Pro-Gly-amino)[2.2]paracyclophane 5.9	218
	(4- <i>N</i> -Pro-Gly-amino)[2.2]paracyclophane 3.43	219
	4-(<i>N</i> -benzylidene)-[2.2]paracyclophane-13-carboxylic acid 5.10	219
	4-(<i>N</i> -benzylamino)-[2.2]paracyclophane-13-carboxylic acid 5.11	220
	(<i>S</i>)- <i>N</i> -(<i>tert</i> -butoxycarbonyl)prolinal 3.46	221
	Imine 5.12	221
	<i>tert</i> -Butyl (2 <i>S</i>)-2-[(<i>p</i> -toluenesulfonyloxy)methyl]pyrrolidine-1-	
	carboxylate 3.50	222
	Boc-L-proline, <i>N</i> -hydroxysuccinimide ester 3.38	223
	Boc-Pro-Pca-OMe 3.54	223
	Boc-Pro-Pca 3.57	224
	Pro-Pca 3.7	225
	4- <i>N</i> -Boc-Pro-amino[2.2]paracyclophane 3.53	226
	4- <i>N</i> -Pro-amino[2.2]paracyclophane 3.61	226
5.2.5	Michael addition	227
	Protocol for Michael reaction of <i>trans</i> - β -nitrostyrene and hexanal	227
5.2.6	2-Butyl-4-nitro-3-phenylbutanal 5.13	228
	Sulfide 4.9 , methyl ester	228
	Sulfide 4.10	229

List of Figures

1.1	Cyclophanes.	1
1.2	Models of [2.2]paracyclophane showing the boat-like structure and twist.	2
1.3	[4.4]Paracyclophane 1.5	3
1.4	Substitution patterns for disubstituted [2.2]paracyclophane. Numbering is explained in Figure 1.11.	3
1.5	Synthesis of PhanePhos	5
1.6	Cram and Steinberg's synthesis of [2.2]paracyclophane	5
1.7	Weinberg <i>et al.</i> 's 1,6-Hofmann elimination route to [2.2]paracyclophane.	6
1.8	Preparation of [2.2]paracyclophane by sulfur photoextrusion.	6
1.9	<i>Meso</i> dibromo-[2.2]paracyclophane regioisomers.	7
1.10	Planar chiral metallocenes.	7
1.11	Atom numbering and stereochemical assignment of [2.2]paracyclophane molecules.	8
1.12	Structural similarity of ferrocene (left) and [2.2]paracyclophane (right)	9
1.13	Diastereomers and enantiomers of 1.13	9
1.14	Differing regioselectivity depending on stereochemistry in palladation of oxazolines.	10
1.15	Diastereomeric ligand and catalyst examples.	11
1.16	Bräse's ketimine ligands in asymmetric diethylzinc addition of aldehydes.	12
1.17	Nájera's BINAM prolinamide catalyst in aldol reactions between ketones and β -ketoesters.	13
1.18	Kinetic resolution of 1.17	14
1.19	Diastereomeric esters of 4-hydroxy[2.2]paracyclophane.	15

1.20	Diastereomeric imine for resolution of 4-hydroxy[2.2]paracyclophane.	16
1.21	PhanePhos-Rh complex catalysed hydrogenation.	16
1.22	PhanePhos in asymmetric hydrogenation of the Crixivan precursor 1.25 .	17
1.23	Bräse's bidentate ligands for asymmetric catalytic aryl transfer and conjugate addition.	17
1.24	Glatzhofer's cyclopropanation.	18
1.25	Nozaki ligand 1.30 for cyclopropanation.	19
1.26	Examples of natural and unnatural amino acids.	20
1.27	Cyclic amino acid synthesis by hydantoin hydrolysis.	21
1.28	Cyclic amino acid synthesis by azide substitution and reduction.	22
1.29	Amine and carboxylic acid functionalised ferrocenes.	22
1.30	Parallel (left) and anti-parallel (right) peptide strand configuration on ferrocene derivatives.	23
1.31	<i>Syn</i> and <i>anti</i> configuration for ferrocene compounds with and without hydrogen bonding.	24
1.32	Butler's synthesis of Fca from 1,1'-dibromoferrocene.	25
1.33	Ueyama's synthesis of Fca from <i>N</i> -acetamidoferrocene.	25
1.34	Heinze's synthesis of Fca based on Ueyama's route.	26
1.35	Erb's synthesis of Fca using optimised Curtius rearrangement.	27
1.36	Carboxylic acid activation for peptide coupling with Fca.	27
1.37	Solid phase peptide synthesis of Fca-containing peptides.	28
1.38	Intra- and interchain hydrogen bonding in Fca-containing peptides.	29
1.39	Amine derivatives of adamantane.	30
1.40	Synthesis of Aca using the Ritter reaction <i>via</i> the bromide 1.66 .	31
1.41	Nitrosonium ion-induced carbocation route to Aca.	32
1.42	Phase transfer catalysed synthesis of Aca.	32
1.43	Peptide coupling between two Aca units.	33
1.44	Hajos and Parrish's proline-catalysed asymmetric Robinson annulation.	34
1.45	An example of Jacobsen's thiourea/imine catalysts in asymmetric Strecker reaction.	35
1.46	Transition state of Strecker reaction catalysed by 1.77	36
1.47	MacMillan's imidazolidinone catalysts	37

1.48 Jørgensen's diphenylprolinyl silyl ether catalyst	38
1.49 Jørgensen's diphenylprolinyl silyl ether catalyst	39
1.50 Enamine-type mechanism of organocatalytic reactions.	41
1.51 Iminium-type mechanism of organocatalytic reactions.	41
1.52 List's proline-catalysed asymmetric aldol reaction.	42
1.53 1,3-Dipolar cycloaddition side reaction between proline and 4-nitro- benzaldehyde.	42
1.54 <i>Trans</i> -4,5-methano-L-proline-catalysed addition of 2-nitropropane to 2-cyclohexenone.	43
1.55 Hydrogen bonding in a β -turn.	45
1.56 Juliá <i>et al.</i> 's polyalanine peptide for asymmetric catalytic epoxidation of chalcone.	45
1.57 Miller's octapeptides for asymmetric acylation.	46
1.58 Asymmetric acylation of (\pm)- <i>N</i> -(2-hydroxycyclohexyl)acetamide. . . .	47
1.59 Miller's peptide 1.99 in a general catalytic acylation for kinetic resolu- tion of alcohols.	48
1.60 Epoxidation catalysed by Miller's peptide catalysts 1.100 and 1.101 . . .	49
1.61 Possible intermolecular hydrogen bonding interactions stabilising tran- sition state in epoxidation of polyenes.	50
1.62 Wennemers' tripeptide in asymmetric Michael addition of butanal to <i>trans</i> - β -nitrostyrene.	51
1.63 Wennemers' alkylated tripeptide catalyst 1.109	51
1.64 Ester hydrolysis catalysed by Reymond's peptide dendrimers.	52
1.65 Enantioselective Dakin-West reaction catalysed by Schreiner's Aca- containing peptide 1.111	54
1.66 Mechanism of the Dakin-West reaction.	55
1.67 Stabilising interactions in the transition state of organocatalysed Dakin- West reaction.	56
1.68 One-pot desymmetrisation and oxidation of 1.123 by Schreiner's pep- tide catalyst 1.122	57
1.69 Predicted catalytic binding pocket of Schreiner's peptide 1.122 in acyl transfer.	58

1.70	Schreiner's multicyclic catalyst 1.122 employed in kinetic resolution of diol 1.125 with oxidative esterification.	59
1.71	Schreiner's dicarboxylic acid/histidine peptide catalyst in epoxidation and enantioselective acyl transfer.	59
1.72	Nájera's BINAM prolinamide catalyst in aldol reactions between ketones and β -ketoesters.	61
1.73	Generic Michael addition.	62
1.74	Takasu <i>et al.</i> 's aza-Michael addition to form tetrahydroisoquinoline 1.131 with asymmetric organocatalyst 1.130	62
1.75	Phase-transfer-catalysed asymmetric aza-Michael addition in synthesis of Letermovir 1.133	63
1.76	Iron(III)-salen complex catalysed asymmetric and regioselective thia-Michael addition.	64
1.77	Michael addition in enantioselective synthesis of steroid precursor cardenolide 1.137	64
1.78	Cu(OTf) ₂ as asymmetric catalyst in Michael addition in synthesis of 1.137	65
1.79	Asymmetric intramolecular Michael addition in the synthesis of lycoposerramine-Z with chiral phosphoric acid 1.138	66
1.80	4-Amino[2.2]paracyclophane-13-carboxylic acid 1.141	68
2.1	Pearson's pseudopeptide 2.1 and analogous [2.2]paracyclophane pseudopeptide 2.2	70
2.2	Unnatural cyclic amino acids.	70
2.3	<i>Ortho</i> , pseudo- <i>geminal</i> , and pseudo- <i>ortho</i> substitution of Pca.	71
2.4	A β -turn-like conformation.	71
2.5	Substitution patterns for disubstituted [2.2]paracyclophane.	72
2.6	Ma <i>et al.</i> 's synthesis of pseudo- <i>ortho</i> 4-amino[2.2]paracyclophane-12-carboxylic acid.	74
2.7	Pelter's first synthesis of pseudo- <i>geminal</i> Pca.	75
2.8	Pelter's pseudo- <i>geminal</i> Pca synthesis <i>via</i> an oxazoline.	76
2.9	Ma's pseudo- <i>geminal</i> Pca synthesis <i>via</i> an oxazoline.	77

2.10 Oxime route for Pca synthesis.	79
2.11 Friedel-Crafts acylation of [2.2]paracyclophane.	80
2.12 Acyl chloride formation with oxalyl chloride and catalytic DMF.	81
2.13 Methyl ester formation from acyl chloride.	82
2.14 Reiche formylation of 4-formyl[2.2]paracyclophane 2.13	83
2.15 ¹ H NMR spectrum of 2.19	84
2.16 13-Formyl[2.2]paracyclophane-4-carboxylic acid 2.19	85
2.17 Hydroxylamine condensation with 2.19 , affording oxime product 2.20	86
2.18 Mechanism for proposed Beckmann rearrangement to form amine.	86
2.19 Koser's reagent 2.31	87
2.20 Oxime rearrangement to hydroxamic acid mediated by Koser's reagent.	87
2.21 Proposed mechanism for Lossen-type rearrangement to amine <i>via</i> an isocyanate.	88
2.22 Synthesis of 4-amino-13-bromo[2.2]paracyclophane 2.37	89
2.23 Ester hydrolysis of Pca-OMe 2.21 to Pca 2.3	90
2.24 Basic ester hydrolysis mechanism.	90
2.25 Nitro route for synthesis of Pca.	92
2.26 Methyl ester protection of carboxylic acid in nitro methodology.	93
2.27 Nitration of [2.2]paracyclophane.	94
2.28 Formylation of 4-nitro[2.2]paracyclophane.	95
2.29 Synthesis of 2.45	95
2.30 The C(H)=N peak region on the ¹ H NMR spectrum of 2.45	96
2.31 Pinnick oxidation of 2.39	98
2.32 Oxidation mechanism of aldehyde 2.39 using Pinnick conditions.	98
2.33 2-Methyl-2-butene as chlorine scavenger.	98
2.34 Oxidation of aldehyde 2.39 using KMnO ₄	100
2.35 Acid/base work up procedure for aldehyde oxidation.	101
2.36 Resolution of 2.48 by crystallisation of the cinchonine salt.	103
2.37 Cinchonidine.	104
2.38 Attempted resolution of 2.40 with cinchonine.	104
2.39 Reduction of the aryl nitro group to the amine with zinc and ammo- nium chloride.	107

2.40	Methyl ester protection of carboxylic acid <i>via</i> acyl chloride.	108
2.41	Optimised route for synthesis of Pca.	109
2.42	Diastereomer formations for attempted resolution by recrystallisation during Pca synthesis.	110
3.1	Model peptide structure design.	111
3.2	Examples of potential peptide structures with variations at the N- terminus.	112
3.3	Examples of potential peptide structures with variations at the C- terminus.	113
3.4	Pca analogues.	114
3.5	Example 2,6-diaminobenzoic acid peptide derivative of 2,6-diaminotoluene as Brønsted acid catalyst.	114
3.6	Coupling of <i>N</i> -pivaloyl valine to <i>o</i> -toluidine <i>via</i> benzotriazole ester. . .	115
3.7	Carbodiimide coupling reagents	116
3.8	Carbodiimide peptide coupling mechanism.	117
3.9	Racemisation mechanism in oxazolone route.	117
3.10	Example benzotriazole derivative additives.	118
3.11	Formation of <i>N</i> -acylurea isomer.	118
3.12	Neighbouring group effect in HOAt.	118
3.13	Benzotriazole additives in peptide coupling with carbodiimides. . . .	119
3.14	Attempted coupling conditions between <i>N</i> -pivaloyl valine and an- thranilic acid's nitrogen atom.	119
3.15	Attempted coupling between <i>N</i> -protected valine and 2,6-diaminotol- uene.	120
3.16	Boc protection of amino acids.	120
3.17	Attempted coupling between <i>N</i> -pivaloyl valine and 2,6-diaminotoluene <i>via</i> acyl chloride.	120
3.18	Attempted coupling between <i>N</i> -pivaloyl valine and 2,6-diaminotoluene with peptide coupling reagents.	121
3.19	Attempted coupling of <i>N</i> -pivaloyl valine to 3.23	121
3.20	Attempted coupling to <i>N</i> -pivaloyl chloride to 3.23	122

3.21 Aminium-uronium salt peptide coupling reagents.	123
3.22 Peptide coupling mechanism with TBTU.	123
3.23 Undesirable guanidino derivative formation.	124
3.24 Pca-Phe synthetic scheme.	124
3.25 Phenylalanine coupling to [2.2]paracyclophane carboxylic acid 3.24 via acyl chloride 3.27	125
3.26 Acyl chloride formation mechanism with thionyl chloride.	125
3.27 Diastereomers of Pca-containing dipeptide.	126
3.28 (<i>R_P</i> , <i>S</i>)- 3.25	127
3.29 X-ray crystal structure of (<i>R_P</i> , <i>S</i>)- 3.25	127
3.30 H NMR spectra of 3.25	128
3.31 Reduction of nitro group to give Pca-Phe.	129
3.32 Pseudo-dipeptide 3.26	129
3.33 Attempted coupling of amino acid to Pca-Phe's N-terminus. R = L- amino acid residue.	130
3.34 Peptide bond formation (A) from mixed carbonic anhydrides and car- bamate formed from side reaction (B).	131
3.35 Chloroformate peptide coupling reagents.	131
3.36 Mixed anhydride formation mechanism with ethyl chloroformate and N-methylmorpholine.	131
3.37 Proposed synthetic scheme for tripeptide synthesis starting with Pca- OMe.	133
3.38 Nitrogen lone pair participation in aromatic resonance in Pca-OMe. . .	134
3.39 Orbital overlap in Pca-OMe.	134
3.40 Tosylation of methyl 4-amino[2.2]paracyclophane-13-carboxylate 3.30 . .	135
3.41 Synthesis of triazene 3.33	135
3.42 Carbonyldiimidazole.	136
3.43 Active ester formation with CDI showing generation of an imidazole molecule.	136
3.44 Boc-valine coupling with aniline.	137
3.45 Pivaloyl amide formation with Pca.	138
3.46 Amide coupling between Boc-proline and 4-amino[2.2]paracyclophane. .	138

3.47	Peptide coupling between Boc-proline and Pca-OMe.	139
3.48	<i>N</i> -Hydroxysuccinimide (NHS).	139
3.49	Peptide coupling mechanism between Boc-proline and Pca-OMe using DCC and NHS.	140
3.50	Possible neighbouring group effect between Pca-OMe and Boc-Pro-OSu.	141
3.51	Boc-Pro-Pca-OMe, numbered.	142
3.52	Proline coupling to Pca compared with the Pca starting material.	142
3.53	Proposed oxime reduction to methylamine 3.45	143
3.54	Proposed reductive amination with Boc-prolinal 3.46	143
3.55	Reductive amination of Pca with benzaldehyde.	144
3.56	Imine formation mechanism.	144
3.57	Reduction of the imine to complete reductive amination.	145
3.58	Proposed reaction between Boc-Pro-OTs 3.50 and Pca-OMe 3.30	146
3.59	Methyl ester cleavage of Boc-Pro-Pca-OMe.	147
3.60	Mechanism of Boc cleavage with TFA.	148
3.61	Pro-Pca 3.7	149
3.62	¹ H NMR spectrum of 3.7	149
3.63	Synthetic scheme for mono-substituted 4-prolinamido[2.2]paracyclophane from 4-nitro[2.2]paracyclophane.	151
3.64	Gly-Pca-OH 3.34 , with its ethanamide moiety.	151
3.65	Synthetic route to Gly-Pca-OMe.	152
3.66	Mechanism of formation of 3.35	152
3.67	Orbital diagram of the α -carbonyl bromide of 3.35 demonstrating the orbital blending.	153
3.68	Transformation of bromide 3.35 to azide 3.36	153
3.69	Reduction with triphenylphosphine following the Staudinger mechanism.	154
3.70	Reduction of the azide to the amine.	154
3.71	Gly-Pca 3.34	155
3.72	Attempted imine formation between Gly-Pca and camphor.	155
3.73	Coupling Boc-Pro-OSu 3.38 to Gly-Pca-OMe 3.39	156
3.74	Deprotection of tripeptide 3.39	156

3.75	¹ H NMR of Boc-Pro-Gly-Pca.	157
3.76	Delocalisation of nitrogen lone pair causing hindered rotation about the amide bond.	157
3.77	Attempted couplings between pseudo-tripeptide 3.40 and natural amino acids.	158
3.78	Isobutyl ester of Boc-Pro-Gly-Pca-OH.	159
3.79	Coupling phenylalanine to the carboxylic acid of [2.2]paracyclophane derivatives <i>via</i> the acyl chloride.	160
3.80	Acyl chloride formation with cyanuric chloride.	160
3.81	Attempted coupling of Phe-OMe to Boc-Pro-Gly-Pca-OH.	161
3.82	Attempted coupling of glycine to Boc-Pro-Gly-Pca-OH 3.40	162
3.83	Pseudopeptide 3.41	162
3.84	N-H region of the Pro-Gly-Pca spectrum in variable temperature ¹ H NMR	162
3.85	Synthesis of the mono 4-Pro-Gly-amido[2.2]paracyclophane. i) Zn, NH ₄ Cl ii) a. bromoacetyl bromide, b. NaN ₃ , c. H ₂ , Pd/C iii) Boc-Pro-OSu iv) CF ₃ COOH	164
3.86	Attempted synthesis of Gly-Pca-Phe.	164
3.87	Attempted amide coupling between Pca-Phe-OMe 3.44 and bromoacetyl bromide.	165
3.88	Pca derivatives synthesised this project.	166
4.1	Asymmetric Michael addition between <i>trans</i> -β-nitrostyrene and hexanal.	167
4.2	Mechanism of Michael addition between <i>trans</i> -β-nitrostyrene and hexanal catalysed by proline.	168
4.3	<i>Syn</i> product formation.	169
4.4	Aldehyde proton peak for the <i>syn</i> and <i>anti</i> diastereomers of 2-butyl-4-nitro-3-phenylbutanal.	171
4.5	Major and minor <i>syn</i> product HPLC peaks.	171
4.6	Catalysts tested in asymmetric organocatalysed Michael addition.	172
4.7	Newman projections of Michael addition with DL-proline catalyst.	173

4.8	<i>Syn</i> and <i>anti</i> transition states in Wennemers' <i>anti</i> -selective Michael addition.	176
4.9	Possible configurations of the enamine intermediate.	177
4.10	Computational model of R_P,S -Pro-Gly-Pca.	178
4.11	Computational model of S_P,S -Pro-Gly-Pca.	178
4.12	Computational model of R_P,S -Pro-Pca.	179
4.13	Computational model of S_P,S -Pro-Pca.	180
4.14	R-group functionalisation of glycine.	182
4.15	Wennemers' <i>N</i> -alkylated tripeptide and a Pca analogue.	183
4.16	Acyl fluoride activation for peptide coupling with Pca-OMe.	184
4.17	Synthesis of thioether 4.10	184
4.18	Exemplar sulfide-catalysed asymmetric bromolactonisation.	185

List of Tables

2.1	Conditions tested for ester hydrolysis of Pca-OMe 2.21	91
4.1	Results of asymmetric Michael addition between <i>trans</i> - β -nitrostyrene and hexanal catalysed by peptides.	172

List of Abbreviations

22PC	[2.2]paracyclophane
2D	two-dimensional
Ac	acetyl
Aca	γ -aminoadamantanecarboxylic acid
Ar	aryl
ATR	attenuated total reflectance
aq.	aqueous
approx.	approximately
BEP	2-fluoro-1-ethyl pyridinium tetrafluoroborate
BINAM	1,1'-binaphthyl-2,2'-diamine
BINAP	2,2'-bis(diphenylphosphino)-1,1'-binaphthyl
BINOL	1,1'-bi-2-naphthol
Boc	<i>tert</i> -butoxycarbonyl
Bn	benzyl
Bu	butyl
Cbz	carboxybenzyl
CDI	1,1'-carbonyldiimidazole
CIP	Cahn-Ingold-Prelog
conc.	concentrated
cp	cyclopentadienyl
Cy	cyclohexyl
DAT	2,6-diaminotoluene
dba	dibenzylideneacetone
DBU	1,8-diazabicyclo[5.4.0]undec-7-ene
DCC	<i>N,N'</i> -dicyclohexylcarbodiimide
de	diastereomeric excess
DIC	<i>N,N'</i> -diisopropylcarbodiimide
DIPEA	<i>N,N</i> -diisopropylethylamine
DMAP	4-(dimethylamino)pyridine
DMF	dimethylformamide
DMSO	dimethylsulfoxide
dr	diastereomeric ratio
DPPA	diphenylphosphoryl azide
DPPF	1,1'-bis(diphenylphosphino)ferrocene
EDC	1-ethyl-3-(3-dimethylaminopropyl)carbodiimide
ee	enantiomeric excess
eq.	equivalents
er	enantiomeric ratio
ESI	electrospray ionisation
Et	ethyl
EWG	electron-withdrawing group
Fca	1'-aminoferrocene-1-carboxylic acid

Fmoc	fluorenylmethoxycarbonyl
g	grams
GABA	γ -aminobutyric acid
HATU	hexafluorophosphate azabenzotriazole tetramethyl uronium
HBTU	hexafluorophosphate benzotriazole tetramethyl uronium
HOAt	1-hydroxy-7-azabenzotriazole
HOBt	hydroxybenzotriazole
HOMO	highest occupied molecular orbital
HPLC	high-performance liquid chromatography
HRMS	high-resolution mass spectrometry
Hz	hertz
<i>i</i>-Bu	isobutyl
<i>i</i>-Pr	isopropyl
IR	infrared
L	litres
m	metres
M	molar
<i>m</i>-CPBA	<i>meta</i> -chloroperoxybenzoic acid
Me	methyl
mmol	millimoles
MP	melting point
MS	mass spectrometry
NHS	<i>N</i> -hydroxysuccinimide
NMM	<i>N</i> -methylmorpholine
NMR	nuclear magnetic resonance
<i>p</i>-NO₂DPPA	bis(<i>p</i> -nitrophenyl)phosphorazidate
Pca	4-amino-[2.2]paracyclophane-13-carboxylic acid
Ph	phenyl
ppm	parts per million
<i>R_f</i>	retention factor
ROESY	rotating frame overhauser effect spectroscopy
RSM	returned starting material
RT	room temperature
SPPS	solid-phase peptide synthesis
Su	succinimide
<i>t</i>-Bu	tertiary butyl
TBTU	<i>o</i> -(benzotriazol-1-yl)- <i>N,N,N',N'</i> -tetramethyluronium tetrafluoroborate
TEMPO	(2,2,6,6-tetramethylpiperidin-1-yl)oxyl
tf	trifluoromethanesulfonate
TFA	trifluoroacetic acid
TFAA	trifluoroacetic anhydride
THF	tetrahydrofuran
TLC	thin layer chromatography
Ts	<i>p</i> -toluenesulfonyl
UV	ultraviolet

Chapter 1

Introduction

1.1 [2.2]Paracyclophane: a peculiar pro-planar chiral compound

The cyclophanes are a class of polycyclic hydrocarbons with one or more aryl rings joined by hydrocarbon chains of varying length. Examples are shown in Figure 1.1. Among them, [2.2]paracyclophane (**1.1**) is a cyclophane with peculiar properties arising from its rather disfavoured conformation. Two ethyl bridges link the two aryl rings with *para* substitution, holding them stacked face-to-face. This gives rise to great steric strain and rigidity, and π - π transannular electronic interactions. These properties give [2.2]paracyclophane its range of useful and interesting applications, for instance in polymeric surface films and coatings,^{1,2} optoelectronic materials,³⁻⁶ and asymmetric catalysis.⁷⁻¹⁰

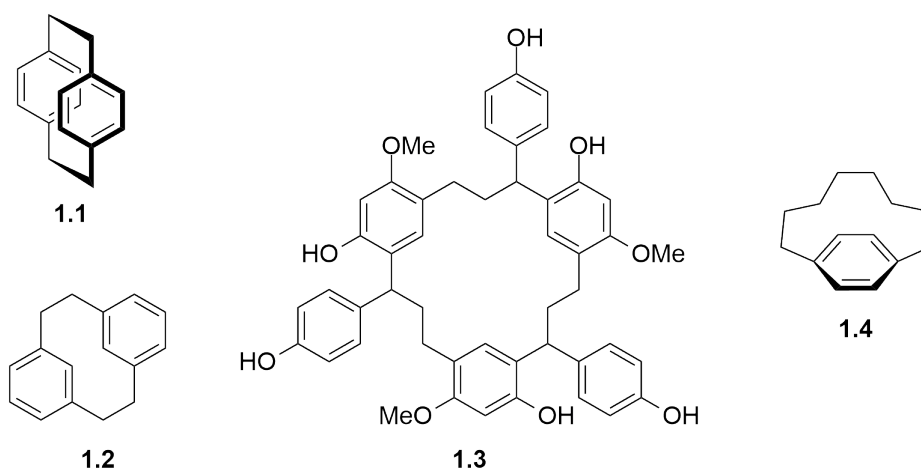


FIGURE 1.1: Cyclophanes. **1.1** [2.2]paracyclophane, **1.2** [2.2]metacyclophane, **1.3** dracophane, a natural metacyclophane isolated from *Dracaena cinnabari* Balf,¹¹ **1.4** [8]Paracyclophane.

1.1.1 [2.2]Paracyclophane structure

[2.2]Paracyclophane's structure (Fig. 1.2) with its "bent and battered"¹² benzene rings gives it unique properties. The rings are held within each other's van der Waals radii giving them a shared π -electron system. The ethylene groups that bridge the two benzene rings are longer than a normal C-C single bond (1.63 Å compared with 1.54 Å). The bond angles of these four bridging carbon atoms, at 114.5°, are also wider than an ideal tetrahedral bonding angle of 109.5°.¹³ The rings are not truly eclipsing, but rather rotate about 5° in plane.¹⁴ They are deformed into a shallow boat-like conformation due to the large amount of strain, rather than being perfectly parallel and planar as most (including Figure 1.1) diagrammatic representations suggest. The HOMO of [2.2]paracyclophane is higher than the analogous alkylbenzene, which one on hand increases its reactivity.¹⁵ On the other hand, [2.2]paracyclophane can be resistant to some transformations, due to its buckled structure, steric effects and its unique π - π interactions.

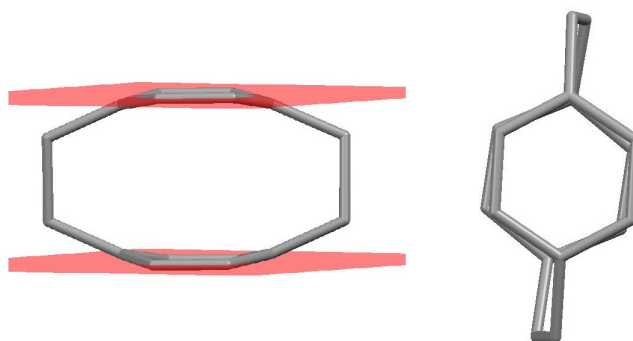
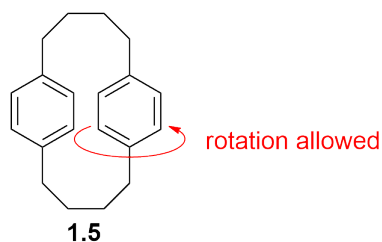


FIGURE 1.2: Models of [2.2]paracyclophane showing the boat-like structure and twist.

The proximity of [2.2]paracyclophane's aryl rings prevents rotation of the rings around the axis between the carbon atoms attached to the ethylene bridges without bond breaking. This gives [2.2]paracyclophane higher rigidity than similar cyclophanes. In cyclophanes with *meta* bridging substitutions or longer bridging alkyl chains, for example [4.4]paracyclophane (1.5, Fig. 1.3), the rings may freely rotate about their axes, so their conformation is less rigidly defined.

The rigid structure of [2.2]paracyclophane allows a high degree of control over the conformation of its derivatives. Chemical moieties may be arranged in space with

FIGURE 1.3: [4.4]Paracyclophane **1.5**.

precise design in a number of substitution patterns. The common nomenclature for the substitution patterns of disubstituted [2.2]paracyclophane compounds is shown in Figure 1.4. Certainly, higher levels of substitution are also possible, however it is unnecessary to discuss these here since this project deals only in mono- or disubstituted [2.2]paracyclophane compounds. Depending on the desired derivative, some substitution patterns are more accessible than others.¹⁶

Aryl directing effects apply to [2.2]paracyclophane substitutions, however due to its unique electronic properties there are some unexpected differences. For example, the nitro group is a *meta*-directing group due to its electron withdrawing nature; thus we expect *meta*- or pseudo-*meta* electrophilic aromatic substitutions to occur. As illustrated in Chapter 2, formylation of 4-nitro[2.2]paracyclophane selectively occurs instead at the pseudo-*geminal* position. This is due to transannular electronic effects, as well as the nitro group's ability to abstract a proton, facilitating the final restoration of aromaticity.

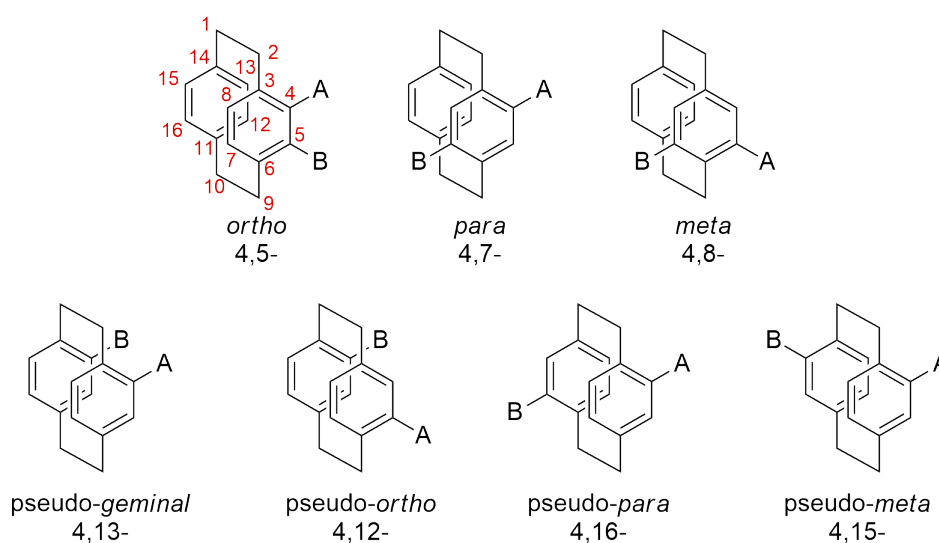


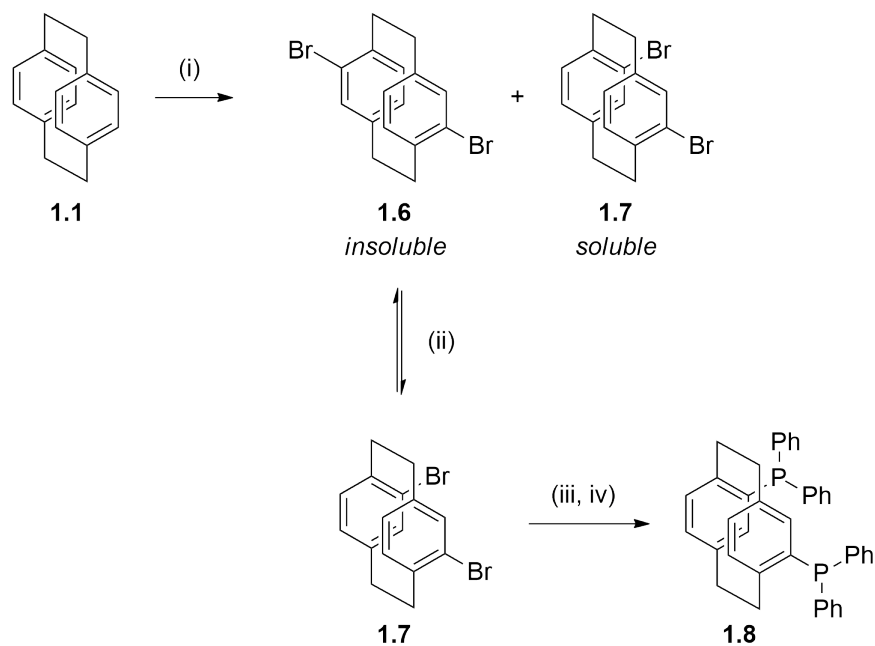
FIGURE 1.4: Substitution patterns for disubstituted [2.2]paracyclophane. Numbering is explained in Figure 1.11.

Transannular electronic effects are the interaction of π -electrons between the two aryl decks due to their close proximity in space.^{17,18} Electron-withdrawing groups on one deck, which would be *meta*-directing on a single aromatic ring, may direct to the corresponding pseudo-*meta* or pseudo-*geminal* position on the opposing ring; similarly electron-donating groups on one deck will encourage pseudo-*ortho* and pseudo-*para* substitution on the opposite deck. The electrons of the two aryl rings exhibit transannular delocalisation through overlap of their orbitals. It helps explain some of the interesting reactivity and properties [2.2]paracyclophane possesses, such as increased reactivity to some processes and decreased reactivity to others.^{19,20}

There is also some evidence to suggest that substituents on one deck can sterically hinder substitution on the opposing deck of [2.2]paracyclophane.²¹ These effects must be taken into consideration when designing a synthetic route; however, trial and error often prevails.

Under normal circumstances, the [2.2]paracyclophane regioisomers do not interconvert. However, the ethylene bridges of [2.2]paracyclophane will cleave above 200°C to give a diradical species that permits substituted examples to undergo regioisomerisation. The bridge-cleaving rotational isomerisation is a useful way of generating regioisomers, particularly where one isomer is difficult to form or isolate.

An example of the utility of this regioisomerisation is the formation of 4,12-dibromo-[2.2]paracyclophane (**1.7**) which is usually synthesised *via* the 4,16-dibromo-[2.2]paracyclophane (**1.6**) regioisomer. Thermal isomerisation at 230°C gives a 50:50 mixture of the pseudo-*para* and pseudo-*ortho* isomers; the pseudo-*para* dibromo-[2.2]paracyclophane regioisomer is highly insoluble and may be separated from the reaction mixture by recrystallisation. This leaves the mother liquor enriched with 4,12-dibromo-[2.2]paracyclophane. This recrystallisation and thermal isomerisation process may be repeated several times to give reasonable (around 70%) yields of the desired pseudo-*ortho* regioisomer. The synthesis of PhanePhos (**1.8**) proceeds in this manner (Scheme 1.5).^{22,23}

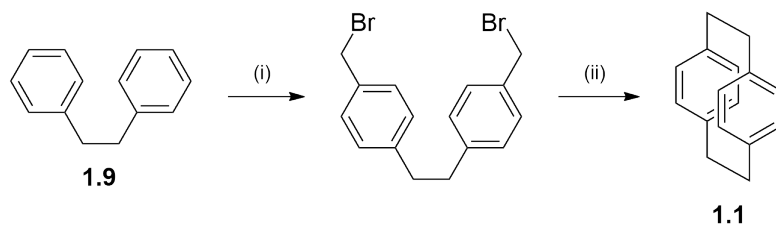


SCHEME 1.5: Synthesis of PhanePhos: i) Br_2/Fe . ii) Diglyme, heat. iii) a. *t*-BuLi; b. $\text{MgBr} \cdot \text{OEt}_2$; c. $\text{Ph}_2\text{P}(\text{O})\text{Cl}$. iv) HSiCl_3 , 140°C .

1.1.2 Synthesis of [2.2]paracyclophane

[2.2]Paracyclophane was first described in 1949 by Brown and Farthing, who isolated it as a dimerisation product from the pyrolysis of *p*-xylene.¹³ They suspected that “the strained system may only be formed under drastic pyrolysis conditions and low pressures”. However, perhaps unsurprisingly, only two years later Cram and Steinberg reported the “standard organic synthesis” of the molecule, which had gained interest due to its suspected electronic and aromatic properties.²⁴

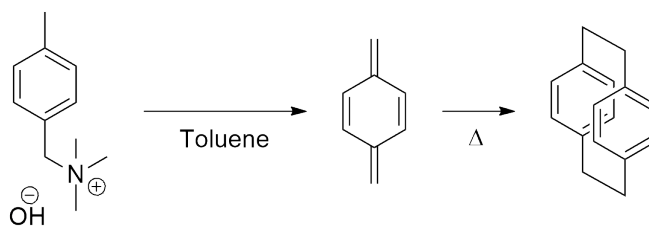
This first synthetic route (Scheme 1.6) involved bromomethylation of 1,2-diphenylethane (**1.9**) followed by intramolecular Wurtz coupling to give [2.2]paracyclophane (**1.1**) with an overall yield of 49%.



SCHEME 1.6: Cram and Steinberg's synthesis of [2.2]paracyclophane: i) HBr , 1,3,5-trioxane. ii) Na .

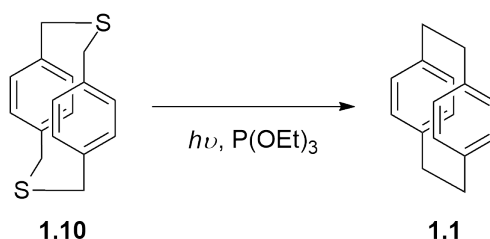
Another synthetic route to [2.2]paracyclophane uses Hofmann elimination, described

in 1960 by Winberg *et al.* (Scheme 1.7).²⁵ This route is quite low-yielding (17%), however, since the main product is poly(*p*-xylene), also known as parylene.



SCHEME 1.7: Weinberg *et al.*'s 1,6-Hofmann elimination route to [2.2]paracyclophane.

Other synthetic routes used include sulfur-photoextrusion of dithiaphane **1.10** (Scheme 1.8) and regiospecific syntheses of polysubstituted [2.2]paracyclophanes based on Winberg's method.^{26,27} The synthesis of [2.2]paracyclophane for study of its derivatives is unnecessary, however, since it is available cheaply in bulk from industrial suppliers due to its use in functionalised electronics coatings.²⁸



SCHEME 1.8: Preparation of [2.2]paracyclophane by sulfur photoextrusion.

1.1.3 Planar chirality

Most [2.2]paracyclophane derivatives are planar chiral, with certain exceptions, such as *meso* compounds like 4,5- or 4,13- or 4,16-dibromo[2.2]paracyclophane (Fig. 1.9), where the internal mirror plane or rotation axis of the identical substituents introduces symmetry.

Planar chirality is derived from two elements that are held out-of-plane with restricted rotation about the bridging bond or bonds.²⁹ The most well-known examples of planar chirality in chemistry are based on metal-organic complexes such as ferrocene or η^6 -metal aryl complexes, examples of which are shown in Figure 1.10.³⁰

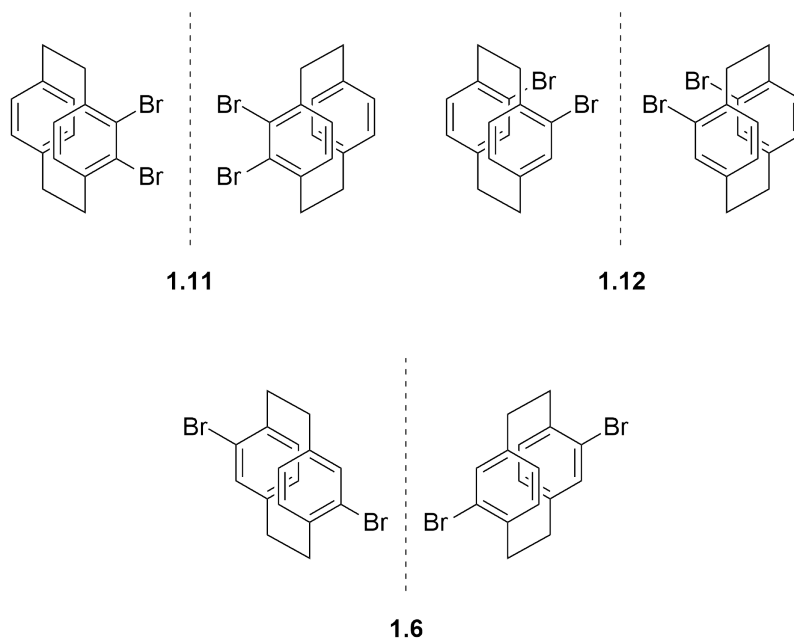


FIGURE 1.9: *Meso* dibromo-[2.2]paracyclophane regioisomers. **1.11**: 4,5-; **1.12**: 4,13-; **1.6**: 4,16-.

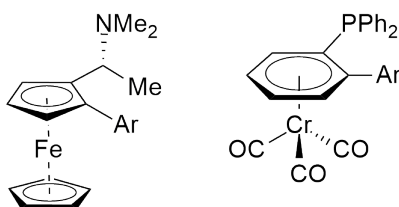


FIGURE 1.10: Planar chiral metallocenes based on ferrocene (left) and (η^6 -arene)chromium.

Planar chirality is assigned using the designators R_P and S_P using the same general method as assigning an asymmetrical carbon atom with the Cahn-Ingold-Prelog priority rules (CIP rules). For [2.2]paracyclophane, the more highly-substituted aryl ring will be treated as the chiral plane. The closest out-of plane carbon atom to the chiral plane is designated as the pilot atom (labelled "1" in Fig. 1.11). Where two or more candidates exist, the atom closest to the highest priority group according to the CIP rules is chosen ("X" in Fig. 1.11). Viewing the molecule from the pilot atom, the three closest adjacent atoms in the chiral plane will be clockwise in an R_P molecule and anticlockwise in an S_P molecule.³¹

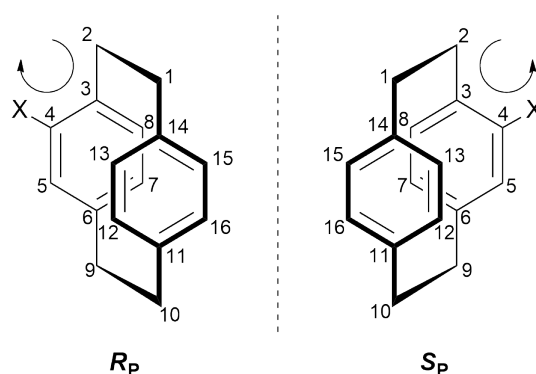


FIGURE 1.11: Atom numbering and stereochemical assignment of [2.2]paracyclophane molecules.

It is also possible to assign [2.2]paracyclophane compounds M/P based on a sense of helicity. This work will use R_P and S_P designations in accordance with the bulk of the [2.2]paracyclophane literature.

Most research on the effect of planar chirality on stereoselective processes has focused on ferrocene and other aromatic transition metal complexes.^{32,33} [2.2]Paracyclophane offers an alternative to these organometallic complexes due to its more robust nature. It is not as sensitive to atmosphere or harsh reagents and conditions. It offers the additional distinction that ferrocene and η -6 aryl complexes require 2 or more substituents on a single ring to be chiral, whereas [2.2]paracyclophane requires one (Fig. 1.12). This can also be considered a disadvantage for [2.2]paracyclophane, as a directing group on the metallocene ring may be used to make a single enantiomer. In the synthesis of enantiopure [2.2]paracyclophane compounds, the addition of the first substituent must be controlled, or else the two enantiomers must be

resolved. The former is hard, while the latter is wasteful.

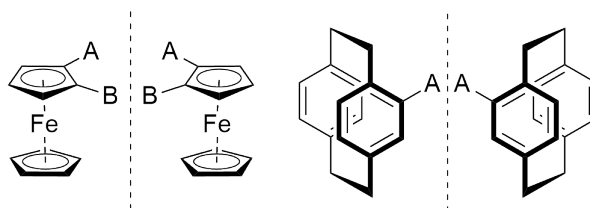


FIGURE 1.12: Structural similarity of ferrocene (left) and [2.2]paracyclophane (right)

The utility of [2.2]paracyclophane's planar chirality is widely studied; of course to investigate chirality one must first separate stereoisomers. [2.2]Paracyclophane derivatisation reactions do not occur stereospecifically but form mixtures of the R_p and S_p enantiomers. Selective derivatisation of unsubstituted [2.2]paracyclophane is highly sought-after but currently, to the best of our knowledge, unattained. The situation becomes more complicated when another chiral entity is introduced to [2.2]paracyclophane; for instance, in the case of the DL-phenylalanine coupling with [2.2]paracyclophane-4-carboxylic acid (Fig. 1.13). The resulting amide 1.13 now exists as 4 stereoisomers: S_p,R , R_p,S , S_p,S , and R_p,R .

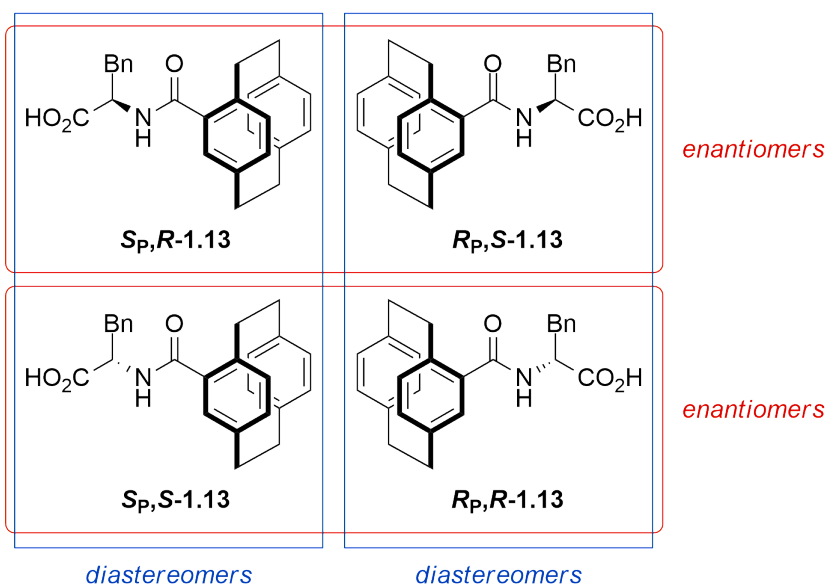
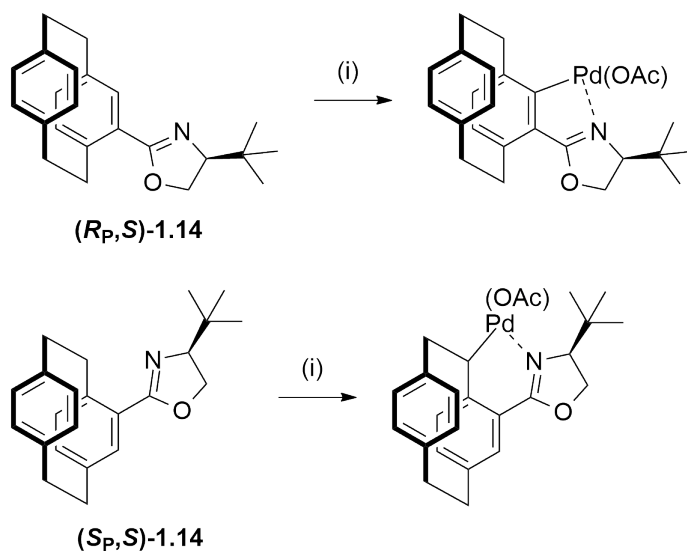


FIGURE 1.13: Diastereomers and enantiomers of 1.13.

The formation of mixtures of stereoisomers is undesirable as this leads to challenging separation and lower yields. A better strategy is to selectively form only the desired stereochemistry of the compound to limit wasted material and time spent resolving the stereoisomers. In some cases, the diastereomers can have different reactivities,

which can be helpful if trying to isolate one particular stereoisomer, or a hindrance if more than one is required. It can further increase the complexity of the mixture of products obtained which potentially makes separation more problematic.

An example of reactivity differing between diastereomers is in Bolm's palladation of oxazolines (R_P,S)-**1.14** and (S_P,S)-**1.14**, which resulted in metal insertion at different locations depending on the diastereomer (Scheme 1.14).³⁴ Bolm separates the oxazoline diastereomers before formation of the Pd complexes, which may indicate that these regioisomers are difficult to separate. It is considered ideal to complete as many transformations as possible before separating isomers, otherwise every step after resolution must be performed twice.



SCHEME 1.14: Differing regioselectivity depending on stereochemistry in palladation of oxazolines. i) $\text{Pd}(\text{OAc})_2$, AcOH.

Ligands with two or more chiral elements have the possibility of co-operation or antagonism between them, resulting in differing activities between diastereomers, such as observed with [2.2]paracyclophane with Bräse's chiral ketimines (**1.15** and **1.16**), Hou's chiral oxazolines (**1.17**), and Bolm's oxazoline palladium complexes (**1.14**, Scheme 1.14).^{34–37} Similar systems have been investigated in Nájera's BINAM catalysts (**1.18**) or in the ferrocene-analogue ruthenocenylobisphosphines (**1.19**) (Fig. 1.15).^{38,39}

These studies suggested varying importance of the planar chiral elements of their

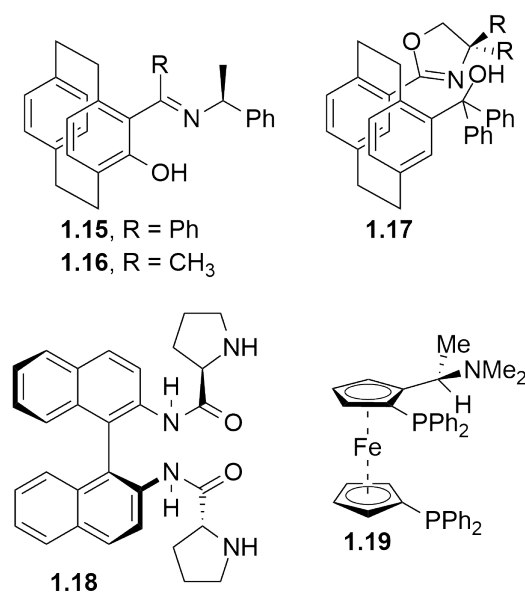
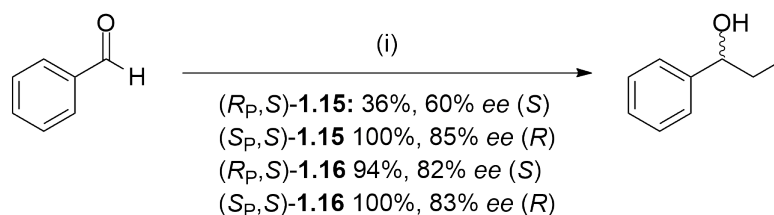


FIGURE 1.15: Diastereomeric ligand and catalyst examples.

systems. In asymmetric catalysts with more than one chiral element, the diastereomer of the catalyst giving the best performance does so due to a cooperative effect between the chiral elements, since these groups are arranged in space differently depending on their absolute configuration. Diastereomers with complementary stereochemistry give better yields and selectivities.

For Bräse's ketimine compounds **1.15** and **1.16**,³⁶ the compounds with complementary chirality (S_P, S) had better yield and selectivity in enantioselective addition of diethylzinc to aldehydes than its R_P, S diastereomer (Scheme 1.16). The reaction mechanism involves formation of a complex between the zinc and the [2.2]paracyclophane ligand. They found that the difference in side chain between **1.15** and **1.16** influenced the stereochemical outcome of the product, with **1.15** giving in general better enantioselectivity, probably due the additional steric bulk of the phenyl group. The $R_P S$ diastereomers had lower catalyst activity, pointing to a decreased affinity for the substrate in the catalyst binding pocket. Bräse found that the planar chiral element had a decisive effect on product configuration, with the R_P and S_P giving reciprocal stereochemical outcomes in the reaction product regardless of the point chirality.

Hou's oxazoline compounds (**1.17**) were tested in the same diethylzinc addition reaction as Bräse's, albeit with a higher catalyst loading (5 mol %).³⁷ They found similar



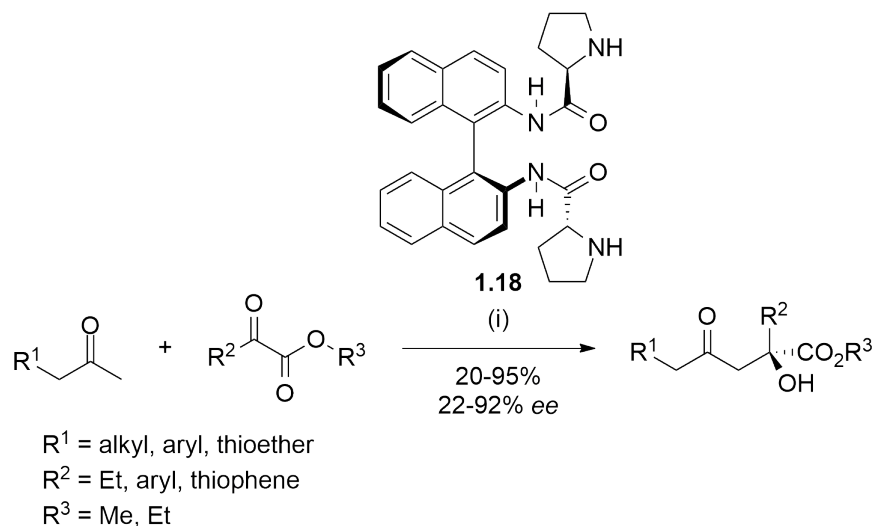
SCHEME 1.16: Bräse's ketimine ligands in asymmetric diethylzinc addition of aldehydes. i) $\text{Zn}(\text{C}_2\text{H}_5)_2$, 1 mol % **1.15** or **1.16**.

results, where there was a clear difference in activity and selectivity between the catalysts with complementary stereochemistry ((R_P, R) , giving the *R* product) and those with antagonistic stereochemistry. The catalyst with the best selectivity had a bulky benzyl R group on the side chain, echoing Bräse's results. Hou tested an additional variable in the reaction where the configuration of the point chiral side chain was reversed; in these reactions, it was the (S_P, S) diastereomer that gave better yield and ee (of the *S* product). The absolute chirality of either chiral element was less important than the relative configuration between them; either enantiomer of the alcohol product of the reaction may be obtained by using the corresponding catalyst.

In Nájera's examination of asymmetric aldol condensation catalysed by prolinamide BINAM derivatives (discussed further in Section 1.4, Scheme 1.72), one diastereomer (S_a, R -**1.18**) gave better enantioselectivity than the other (S_a, S) (64% ee (*S*) vs. 32% ee (*R*)) in aldol reaction with acetone and 2-phenyl-2-oxoacetate, Scheme 1.17).³⁸ Computational models showed that S_a, R -**1.18** gave a greater difference in steric hindrance between phenyl group of the substrate and the binaphthyl portion of the catalyst, favouring formation of the less hindered enantiomer more heavily. The stereoisomers with opposite axial configuration (R_a, S and R_a, R) were not tested; it would be interesting to see if, as for the [2.2]paracyclophane compounds described above, the bulky binaphthyl element had a greater effect on ee than the point chiral prolines.

1.1.4 Resolution

There are several methods for resolving enantiomers of [2.2]paracyclophane compounds. Not all methods will be discussed here, but examples will be given of derivatisation; salt formation; and chromatographic methods such as flash chromatography and HPLC. All these methods tend to involve some trial and error to



SCHEME 1.17: Nájera's BINAM prolinamide catalyst in aldol reactions between ketones and β -ketoesters. i) 20 mol % **1.18**, $\text{ClCH}_2\text{CO}_2\text{H}$.

find a suitable or optimal resolution. Additionally, one must consider that if both enantiomers, or several diastereomers, are desired, the earlier in a synthetic pathway the separation is performed, the more synthetic steps must be performed multiple times - once for each stereoisomer. If all stereoisomers are not required then material is wasted.

Kinetic resolution

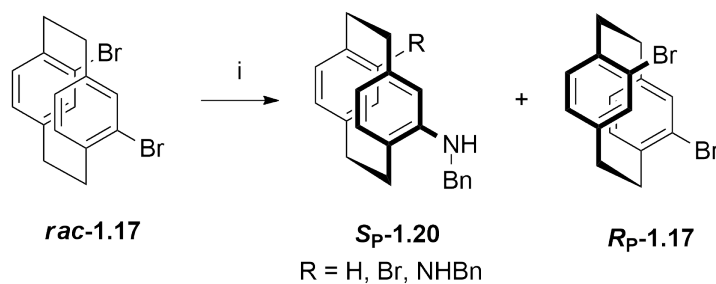
Kinetic resolution is an attractive option but is not widely applicable. In kinetic resolution, an asymmetric catalyst is used in the reaction of a racemic starting material to give a single enantiomer of product while the other enantiomer is returned as starting material. The name *kinetic resolution* refers to its utilisation of differing rates of reaction of each enantiomer due to differing transition state energies with a chiral catalyst. It relies on one enantiomer reacting faster than the other and this leads to two different compounds. This makes separation easier; it also gives two different enriched enantiomers. It is an efficient way of preparing a single enantiomer if only one is required.

Kinetic resolution relies on one enantiomer reacting faster than the other to give two separable products. The efficiency can be measured by k_{rel} , which is a measure of the difference in rate of reaction of one enantiomer compared to the other. For $k_{\text{rel}} > 1$,

kinetic resolution can theoretically give a high % *ee* of the recovered starting material at the expense of yield: as the reaction time goes on longer, more of the enantiomer which reacts at a slower rate will be converted. For the product, high *ee* can only be obtained with a very high k_{rel} since with low k_{rel} there will almost immediately be some small conversion of the undesired enantiomer of the product.

Kinetic resolution is useful in situations where a very high *ee* is required; where the racemic substrate and catalyst are readily prepared or accessible; and where the starting material and product are easily separated. Common kinetic resolution reactions in synthetic chemistry include acylation of alcohols, epoxidation of alkenes, ring-closing metathesis, and many other examples.⁴⁰⁻⁴⁵

For example, enantiomerically pure PhanePhos may be produced by kinetic resolution; interestingly, using PhanePhos itself as a ligand. The R_P enantiomer of the racemic pseudo-*ortho* dibromo[2.2]paracyclophane precursor **1.17** may be selectively prepared by Buchwald-Hartwig amination, giving a mixture of products including the S_P -benzylamine **1.20**, $R = \text{Br}$, and R_P -**1.17**, with the S_P enantiomer reaction 3-4 times faster than the R_P enantiomer (Scheme 1.18). The R_P -**1.17** is then separated by chromatography.⁴⁶



SCHEME 1.18: Kinetic resolution of **1.17**. i) BnNH_2 , NaOt-Bu , (*S*)-PhanePhos, Pd_2dba_3 .

Chromatography

Column chromatography using silica or alumina gel is a more appealing method for resolving diastereomers which have different R_f values. Chiral chromatography may be used to separate enantiomers with a chiral stationary phase. This can be limited by suitability of the chiral stationary phase available, and/or the HPLC

throughput capacity; but this is still the most common method of isolating enantiomerically pure 4,12-dibromo[2.2]paracyclophane **1.17**- the other being the kinetic resolution described above.⁴⁷

Recrystallisation

Resolution by recrystallisation of diastereomers is another advantageous option if both the R_P and S_P forms of the compound are needed, and if the two diastereomers have different solubilities. It is particularly attractive if diastereomers can be formed through making a salt with a chiral partner, since it is trivial to form and neutralise salts. Derivatives of [2.2]paracyclophane tend to be crystalline because [2.2]paracyclophane's shape and aryl decks encourage regular stacking. Pye and Rossen's original synthesis of PhanePhos involved selective crystallisation of diastereomeric salts formed between tartaric acid and the phosphine oxide.²²

Resolution using recrystallisation can also be achieved with chiral auxiliaries, covalently adding a stereogenic centre. Enantiopure 4-hydroxy[2.2]paracyclophane may be prepared *via* diastereomeric esters, using the chiral auxiliary (1*S*)-camphanoyl chloride (**1.21**) or (*S*)-naproxene acid chloride (**1.22**) (Fig. 1.19) or the imine **1.23** with chiral auxiliary (*R*)-1-phenylethylamine (Fig. 1.20).⁴⁸⁻⁵¹ The diastereomers in each case are separated by fractional recrystallisation giving *de* of >98% in each case and between 14 and 22% yield.

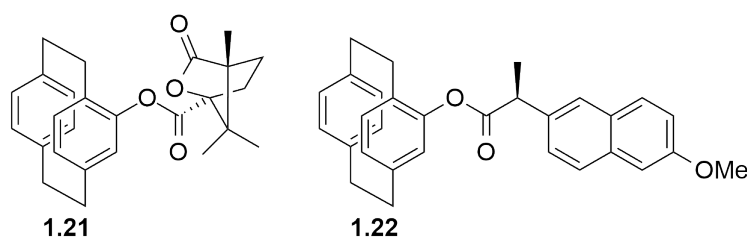


FIGURE 1.19: Diastereomeric esters of 4-hydroxy[2.2]paracyclophane.

1.1.5 [2.2]Paracyclophane in asymmetric catalysis

[2.2]Paracyclophane's planar chirality makes it an attractive scaffold for asymmetric catalysis. PhanePhos (**1.8**) is a ligand for hydrogenation and is one of the most commonly-used [2.2]paracyclophane-centred asymmetric ligands (Fig. 1.21). This

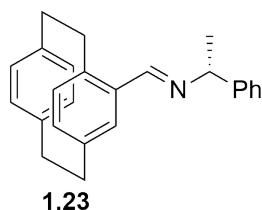
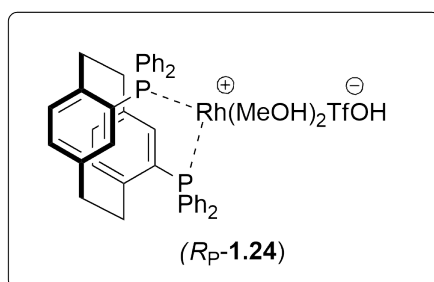
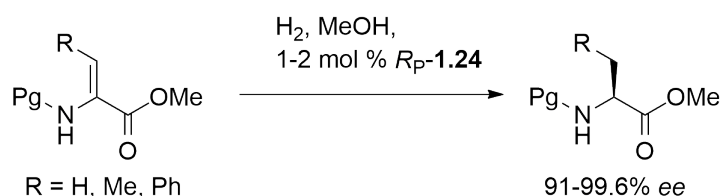


FIGURE 1.20: Diastereomeric imine for resolution of 4-hydroxy[2.2]paracyclophane.

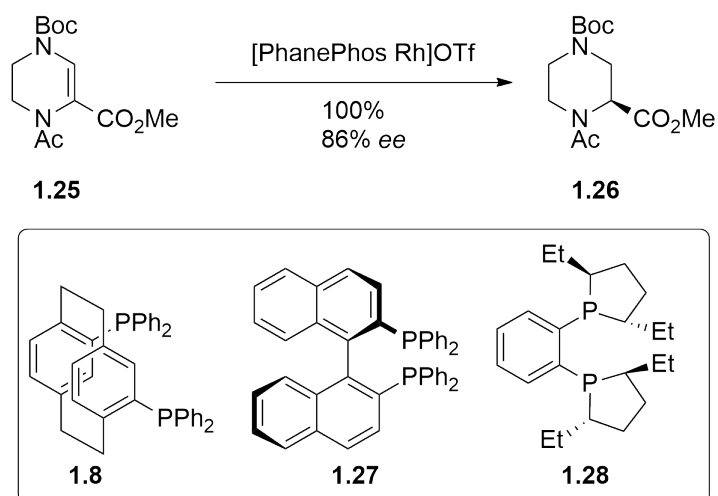
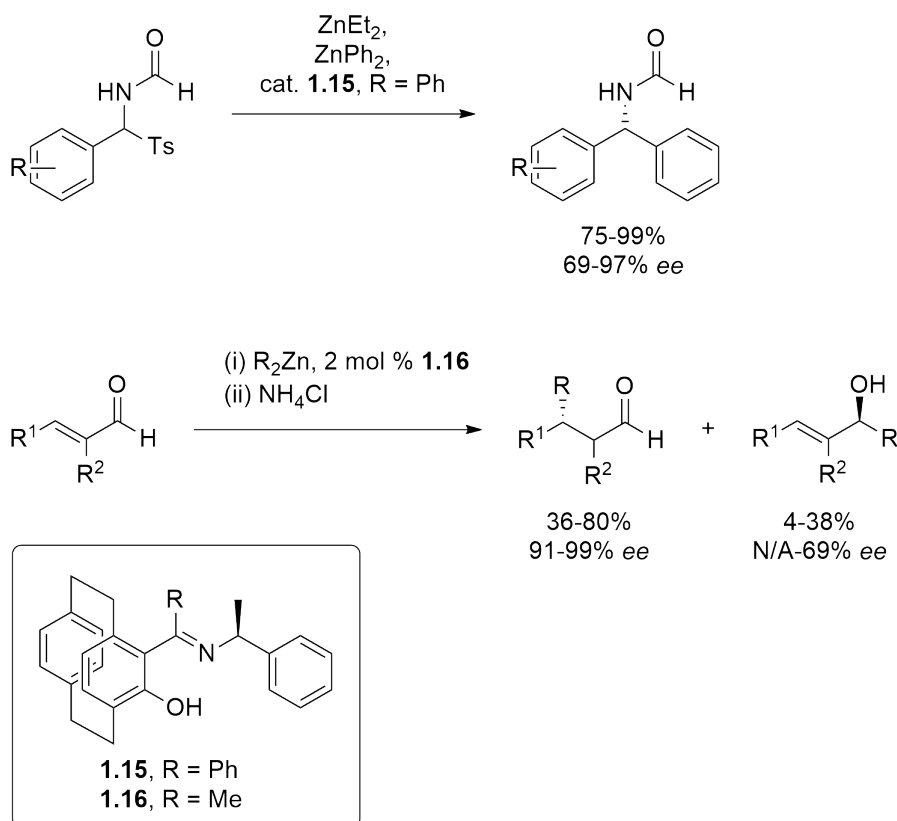
is due to its excellent selectivity compared with other similar catalysts.²² Pye and Rossen demonstrated that PhanePhos performs well in challenging transformations that similar rhodium bisphosphine catalysts achieved only moderate enantioselectivities under harsh conditions.



SCHEME 1.21: PhanePhos-Rh complex catalysed hydrogenation.

In an example reduction of tetrahydropyrazine **1.25** to give the HIV drug Crixivan precursor **1.26**, BINAP (**1.27**) gave 56% *ee* and Et-DuPHOS (**1.28**) gave 50% *ee* with strong conditions (70 bar, 40 °C, 24 hours); PhanePhos **1.8** performed the same reduction under milder conditions (1.5 bar, -40°C, 6 hours) with 86 % *ee* (Scheme 1.22).

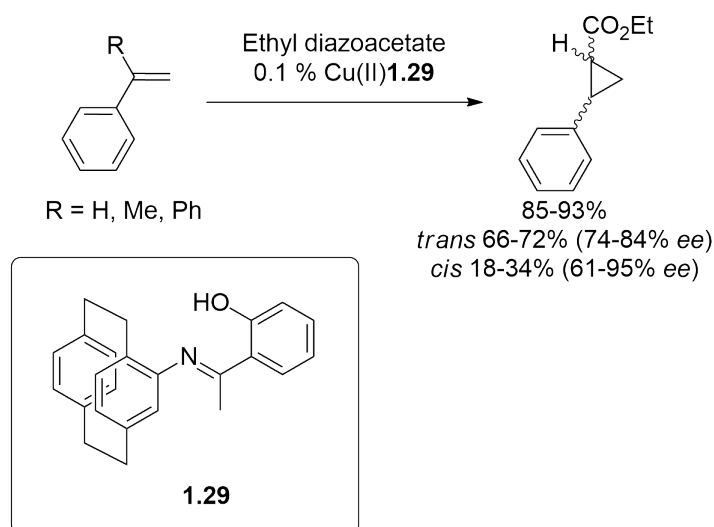
Bräse's [2.2]paracyclophane catalysts have been discussed above (Section 1.1.3) as interesting examples of [2.2]paracyclophane compounds that contain planar and point chirality. They are efficient catalysts with **1.15** (R=Ph) performing enantioselective addition of diphenylzinc to imines *via* an imine precursor (Scheme 1.23, top reaction). The best example gave the product where R = 4-Me in 99% yield and 94% *ee* with 5 mol % catalyst loading.

SCHEME 1.22: PhanePhos in asymmetric hydrogenation of the Crixivan precursor **1.25**.

SCHEME 1.23: Bräse's bidentate ligands for asymmetric catalytic aryl transfer and conjugate addition.

Ligand **1.16** (R=Me) performs well in an enantioselective copper-free conjugate addition of organozinc compounds to α,β -unsaturated aldehydes (Scheme 1.23, lower reaction) with low catalyst loading (2 mol %). Addition to cinnamaldehyde (R¹ = Ph, R² = H) with diethylzinc and *S_P*,*S*-**1.16** gave 46% of the (*R*) 1,4-product with 97% *ee*. The *R_P*,*S*-**1.16** gave the (*S*) 1,4-product with 43% yield and 98% *ee*, again showing the important of the planar chiral element of the catalyst in determining the configuration of the product.

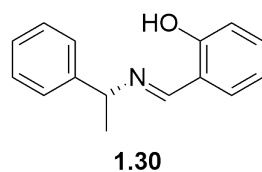
Glatzhofer's salicylidene [2.2]paracyclophane ligand **1.29** was effective for copper-catalysed cyclopropanation with very low catalyst loadings (0.1 mol %).⁵² In a reaction between styrene and ethyl diazoacetate, **1.29** gave 93% conversion in a 1.9:1 *trans/cis* ratio; the *trans* isomer has 76% *ee* and the *cis* isomer had 61% *ee* (Scheme 1.24).



SCHEME 1.24: Glatzhofer's cyclopropanation.

This compares favourably with Nozaki's analogous ligand **1.30**, which gave 72% yield of a 2:1 *trans/cis* ratio and 6% *ee* of each isomer in the same reaction.⁵³ The [2.2]paracyclophane ligand gives better enantiomeric excess due to the hindered rotation between the imine methyl group and the [2.2]paracyclophane scaffold. This makes a more structurally rigid binding pocket around the catalytic copper centre which is more sterically demanding.

These examples illustrate how [2.2]paracyclophane, with its unique structural properties, is an excellent planar chiral scaffold for asymmetric catalysts. The selectivities

FIGURE 1.25: Nozaki ligand **1.30** for cyclopropanation.

and yields of these examples indicate that [2.2]paracyclophane-based asymmetric catalysts are a worthwhile target for further development.

1.2 Unnatural amino acids

1.2.1 Terminology

The term *amino acid* is generally accepted to refer to the 20 “canonical” amino acids that are encoded by DNA. These are composed of an amine, a carboxylic acid, and a side chain, or *R group*, all attached to the same, central tetrahedral carbon atom. All of these “natural” amino acids, with the exception of glycine, whose R group is simply -H, have a stereocentre at the central α -carbon (Fig. 1.26, **1.31**). The R group determines the identity and function of the amino acid, and these vary from short alkyl chains to functionalised side chains such as glutamic acid, which has a carboxylic acid; asparagine, which has an amine; histidine, which has an imidazole; and phenylalanine, which contains an aryl ring. The natural amino acid proline (**1.32**) is a special case in which the R group forms a ring linking to the α -N.

Technically, any molecule containing an amine and a carboxylic acid, no matter how many other atoms and/or functional groups are present, might be considered an amino acid. A slightly narrower definition refers to all such amino acids found in biological systems, including those that are not coded by DNA: some amino acids may undergo additional structural modifications (for example, 4-hydroxyproline, **1.33**), or post-translational modifications (for instance, glycosylation or acylation) after incorporation into peptides. Somewhere between natural and unnatural amino acids exist a vast array of biologically created molecules that are non-proteinogenic: for instance, γ -aminobutyric acid (**1.34**), a neurotransmitter, and folic acid (**1.35**), a B vitamin.

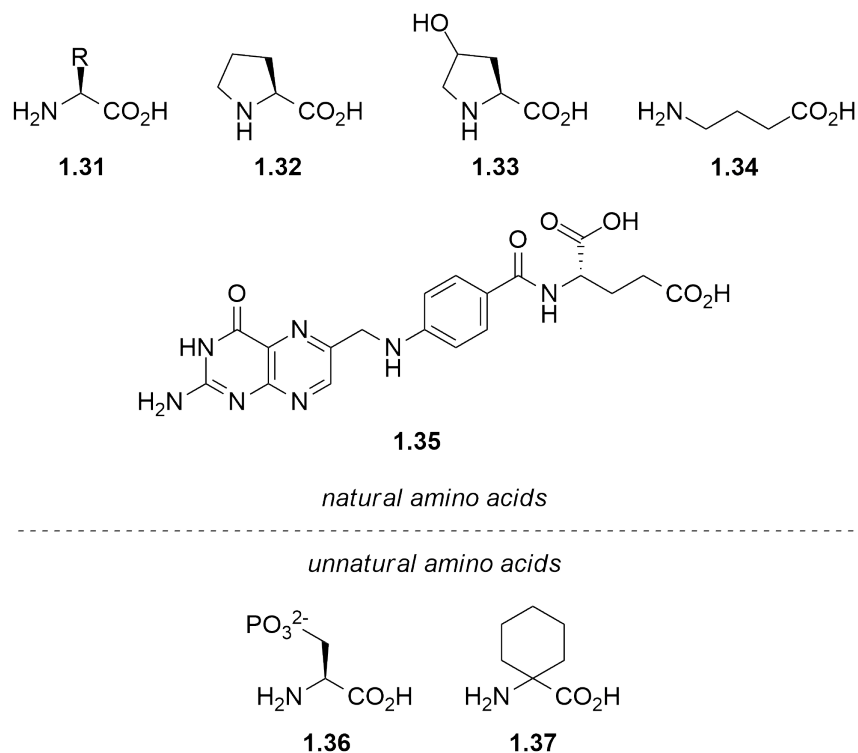


FIGURE 1.26: Examples of natural and unnatural amino acids.

The term *unnatural amino acid* will refer to synthetic molecules which resemble a natural amino acid but with side-chain (1.36) or backbone (1.37) modifications, rather than any molecule that contains both amine and carboxylic acid functional groups.^{54,55} This review will focus on a few synthetic unnatural amino acids that have clear relevance to this project.

1.2.2 Unnatural cyclic amino acids

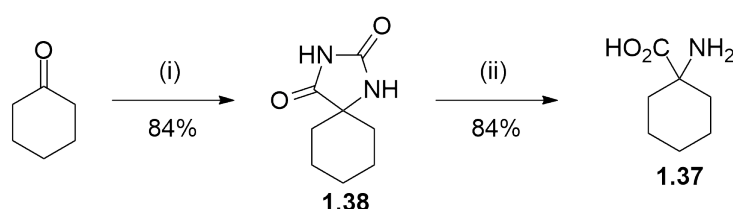
The synthesis, characteristics, and utility of cyclic amino acids will be discussed here, as they restrict conformational freedom; something the target of this project will also do, albeit while differing from these examples in many ways. Proline is the only canonical cyclic amino acid. This gives it a number of powerful functions, like manipulating the conformation of amide bonds in peptide secondary structure, for instance causing the important hairpin turn structural motif. Proline residues function prevalently as a catalytic site in enzymes and synthetic catalysts. Chemists have wanted to mimic these properties, so many cyclic unnatural amino acids have been produced, too.

There are many unnatural cyclic amino acids; and similarly innumerable ways to make them. Three examples have been chosen which show the variety of synthetic approaches available and their utility. These examples are all fundamentally different to the unnatural amino acids synthesised for this project; the closest example to a [2.2]paracyclophane containing amino acid is the ferrocene-centred example, below (Section 1.2.3).

1-Aminocyclohexanecarboxylic acid

An example of an unnatural cyclic amino acid is the α,α -disubstituted 1-aminocyclohexanecarboxylic acid **1.37**. It has seen some interest in peptide structural studies since its increased steric bulk and hindered rotation increases rigidity in the peptide chain, leading to increased conformational stability; thus peptides containing this unnatural amino acid residue might find use as catalysts.^{55,56} However, outside of this arena its potential is largely untapped, probably because it is achiral.

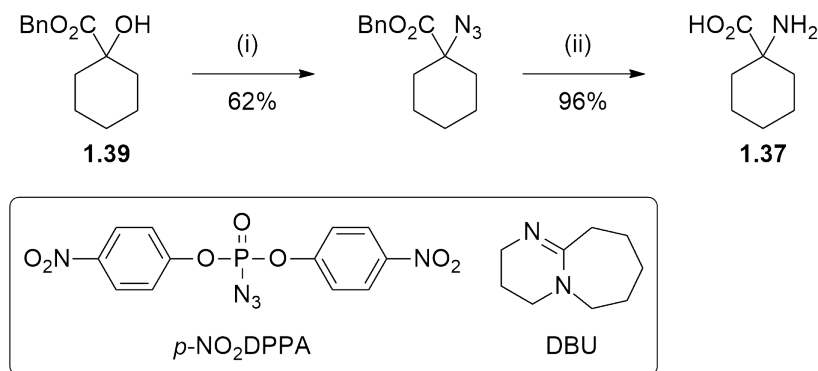
A popular synthetic route to 1-aminocyclohexanecarboxylic acid proceeds *via* a hydantoin **1.38** which is hydrolysed to the amino acid (Scheme 1.27).^{57,58}



SCHEME 1.27: Cyclic amino acid synthesis by hydantoin hydrolysis.
i) KCN, (NH₄)₂CO₃, EtOH/H₂O. ii) 60% H₂SO₄, 160°C.

Another produces the amine by azidation of the corresponding alcohol **1.39** using bis(*p*-nitrophenyl)phosphorazidate followed by azide reduction to the amine by catalytic hydrogenation (Scheme 1.28).⁵⁹ The azide substitution is an S_N2 mechanism which is unfavourable on quaternary carbons; here it is achieved using the reagent bis(*p*-nitrophenyl)phosphorazidate (*p*-NO₂DPPA), which is more active than the unsubstituted parent DPPA due to the presence of the electron-withdrawing *p*-nitro groups.

These synthetic methods also work for cyclic amino acids of other ring sizes and, in the case of the hydantoin methodology, with other substituents. The hydantoin



SCHEME 1.28: Cyclic amino acid synthesis by azide substitution and reduction. i) *p*-NO₂DPPA, DBU. ii) Pd/C, H₂.

methodology is also seen in the synthesis of ferrocene-containing amino acids (Section 1.2.3) as well as industrial synthesis of the natural amino acid methionine.⁶⁰

1.2.3 Ferrocene-centred amino acid

Arguably the closest unnatural amino acid to the work described in this thesis involves ferrocenes with amine and carboxylic acid functionality (Fig. 1.29).⁶¹ The earliest example of a ferrocene-centred amino acid analogue was from Herrick showing 1,1'-ferrocenedicarboxylic acid (**1.40**) can be used as a β -turn mimic in peptides.⁶²

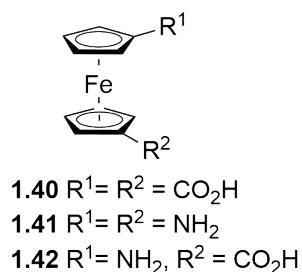


FIGURE 1.29: Amine and carboxylic acid functionalised ferrocenes.

The corresponding 1,1'-ferrocenediamine (**1.41**) may be used similarly; these symmetrically functionalised compounds form parallel peptide strands (**1.43**, Fig. 1.30). This was followed by studies showing 1'-aminoferrocene-1-carboxylic acid (*Fca*, **1.42**) incorporating peptide strands are antiparallel (**1.44**) as is characteristic in nature.⁶³

Ferrocene derivatives, like [2.2]paracyclophanes, can be planar chiral, however the compounds described in Figures 1.29 and 1.30 hold a single substituent on each ring and do not exhibit planar chirality. Ferrocene derivatives require two substituents on

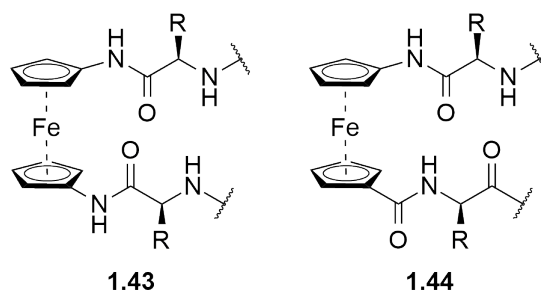


FIGURE 1.30: Parallel (left) and anti-parallel (right) peptide strand configuration on ferrocene derivatives.

one ring to be planar chiral. This is a limitation of ferrocene compared to [2.2]paracyclophane: Fca is essentially a bulky glycine analogue with no inherent chirality. The distance between the rings of ferrocene is 3.32 Å; this is close to the distance between hydrogen bonded N-O pairs in a β -sheet, which makes ferrocene an attractive backbone for the construction of peptides.⁶⁴

Typically, ferrocene derivatives with substituents on both cyclopentadienyl (*cp*) decks tend toward an anti configuration since this configuration is sterically favoured, however Fca-containing peptides are held closer to an eclipsed configuration due to the hydrogen bonding between the peptide strands on either deck (1.45). Where no hydrogen bonding is possible, for instance in the case of the bisproline compound 1.46, the compound's crystal structure shows that it adopts the staggered conformation.⁶²

NMR spectra of the Fca peptides reveals the effects of hydrogen bonding, or lack thereof, between the peptide strands. Hydrogen bonded carbonyl carbons have higher ¹³C chemical shifts because of deshielding from the hydrogen bond, and indeed this is seen in the difference between the spectra of the mono- and bisvaline compounds 1.45 and 1.47 in their ester carbonyl chemical shifts with a difference of 2.1 ppm. Meanwhile, the mono- and bisproline compound's ester carbonyl chemical shifts are virtually identical, differing by only 0.2 ppm, which is expected since hydrogen bonding is not possible between the two proline residues. Additionally, only 3 *cp* C chemical shifts are observed for the bis(proline) compound 1.46, indicating the rings may rotate; 5 *cp* chemical shifts are seen for the analogous bis(valine) compound, indicating the rotation is hindered by the hydrogen bonding between then NH and ester CO groups (Fig. 1.31). Similar differences are observed for the IR

spectra of these compounds.

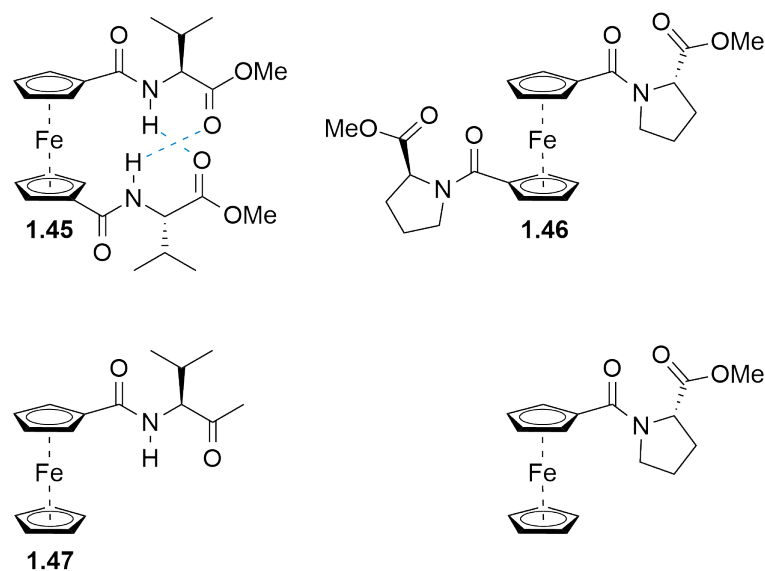


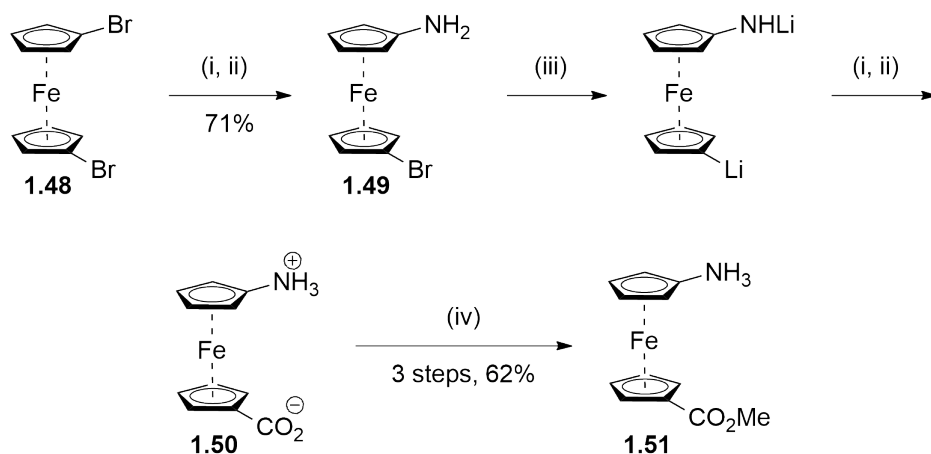
FIGURE 1.31: *Syn* and *anti* configuration for ferrocene compounds with and without hydrogen bonding.

Synthesis of ferrocene amino acid

A number of groups have shown interest in the attractive structural and electronic properties and applications of Fca. Therefore, several synthetic approaches to Fca are described below.

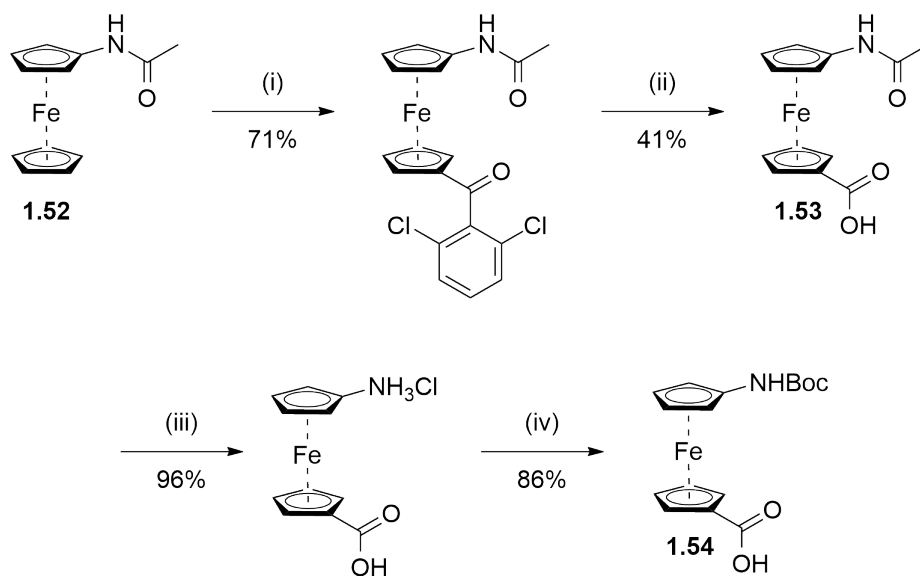
The first synthesis of Fca was published by Butler's group and started with metal-halogen exchange of 1,1'-dibromoferrocene **1.48** (Scheme 1.32).⁶⁵ Benzylhydroxylamine reacts with the mono-lithiated product to form 1'-bromoferrocene-1-amine **1.49**. A further metal-halogen exchange followed by quenching with carbon dioxide gives the Fca as the zwitterion **1.50**. The group described difficulties in this synthesis with the formation of intermediates and side products, and with the stability of the compounds; this also led to complications purifying products, and it was found that Fca-OMe **1.51** had the best stability and ease of isolation.

Ueyama *et al.* followed with a synthetic route that began with a synthesis of *N*-acetamidoferrocene **1.52** previously described in the literature (Scheme 1.33).⁶⁶ Friedel-Crafts reaction with 2,6-dichlorobenzoyl chloride and subsequent hydrolysis with *t*-BuOK afforded the carboxylic acid **1.51** specifically at the opposing ring due to the acetamide's deactivating effect. Acetamide cleavage with HCl gave Fca as the



SCHEME 1.32: Butler's synthesis of Fca from 1,1'-dibromoferrocene. i) *n*-BuLi, ii) BnONH₂, iii) CO₂, iv) AcCl, MeOH.

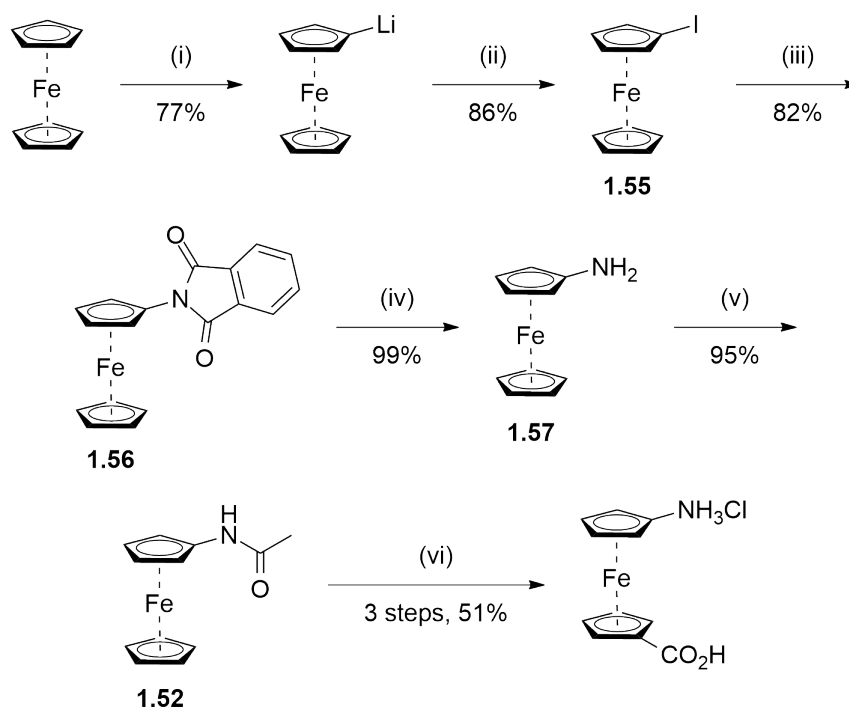
HCl salt **1.42** · HCl, which was stable at low pH, but *N*-protection with Boc **1.54** was found to provide stability at higher pH.



SCHEME 1.33: Ueyama's synthesis of Fca from *N*-acetamidoferrocene. i) 2,6-Cl₂C₆H₃COCl, AlCl₃, ii) *t*-BuOK, iii) 6 M HCl, iv) Boc₂O.

A synthesis which improved upon Ueyama's route was reported by Heinze *et al.* in 2004 which increased their low yield (from 28% to 51%) by altering the initial synthesis of *N*-acetamidoferrocene **1.52** (Scheme 1.34). They also reported better yields in the subsequent introduction of the carboxylic acid moiety to the opposing ring.⁶⁴

The original conditions involved the reaction of iodoferrrocene **1.55** with phthalimide

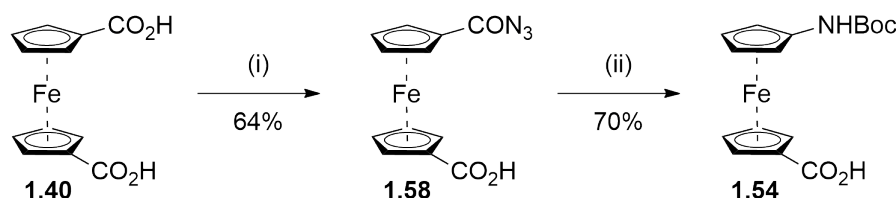


SCHEME 1.34: Heine's synthesis of Fca based on Ueyama's route.
 i) *t*-BuLi, ii) I₂, iii) copper phthalimide, iv) NH₂NH₂ · H₂O, v) Ac₂O, NaOAc. vi) a. 2,6-Cl₂C₆H₃COCl, AlCl₃, b. *t*-BuOK, c. 6 M HCl.

catalysed by Cu₂O in pyridine in Gabriel-like conditions.⁶⁷ Along with the desired product **1.56**, ferrocene dimers were formed. Pre-forming the copper-phthalimide and using solvent-free conditions prevents dimerisation. Reaction with hydrazine (the Ing-Manske procedure) gives aminoferrocene **1.57**, and finally *N*-acetamidoferrocene **1.52** is formed by amide formation with acetic anhydride. Optimisation of reaction conditions from Ueyama's paper increased their yields to give the hydrochloride salt of Fca **1.42** · HCl. The major improvement was in the hydrolysis step to furnish the carboxylic acid, which was increased from 41% to 70% by optimising the stoichiometry of the added water.

Ueyama and Heine's methods suffered from long linear synthetic routes necessitated by addition and removal of protecting groups, while Butler's synthesis where the amine is formed followed by the carboxylic acid results in a mixture of inseparable compounds. An alternative strategy used by Erb *et al.* employed the selective reaction of a single carboxylic acid of ferrocene-1,1'-dicarboxylic acid **1.40** (Fig. 1.35).⁶¹ One acid was converted to an aniline by the Curtius rearrangement. Whereas previous methods which formed the amine by Curtius rearrangement employed sodium

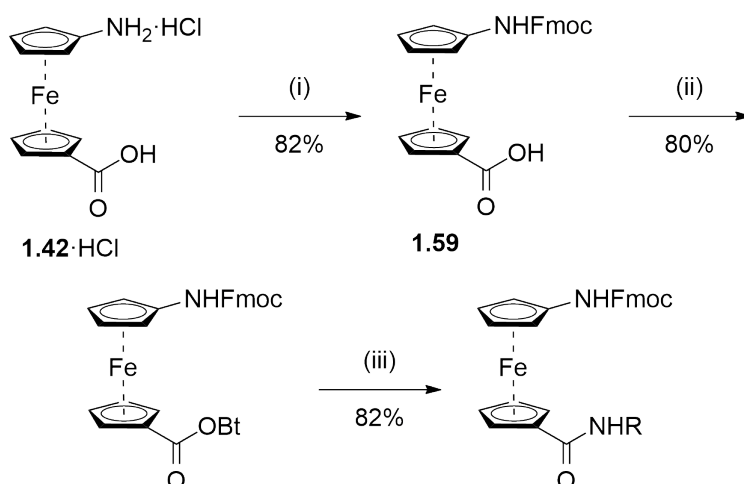
azide, here, diphenylphosphoryl azide (DPPA) was used to promote desymmetrisation of the dicarboxylic acid and limit formation of side products such as the di-azide. The Curtius rearrangement of the resulting acyl azide **1.58** with *t*-BuOH gives the *N*-Boc-protected Fca **1.54**. This method has a lower yield (around 40% from the dicarboxylic acid), however it has the advantage of fewer synthetic steps.



SCHEME 1.35: Erb's synthesis of Fca using optimised Curtius rearrangement. i) DPPA, Et₃N, ii) *t*-BuOH, 110°C.

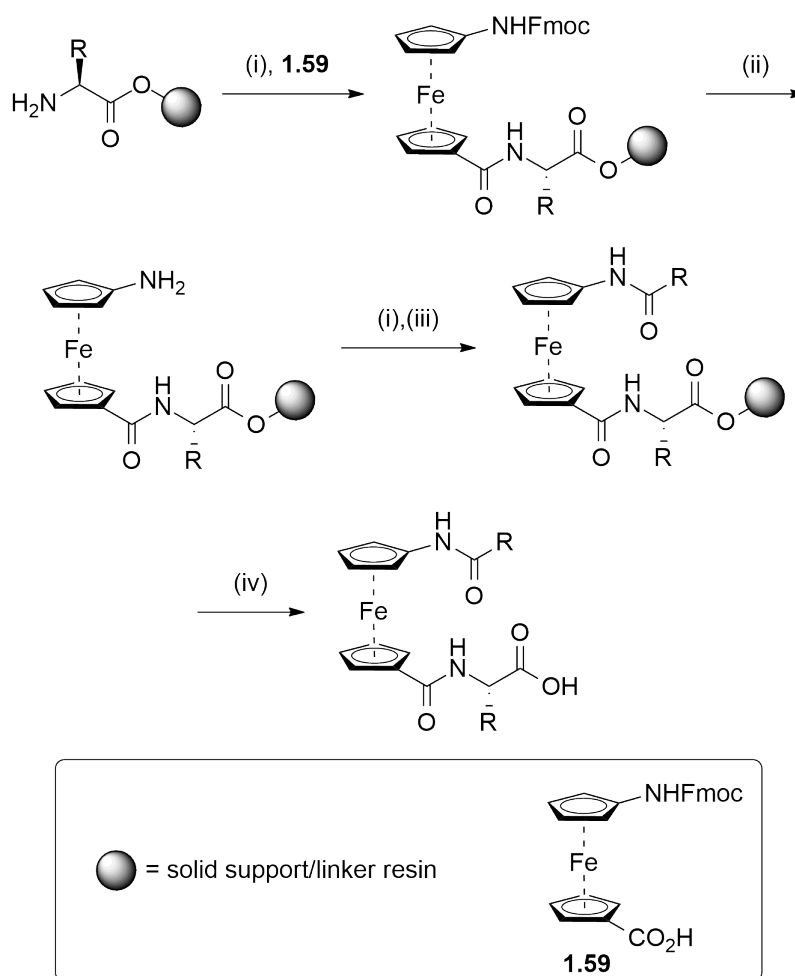
Ferrocene amino acid peptides

Fca can be incorporated into a peptide using standard coupling conditions such as the use of classic peptide coupling reagents such as EDC/HOBt, DCC/HOBt, HBTU/HOBt; and acyl chloride and acyl fluoride activation of the carboxylic acid moiety.^{63,64,68–75} An example using DDC and HOBt is shown below (Scheme 1.36). Fmoc-protection of the N-terminus (**1.59**) with Fmoc-Cl should be carried out in buffered solution since Fca is sensitive to basic conditions. Boc-protection is generally avoided for organometallic complexes since its removal required the use of strong acid.



SCHEME 1.36: Carboxylic acid activation for peptide coupling with Fca. i) 9-Fluorenylmethyl chloroformate. ii) DCC, HOBt. iii) C-terminus protected amino acid or peptide R-NH₂.

Solid-phase peptide synthesis (SPPS) protocols have also been employed in the synthesis of Fca-containing peptides (Scheme 1.37).^{76,77} SPPS is a well-established method for building synthetic peptides.⁷⁸ While Fmoc was used in the example above, in this example, the Fmoc-terminated oligopeptides were unstable so a combination of Boc- and Fmoc-protection was used. SPPS facilitates the multiple couplings and purifications required for stepwise production of oligopeptides since the peptide remains bound to the resin beads while the excess reagents and side products are washed away by appropriate solvents.



SCHEME 1.37: Solid phase peptide synthesis of Fca-containing peptides. i) DIC, HOBT. ii) piperidine. iii) N-terminus protected amino acid or peptide R'-COOH, iv) TFA.

1'-Aminoferrocene-1-carboxylic acid-centred peptides have been used for structural studies, confirming the importance of intramolecular hydrogen bonding and, to a smaller extent, steric hindrance as conformational determinants in the secondary

structure of these peptide strands.^{69,73,79,80} Heinze *et al.* found the hydrogen bonding motif seen in compound **1.45** (Fig. 1.31) with the hydrogen bonds crossing the side chains forming 9- and 11- membered rings was most common and encouraged the β -like sheet arrangement.⁷⁹ Barišić *et al.* found that absolute configuration of natural amino acid residues in Fca-centred peptides did not influence the peptide's conformation, nor did the steric bulkiness of side chain protecting groups.⁶⁹ Rather, the most important factor dictating the conformation was the number and position of hydrogen bonding donor and acceptor groups. This can be seen in the different hydrogen bonding seen in **1.61**, which has exclusively interchain hydrogen bonds; while the constituents of **1.60** allow both inter- and intrachain hydrogen bonds (Fig. 1.38).

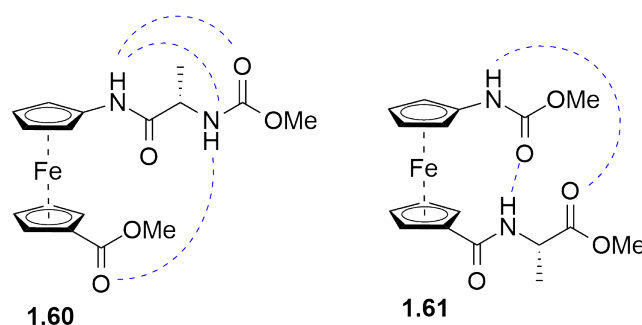


FIGURE 1.38: Intra- and interchain hydrogen bonding in Fca-containing peptides.

The structure of and electronic interaction and communication between redox-active centres of polypeptides containing several Fca units has been studied: ferrocene polymers often display electronic communication between the metal sites modulated by the distance between the ferrocene units; however large organic groups between the ferrocene units insulate against this electronic communication.^{74,75,81–83}

The activity of Fca peptides have also been studied: a group of proline-containing Fca peptides were tested for anticancer activity and mostly found wanting; Kraatz's group has found promising results with their Fca peptides as surface-bound nerve agent detectors and protein detectors; naphthyl-derived Fca peptides show promise as anion receptors.^{70–72,84}

1.2.4 Adamantane-centred amino acids

Schreiner's γ -aminoadamantanecarboxylic acid (*Aca*, **1.62**) is of pertinence to the work presented in this thesis due to the fact adamantane is very rigid and places functionality in specific points in 3-dimensional space. This is analogous to the structure of [2.2]paracyclophane which is also used as a scaffold about which functional groups may be precisely arranged.

Schreiner's research on *Aca* followed studies on aminoadamantanes found in several earlier potential pharmaceuticals such as the antiviral adamantidine (**1.63**) and tromantidine (**1.64**), and the Alzheimer's treatment drug memantine (**1.65**) (Fig. 1.39).^{85,86}

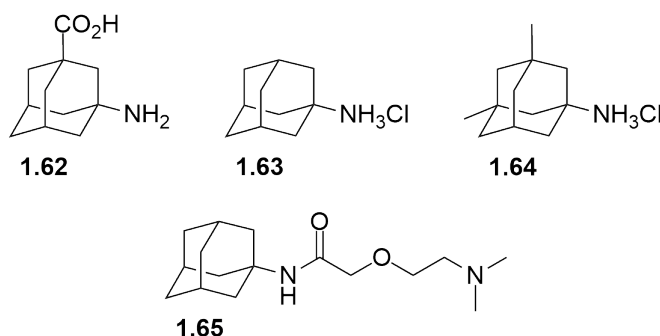


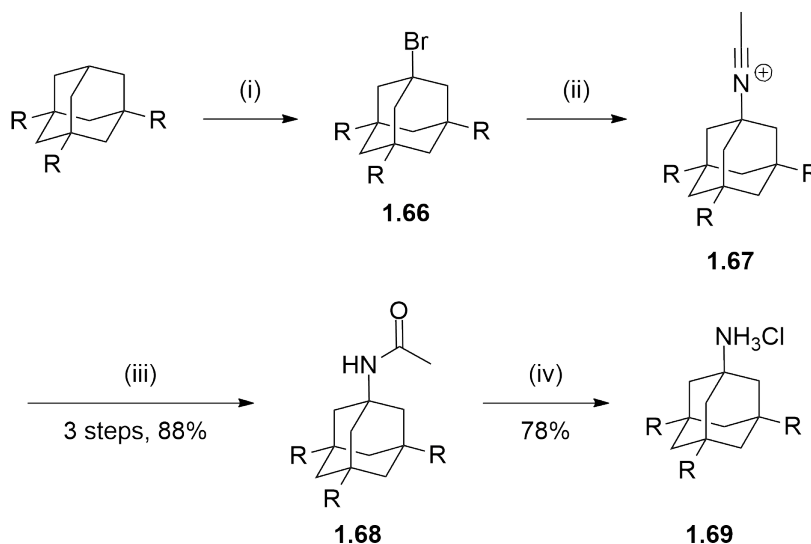
FIGURE 1.39: Amine derivatives of adamantane.

Aca resembles a class of GABA analogues used as anticonvulsants; the synthesis of *Aca* and derivatives was studied for their potential use as pharmaceuticals.⁸⁷ The adamantane backbone is a rigid and bulky scaffold that causes restricted conformational rotations that produce turn-like structures. Therefore it presents a compelling target for organocatalysis in reactions known to require rigid turn structures.^{88,89} α -Amino acids with adamantyl side chains have also been synthesised but will not be considered here.^{90,91}

Synthesis of aminoadamantanecarboxylic acid

Synthesis of the amine moiety of *Aca* has been described following several similar routes involving formation and then hydrolysis of an amide. These routes follow the popular method of Ritter C-N bond formation, with electrophilic attack of a nitrile to the tertiary carbocation in the presence of strong acid (Scheme 1.40).⁹²⁻⁹⁴ The

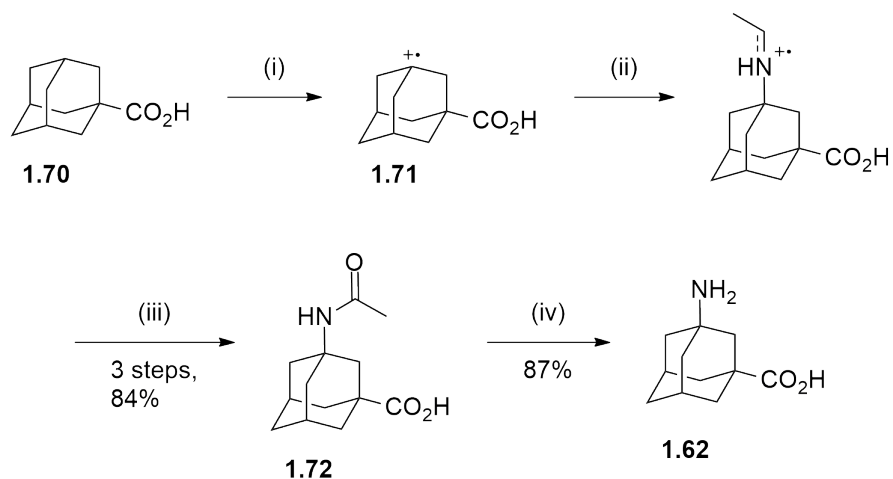
key step is formation of a tertiary carbocation, which proceeds *via* a bromide. The bromide **1.66** is formed with a large excess of bromine, and is eliminated to give the active carbocation. The acetonitrile adds to give the nitrilium ion **1.67** which becomes the amide **1.68** after addition of a water molecule. The amide is hydrolysed under acidic conditions to give the amine as the hydrochloride salt **1.69**.



SCHEME 1.40: Synthesis of Aca using the Ritter reaction *via* the bromide **1.66**. (i) Br₂. (ii) MeCN. (iii) H₂O. (iv) Aq. HCl.

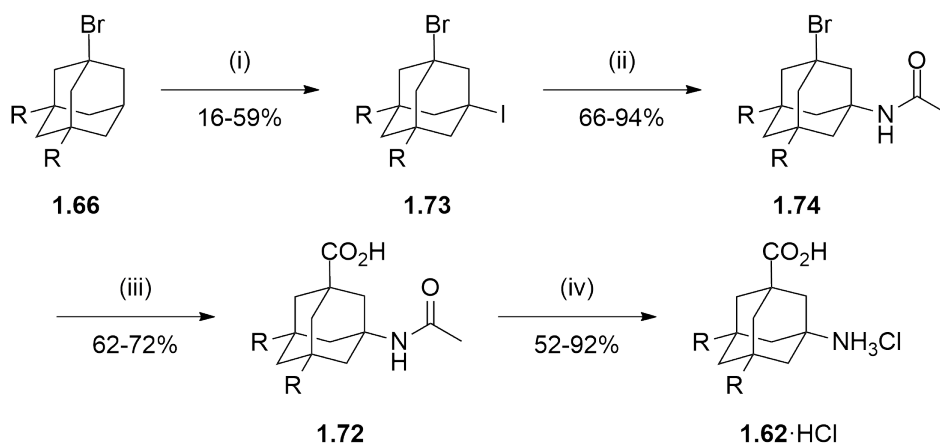
Schreiner *et al.* developed a method that avoided the use of excess bromine through formation of a radical carbocation (Scheme 1.41).⁸⁷ Starting with adamantane-1-carboxylic acid **1.70**, Schreiner's route generates the carbocation **1.71**, by reaction with a mixture of nitric acid and sulfuric acid.⁹⁵ These produce the radical carbocation by single electron transfer from the adamantane derivate to NO₂⁺.⁹⁶ The reaction occurs selectively at the tertiary position as this is the more stable radical cation. The reaction then rejoins the Ritter process with acetonitrile adding to give the acetamide **1.72** after the addition of water. The free amine can be obtained by acid hydrolysis of the amide. This route gives the best yields when the substrate contains either carboxylic acids as this increases the solubility in the reaction medium; and/or alkyl groups that help stabilise the radical carbocation. This methodology can be used to form other amino adamantanes.

A further method developed by Schreiner *et al.* uses phase transfer catalysis to generate the halide **1.73** prior to the formation of the carbenium ion (Scheme 1.42).⁸⁷ Ritter



SCHEME 1.41: Nitrosonium ion-induced carbocation route to Aca. i) $\text{HNO}_3, \text{H}_2\text{SO}_4$. ii) MeCN. iii) H_2O . iv) HCl.

protocol with the carbocation formed by the nitrosonium ion bears the acetamide **1.74**. Finally the carboxylic acid **1.72** is formed by a Koch-Haaf type reaction with formic acid generating carbon dioxide *in situ*. The carbon dioxide attacks the tertiary carbocation formed by the bromide; addition of -OH from water gives the carboxylic acid **1.62**.



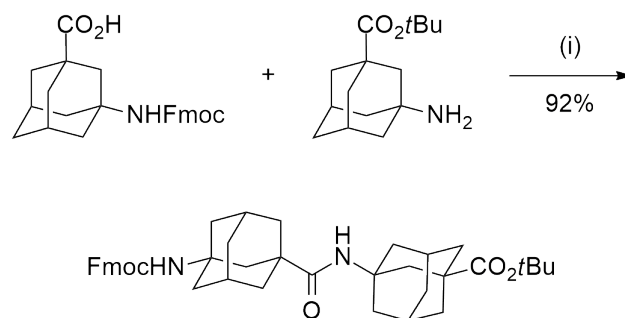
SCHEME 1.42: Phase transfer catalysed synthesis of Aca. i) NaOH, CHI_3 , tetra-*N*-butylammonium bromide, ultrasound, ii) a. NOBF_4 , MeCN, -50 to -15 °C, b. H_2O , iii) a. $\text{H}_2\text{SO}_4, \text{HCO}_2\text{H}$, b. H_2O , iv) 8 M HCl.

Although the oxidative route using the nitrosonium species is more efficient for the formation of **1.62**, the halide-based methods are more versatile and allow a broader scope of R-groups and side chains to be accessed. Side chain functionalisation can be desirable in the chemistry of peptides, so the less appealing halogenation route is still very useful. Whichever method is used, chiral products are racemic and may be

resolved by selective recrystallisation of diastereomeric salts formed from quinine.⁸⁷

Adamantane amino acid peptides

Peptide couplings between Aca units may be performed by using traditional peptide couplings reagents such as HBTU (Scheme 1.43); or solid phase peptide synthesis.^{87,91,97}



SCHEME 1.43: Peptide coupling between two Aca units. i) HBTU, DIPEA

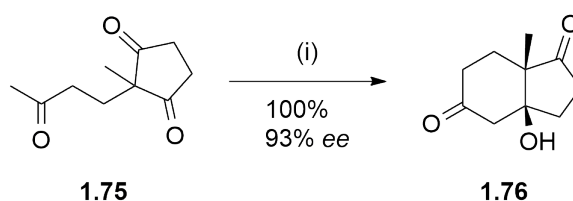
Schreiner's group went on to develop a series of organocatalysts based on Aca-containing peptides. These will be discussed in Section 1.4.4. Schreiner's array of peptide multicatalysts illustrate the power of using peptides in order to easily alter the functionality of the molecule through use of different amino acids. The variety of functionality available in natural amino acids gives scope to alter catalytic function, solubility, and conformational control simply by introducing a different amino acid residue.⁹⁸ The modular nature of the chain of amino acids and well-developed peptide coupling chemistry allows this ease of elaboration.

1.3 Asymmetric organocatalysis

The demand for chiral compounds is ever-increasing, due to their biological importance, their utility in industry, and their remarkable structures. Of the many approaches available for synthesis of chiral compounds, asymmetric catalysis is attractive because of its efficiency. Traditionally, chiral catalysts were organometallic complexes, or biologically derived enzymes. Both of these have shortcomings. Metal-containing complexes are often sensitive to air and may not be compatible with many solvents, or with harsh reaction conditions. They tend to be specific for

a small set of substrates. Enzymes must either be synthesised, which is a significant challenge considering the molecular weight of even the smallest of these biological polymers; or extracted from a biological source. Like organometallic catalysts, enzymes are sensitive to reaction conditions, particularly temperature, pH, and organic solvent. Organocatalysts, composed of small molecules with no metal atoms complexed, hold the advantage of being more stable to reaction conditions, with generally lower toxicities than organometallic compounds.

Arguably the first organocatalysts were 4-dimethylaminopyridine (DMAP) in Steglich esterification or piperidine in Knoevenagel condensation; however these are not asymmetric catalysts.^{99,100} The first asymmetric organocatalyst emerged in the 1970s with Hajos and Parrish's discovery of proline-catalysed Robinson annulation: now called the Hajos–Parrish–Eder–Sauer–Wiechert reaction due to the contributions of many chemists to the investigation of scope and mechanism of this useful aldol reaction.¹⁰¹ Their work described the proline-catalysed stereoselective intramolecular aldol reaction of ketone **1.75** to give alcohol **1.76** in quantitative yield and 93% *ee* (Scheme 1.44).



SCHEME 1.44: Hajos and Parrish's proline-catalysed asymmetric Robinson annulation. i) 3 mol % L-proline.

Amino acids with primary amines were found to have lower stereoselectivity; proline's secondary amine in a 5-membered ring has a more rigid conformation and increases stereoselectivity. The reaction mechanism has been proposed to proceed *via* an enamine intermediate.¹⁰²

The versatility of organocatalysts in asymmetric catalysis have been recognised more recently. The last 20 years have seen a huge explosion in this area and it would be infeasible to discuss its entire scope. Interested readers are directed to the reviews by Taylor and Jacobsen, Schreiner, Seayad and List, and Dalako and Moisan.^{103–106} Some pioneering organocatalysts will be mentioned briefly but more attention will

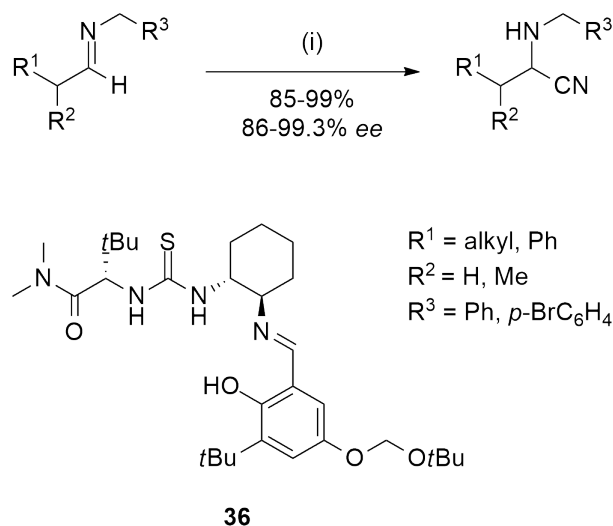
be paid to those with resemblance to amino acids and peptides. Since amine-based organocatalysts follow either standard enamine or iminium catalytic mechanisms they have the advantage of being more general for types of functional group: examples of each mechanism are discussed in the sections to follow.

1.3.1 Early asymmetric organocatalysis

Two distinct areas start quite early in the growth of organocatalysis. These can broadly be termed Brønsted acid catalysis and Lewis base catalysis.¹⁰⁷

Brønsted acid catalysis

Acids were known to be useful as non-chiral catalysts before interest in chiral versions became apparent, inspired by the prevalent motif of proton transfer in enzymatic catalysis.¹⁰³ One of the first asymmetric examples is Jacobsen's urea or thiourea imines for the asymmetric Strecker reaction, a reaction which is useful for forming highly enantiopure amino acid precursors.¹⁰⁸ These catalysts were discovered by accident: Jacobsen included a control experiment without metal and found the ligand gave better results than the complex.¹⁰⁹ Jacobsen's catalysts displayed impressive enantioselectivity and substrate range, with the thiourea **1.77** giving the best enantioselectivity (Scheme 1.45).



SCHEME 1.45: An example of Jacobsen's thiourea/imine catalysts in asymmetric Strecker reaction. i) Trimethylsilyl cyanide, 2 mol % **1.77**, then TFAA.

In thiourea **1.77**, the active site of the catalyst is the N-H bonds of the thiourea as seen in the simplified transition state in Figure 1.46. Replacing the oxygen of the urea in initial catalysts (not shown) with a sulfur increased the stereoselective power of the catalyst because thiourea protons are more acidic. Both thiourea protons hydrogen bond with the imine in *cis*-configuration as the only essential points for catalyst activity. This points the large group on the imine carbon away from the catalyst, allowing for this catalyst's broad substrate scope for aldimines since this group does not interact strongly with the catalyst; ketimines on the other hand are not ideal substrates for this reaction since their additional R group is too big to occupy the space. The HCN addition occurs over the cyclohexane ring, inducing *S* configuration in the product.

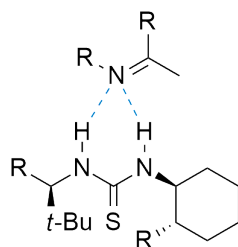


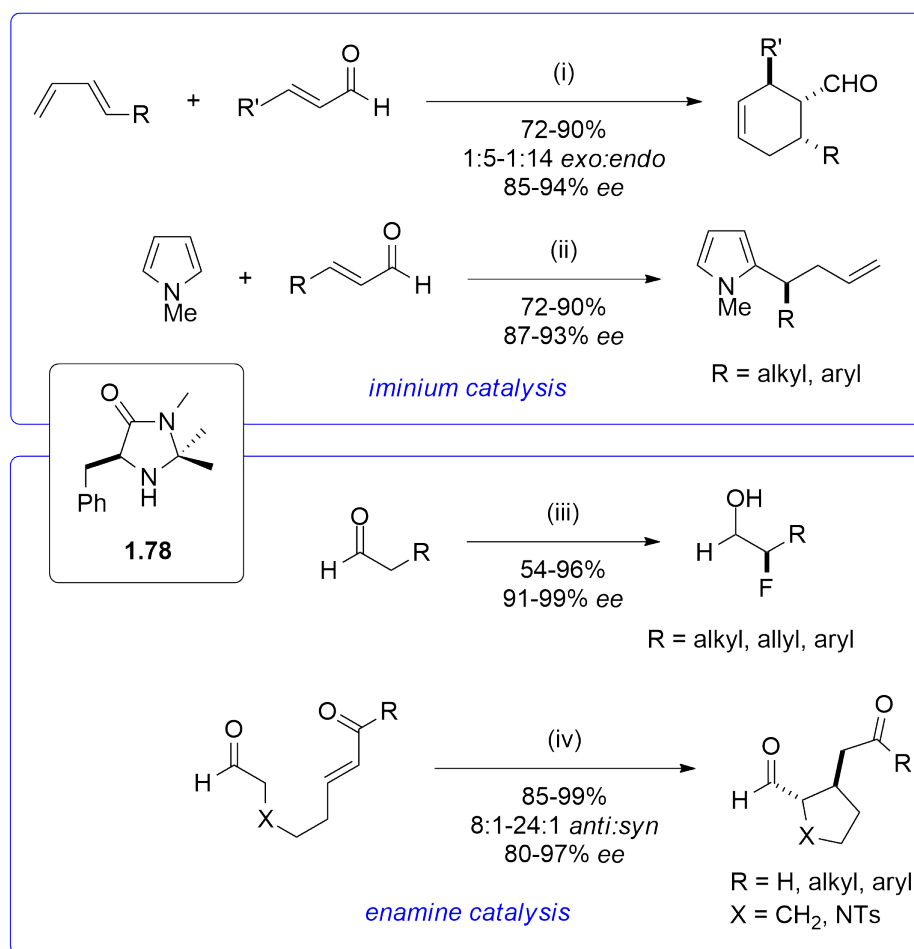
FIGURE 1.46: Transition state of Strecker reaction catalysed by **1.77**

Lewis base catalysis

Lewis base catalysis is less well-defined, covering a range of processes like Denmark's activation of silicon Lewis acids with phosphoramides, to nucleophilic catalysts such as carbenes used in the Stetter reaction.^{110,111}

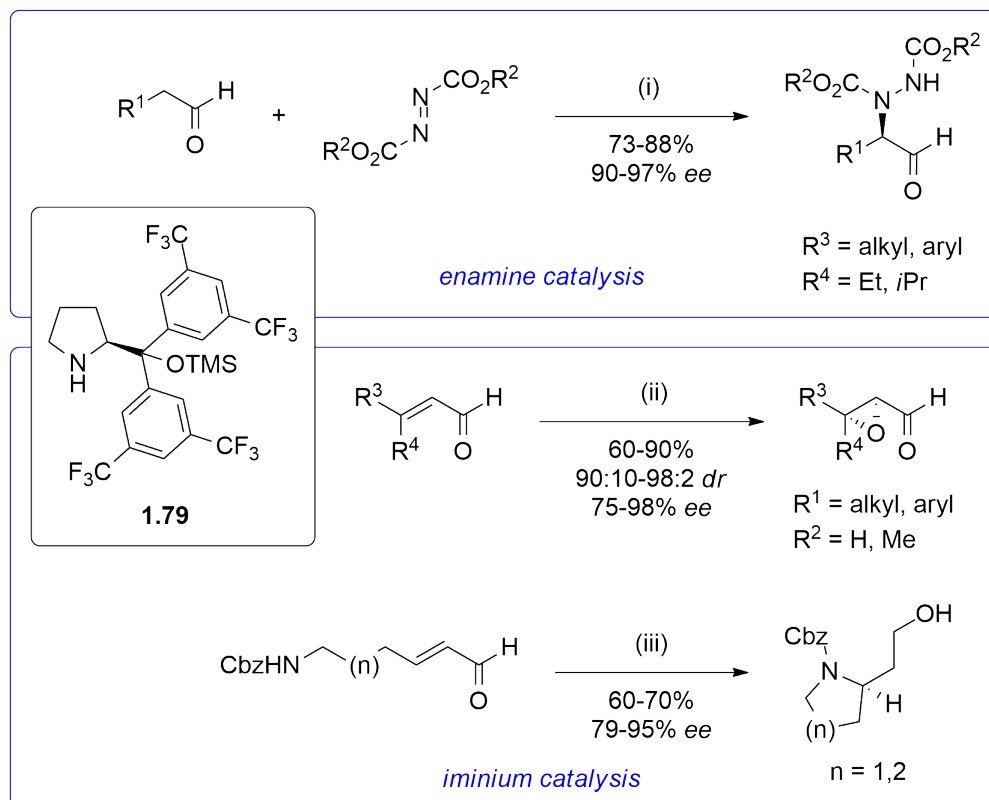
It would be remiss to discuss early examples of Lewis base asymmetric organocatalysts without mention of MacMillan's well-known imidazolidinone catalysts, for example **1.78**. They were first shown to be effective in a Diels-Alder reaction, followed by an array of other reactions including Friedel-Crafts alkylation, variants of the Michael addition, and α -halogenation (Scheme 1.47).¹¹²⁻¹¹⁷ The beauty of these catalysts is that they offer a general strategy to promote many reactions. The catalysts may act in either the enamine or iminium catalytic mechanisms.

Jørgensen's diphenylprolinyl silyl ethers (for example, **1.79**) are an example of chiral secondary amine compounds that will catalyse a number of different reactions



SCHEME 1.47: MacMillan's imidazolidinone catalysts in (from top to bottom) Diels-Alder reaction, Friedel-Crafts reaction, α -fluorination, and intramolecular Michael addition. i) 20 mol % **1.78**, HCl; ii) 20 mol % **1.78**, TFA; iii) a) 20 mol % **1.78**, dichloroacetic acid, *N*-fluorobenzenesulfonimide, b) NaBH₄; iv) 5 mol % **1.78**, HCl.

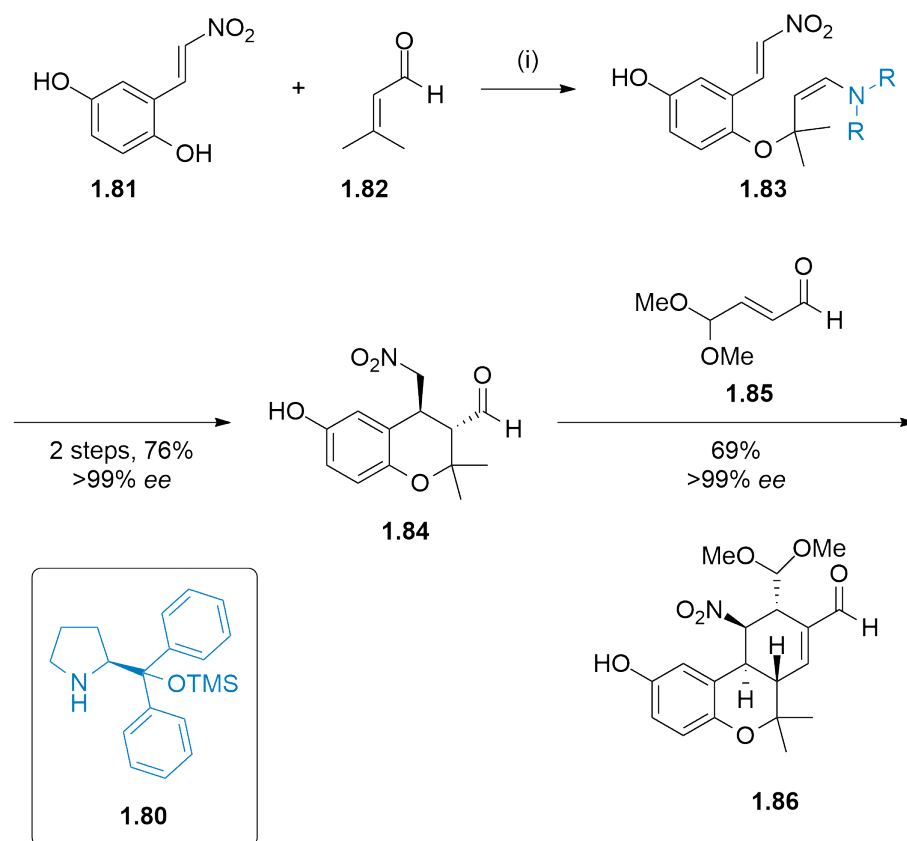
of carbonyl compounds (Scheme 1.48), such as the α -functionalisation of aldehydes and the epoxidation of α,β -unsaturated aldehydes.^{118–120} They are also widely used in the Michael addition and its variants, including aza-Michael additions, with some examples in the literature detailing elegant syntheses using these catalysts in cascade reactions, installing as many as four stereocentres concurrently.^{121–123}



SCHEME 1.48: Jørgensen's diphenylprolinyl silyl ether catalyst in (from top to bottom) α -amination, epoxidation of α,β -unsaturated aldehydes, and aza-Michael addition. i) 10 mol % **1.79**; ii) 10 mol % **1.79**, H_2O_2 ; iii) a) 20 mol % **1.79**, b) $NaBH_4$.

An exemplar of a cascade reaction using Jørgensen's diphenylprolinyl silyl ether catalyst is the total synthesis of (+)-Conicol **1.86**, where it installs four stereocentres in a one-pot, two-step reaction in 55% total yield with >99% ee (Scheme 1.49). Jørgensen's catalyst **1.80** enabled the installation of these stereocentres from achiral substrates. This is a cascade reaction of four steps: (oxa-Michael)-Michael-Michael-aldol. The first step in the cascade is tandem oxa-Michael addition of a phenol oxygen of (*E*)-2-(2-nitrovinyl)benzene-1,4-diol (**1.81**) to 3-methylbut-2-enal (**1.82**), and Michael addition of the resultant enamine species **1.83** to the α,β -unsaturated nitro

group. The next step was addition of 4,4-dimethoxybut-2-enal **1.85** to the same reaction vessel for a tandem Michael-aldol condensation. The Michael addition occurs between the α -nitro carbon of **1.84** and 4,4-dimethoxybut-2-enal; the aldol reaction occurs between the aldehyde of **1.84** and 4,4-dimethoxybut-2-enal.



SCHEME 1.49: An example of Jørgensen's diphenylprolinyl silyl ether catalyst in the synthesis of (+)-Conicol in a cascade reaction. i) 20 mol % **1.80**, HOAc.

4,4-Dimethoxybut-2-enal was chosen to represent the final ring's three-carbon synthon since Hong *et al.* found using crotonaldehyde led to the formation of an unstable α,β -unsaturated cyclic ketone later in the synthetic pathway which aromatised to form a phenol; the dimethoxy compound gave a more stable intermediate. The successful crotonaldehyde Michael-aldol reaction was remarkable since its γ -H could have caused γ -amination side reactions. This synthetic strategy lends itself to diverse products based on the central three-ring skeleton which is found in many natural products being studied for biological activity. Two variants were synthesised in Hong *et al.*'s study.¹²³

1.3.2 Enamine catalysis

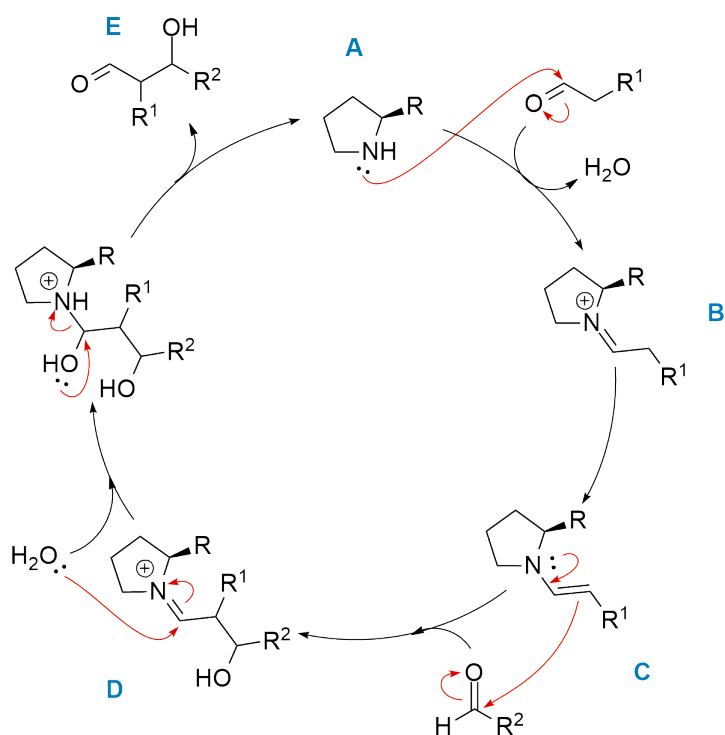
The difference between enamine and iminium catalysis for an asymmetric amine catalyst hinges on whether the nucleophile or the electrophile is activated. For enamine catalysis, the nucleophile is activated *via* an initial iminium species. The enamine intermediate forms because of the increased C-H acidity in the iminium-enamine equilibrium.

Many amine catalysts proceed through the enamine catalysis mechanism.¹²⁴ Scheme 1.50 shows the mechanism in an enamine aldol reaction catalysed by proline or a proline derivative such as Jørgensen's catalysts (Schemes 1.48 and 1.49). This mechanism is the same with small variances for all enamine-route catalyses. The first step is formation of the enamine **B** through nucleophilic attack from the amine **A** to the carbonyl carbon. This step proceeds *via* an iminium intermediate **C** but here, the next step proceeds *via* the enamine species. The nitrogen lone pair reforms the C=N double bond **D** and the enamine double bond acts as the nucleophile to attack the electrophilic atom. In the aldol reaction, this is the carbonyl carbon; in the Michael addition, this is the 4-position. The resultant iminium species is hydrolysed to form the product **E** and the regenerated amine catalyst **A**.

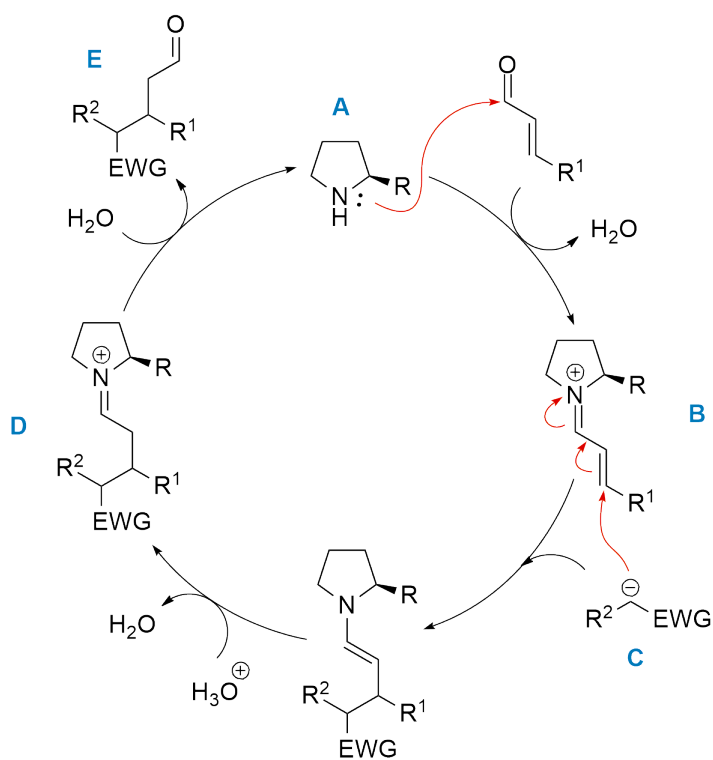
1.3.3 Iminium catalysis

In iminium catalysis, the electrophile is activated. As shown in Scheme 1.51 the first step is the same and the amine catalyst **A** will form an iminium species **B** with the carbonyl group. This charged species increases the electrophilicity of the carbon atom. The nucleophile **C** attacks the electrophilic carbon, which has been activated by the iminium formation. Hydrolysis of the iminium intermediate **D** allows formation of the product and catalyst regeneration.^{125,126}

Michael addition is shown in the iminium catalysis exemplar. It is an important reaction catalysed by many chiral amines and may undergo either enamine or iminium catalysis depending on the reagents. The iminium route prevails when the Michael acceptor (the α,β -unsaturated substrate) is an enal as opposed to a nitrile or nitro, for instance.



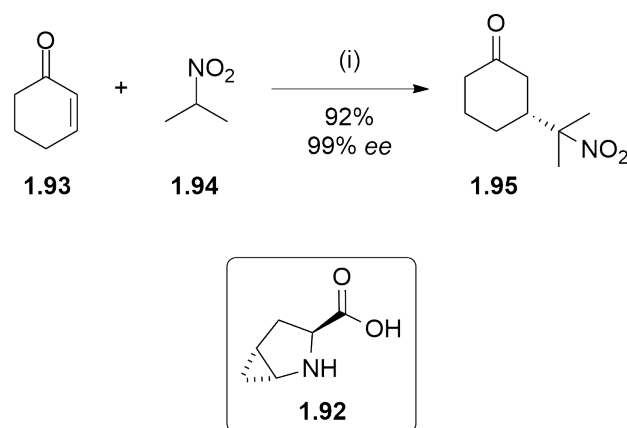
SCHEME 1.50: Enamine-type mechanism of organocatalytic reactions.



SCHEME 1.51: Iminium-type mechanism of organocatalytic reactions.
EWG = electron-withdrawing group.

1.3.5 *Trans*-4,5-methano-L-proline in iminium mechanism of catalysis

Hanessian and coworkers found *trans*-4,5-methano-L-proline (**1.92**) was a more stereoselective catalyst in conjugate addition of symmetrical nitroalkanes to 2-cycloalkenones than L-proline.¹²⁶ In the addition of 2-nitropropane **1.94** to 2-cyclohexenone **1.93**, *trans*-4,5-methano-L-proline gave **1.95** with a yield of 92% with 99% *ee*, while using L-proline as a catalyst gave 83% yields with 89% *ee* under the same conditions (Scheme 1.54). Here, the catalysis mechanism is the iminium route (Scheme 1.51). The base additive, *trans*-2,5-dimethylpiperazine, forms a salt with 2-nitropropane. 2-Cyclohexenone forms the iminium species with the catalyst's amine. The piperazinium nitronate anion adds to the activated iminium species selectively in an *anti*-configuration with respect to the carboxylic acid group of the catalyst, giving the *R*-form of the product. It is unclear why the bicyclic catalyst is superior to proline but it is thought that the extra rigidity improves selectivity.



SCHEME 1.54: *Trans*-4,5-methano-L-proline-catalysed addition of 2-nitropropane to 2-cyclohexenone. i) 10 mol % **1.92**, *trans*-2,5-dimethylpiperazine.

Peptide catalysts are capable of performing all of the above and more. Some examples will be discussed in the next section.

1.4 Peptide organocatalysis

It has been established that asymmetric organocatalysis is a broad and growing area of research. Since the work presented in this thesis is focused on peptide catalysts,

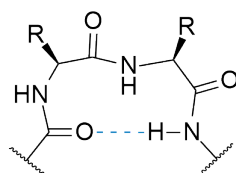
the scope and function of peptide organocatalysts will be explored here in more detail.

Proteins perform a wealth of functions in living systems. They can be molecular transporters, structural support, intra- and extra-cellular communicators, and catalysts. All these functions, and many more besides, are carried out by combinations of the same twenty or so natural amino acids. That Nature gets such variety of function from such a small number of building blocks is a result of how they are linked together and then the shape these macromolecules adopt. There is a strong structure-function relationship in biological polymers.

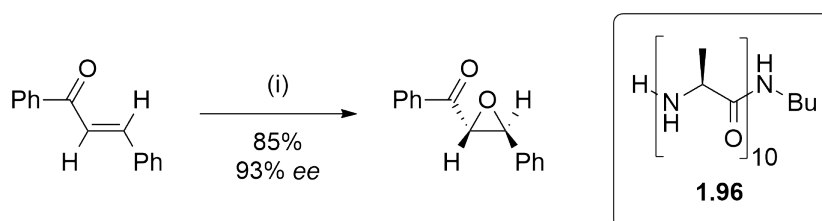
A protein is a polymeric macromolecule that comprises a linear chain of amino acids linked through amide bonds, which are specifically called peptide bonds when referring to the amide linkage between two amino acids. This is the primary structure. Local areas of shape and specific conformations arise due to weak intramolecular and intermolecular interactions, particularly hydrogen bonding between C=O and N-H groups on the peptide backbone. The conformation of a protein's peptide chain is a vital component of its function. This is the secondary structure. Further levels of protein structure are: tertiary structure, which is the three dimensional shape of a protein, stabilised mainly by hydrophobic interactions, and ionic bonds, hydrogen bonds, and disulfide bridges between the R groups of the amino acid residues; and quaternary structure, stabilised in much the same way as tertiary structure, with interactions between two separate peptide strands. These levels of protein structure are less relevant to this project which deals only with short peptides.

The conformation of a protein's peptide chain is a vital component of its function. Many secondary structural motifs exist but a common conformational motif found in proteins, and in the active sites of many enzymes, is the β -turn (Fig. 1.55). The β -turn is a sharp four-residue hairpin shape in the chain, stabilised by hydrogen bonds, which induces a change in direction of the peptide strand.

Enzymes were discovered to be proteins in the early 1900s and early examples of synthetic peptide catalysts were published in the 1980s: for example, Juliá *et al.*'s

FIGURE 1.55: Hydrogen bonding in a β -turn.

polyalanine **1.96** and polyglutamates (Scheme 1.56).¹³³ The study of enzymes catalysis was more popular, with examples such as pig liver esterase being very useful, and is an ongoing area of compelling research.^{134–138} Research activity on peptide organocatalysis was specialised to a small number of groups until the explosion of interest in asymmetric organocatalysis and, in particular, the discovery of proline as an efficient asymmetric catalyst with diverse applications.



SCHEME 1.56: Juliá *et al.*'s pioneering polyalanine peptide for asymmetric catalytic epoxidation of chalcone. (i) 80 mol % **1.96**, H_2O_2 , NaOH.

Enzymes are proteins that catalyse the reactions of an organism's metabolism - often asymmetrically and with site specificity, as well as excellent efficiency. It follows, then, to seek to mimic the structures and functions of enzymes to produce catalysts capable of performing with high yield and enantioselectivity. Enzymes themselves can be difficult to work with, being sensitive to the reaction environment and difficult to obtain and purify in high yield. Their specificity, an advantage in nature, can be a limitation to a chemist, as only a limited number of substrates can be used. Further, the complexity of an enzyme means that producing its mirror image, allowing synthesis of either enantiomer of the product, is challenging. Proteins are often too long or too sensitive to be practical; single amino acids by themselves are too limited: peptides strike a happy medium. Short peptides, or *oligopeptides*, are relatively easy to synthesise by established peptide synthesis protocols. Accordingly, synthetic peptide sequences have seen increasing use in asymmetric catalysis.

1.4.1 Miller's peptide organocatalysts

Undoubtedly the leader in this field is Miller and coworkers. Their studies on peptide-based asymmetric catalysts have opened the doors for the outpouring of new peptide catalysts being discovered, and has covered numerous transformations including acyl transfer among many others.⁴⁰

Early studies modified common physiological processes. A prime example is the development of acyl transfer catalysts that mimic many metabolic reactions and were modified to allow the desymmetrisation or kinetic resolution of alcohols. Desymmetrisation alters a symmetrical compound to remove a symmetry element, such as mono-acylation of a pro-chiral alcohol, to give one enantiomer of the product.¹³⁹ This is useful when done stereoselectively.

Miller's work started with tripeptides containing modified histidine residues, and found that increasing length of the peptide chain up to 8 amino acid residues created catalysts with well-defined shape due to intramolecular hydrogen bonding.⁴⁰ This increases the stereoselectivity of the catalyst. Octapeptides that mimic the β -hairpin turn (Fig. 1.57) motif also exhibit greater selectivities than those which do not.

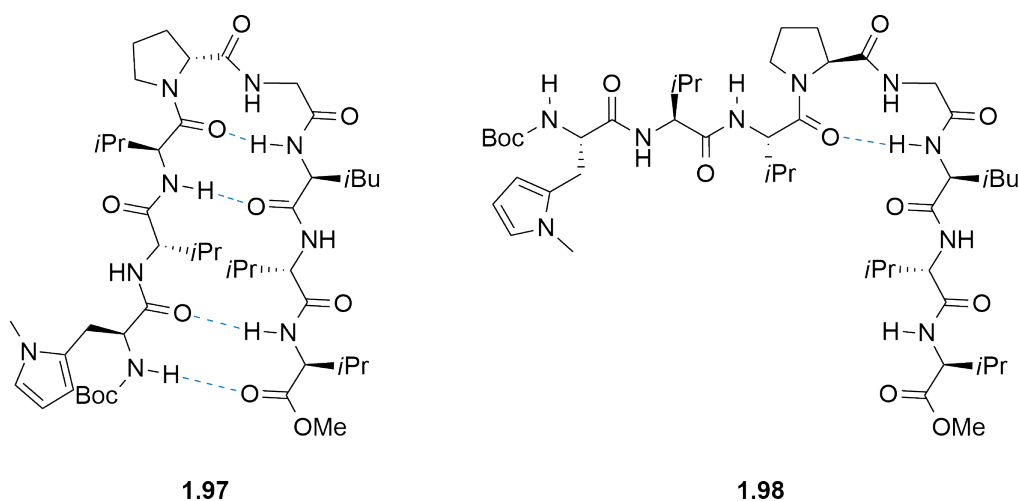
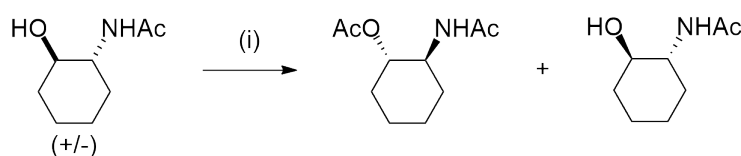


FIGURE 1.57: Miller's octapeptides for asymmetric acylation; **1.97** exhibiting β -hairpin turn; **1.98** does not have the β turn.

Compounds **1.97** and **1.98** differ only in the chirality at the proline residue. In **1.97** the D-proline residue, which forces the twist with its 5-membered ring and disrupts

hydrogen bonding, is integral in the formation of the β -hairpin conformation. Compound **1.98** is identical to **1.97** except for the inclusion of L-proline instead of D-proline, and is less rigid and does not exhibit the β -turn conformation; its substrate selectivity is lower and performs the kinetic resolution with lower stereoselectivity.

For the kinetic resolution of (\pm)-*N*-(2-hydroxycyclohexyl)acetamide (Scheme 1.58), turn-containing **1.97** had a k_{rel} of 51 with a conversion of 50%, which translates to an *ee* of approximately 90%; compared to non-turn-containing **1.98**'s k_{rel} of 7 with conversion of 46%. The imidazole of the π -methyl histidine residue captures the acetic anhydride; in the turn-containing **1.97**, hydrogen bonding between the peptide and oxygen and nitrogen of the substrate induce an enantiomer-specific transition-state hydrogen bonding interaction which accelerates the reaction rate of the (*R,R*)-enantiomer.



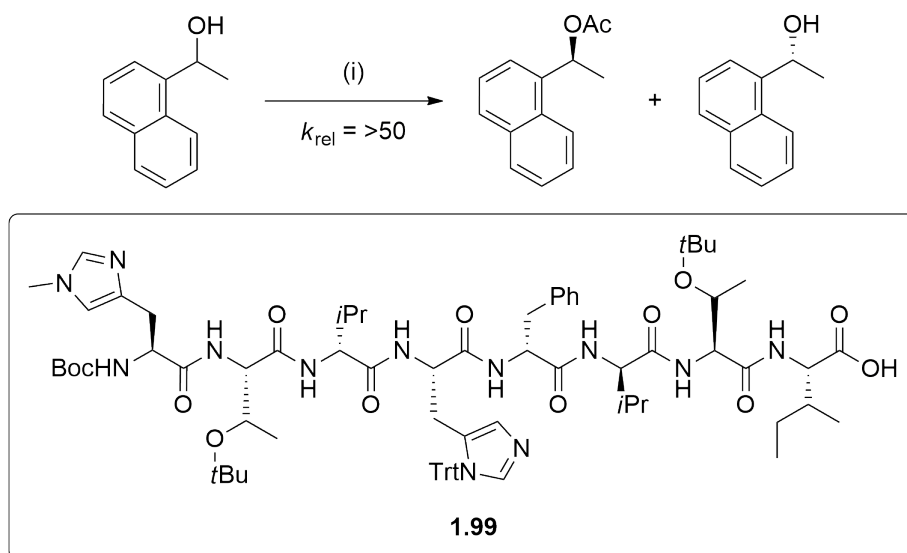
SCHEME 1.58: Asymmetric acylation of (\pm)-*N*-(2-hydroxycyclohexyl)acetamide. i) Ac_2O , 2 mol % **1.97** or **1.98**.

Using combinatorial chemistry and the inclusion of both L- and D-amino acids, further octapeptide sequences were prepared and screened in acylation resolution reactions.¹⁴⁰ While **1.97**, above, gave good selectivity with limited examples of amide-functionalised alcohols, the search was for a more general acylation catalyst. Iterative combinatorial peptide library preparation allowed synthesis of a large number of potential catalysts that could quickly be screened to find the candidates most likely to perform well as asymmetric catalysts.

Indeed, the best peptide, **1.99**, gave good k_{rel} for the kinetic resolution for a variety of racemic alcohols. Predictably, greater selectivity was observed for more sterically bulky substrates. The best example is shown in Scheme 1.59. The group performed structural and modelling analysis after the fact to determine reasons for this peptide sequence's good performance and found certain residues to be responsible for the lowered conformational variability thought to increase stereoselectivity. This example shows one benefit of using peptides as catalysts: their highly functionalised side

chains offer the possibility to tune regioselectivity and activity simply by altering an amino acid residue.

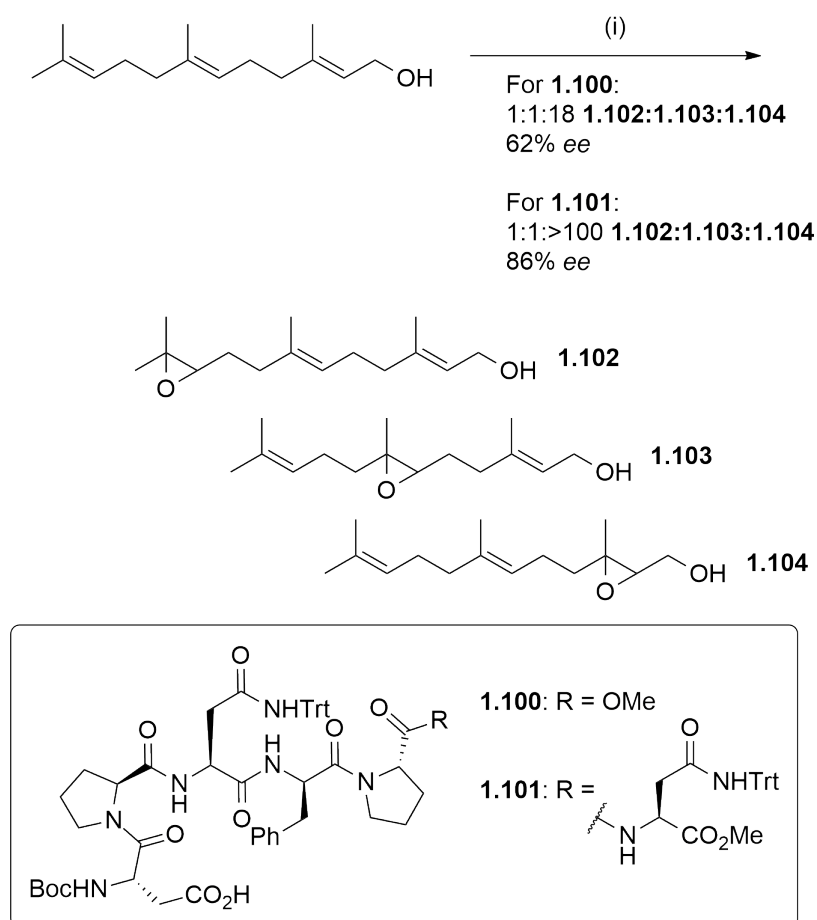
The N-terminal π -methyl histidine residue contains the imidazole nucleophile that activates the acyl reagent. The C-terminal isoleucine residue replaced residues with less sterically bulky R-groups in less selective catalysts; this suggests conformational proximity between the N- and C-terminus residues during the transition state. The fourth residue is a trityl histidine which is shared between the peptides with greatest activity; it is thought that π stacking with the aryl rings of the substrate enhances selectivity. The two *t*-butyl ethers provide hydrogen bonding donors for the substrate to position it.



SCHEME 1.59: Miller's peptide **1.99** in acylation for kinetic resolution of alcohols. i) 2.5 mol % **1.99**, Ac₂O.

Having found success mimicking nature, Miller began to investigate reactions that are rarer in nature or require metalloenzymes. One of these was regio- and stereoselective epoxidation of polyenes. For this transformation, Miller's peptides consisted of a peracid-derivatised aspartic acid residue as the catalytic moiety.¹⁴¹ Small alterations to the peptide structure were also found to be important for efficient epoxidation. Studying the effect of peptide length, a shortening from trityl-protected asparagine **1.101** to a methyl ester **1.100** (Scheme 1.60) produced a significant decrease in regioselectivity and stereospecificity. **1.100** produced **1.104** with 62% *ee* and 4.2:1 site specificity while **1.101** catalysed the reaction with *ee* of 86% and 13:1 site

specificity.



SCHEME 1.60: Epoxidation catalysed by Miller's peptide catalysts **1.100** and **1.101**. (i) 10 mol % peptide catalyst, 10 mol % HOBT, 10 mol % DMAP, DIC, H₂O₂.

This terminal region containing the trityl asparagine residue in **1.101** is involved in stabilising conformations of the peptide that increase both stereo- and regioselectivity. This is evidenced by the ¹H NMRs of the two peptides; **1.101** has sharper peaks indicating less conformational freedom. According to their model, the hydroxyl group of the substrate participates in hydrogen bonding that directs it to present the face of the bond that is epoxidised to the peracid-activated aspartic acid residue that carries out the epoxidation. Several possible hydrogen bonding sites are possible as suggested by ROESY NMR spectra which determines through-space interactions. One option is with with two backbone carbonyl oxygens; Henbest and others have shown that the hydroxyl group may interact solely with the peracid; or it may be a mixture of these two hydrogen bonding modes (Fig. 1.61).¹⁴²⁻¹⁴⁴

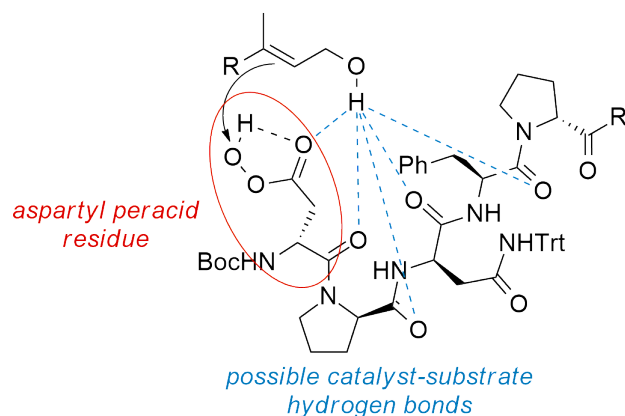
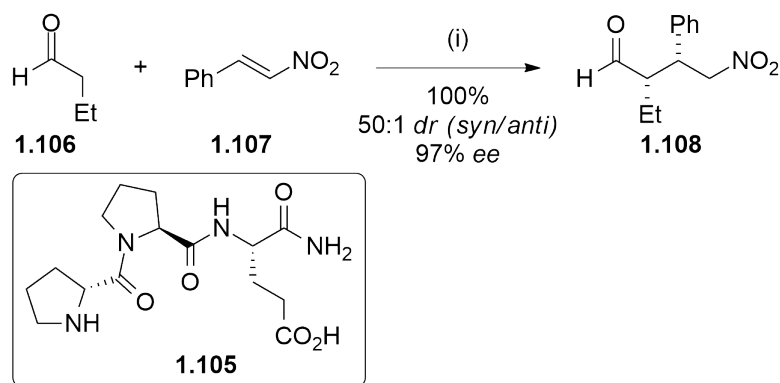


FIGURE 1.61: Possible intermolecular hydrogen bonding interactions stabilising transition state in epoxidation of polyenes.

1.4.2 Wennemers' peptide organocatalysts

Small peptides with the sequence Pro-Pro-Xaa-NH₂ (where Xaa is a generic acidic amino acid with various functionality and modification) have been used by Wennemers' group in asymmetric catalysis of Michael addition of aldehydes to nitroalkenes including demanding disubstituted nitrostryenes.¹⁴⁵ The sequence (D-Pro-Pro-Glu-NH₂) **1.105** was screened along with all its diastereomers and gave the best yield and stereoselectivity in Michael addition between butanal **1.106** and *trans*- β -nitrostyrene **1.107** (quantitative conversion, 50:1 *dr* (*syn/anti*), and 97% ee for (*S,R*)-**1.108**, Scheme 1.62).

Introduction of a fourth amino acid residue gave little increase in yield and no change in stereoselectivity.¹⁴⁶ More important was the conformation of the two proline residues, which due to their tertiary amide bond, force a turn-like structure.¹⁴⁷ In the ground state, the tripeptide has a hydrogen bond between the terminal proline residue's amine proton and the glutamic acid side chain's carboxylate oxygen. This induces the amide bonds of both proline residues to prefer the *cis* configuration that creates the turn-like structure. Formation of the enamine with the Michael donor substrate releases the carboxylic acid of the glutamic acid side chain from its hydrogen bond with the N-terminus proton; this carboxylic acid then serves as a proton donor for the incoming nitroalkene and guides the substrate to form the *syn* product.



SCHEME 1.62: Wennemers' tripeptide in asymmetric Michael addition of butanal to *trans*- β -nitrostyrene. i) 5 mol % **1.105**.

Iterative design changes in the catalysts optimised them to perform in aqueous conditions: here, addition of alkyl groups helps the catalyst mirror the hydrophobic environment of enzyme active sites.¹⁴⁸ Without this alteration, the tripeptide catalyst must be used in dry solvents since excess water interferes with reaction rate. The alkyl chain permitted the formation of an emulsion in aqueous solvent. Michael additions between aldehydes and nitroalkenes were performed with very good yield and chemoselectivity: the peptide catalysts favour the conjugate addition over the homo-aldol reaction. Peptide **1.109** (Fig. 1.63) gave >95% yield and 91% ee for the reaction above (Fig. 1.62).

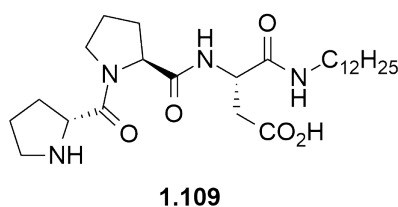


FIGURE 1.63: Wennemers' alkylated tripeptide catalyst **1.109**.

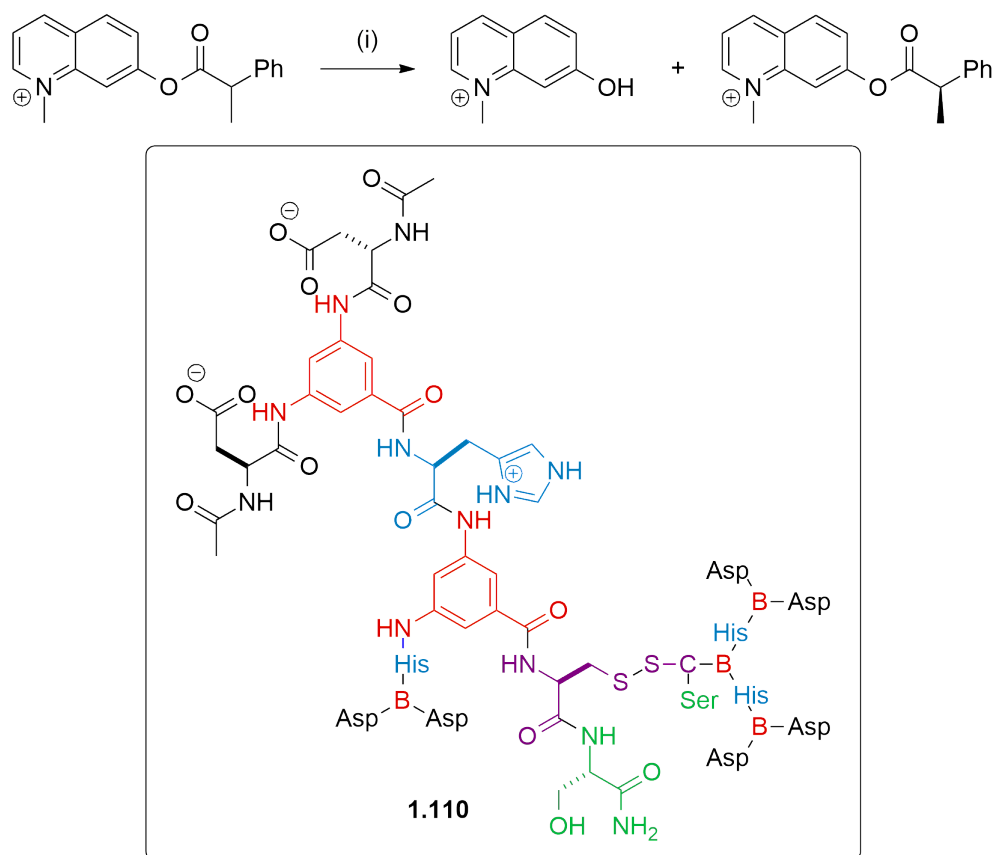
1.4.3 Reymond's aryl peptide dendrimers

Conformational stability of peptide catalysts has been shown to be important for catalyst selectivity and activity. Even small peptides contain numerous functional groups and their conformation is difficult to predict. In Miller's combinatorial libraries of peptides (above), only the conformation of the effective catalysts was determined. Knowing the conformation of a successful peptide, it would be interesting

to know if a structure with fixed shape could be introduced that would allow rational design of a peptide catalyst with inbuilt conformational rigidity that has similar catalytic power.

Reymond's group looked at constricting conformational freedom using 3,5-diaminobenzoic acid as a rigid backbone unit on which branching amino acid chains were coupled.¹⁴⁹ They used a combinatorial approach to build branched peptides, allowing the screening of a variety of similar peptides in an ester hydrolysis reaction (Scheme 1.64).¹⁵⁰

The peptide dendrimer shown (**1.110**) had good activity in the ester hydrolysis ($k_{\text{cat}}/k_{\text{uncat}} = 4,000$) and stereoselectivity (74% *ee*). The figure shows a simplified cartoon of the peptide dendrimer's structure; the two branches extending from the central 3,5-diaminobenzoic acid scaffold have the same structure and linkages, and the two halves of the dendrimer joined by the cysteine-cysteine disulfide bridge are identical.



SCHEME 1.64: Ester hydrolysis catalysed by Reymond's peptide dendrimers. (i) 10 mol % **1.110**, pH 6 buffer.

They found that catalytic activity increased when their peptide was built on a more rigid backbone. They hypothesised that rigidity inhibited folding, making the conformation more open and allowing the substrate to access the active site. This is another example of kinetic resolution and the mechanism involves two histidine side-chains, one acting as the nucleophile activating the acyl group; the other acts as a general base. The selectivity is mediated by electrostatic interactions between the aspartate anions presented on the surface of the peptide dendrimer and the quino-
lium cation. A decrease in selectivity is observed when a single amino acid residue is altered in the peptide, which suggests additional interactions within the peptide which influence stereoselectivity. Further studies or modelling would help elucidate exact interactions.

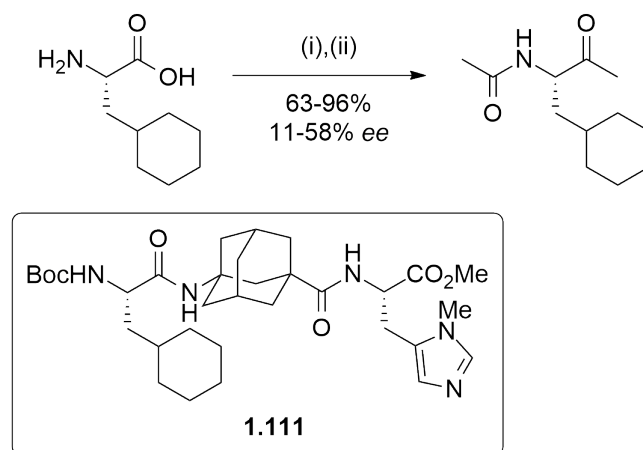
1.4.4 Schreiner's peptide organocatalysts

Schreiner's work with an adamantane-containing amino acid (*Aca*, see Section 1.2.4) is another example of the utility of a rigid backbone element in peptide catalysts. Schreiner's research has revealed that changing the amino acids attached to the central adamantane unit allows a broad scope of reactions to be promoted.^{151–153}

Dakin-West reaction

An *Aca*-containing peptide catalyst from Schreiner's group performed the first enantioselective Dakin-West reaction (Scheme 1.65).¹⁵¹ The Dakin-West reaction is often used for the conversion of an amino acid to a keto-amide. The catalyst **1.111** contains the methyl histidine residue common to all Schreiner's *Aca* catalysts with its imidazole side chain, as well as a cyclohexylalanine residue, which was important for forming the catalytic binding pocket to provide stereocontrol. The catalyst gives enantioselectivity with a range of aryl and alkyl substrates that is on par with other organocatalytic decarboxylative protonations, with moderate to good yields.

In the first step of the reaction mechanism (Scheme 1.66), the amino acid is *N*-acylated to give **1.112**, which then forms a mixed anhydride **1.113**, with two equivalents of the acetic anhydride. Cyclisation gives the oxazolone **1.114**, which is deprotonated to give the resonance-stabilised enolate **1.115**. The enolate oxygen is

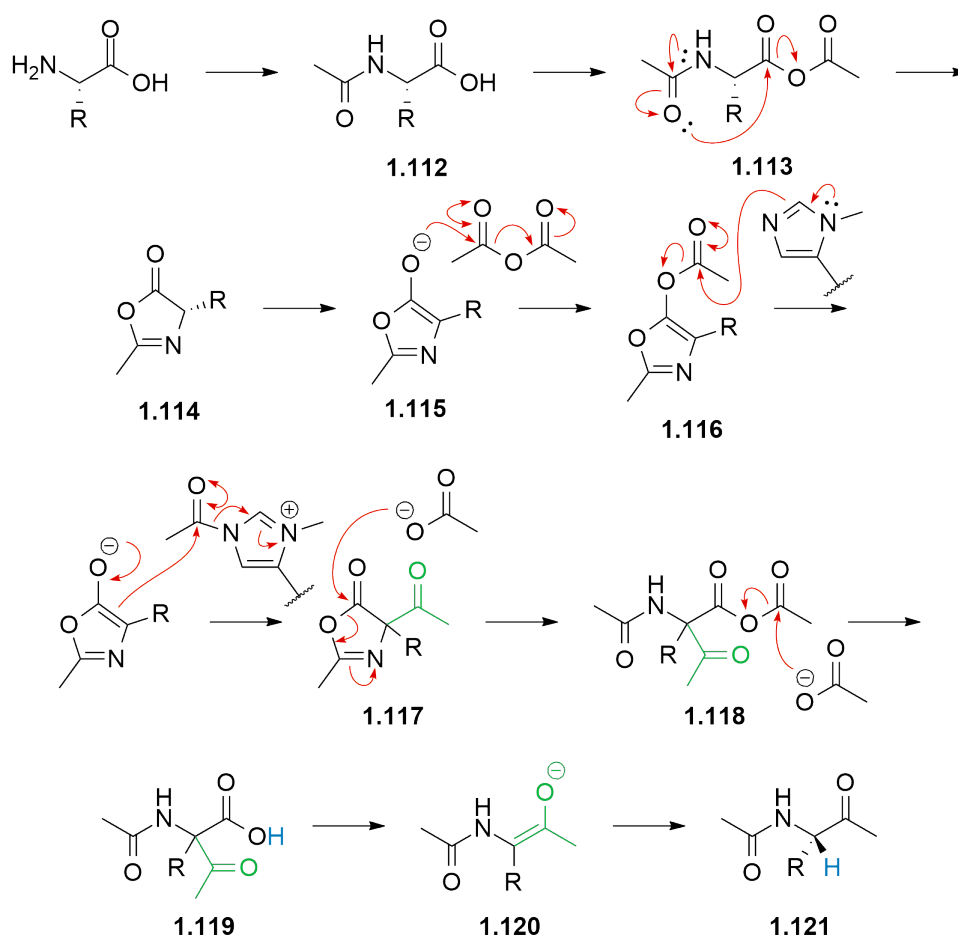


SCHEME 1.65: Enantioselective Dakin-West reaction catalysed by Schreiner's Aca-containing peptide **1.111**. i) 10 mol % **1.111**, DCC, Ac₂O. ii) AcOH. R = aryl, alkyl, H.

acetylated and this *O*-acyl species **1.116** undergoes Steglich esterification catalysed by **1.111** to give **1.117**. Acetic acid opens the oxazolone ring to give **1.118** and the transacylation of acetic acid gives the β -ketoacid **1.119**. Upon deprotonation by the methylimidazole group of **1.111**, **1.119** is decarboxylated, forming the enolate **1.120**, and then re protonated to give the methylketo-acetamide **1.121**.

The catalyst is proposed to be active at two points in the reaction mechanism.¹⁵⁴ The methyl histidine acts as a Lewis base for the acetyl transfer on **1.116**, and as a Brønsted base in the final protonation. The reaction is usually non-stereoselective, giving the product as a racemate because of intermediates **1.115** and **1.120**. The methylimidazole moiety by itself is not basic enough to deprotonate the oxazolone **1.114**, and using an external base in the reaction reduces enantioselectivity of the final step. DCC was used as an additive because it furnishes the cyclised oxazolone with a good reaction rate, and assists in the subsequent deprotonation. Since its side product, dicyclohexylurea (discussed in Section 3.3.3), does not act as a base, it did not interfere with the final protonation step's enantioselectivity.

The adamantane catalyst performed the final protonation of **1.120** enantioselectively, affording the enantioenriched product **1.121**. The *S*-product is favoured due attractive interactions between the catalyst and substrate during the final deprotonation, decarboxylation and the ensuing stereoselective protonation. Hydrogen bonding interactions between the substrate's amide proton and the catalyst's cyclohexylalanine



SCHEME 1.66: Mechanism of the Dakin-West reaction.

residue's carbonyl oxygen, and the enolate oxygen of the substrate binding with the amide proton of cyclohexylalanine residue, bring the α -carbon close to the protonated imidazole of the π -methyl histidine (Fig. 1.67). This proximity and additional dispersive interactions between the cyclohexyl rings on the substrate and catalyst lead to preferential protonation from one face to give the *S*-product.

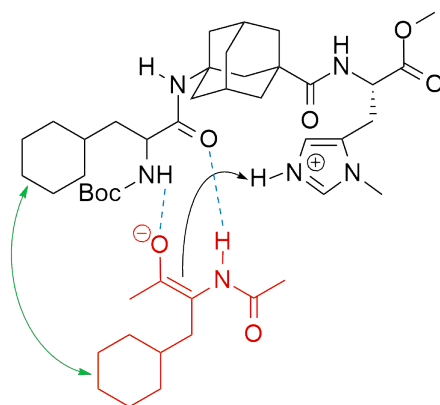


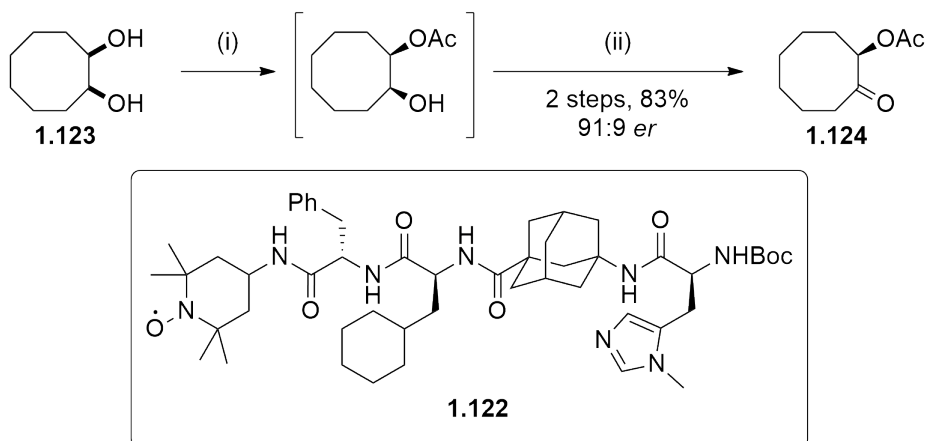
FIGURE 1.67: Stabilising interactions in the transition state of organocatalysed Dakin-West reaction.

Peptide multicatalysts

Multicatalysts are molecules that contain several active sites within one catalyst. They differ from molecules such as bifunctional catalysts in that their sites act independently of each other. By allowing the catalysis of multiple reactions in a single vessel they permit complexity to be built quickly. Peptides are suited to this because it is easy to add discrete functionality and then separate these groups along the peptide chain. Schreiner's Aca-containing peptides are particularly appropriate for this purpose due to the functional group separation introduced by the adamantane scaffold.

An example of Schreiner's multicatalysts combined two known catalytic groups on a constrained peptide backbone: multicatalyst **1.122** combines (2,2,6,6-tetramethylpiperidin-1-yl)oxyl (TEMPO) for oxidation of aldehydes; and a π -methyl histidine to promote acyl transfer (Scheme 1.68). Compound **1.122** is added in the first step of the one-pot reaction and catalyses reactions in both steps. First it desymmetrises the *meso*-diol **1.123** by selectively acylating one hydroxyl group, then oxidises the remaining alcohol to form the aldehyde **1.124** and prevent intramolecular acyl shift.⁹⁸

As per the previous discussion of kinetic resolution (Section 1.4.1), the importance of removing the unreacted enantiomer is obvious; the prevention of intramolecular acyl shift ensures the selectivity of the desymmetrisation is not wasted by racemisation after the fact. The best yield and stereoselectivity was found for *cis*-cyclooctane-1,2-diol **1.123**, as smaller products suffered from a fast-acting Baeyer-Villiger oxidation with *m*-CPBA.



SCHEME 1.68: One-pot desymmetrisation and oxidation of **1.123** by Schreiner's peptide catalyst **1.122**. i) 5 mol % **1.122**, Ac₂O. ii) Bu₄NBr, *m*CPBA.

Expanding on Miller's work with oligopeptides in kinetic resolution of chiral alcohols, their inclusion of an Aca residue solved several problems. The bulky hydrocarbon group prevented the peptide self-associating, increased its affinity for organic solvents, and promoted hydrophobic interactions in the transition state (Figure 1.69).⁹⁷ The cyclohexyl amino acid's side chain increases lipophilicity, which had previously been shown to increase selectivity of the catalyst.⁸⁹ Molecular modelling sought to explain the role of adamantane in the catalyst's increased efficiency: it was predicted that adamantane held an important C=O group in correct conformation for hydrogen bonding with the cyclic diol. The carbonyl group acted as a hydrogen bond acceptor and was important for stereoselective receipt of the substrate. Additionally, London dispersion forces (hydrophobic interactions) between the acyl adduct and the cyclohexyl side chain stabilised the catalytic pocket formed upon association of the diol.

By varying the order reagents are added to the reaction, the above histidine-TEMPO multicatalyst **1.122** could be made to facilitate an even more efficient variant of this

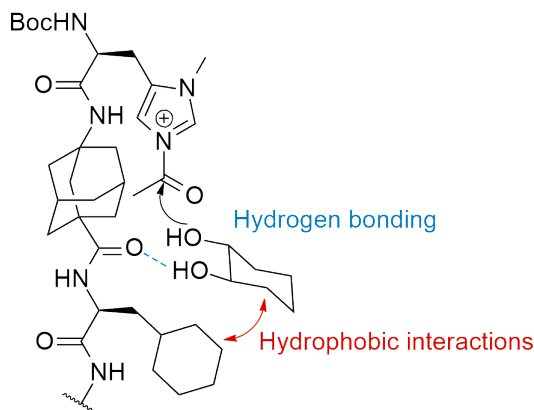
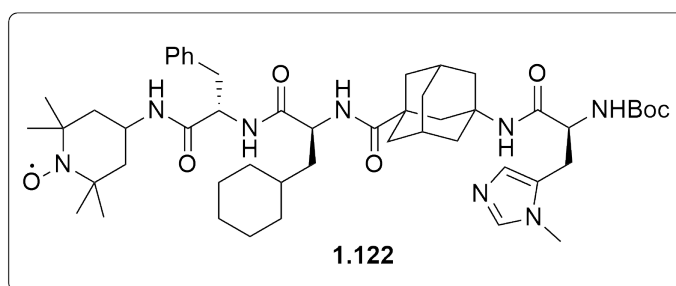
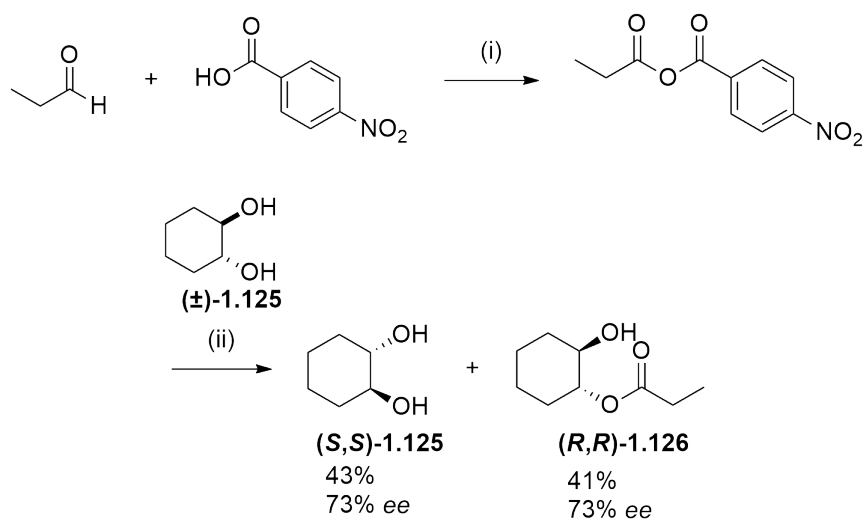


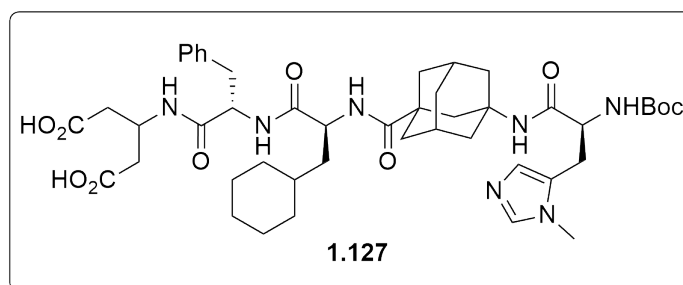
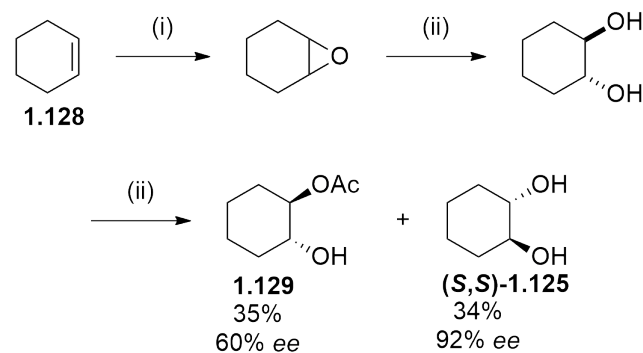
FIGURE 1.69: Predicted catalytic binding pocket of Schreiner's peptide **1.122** in acyl transfer.

transformation. The order of each reaction was reversed so that the catalyst oxidised an aldehyde and which formed an anhydride *in situ*. This anhydride participated in the enantioselective acylation reaction. This one-pot oxidative esterification allowed the kinetic resolution and the resolution of *meso* diols; additionally it represented an alternative route to ester formation.¹⁵⁵ The combined multicatalyst gave the same products as the two catalysts individually, with only slightly lower ee. Shown in Scheme 1.70, the reactions catalysed by the π -methyl histidine-containing peptide (step i) and TEMPO (step ii) separately gave **1.125** (46%, 81% ee) and **1.126** (43%, 88% ee); catalysed by **1.122** (added in step i) gave **1.125** (43%, 73% ee) and **1.126** (41%, 73% ee) in a one-pot reaction.

Schreiner's research with these multicatalysts has shown that they are amenable to other kinetic resolutions simply by altering the amino acid residue added to the central adamantane core. By adding a dicarboxylic acid, in addition to the histidine residue, a multicatalyst that promoted alkene epoxidation followed by ring opening then the familiar acyl transfer could be created. Cyclohexene **1.128** was first epoxidised, reacted and resolved, to give (*R,R'*)-**1.129** with 35% yield and 60% ee and (*S,S'*)-**1.125** with 34% yield and 92% ee (Scheme 1.71).^{43,44} Other alkenes gave similar yields and selectivities. This is a remarkable reaction considering three separate reactions are promoted by the same catalyst.



SCHEME 1.70: Schreiner's multicatalyst **1.122** employed in kinetic resolution of diol **1.125** with oxidative esterification. i) 5 mol % **1.122**, pyridine, *t*-BuOCl, ii) rac-**1.125**, DIPEA.



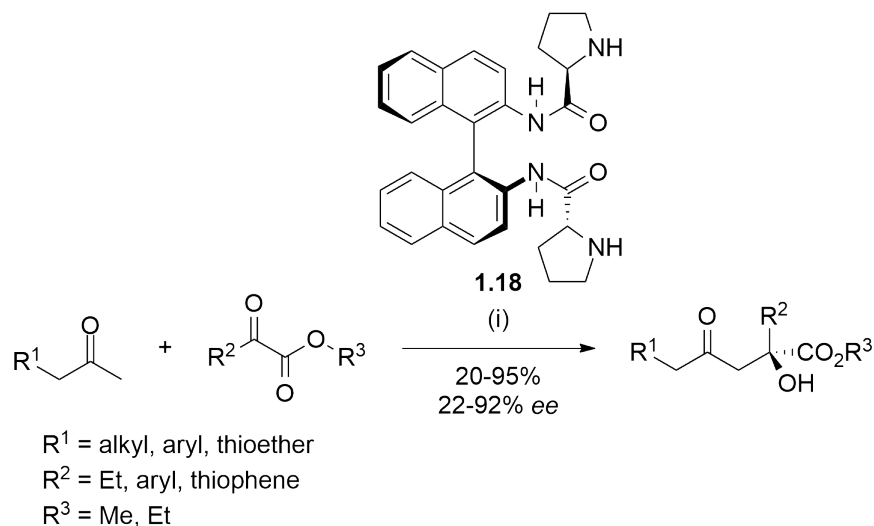
SCHEME 1.71: Schreiner's dicarboxylic acid/histidine peptide catalyst in epoxidation and enantioselective acyl transfer. i) 5 mol % **1.127**, H_2O_2 , DIC; ii) H_2O , $N_2H_4 \cdot H_2SO_4$; iii) Ac_2O , DIPEA.

1.4.5 Prolinamide BINAM derivative organocatalyst

A more well-known motif is the binaphthyl backbone found in many ligands and catalysts. Nájera has used (*S*_a)-1,1'-binaphthyl-2,2'-diamine (BINAM) as a rigid backbone that constrains the conformation of the resulting peptide.^{156,157} Proline-functionalised BINAM **1.18** was used to promote the aldol reaction.³⁸ The sterically-hindered BINAM introduced axial chirality into the molecule and allowed stereochemical control of the alcohol product. Here, the backbone is not an amino acid, but a diamine, with both proline residues coupled through their carboxylic acids. It is included in the review as an interesting example of an organocatalyst that harnesses the catalytic power of amino acid residues. Proline is a popular catalytic moiety for aldol condensation; it was combined with BINAM, which is a scaffold that provides rigidity and steric bulk, as well as a chiral platform that the substituents can be arranged about.

In one example of the aldol reaction (Scheme 1.72), acetone was used as the nucleophile ($R^1 = H$) and 2-phenyl-2-oxoacetate ($R^2 = Ph$, $R^3 = Me$) as the aldol acceptor, or electrophile. When (*S*_a)-BINAM-L-prolinamide was the catalyst, the yield was >90% and the chiral tertiary alcohol had 15-32% ee of the *R* isomer; (*S*_a)-BINAM-D-prolinamide produced >90% yields of the *S* isomer with 55-60% ee. A range of other alkyl and aryl derivatives was tolerated in the reaction, giving the desired products with good yield and enantioselectivities: up to 95% and 92% ee. Some more challenging derivatives with $R^1 = CH_2Cl$ or CH_2SCH_3 gave lower yields of 60% and 20%, respectively; these substrates are less reactive nucleophiles. An alkyl β -ketoester ($R^2 = Et$) reacted with lower enantioselectivity; possibly due to lower difference in steric hindrance between the *Re* and *Si* intermediates because of the less bulky ethyl group. The diastereomers of the catalyst gave different results. From molecular modelling calculations, it appears that the amino acid controls enantioselectivity while BINAM improves arrangement of the substrates. The axial chirality introduces a spatial arrangement that favoured formation of the *S* isomer's transition state due to steric hindrance between the substrate and the binaphthyl portion of the catalyst.

The above examples of asymmetric peptide organocatalysts show the importance of



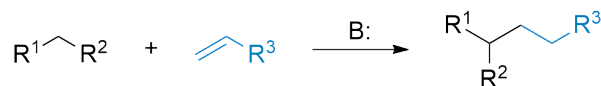
SCHEME 1.72: Nájera's BINAM prolinamide catalyst in aldol reactions between ketones and β -ketoesters. i) 20 mol % **1.18**, $\text{ClCH}_2\text{CO}_2\text{H}$.

structural or conformational restriction (or both) on catalyst performance and stereoselectivity, regardless of the type of reaction. Merely a brief overview of the possibilities afforded by peptide catalysts has been given. The rapidly growing field of peptide organocatalysis has developed broad avenues into a variety of useful reactions. The array of functionality and well-established chemistry for peptide synthesis makes it an attractive field for further study.

1.5 Michael addition

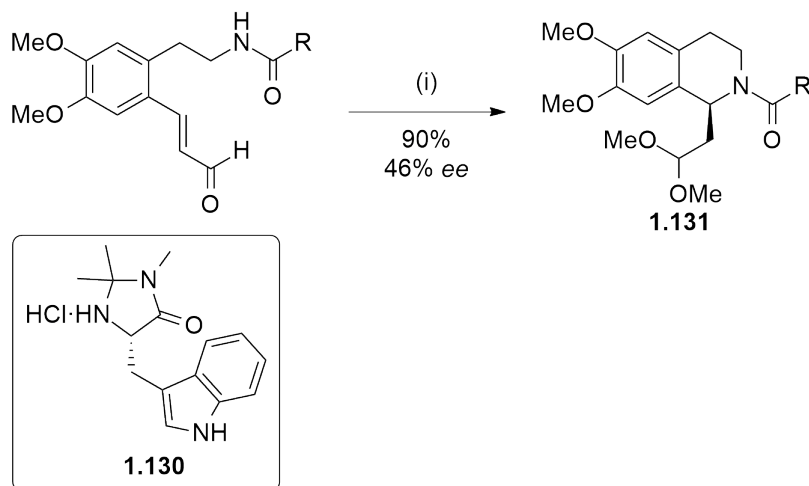
The Michael addition is a generic term that now refers to the nucleophilic addition of methylene nucleophile to an activated α,β -unsaturated compound, which has been widely used as a source of C-C bond formation (Scheme 1.73). It is another term for conjugate addition. Depending on the substrates and catalysts used the Michael addition may be used for the stereoselective introduction of chiral centres. For the research discussed in this work, a control experiment was required to test our new catalysts. Michael addition was chosen because it has been well studied, and would allow us to gain insight into catalyst behaviour and alter reaction conditions with known variables.

The Michael addition was first described by Arthur Michael in the late 19th century



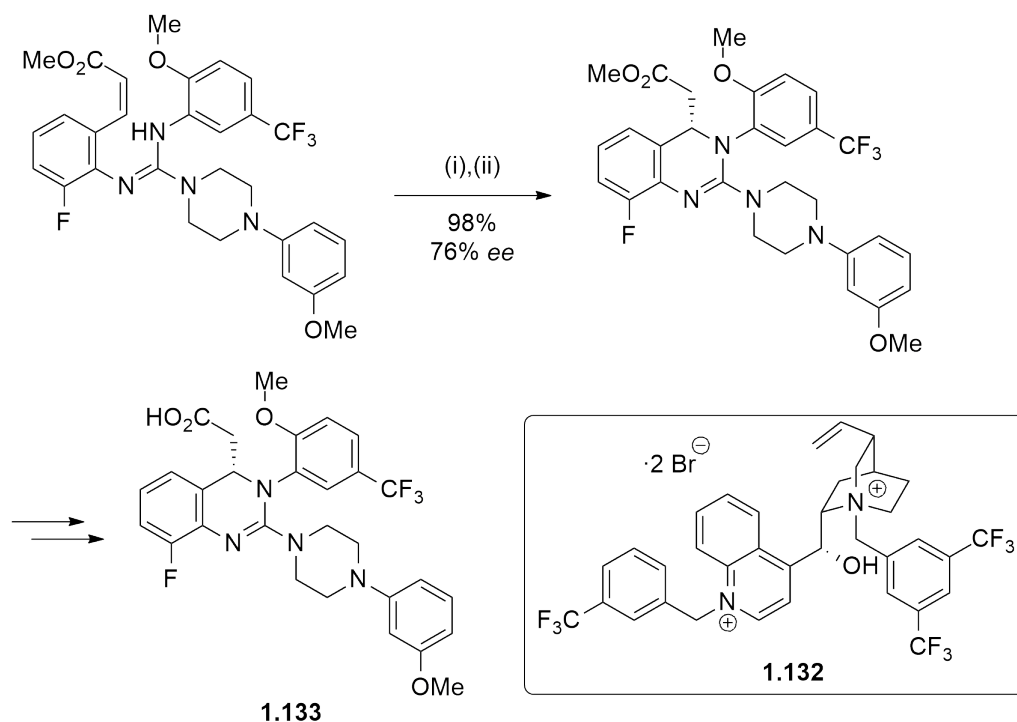
SCHEME 1.73: Generic Michael addition. R^1 and/or R^2 are electron-withdrawing groups. The base B: abstracts a proton from the methylene hydrogen. R^3 is an electron-withdrawing group that causes resonance stabilisation such as a carbonyl, nitrile, sulfone or nitro group, activating the alkene.

as the addition of the enolate of an aldehyde or ketone to the β carbon of an α,β -unsaturated carbonyl compound. Since then, the definition of the Michael reaction has broadened from its original specification to include unsaturated compounds that contain other electron-withdrawing groups, such as nitriles and nitro groups like *trans*- β -nitrostyrene (Section 1.3, Scheme 1.62); and also any 1,4-addition to an α,β -unsaturated carbonyl compound, rather than only aldehydes; for instance the aza-Michael reaction refers to the addition of a nitrogen nucleophile (Schemes 1.74 & 1.75); and thia-Michael addition involves addition of sulfur to the Michael acceptor (Scheme 1.76).^{158–161}



SCHEME 1.74: Takasu *et al.*'s aza-Michael addition to form tetrahydroisoquinoline **1.131** with asymmetric organocatalyst **1.130**. i) 20 mol % **1.130**, MeOH.

An example of an intramolecular aza-Michael reaction is the asymmetric organocatalytic synthesis of tetrahydroisoquinoline **1.131** by Takasu *et al.*¹⁵⁸ This reaction was completed in "green" conditions, with only the organocatalyst required as reagent and methanol and water as solvents. The opposite enantiomer of the product was produced by changing the two 2-methyl groups of the catalyst for a *t*-butyl substituent.

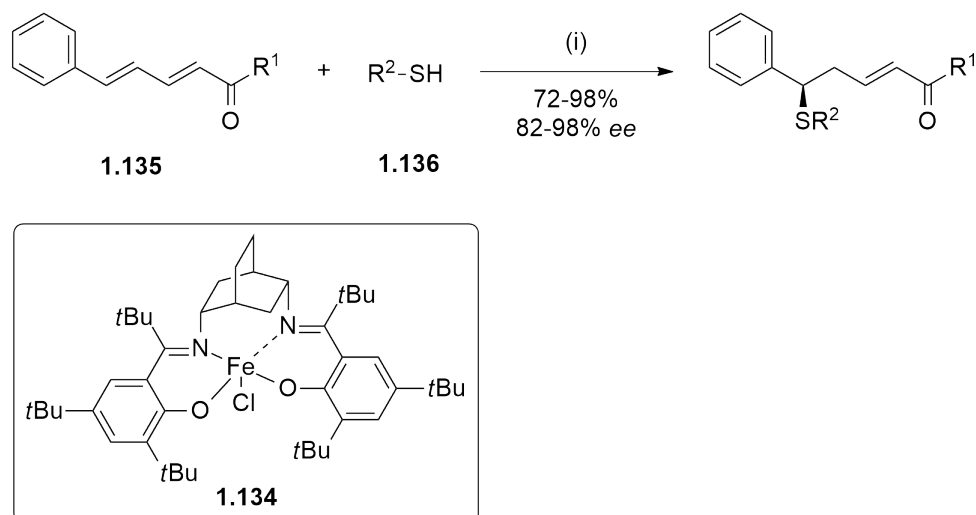


SCHEME 1.75: Phase-transfer-catalysed asymmetric aza-Michael addition in synthesis of Letemovir **1.133**. i) K_3PO_4 ; ii) 5 mol % **1.132**, K_3PO_4 .

Similar reactions can be catalysed by many different catalysts. The next is an example of phase transfer catalysis in an aza-Michael addition in the synthesis of Letemovir (**1.133**, Scheme 1.75). In this reaction, toluene was used in place of alcoholic solvents to suppress background cyclisation of the guanidine, which is catalysed by Brønsted acids. The phase transfer catalyst **1.132** benefited from the inclusion of electron-deficient $-\text{CF}_3$ groups which increased performance; $>99\%$ *ee* was achieved by recrystallisation of **1.133** as the di-*p*-toluoyl-(*S,S*)-tartaric acid salt.

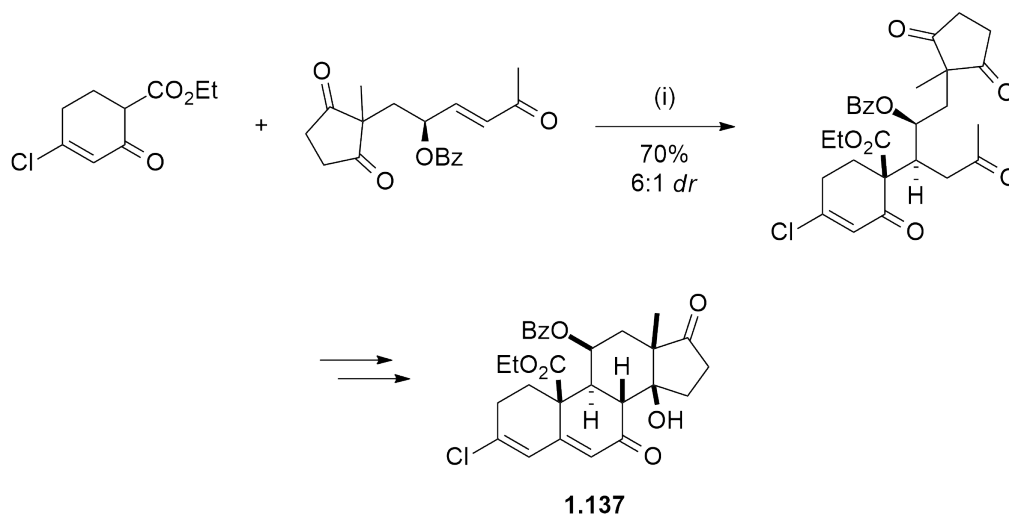
An example of thia-Michael addition is the addition of thiol **1.136** to conjugated carbonyl compounds **1.135** catalysed by iron(III)-salen complex **1.134** (Scheme 1.76). Regioselectivity for δ -addition over β -addition was enhanced by adding sterically bulky groups at the iminyl carbons.

Michael additions are useful for synthetic chemistry since they are a gentle approach to forming C-C bonds with β -functionalisation while controlling both regio- and stereoselectivity. The Michael addition has been used for, for example, stereoselective installation of cyclic aldehydes in the total synthesis of the cardiotonic steroid precursor cardenolide **1.137**, with the catalyst $\text{Cu}(\text{OTf})_2$ providing stereochemical



SCHEME 1.76: Iron(III)-salen complex catalyzed asymmetric and regioselective thia-Michael addition. i) 10 mol % **1.134**, AgBF_4 .

control of the addition (Scheme 1.77).¹⁶²



SCHEME 1.77: Michael addition in enantioselective synthesis of steroid precursor cardenolide **1.137**. i) 50 mol % $\text{Cu}(\text{OTf})_2$.

Nagorny and coworkers suggested $\text{Cu}(\text{OTf})_2$ induced formation of the major diastereomer *via* the transition state shown in Figure 1.78. The incoming nucleophile attacks from the face which causes the least allylic strain, with the benzoyl group facing away.

Another example of Michael addition used in natural product synthesis is in the formation of key intermediate **1.139** in the synthesis of lycoposerramine-Z **1.140** by intramolecular Michael addition.¹⁶³ Lycoposerramine-Z is an alkaloid, isolated from club mosses in the *Lycopodium* family, with possible acetylcholinesterase-inhibitory

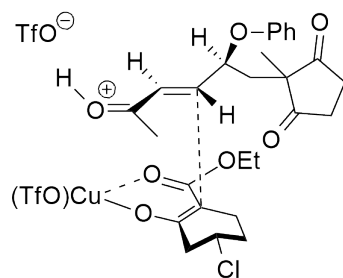


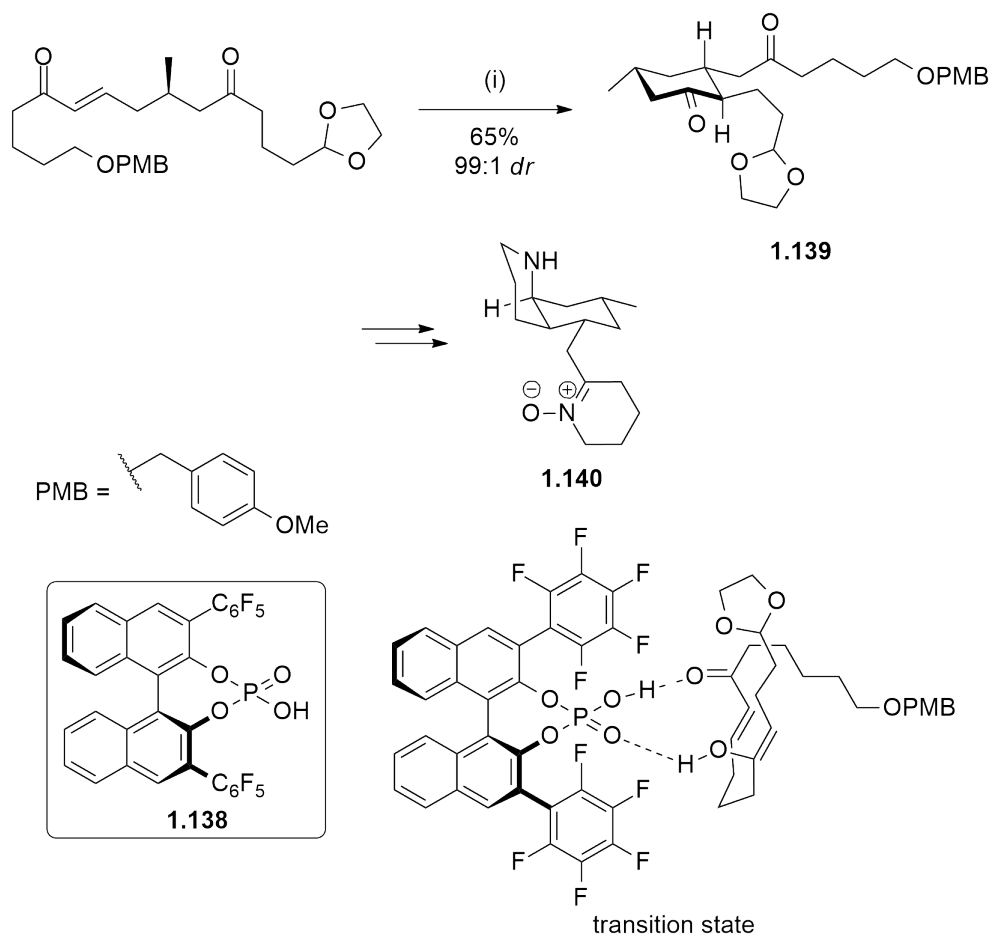
FIGURE 1.78: $\text{Cu}(\text{OTf})_2$ as asymmetric catalyst in Michael addition in synthesis of **1.137**.

activity for treatment of Alzheimer's disease. The BINOL-phosphoric acid **1.138** catalysed the Michael addition with good enantioselectivity (Scheme 1.79, 65% yield, >99:1 dr).

Metal complexes such as copper triflate (Scheme 1.77) and complexes of many other transition metals including aluminium, manganese, nickel, and scandium were developed in stereoselective syntheses.^{164–169} In contrast, organocatalysts offer the advantage of being able to be used in the presence of water, instead of under anhydrous conditions, as is the case for most metal complexes. In some cases the presence of water can even enhance yield or stereoselectivity.¹⁷⁰ Due to the utility of the Michael addition in synthesis, there is still demand for new catalysts that improve either yield, selectivity, functional group tolerance, substrate applicability, have milder or greener reaction conditions, or a combination of any or all of the above.

While organocatalysts such as the phosphoric acid shown in Scheme 1.79 are also used, most organocatalysis of Michael additions usually involve an amine catalyst. Amine catalysis occurs in one of two main mechanisms that start with creation of a covalent bond between the amine nitrogen of the catalyst and one of the substrates: enamine activation and iminium activation, depending on whether the nucleophile or electrophile is activated. Examples of both mechanisms are presented in Section 1.3.

Peptides feature heavily in the literature on asymmetric organocatalysis of Michael additions. Proline-derived catalysts, including proline itself are also good Michael



SCHEME 1.79: Asymmetric intramolecular Michael addition in the synthesis of lycoposerramine-Z with chiral phosphoric acid 1.138. i) 20 mol % 1.138.

addition catalysts. Wennemers' oligopeptide catalysts (see Section 1.4.2) are excellent catalysts of Michael addition between alkyl aldehydes and β -nitrostyrene, giving good yield and selectivity. The suggested mechanism of stereoselectivity in these cases is hydrogen bonding between the enamine catalyst/Michael donor and the nitrate of the Michael acceptor holding the transition state in conformation such that the addition of the Michael donor and the loss of proton occur syn to each other.

1.6 Conclusion

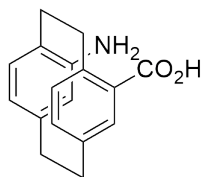
Examples discussed in this chapter illustrate just a small fraction of the utility of peptides in asymmetric organocatalysis. The orientation of active groups in a catalyst plainly impacts its stereoselectivity. [2.2]Paracyclophane offers a convenient scaffold for arranging chemical moieties in 3D space. Therefore, the aim of this project was to investigate new planar chiral amino acids incorporated into peptides, where we could control the placement of substituents in space and determine if altering the active moieties' position and distance relative to each other affected the catalyst's stereoselectivity.

The three chapters to follow each discuss one of the aims of the project:

1. To develop a convenient synthetic route to a [2.2]paracyclophane-centred amino acid;
2. To develop coupling methods for incorporating this amino acid into small peptides with natural amino acids; and
3. To investigate these small peptides' activities as organocatalysts.

Chapter 2 discusses the first aim: to synthesise a [2.2]paracyclophane amino acid. The first target was to develop a scalable synthesis of 4-amino[2.2]paracyclophane-13-carboxylic acid **1.141** (Fig. 1.80). The devised route should allow easy access, give one regioisomer, and ideally allow for resolutions of the planar chirality.

Chapter 2 discusses the second aim: to incorporate **1.141** into small peptides. The ideal peptide coupling conditions should be high-yielding with the challenging [2.2]paracyclophane derivative, and prevent racemisation of the amino acids.

**1.141**FIGURE 1.80: 4-Amino[2.2]paracyclophane-13-carboxylic acid **1.141**

Chapter 3 discusses the third aim: to use the synthesised peptides as organocatalysts to investigate their activity in a stereoselective Michael addition. The small peptides' efficacy could be measured against other peptide catalysts in similar reactions. [2.2]Paracyclophane's unique properties were hypothesised to impact on the catalysts' activities by controlling the geometry of the peptides to some extent.

Chapter 2

Synthesis of 4-amino[2.2]paracyclophane-13-carboxylic acid

A note on nomenclature

The definition of an amino acid is variable and depends greatly on context. Common usage dictates that *amino acid* refers to the 20 or so naturally occurring amino acids coded by DNA. Many variations and modifications exist in nature, and even more small molecules containing both amine and carboxylic acid moieties have been created in vitro. These, too, can be considered amino acids and may be incorporated into amide-linked polymers, or peptides. The [2.2]paracyclophane-centred compound that this work is focused on will be described as a pseudoamino acid, for clarity. It is not naturally-occurring, and strictly speaking it does not contain an amine but is better described as an aniline derivative. This, coupled with the steric bulk and unusual electronic properties of [2.2]paracyclophane change its behaviour in synthesis and reactivity. Thus, peptides containing a pseudoamino acid become pseudopeptides, after Pearson's naming of similar anthranilic acid-containing compounds **2.1** (Fig. 2.1).¹⁷¹

For brevity, the [2.2]paracyclophane-derived pseudoamino acid **2.3** that is the feature of this project will be referred to as *Pca*, following similar naming conventions: by the Heinze group and Barišić group (among others), using *Fca* with ferrocene

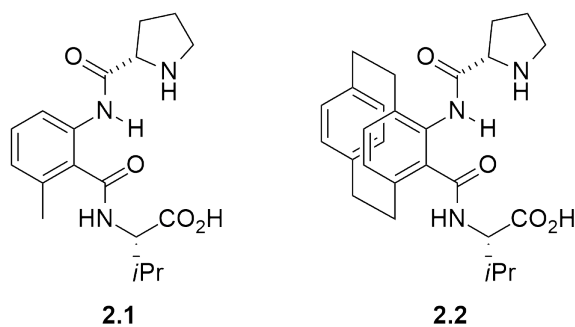


FIGURE 2.1: Pearson's pseudopeptide **2.1** and analogous [2.2]paracyclophane pseudopeptide **2.2**.

2.4^{63,64} and Schreiner's adamantane-derived *Aca* **2.5**⁹⁸ (Fig. 2.2). The pseudo-*geminal* 4-amino[2.2]paracyclophane-13-carboxylic acid synthesised in this thesis will be referred to simply as *Pca*, with other regioisomers given a descriptive prefix. For example, 4-amino[2.2]paracyclophane-12-carboxylic acid (**2.6**) will be called pseudo-*ortho* Pca. Pca-containing peptides will be referred to in the usual fashion for chemistry literature, by their three-letter codes, from N-terminus to C-terminus.

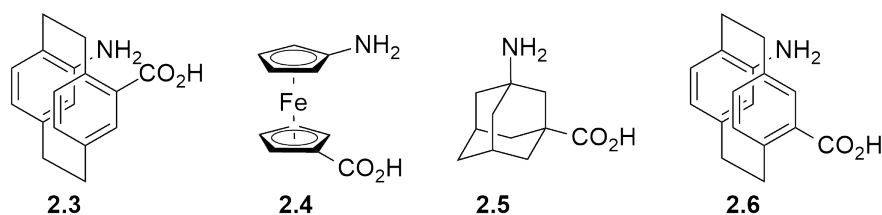


FIGURE 2.2: Unnatural cyclic amino acids.

2.1 Project scope

Asymmetric organocatalysis using small peptides as the catalyst is a young and exciting field of research, but many parts of its utility and control of stereoselectivity are found by trial and error using combinatorial methods, rather than specific design from known mechanistic principles. Much is known about the effect of specific peptide sequences on reaction rate and selectivity, but the effect of conformation is less explored.¹⁷² For instance, in the peptide-catalysed Michael addition introduced in Section 1.5, how does spatial orientation between the amine and the proton donor affect stereoselectivity? Wennemers' study of Michael addition with nitroalkenes (discussed in Section 1.4.2) demonstrates the importance of the proton donor's interaction with the catalytic intermediate.¹⁴⁷

[2.2]Paracyclophane offers a unique opportunity to investigate this question. Its rigid, bulky structure provides a scaffold around which functional groups can be arranged in space with precision. Thus, we can manipulate the distance and angle of these functional groups from each other in order to investigate how these factors may influence stereoselectivity in the Michael addition. By controlling the relative position of functional groups (*ortho*, *pseudo-geminal*, *pseudo-ortho* (Fig. 2.3)) on the [2.2]paracyclophane decks, the separation of functionality is reasonably well-defined and its influence on stereoselectivity can be investigated.

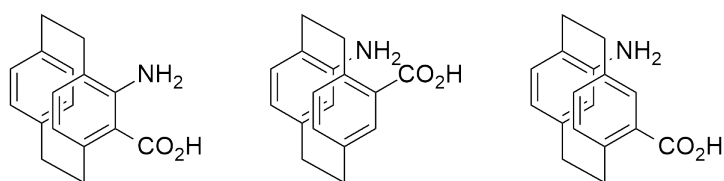


FIGURE 2.3: Left to right: *ortho*, *pseudo-geminal*, and *pseudo-ortho* substitution of Pca.

As illustrated in the literature review, there is significant interest in conformationally restricted and planar chiral amino acids and peptides (using cyclic, polycyclic or organometallic backbones) and their use in catalysis, materials, and medicinal chemistry. In restricting conformational freedom, [2.2]paracyclophane forms a turn-like motif common to many asymmetric organocatalysts (and also found extensively in nature). In the first report of Pca by Pelter in 1997 there was mention of its β -turn mimicking potential (Fig. 2.4).¹⁷³ However, there have been no subsequent reports regarding its properties in the intervening 20-plus years. Perhaps a reason for this is the difficulty in producing the desired compound in reasonable quantity. This project is an opportunity to find an efficient synthetic route to Pca and to explore a small area of its potential use.

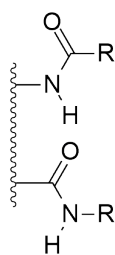


FIGURE 2.4: A β -turn-like conformation.

2.2 Literature syntheses of [2.2]paracyclophane-centred pseudo-amino acids

One of the selling points of [2.2]paracyclophane is the wealth of options available for controlled installation of functional groups. There are many conceivable [2.2]paracyclophane-centred pseudoamino acids (or Pca) (for instance, *ortho*, pseudo-*geminal*, pseudo-*ortho* (Fig. 2.5)) with fascinating possibilities: but none have been studied in this type of chemistry. The closest example is Pelter's preliminary work with the synthesis of these compounds and their proposed, but never fulfilled, investigation into their β -turn-like configuration.¹⁷³

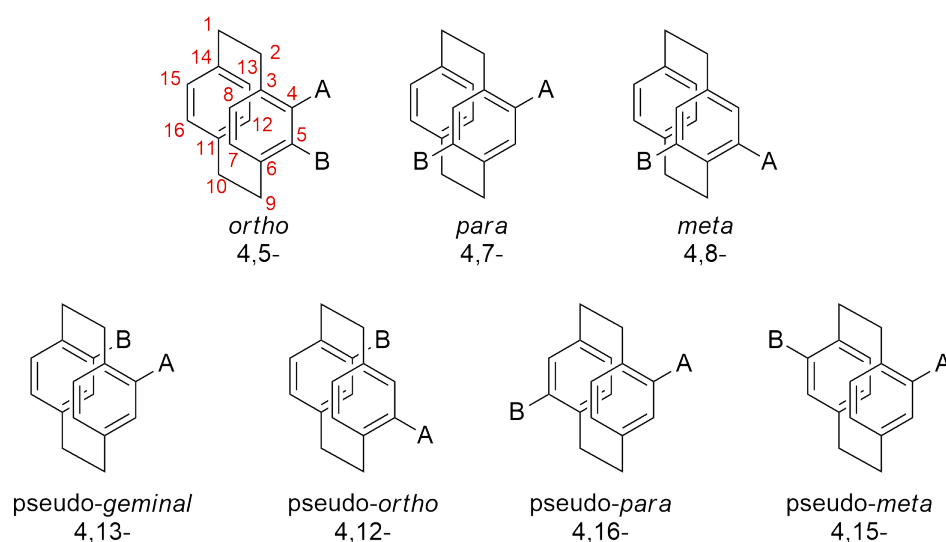


FIGURE 2.5: Substitution patterns for disubstituted [2.2]paracyclophane.

The combination of [2.2]paracyclophane's useful properties also contributes to some of the problems encountered in synthesis. Some of the challenges associated with the production of [2.2]paracyclophane derivatives include low solubility, side-product formation, and difficulty separating regioisomers, enantiomers and diastereomers. [2.2]Paracyclophane's steric bulk can also inhibit reactions.

With this in mind, a good starting place would be the *ortho*-Pca. The configuration of the carboxylic acid and amine groups resembles the successful catalysts of Pearson (Fig. 2.1). This configuration, however, is synthetically troublesome. Obstacles the Rowlands group have encountered in the synthesis of *ortho*-substituted [2.2]paracyclophane amines include instability of the products resulting in decomposition,

and poor reactivity of these *ortho*-substituted compounds.^{20,174} The *N*-phenyl *ortho*-substituted Pca was synthesised previously but the primary amine was never obtained.¹⁷⁴

2.2.1 Pseudo-*ortho* [2.2]paracyclophane amino acid synthesis

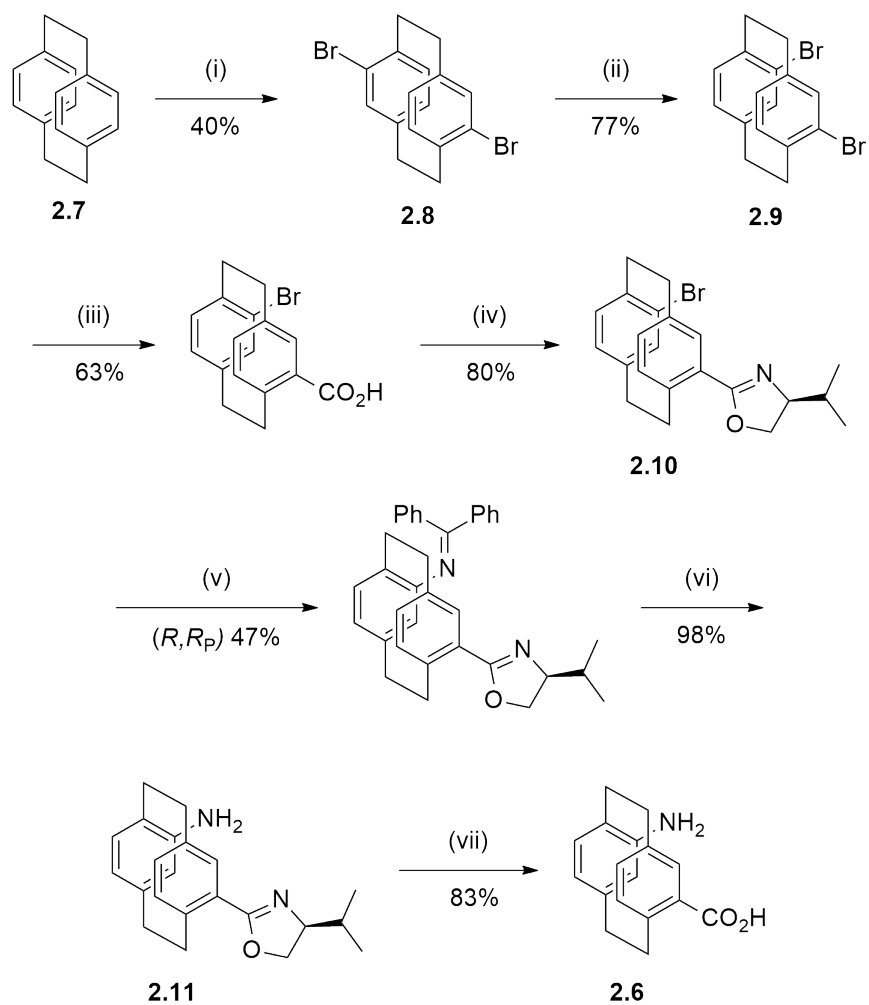
The pseudo-*ortho* Pca **2.6** is the next obvious choice as many good ligands are based on this configuration,^{22,175,176} but at the initiation of this project we thought the chemistry would be too long. One described route (Scheme 2.6)¹⁷⁷ starts with dibromination of [2.2]paracyclophane **2.7**,¹⁷⁸ which always gives a mixture of products with the pseudo-*para* **2.8** and pseudo-*ortho* **2.9** predominating. A useful quantity of pseudo-*ortho* isomer **2.9** can be obtained by the thermal isomerisation of the less soluble pseudo-*para* derivative and separation by recrystallisation based on their solubilities. The route then involves the multi-step formation of the bromo-oxazoline-[2.2]paracyclophane **2.10**, palladium-catalysed formation of the amine **2.11**, and finally oxazoline hydrolysis to give the carboxylic acid. This route did have the advantage of achieving resolution of the planar chirality by the inclusion of the enantiomerically pure oxazoline, which gave diastereomers that were easily separable.

2.2.2 Pseudo-*geminal* [2.2]paracyclophane amino acid synthesis

Pelter's 1997 synthesis of Pca also included a shorter, but very low-yielding synthesis of the pseudo-*ortho* pseudoamino acid **2.6**. Therefore, pseudo-*geminal* Pca **2.3** was chosen as the initial target planar chiral pseudoamino acid for this project, since it appeared, on paper, to be the easiest to synthesise. The discussion of its synthesis that follows might show that looks can be deceiving.

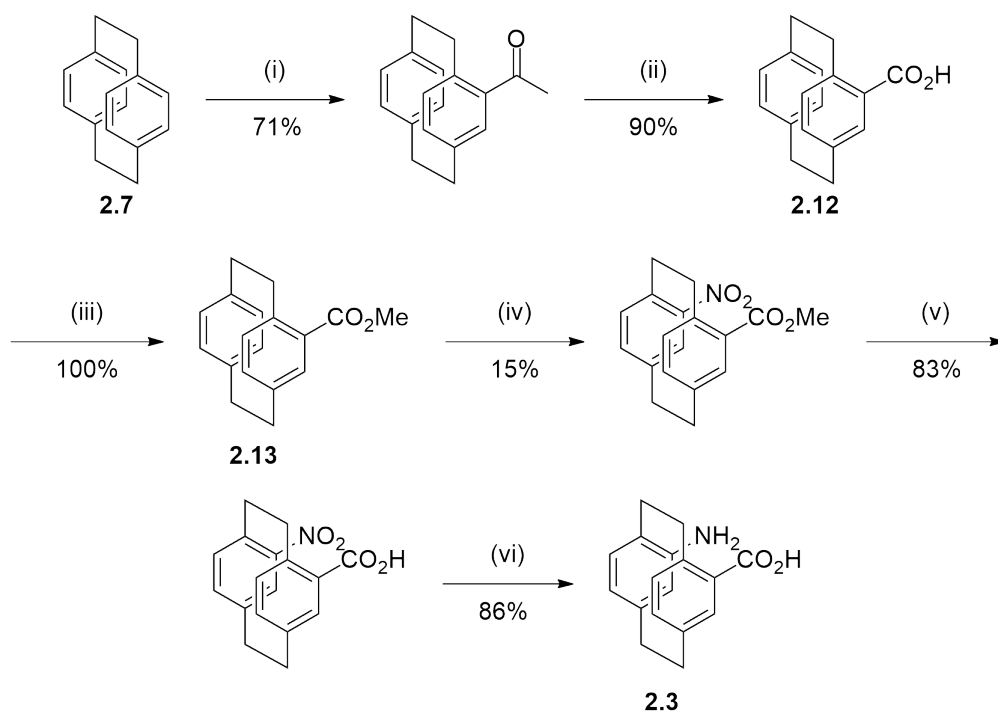
The first strand of this project was development and optimisation of a synthetic route to pseudo-*geminal* Pca. Several groups, including our own, have previously reported syntheses of this compound (or protected versions thereof).

Pelter's first reported synthesis from the late 1990s (Scheme 2.7) started with formation and protection of the carboxylic acid **2.12** to the methyl ester **2.13**.^{173,179,180} The nitration was found to be particularly problematic, giving very low (<15%) yield; additionally the substitution is not regioselective, giving a mixture of three or more



SCHEME 2.6: Ma *et al.*'s synthesis of pseudo-*ortho* 4-amino[2.2]paracyclophane-12-carboxylic acid. i) Fe, Br₂. ii) triglyme, heat (4 repetitions). iii) *n*-BuLi, CO₂. iv) a. SOCl₂, L-valinol b. PPh₃, CCl₄. v) benzhydrylideneamine, Pd-DPPF. vi) 6 M aq. HCl, THF. vii) aq. HCl.

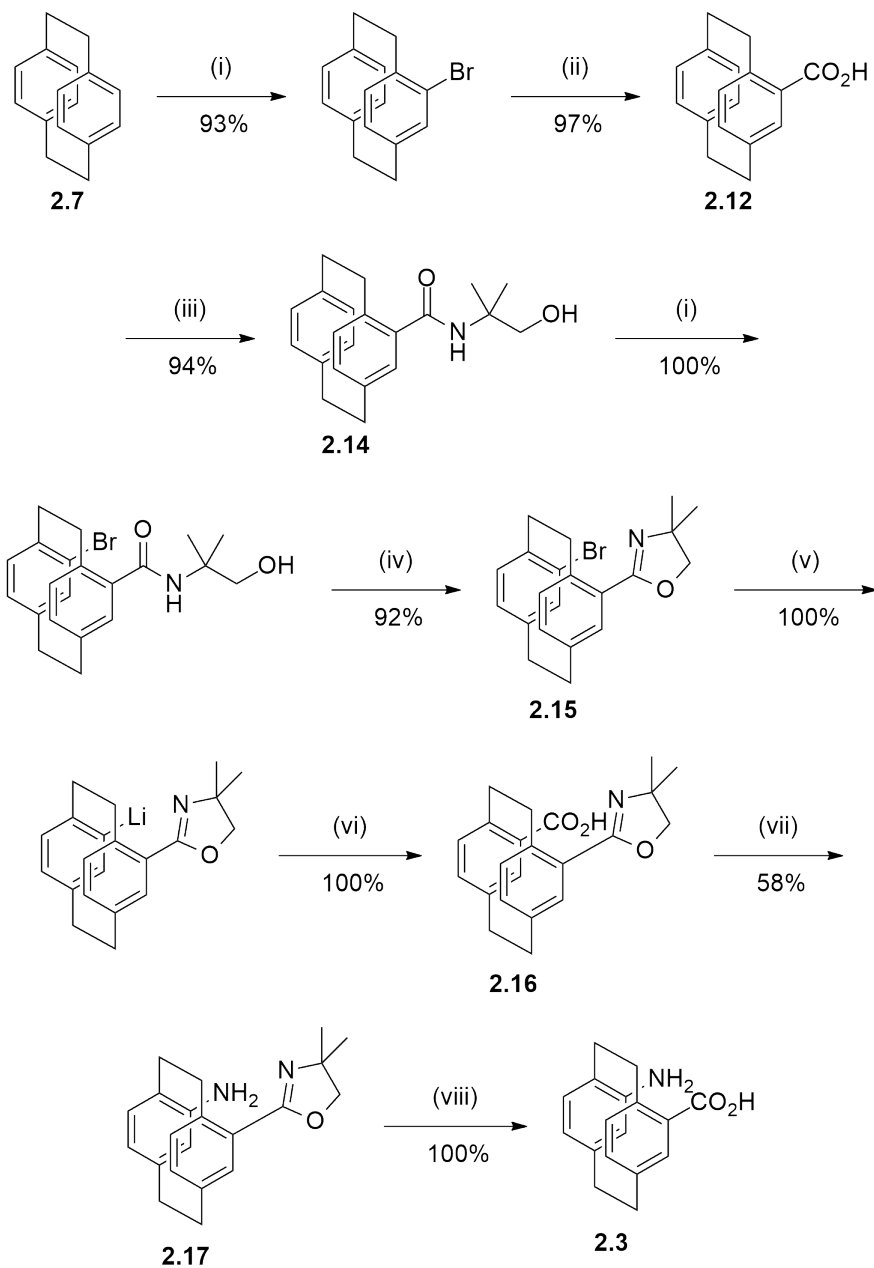
compounds with different substitution patterns. Basic ester hydrolysis and hydrogenation complete this route to the pseudo-amino acid **2.3**.



SCHEME 2.7: Pelter's first synthesis of pseudo-geminal Pca. i) AcCl, AlCl₃. ii) KOB. iii) CH₂N₂. iv) HNO₃, H₂SO₄. v) KOH, EtOH. vi) H₂, Pd-C.

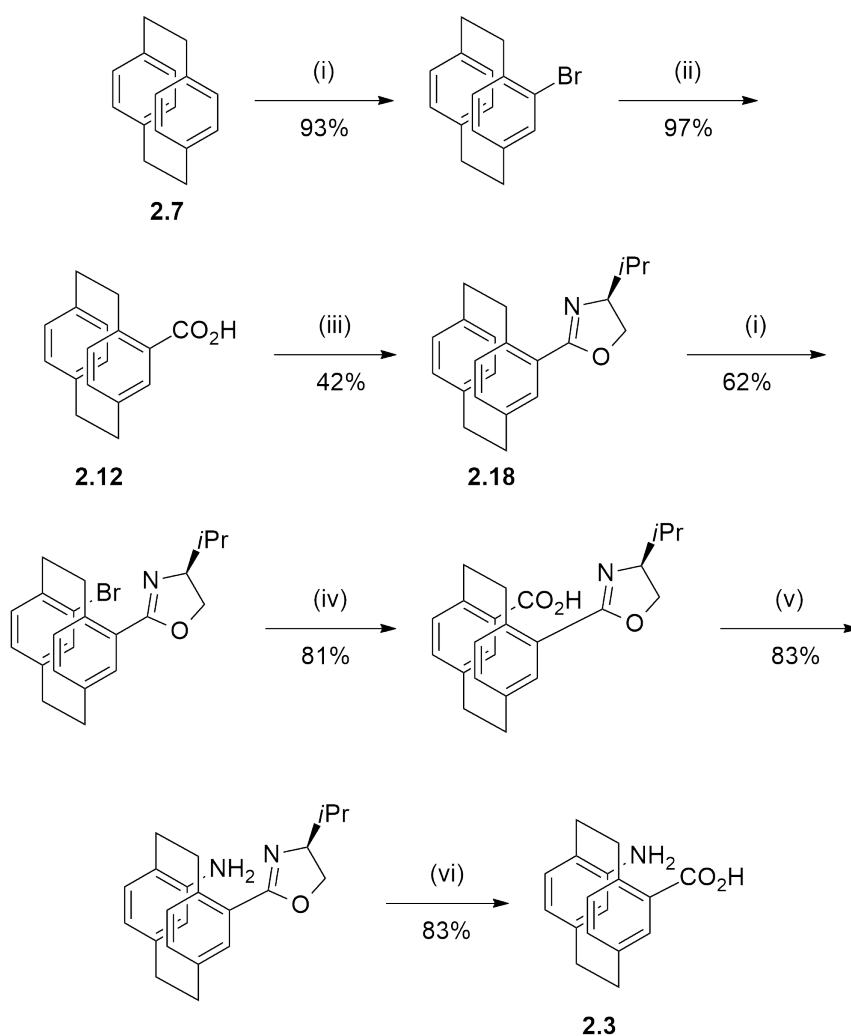
In 2000, Pelter's group reported another synthesis by an altogether different route employing an oxazoline to protect the carboxylic acid from attack during halogen-metal exchange (Scheme 2.8).¹⁸¹ The highest yielding, most convenient synthesis of the oxazoline involved a five-step sequence starting with bromination; a Grignard formation and addition to carbon dioxide gave the carboxylic acid **2.12**; amide formation *via* the acyl chloride; a second, pseudo-geminal bromination; and finally cyclisation of the β-hydroxy amide amide to the oxazoline gave the precursor **2.15**. The second bromine is converted to lithium by halogen-metal exchange and then to a second carboxylic acid **2.16** with addition of carbon dioxide. Finally, the amine **2.17** is formed by a Curtius rearrangement and the oxazoline protecting group is removed to give Pca **2.3**. The amide directs the second bromination to the pseudo-gem position. Although lengthy, the reported overall yield for this route is 45%.

Ma's synthesis (Scheme 2.9) of oxazoline substituted [2.2]paracyclophanyl imidazo[1,5-a]pyridinium triflates included synthesis of Pca as a means of testing absolute



SCHEME 2.8: Pelter's pseudo-geminal Pca synthesis *via* an oxazoline.
 i) Br₂, Fe. ii) a. Mg, CO₂. iii) SOCl₂, 2-amino-2-methylpropan-1-ol.
 iv) Et₃N, PPh₃, CCl₄. v) *n*-BuLi. vi) CO₂ then aq. acid. vii) a. SOCl₂
 b. NaN₃/acetone c. toluene, heat d. aq. KOH. viii) 6 M HCl.

stereochemistry by plane-polarised light rotation.¹⁷⁷ It followed largely the same route as Pelter's oxazoline route; except the amine was formed from the carboxylic acid using different conditions. It first creates the diastereomeric oxazoline species **2.18**, a masked carboxylic acid. Carboxylic acid formation on the pseudo-geminal position by halogen-metal exchange then transformation with DPPA completes the amine formation. This route boasts the advantage of the oxazoline synthetic intermediate being easily resolved by column chromatography, separating the two diastereomers, which after oxazoline cleavage afforded the carboxylic acid, enantiomerically pure.



SCHEME 2.9: Ma's pseudo-geminal Pca synthesis *via* an oxazoline. i) Br₂, Fe. ii) a. Mg, CO₂. iii) a. SOCl₂, L-valinol. b. PPh₃, CCl₄ iv) *n*-BuLi then CO₂. v) DPPA. vi) Aq. HCl.

2.3 Syntheses of 4-amino[2.2]paracyclophane-13-carboxylic acid in this work

The first route to pseudo-*gem* Pca investigated in this project was based on chemistry being performed in the Rowlands group. This oxime methodology is adapted from previous work detailing a one-pot oxime oxidation of an aryl aldehyde to the hydroxamic acid, then Lossen rearrangement to give the amine.^{20,182–184} A second route which formed the amine by nitro reduction was developed in response to difficulties with the former method. These syntheses both started from [2.2]paracyclophane **2.7**, a compound that is available cheaply in large quantities.

2.3.1 Chiral resolution

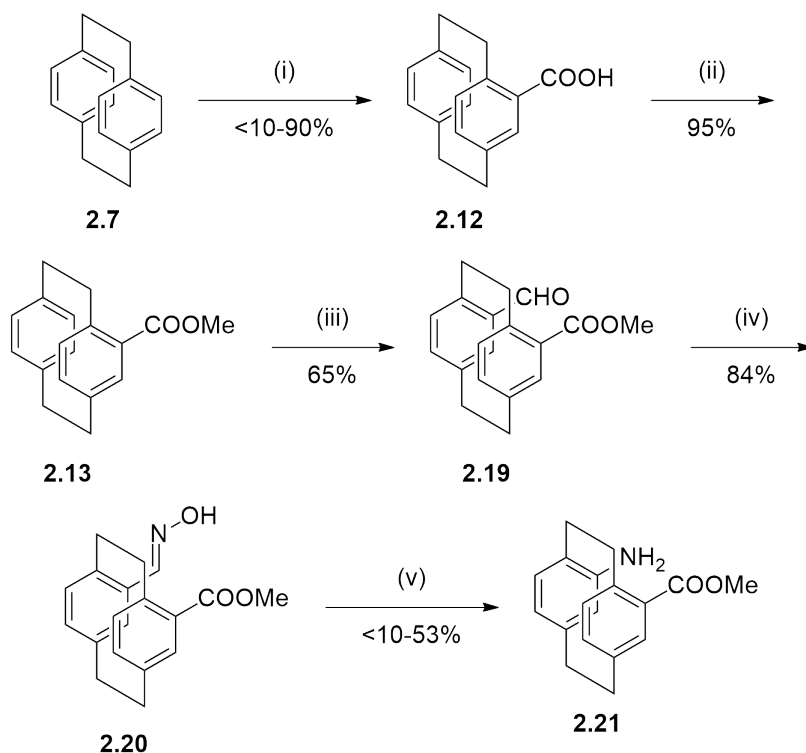
Resolution of the planar chirality of the [2.2]paracyclophane backbone was attempted at several synthetic stages. Resolution before coupling to an amino acid or peptide is possible, and has been shown to work well by Bräse and others; we considered it might be more expedient to resolve the [2.2]paracyclophane backbone at a later stage.⁵¹ The closer to the end of a synthetic route a resolution is performed, the fewer total synthetic steps must be completed if both stereoisomers are desired. Addition of an L-amino acid leads to the formation of diastereomers and it was anticipated that these might be separable by standard flash chromatography.

2.3.2 Oxime methodology

At first, refinement of the oxime methodology was attempted (Scheme 2.10). This route is short and elegant, with the amine **2.21** formed in two steps from the formaldehyde **2.19** by a Lossen-type rearrangement *via* oxime **2.20**. The methyl carboxylate acts as the directing group for the formation of the pseudo-*geminal* isomer.

Friedel-Crafts acylation

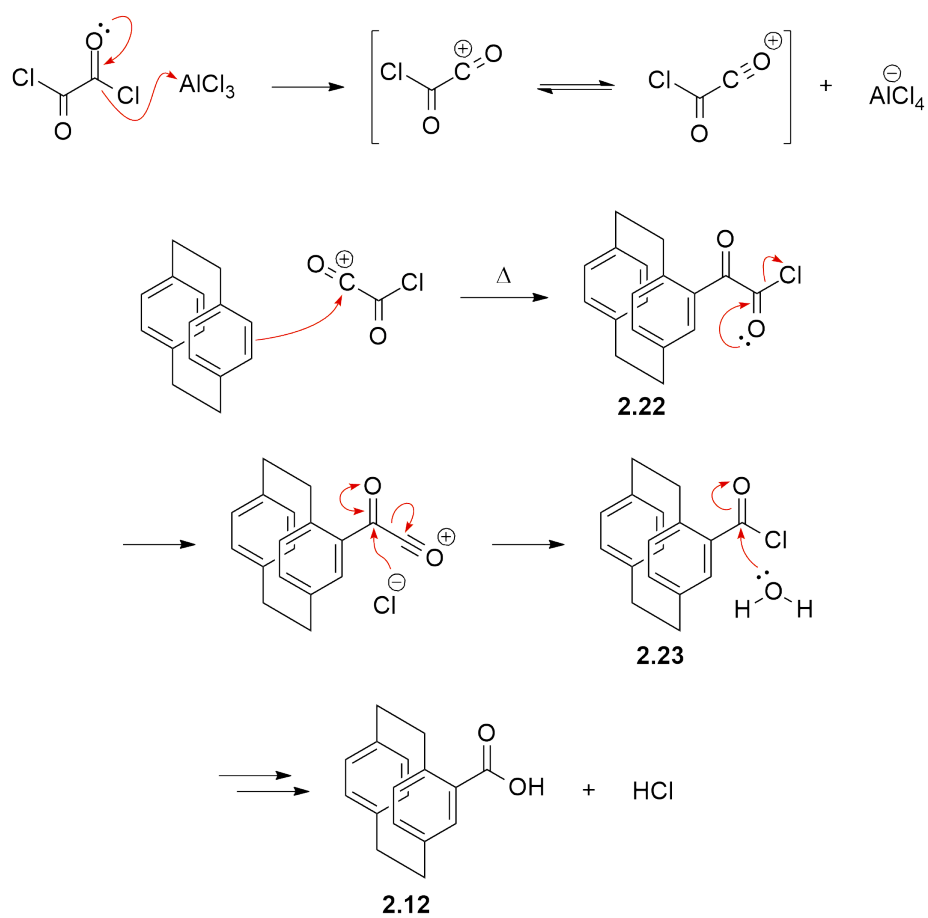
The first synthetic step was the direct synthesis of [2.2]paracyclophane-4-carboxylic acid **2.12** by a Friedel-Crafts reaction between [2.2]paracyclophane and oxalyl chloride (Scheme 2.11). This avoided bromination followed by halogen-metal exchange and addition to carbon dioxide used in the syntheses described above.



SCHEME 2.10: Oxime route for Pca synthesis. i) a. AlCl_3 , $(\text{COCl})_2$, b. chlorobenzene, H_2O . ii) a. $(\text{COCl})_2$, DMF, b. MeOH. iii) $\text{CH}_3\text{OCHCl}_2$, TiCl_4 . iv) NaOAc, $\text{NH}_2\text{OH} \cdot \text{HCl}$. v) a. hydroxy(tosyloxy)iodobenzene, b. NaOH.

The Friedel-Crafts acylation forms [2.2]paracyclophane-4-(2-chloro-2-oxoacetyl) **2.22**, a remarkably stable keto-acid chloride, which may be isolated from the reaction mixture without decomposition.¹⁸⁵ The keto-acid chloride undergoes decarbonylation upon heating, yielding the acyl chloride **2.23** which can be hydrolysed to the carboxylic acid **2.12** by the addition of water. Methanol can be added instead to directly form the methyl ester, however it was found that a mixture of the desired product, the carboxylic acid and unreacted [2.2]paracyclophane was observed; using water to quench the reaction gives only carboxylic acid and starting material.

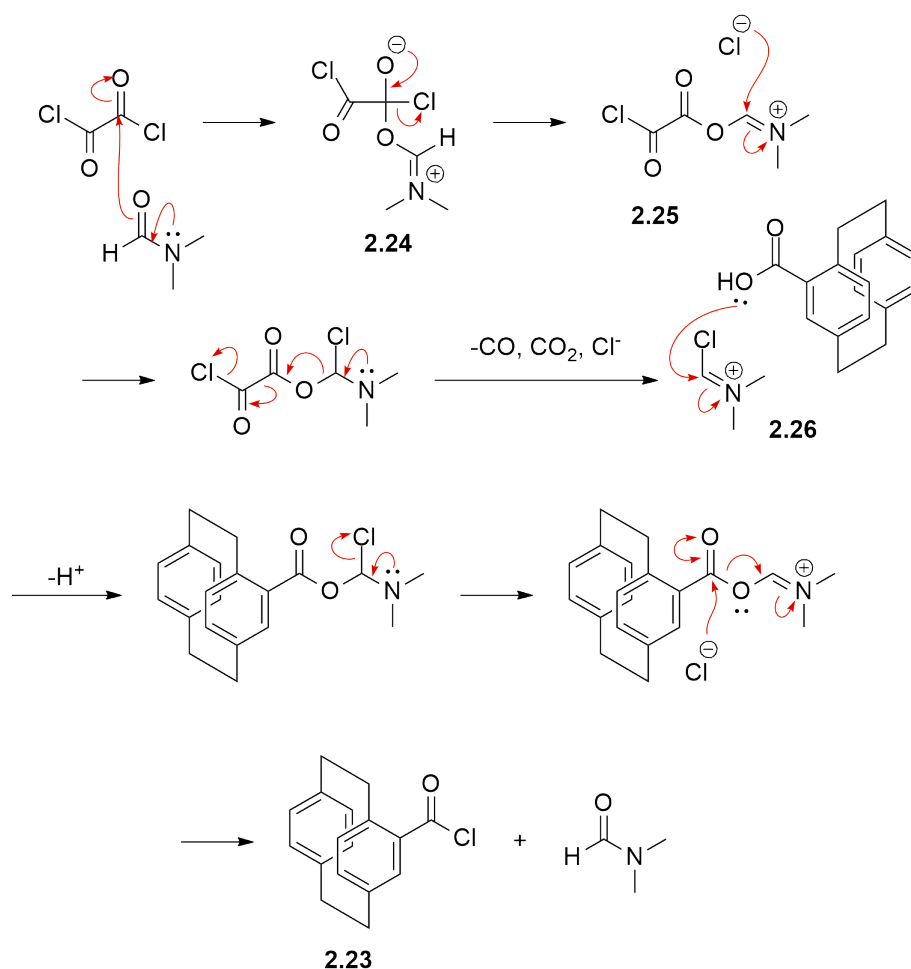
This step is a known reaction, but not widely used.¹⁸⁶ In the course of this project, the reaction was problematic, giving the acid in variable low to moderate yields, and separation from the starting material by column chromatography was far from satisfactory. The first step requires careful exclusion of water from the reaction vessel and many steps were taken to remove any water present in the system. These included flame-drying glassware; running the reaction under an argon balloon and cycling the argon atmosphere with vacuum three times before addition of reagents; driving



SCHEME 2.11: Friedel-Crafts acylation of [2.2]paracyclophane.

off any residual water on reagents with heat under vacuum; and transferring the large volume of solvent to the reaction vessel *via* cannula rather than syringe. These did not seem to improve the efficiency of the reaction, which hardly ever gave above 30% yield.

Instead of forming the methyl ester directly after formation of the oxo-acyl chloride intermediate in the previous step, the methyl ester was formed by activating the carboxylic acid with oxalyl chloride and DMF to form the acyl chloride, which was isolated by removing the solvent to dryness under reduced pressure (Scheme 2.12).

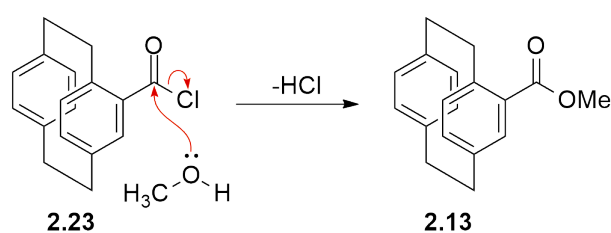


SCHEME 2.12: Acyl chloride formation with oxalyl chloride and catalytic DMF.

The acyl chloride formation occurs first by generating the Vilsmeier reagent **2.26** from oxalyl chloride and DMF. The DMF performs nucleophilic attack on the C=O of oxalyl chloride through its oxygen of the oxalyl chloride C=O forming the tetrahedral intermediate **2.24**. The C=O double bond reforms and a Cl^- is ejected. The

chloride ion attacks the electrophilic C=N double bond of **2.25**. CO, CO₂, and Cl⁻ are generated along with the iminium species **2.26**. This highly electrophilic intermediate is now attacked by the -OH of the carboxylic acid. The iminium reforms, ejecting a chloride ion, which then attacks at the carboxylic acid's electrophilic carbon. The tetrahedral intermediate reforms the C=O bond, reforming the DMF catalyst, and leaving the acyl chloride **2.23**.

The acyl chloride was then reacted with methanol to form the desired methyl ester (Scheme 2.13).



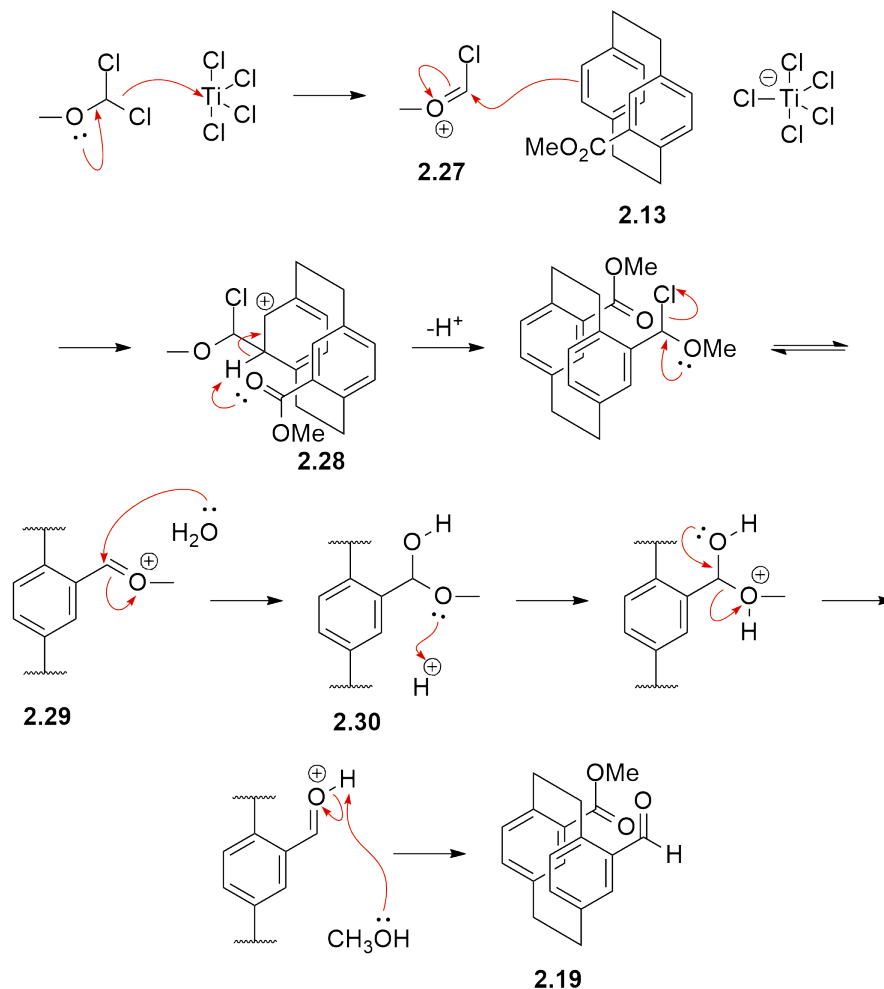
SCHEME 2.13: Methyl ester formation from acyl chloride.

Reiche formylation

The aldehyde **2.19** was then formed using Reiche formylation conditions.¹⁸⁷ These conditions have been used extensively in [2.2]paracyclophane chemistry for substitution specifically at the 13- (pseudo-*geminal*) position when there is an electron-withdrawing group in place at the 4-position.^{186,188,189} This step was high-yielding with good purity, as found in the literature. The only drawback with these conditions is the use of TiCl₄ which requires careful handling since it exothermically forms hydrogen chloride upon contact with water and other weakly basic solvents. This reaction is well-established as a carbon-carbon bond forming method in cyclophane chemistry due to their electron-rich nature making them a suitable substrate.^{51,190,191}

The mechanism of the Reiche formylation begins with generation of the electrophile from 1,1-dichlorodimethyl ether. Nucleophilic attack from the 13-carbon to the chloromethyl carbocation **2.27** of the substrate gives the Wheland intermediate **2.28**. Generally in Reiche formylation, in the next step a chloride ion abstracts a proton, restoring aromaticity. In the [2.2]paracyclophane system, the ester on the opposing ring abstracts this proton. A further chloride ion is ejected and a molecule of water adds

to the oxonium electrophile **2.29**. The hemiacetal **2.30** is protonated at the acetal oxygen, making methanol a good leaving group. Finally, the aldehyde product is deprotonated **2.19** (Scheme 2.14).



SCHEME 2.14: Reiche formylation of 4-formyl[2.2]paracyclophane **2.13**.

The rate-determining step in electrophilic aromatic substitution is usually the initial step which destroys aromaticity. In this formylation, the proton abstraction seems to be the rate-determining step. The transannular effect could be thought of as stabilising the carbocation through resonance, but more important is the ability to remove the proton. This is illustrated by the fact a nitrile group in the same position does not direct addition to the pseudo-*gem* position as it is linear and the lone pair has the wrong orientation. The methyl ester on the opposite deck assists in proton abstraction and directs the substitution to the pseudo-*gem* position. The regioselectivity may also be enhanced by the TiCl_4 coordinating with the oxygen atoms of

the 1,1-dichlorodimethyl ether and methyl [2.2]paracyclophane-4-carboxylate.^{187,192} This aligns the substrate for attack from the 13-position of [2.2]paracyclophane and increases the electrophilicity of the substrate, and hence gives pseudo-*gem* substitution.

Limiting the equivalence of the alkylating reagent (1,1-dichlorodimethyl ether) to 1.05-1.10 helps prevent over-alkylation. Additionally, the steric bulk of the ethylene bridges of [2.2]paracyclophane may help prevent additional aryl carbons being derivatised. This reaction was found to give the best results on smaller scales (up to 5 g): larger scale syntheses than this had a lower yield and decreased purity. This may be simply because inert technique was more difficult on larger scales. Larger flasks are more difficult to evacuate of atmospheric water completely and it is more likely that larger quantities of reagents or solvents will retain residual water after drying. This residual water would quench the reagents before they react with the [2.2]paracyclophane.

The regiochemistry of formylation was confirmed by ¹H NMR spectrum of the formylated product, 13-formyl[2.2]paracyclophane-4-carboxylic acid **2.19** (Fig. 2.15 and Fig. 2.16). The peak pattern of the aromatic protons is consistent with a 4,13-substitution pattern on [2.2]paracyclophane, and can be observed in the spectra of pseudo-*geminal* compounds throughout this work.

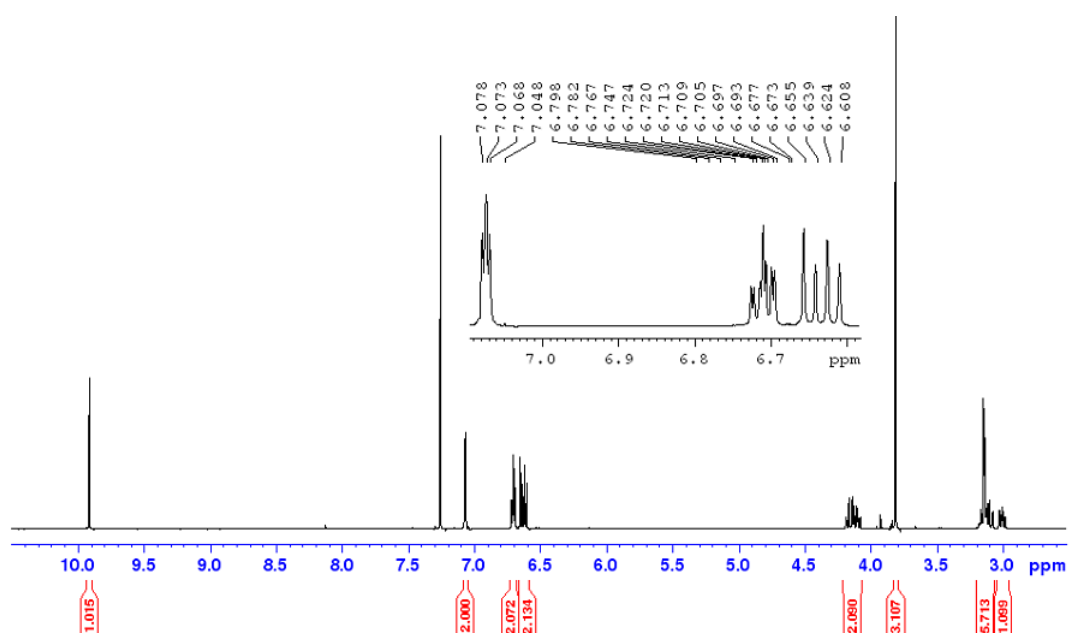


FIGURE 2.15: ¹H NMR spectrum of **2.19**.

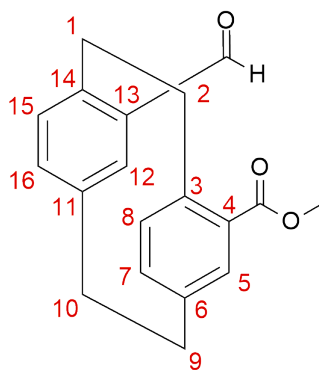


FIGURE 2.16: 13-Formyl[2.2]paracyclophane-4-carboxylic acid **2.19**.

The H^5 and H^{12} protons are assigned to the overlapping peaks at 7.07 ppm with $J = 2.4$ Hz, indicative of *meta* coupling. H^8 and H^{15} are the doublets at 6.64 and 6.61 ppm with $J = 7.8$ Hz. This is the *ortho* coupling; the *para* coupling with H^5 and H^{12} is not present. H^7 and H^{16} are the last pair of aromatic protons seen in the spectrum as the two overlapping dd peaks at 6.7 ppm with $J = 5.7, 2.0$ Hz, indicative of their *ortho* and *meta* coupling partners, respectively. This peak coupling pattern is indicative of pseudo-*gem* substitution.

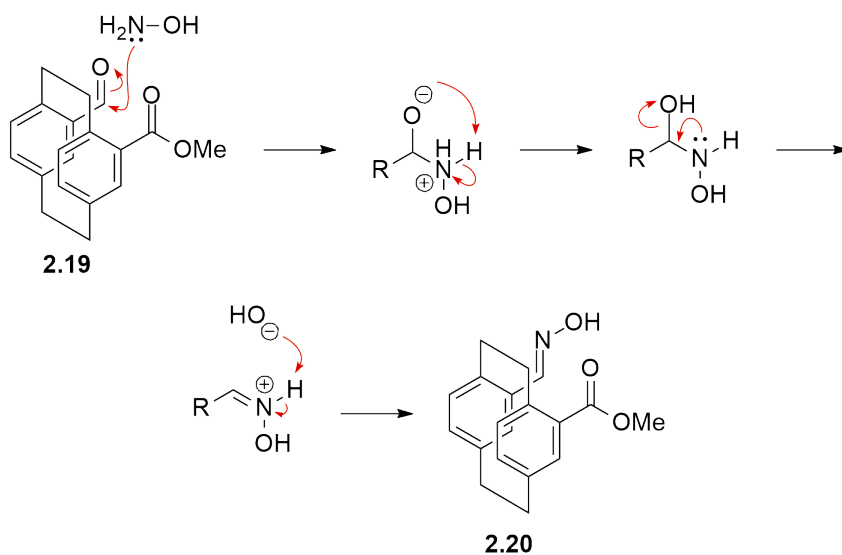
Oximation

The oximation using hydroxylamine hydrochloride was undemanding, using hydroxylamine hydrochloride, with NaOH to remove the hydrochloride salt. In this reaction, hydroxylamine condenses with the aldehyde, forming the resonance-stabilised oxime (Scheme 2.17). This reaction proceeded in high yield and purity.

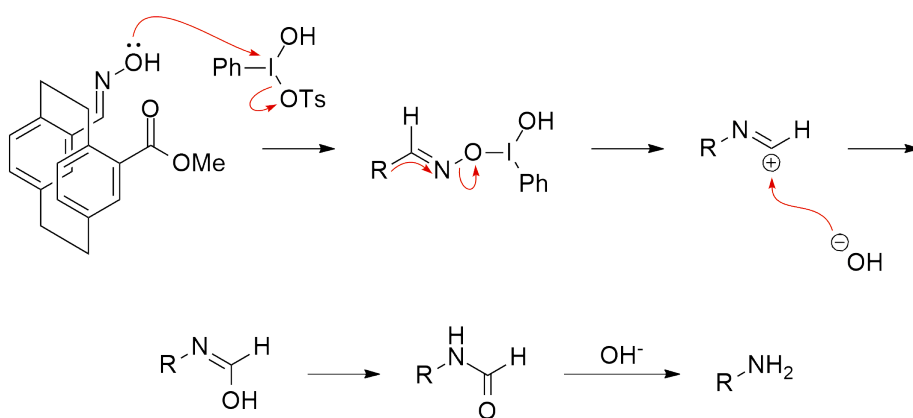
Oxime rearrangement to amine

The final step was one-pot oxidation-rearrangement of the oxime to the amine *via* the hydroxamic acid. This used Koser's reagent and then NaOH. This is presumed to involve a Lossen-type rearrangement.

Originally, the plan was to go directly to the amine. The expected reaction was initially Beckmann rearrangement without competition from fragmentation to form the nitrile; followed by basic amide hydrolysis (Fig. 2.18).¹⁹³ However, isolation of the hydroxamic acid intermediate suggested a different mechanism.



SCHEME 2.17: Hydroxylamine condensation with **2.19**, affording oxime product **2.20**.



SCHEME 2.18: Mechanism for proposed Beckmann rearrangement to form amine.

The first stage of this mechanism is oxidation of the oxime to the hydroxamic acid, mediated by Koser's reagent **2.31**.^{182,184,194} Koser's reagent, or hydroxy(tosyloxy)-iodobenzene (Fig. 2.19), is a useful hypervalent iodine reagent for oxidation as an alternative to heavy metal reagents.

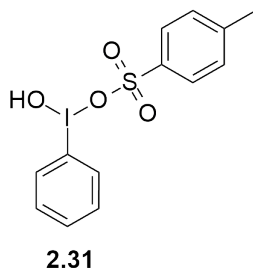
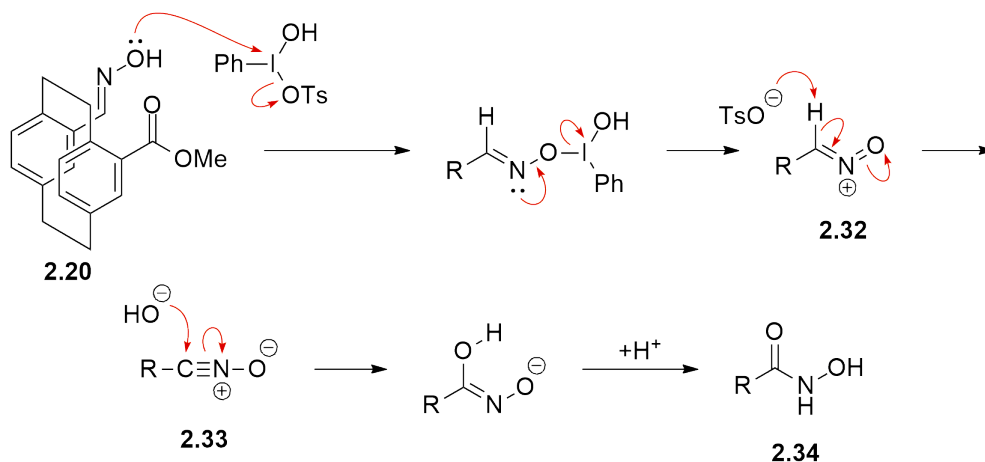


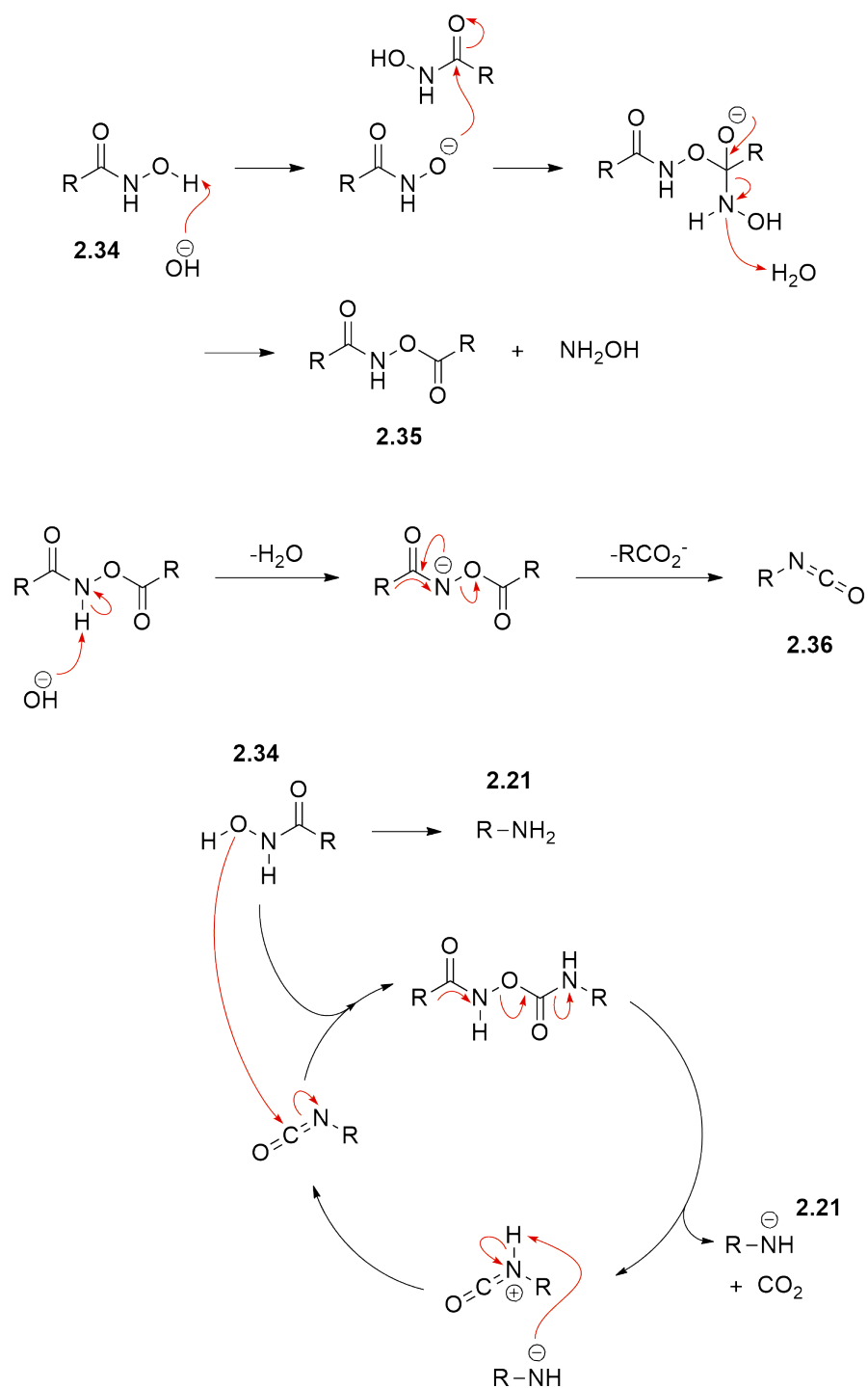
FIGURE 2.19: Koser's reagent **2.31**.

The oxime oxygen attacks the iodine and displaces tosic acid. Rearrangement expels Ph(OH)I, giving the intermediate **2.32**, which is deprotonated to give the nitrile oxide **2.33**. The nitrile oxide undergoes nucleophilic attack by the OH⁻ generated from the Koser's reagent. Tautomerisation results in the hydroxamic acid **2.34** (Scheme 2.20).



SCHEME 2.20: Oxime rearrangement to hydroxamic acid mediated by Koser's reagent.

A modified Lossen rearrangement using base with no external activating reagent was employed to form the amine from the hydroxamic acid.¹⁸³ The apparent pathway involved firstly the generation of a small quantity of the isocyanate **2.36** which then participated in a chain reaction which furnished the final amine (Scheme 2.21).

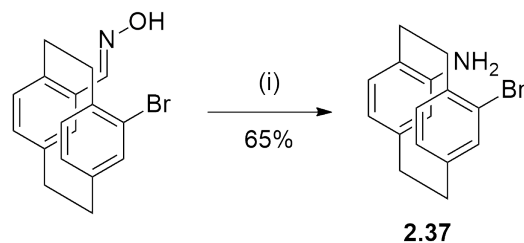


SCHEME 2.21: Proposed mechanism for Lossen-type rearrangement to amine *via* an isocyanate.

First, the isocyanate reactive intermediate is generated from reaction of two hydroxamic acid molecules to give the *O*-acylhydroxamate **2.35**, which rearranges to form the isocyanate **2.36** and a molecule of the corresponding carboxylic acid. This differs from traditional Lossen rearrangement where an activating agent, such as tosyl chloride, is required to make the hydroxyl group into a good leaving group, allowing conversion of the hydroxamic acid to the isocyanate.

Further, in a standard Lossen rearrangement, hydrolysis of the isocyanate requires water, but here, the reaction has a higher yield in anhydrous conditions, since the isocyanate must react with more hydroxamic acid. The formed isocyanate enters the chain reaction cycle and is attacked by the hydroxamic acid. This dimer undergoes rearrangement to produce carbon dioxide, one molecule of the amine, and one molecule of the isocyanate; the latter of which goes on to complete another chain reaction cycle.

The reaction did not behave as predicted through the Beckmann rearrangement, instead proceeding *via* the hydroxamic acid, causing yield and purity issues. The yield was highly variable, ranging from less than 10% to a maximum of 53%, with very poor purity. Column chromatography was inconsistent at affording the pure product. The hydroxamic acid intermediate could be isolated in high yield and purity, indicating that the problematic step of the reaction was the Lossen-type rearrangement. Other members of the Rowlands group found acceptable results forming 4-amino-13-bromo[2.2]paracyclophane **2.37** with 65% yield in the final hydroxamic acid rearrangement (Scheme 2.22).²⁰



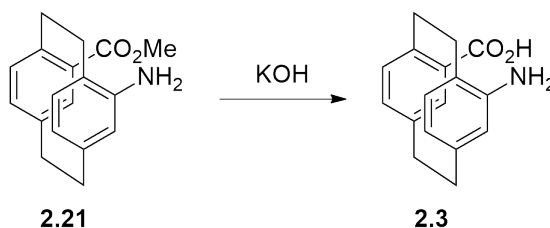
SCHEME 2.22: Synthesis of 4-amino-13-bromo[2.2]paracyclophane **2.37**. i. Koser's reagent then NaOH.

It is possible that intramolecular hydrogen bonding between the hydroxamic acid and carboxylate substituents on the two opposing faces of paracyclophane prevented

the rearrangement from proceeding. Other problems included hydrolysis of the ester and involvement of the acid. Synthesis of the monosubstituted 4-amino[2.2]paracyclophane *via* the oxime, to avoid interference of other functional groups did not improve the yield of the oxime rearrangement. Difficulties were encountered by other members of the Rowlands group in the synthesis of similar molecules, so the roadblock at this final step meant development of an alternative route to Pca was valuable.

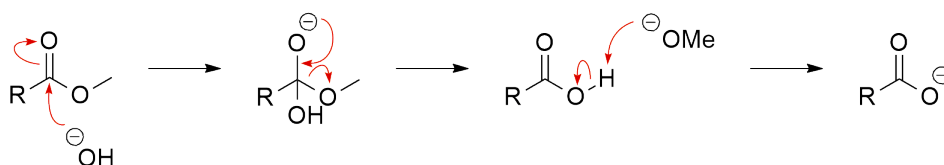
Ester hydrolysis

The first route to Pca concluded with hydrolysis of the methyl ester. A methyl ester was employed as a protecting group in the oxime methodology for synthesis of Pca. Several conditions for hydrolysis of this ester according to Scheme 2.23 were tested and are listed in Table 2.1.



SCHEME 2.23: Ester hydrolysis of Pca-OMe **2.21** to Pca **2.3**.

Basic ester hydrolysis occurs by a hydroxide ion attacking the carbonyl electrophile to form the tetrahedral carbon intermediate. The carbonyl C=O bond is restored, and with loss and gain of a proton, the alkyl protecting group leaves as the corresponding alcohol: here, methanol (Scheme 2.24). Formation of the carboxylate drives the equilibrium to favour the products.



SCHEME 2.24: Basic ester hydrolysis mechanism.

Previously our group used the conditions in the first entry of Table 2.1: 0.067 M 3:1 MeOH/H₂O, 5 eq. KOH, at 50 °C as reported.¹⁹⁵ They were found to return approximately 20% of the material as the methyl ester as determined by ¹H NMR.

This could be avoided by running the reaction either at reflux in the same solvent mixture (entry 2) or at 50 °C in 3:1 EtOH/H₂O (entry 3), which both gave the desired free carboxylic acid with only trace amounts of the appropriate returned ester. Using ethanol as solvent improved the solubility of the starting material, pushing more of the ester to be hydrolysed. The ratio of 3:1 EtOH/H₂O at 50 °C was deemed most desirable since it required a lower energy input.

Solvent system	Temperature	Product yield	Returned ester
3:1 MeOH/H ₂ O	50°C	60%	20%
3:1 MeOH/H ₂ O	reflux	80%	0%
3:1 EtOH/H ₂ O	50°C	90%	0%

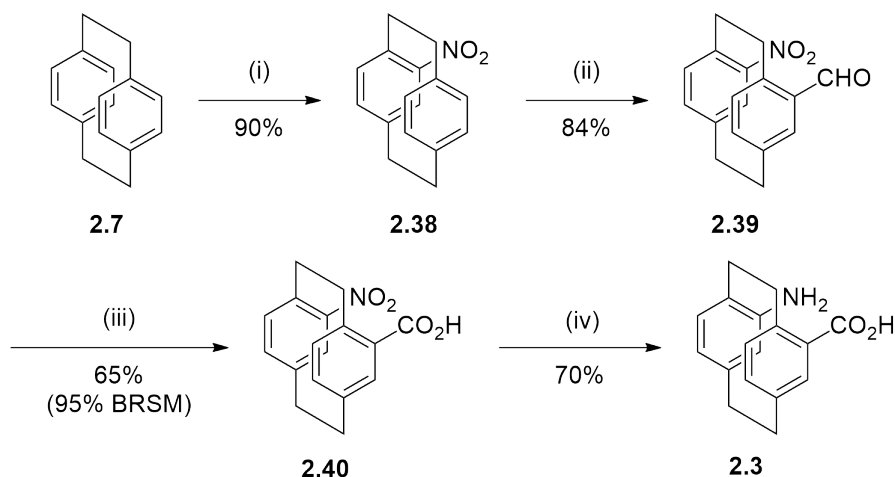
TABLE 2.1: Conditions tested for ester hydrolysis of Pca-OMe **2.21**. All reactions used 5 eq. of KOH, and solvent was used at 0.067 M for the substrate.

2.3.3 The nitro group methodology

The oxime methodology for synthesis of Pca was discarded after several attempts at the oxime rearrangement failed or could not be purified. Additional problems were encountered in yield and purity of the initial carboxylic acid formation. For these reasons, developing a more straightforward and easy to execute synthetic route seemed more efficient. It took much longer than anticipated to optimise this new methodology. However, the nitro methodology performs better, giving moderate yield with high purity, and takes only four steps to obtain Pca. The four steps give Pca in 34% and increases to 47% when considering returned starting material.

This method used simpler transformations that had more potential for optimisation and to be scaled up to allow for production of a large quantity of this key material. First, nitration **2.38** of [2.2]paracyclophane installed the amine precursor. This was followed by formylation **2.39** of the opposing face; then oxidation of the aldehyde to the carboxylic acid **2.40**; and finally reduction of the nitro to the primary amine **2.21**, as summarised in Scheme 2.25.

Both the nitro group or the acid can participate in the transannular effect and direct to the pseudo-*gem* position so either functional group might be appended first. It was advantageous to form the carboxylic acid second since it introduces solubility issues; and its acid-base properties could be utilised for purification of the material.



SCHEME 2.25: Nitro route for synthesis of Pca. i) HNO_3 , H_2SO_4 . ii) TiCl_4 , $\text{CH}_3\text{OCHCl}_2$. iii) KMnO_4 . iv) Zn , NH_4Cl .

Further, at the outset of the development of this method, the nitration was the largest unknown due to the variance and poor performance of conditions used in [2.2]paracyclophane chemistry; this step's success or failure would determine the viability of this synthetic route.

This route, as with the previous oxime methodology, includes methyl ester protection of the carboxylic acid. In the nitro methodology, the carboxylic acid does not need to be protected since the nitro reduction proceeds well with the carboxylic acid unprotected. However, protection of the carboxylic acid was necessary for elaboration of the amine in the completed Pca. The methyl ester protection gave the product in high yield wherever it was carried out in the synthetic route (Scheme 2.26). A convenient place in the route to complete it was before reduction of the nitro group to the primary amine.

Nitration

The route starts with nitration by electrophilic aromatic substitution. This route was not considered as the first choice due to inconsistency in the literature yields, and previous difficulty in the Rowlands lab with nitration of [2.2]paracyclophane compounds. [2.2]Paracyclophane can be considered as an electron rich aromatic system and is prone to multiple reactions or nitrations under standard conditions. Pelter's nitration conditions using 1:1 sulfuric acid and nitric acid at room temperature gave a very low yield and generated side products with multiple points of nitration.¹⁷³

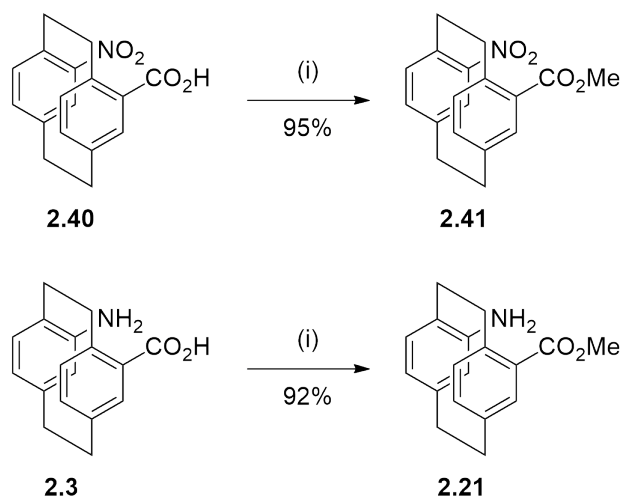


FIGURE 2.26: Methyl ester protection of carboxylic acid in nitro methodology. i) a. SOCl_2 b. MeOH.

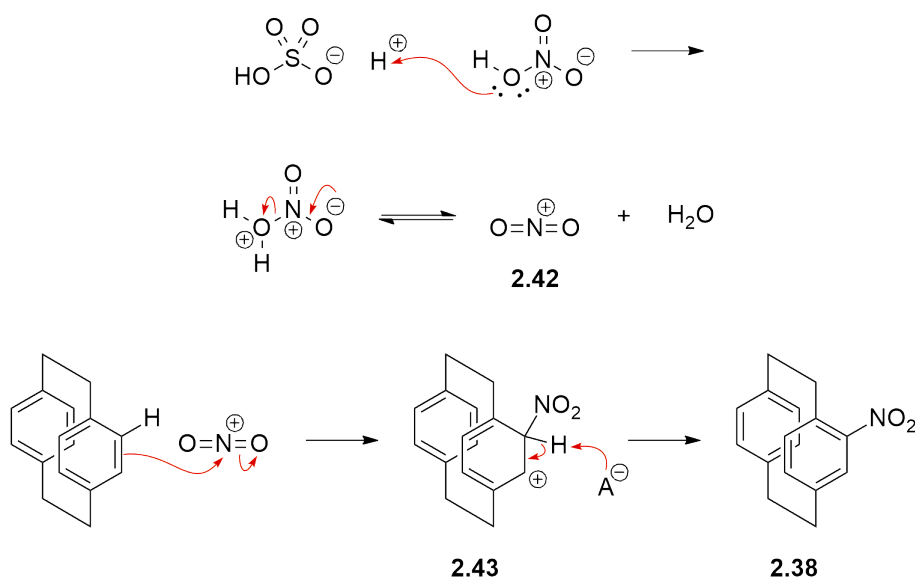
Paradies *et al.* describe a nitration of [2.2]paracyclophane in harsh conditions with heating.¹⁹⁶ In these conditions, glacial acetic acid rather than sulfuric acid is used to generate the nitronium electrophile. Even employing rigorous temperature and time control, the authors report at best a 30% yield. This result was replicated, however these conditions always produce a large proportion of side products and the reaction procedure could perhaps best be described as finicky, with challenging purification.

While giving some limited success, these conditions were discarded in favour of development of more gentle, controlled conditions. Sulfuric and nitric acid were used as in Pelter's nitrations, here in the stoichiometry of 4 and 2 equivalents respectively; however the reaction was performed at low temperature (0°C). Important for the success of this reaction was using dichloromethane and the solvent at low temperature. Dichloromethane has acceptable solubility of [2.2]paracyclophane at (0°C). These conditions were favoured because the formation of side products was slower, allowing the reaction to be run overnight. Even under these conditions a black, tar-like substance was formed. It was essential that the reaction mixture was decanted from this tar otherwise the work-up became difficult. An emulsion would form that prevented a good yield being obtained.

These conditions gave higher yield, usually between 80 - 90%, with the side products able to be removed using column chromatography or recrystallisation. The difference

in yield is probably due to the lower reaction temperature simply slowing the formation of undesirable products such as multiply-nitrated [2.2]paracyclophane.

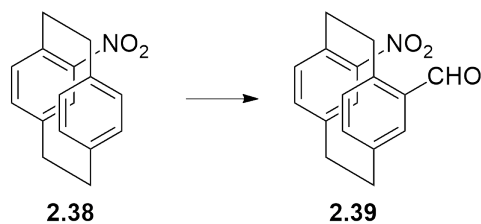
The mechanism of all the methods described above is the same: an electrophilic aromatic substitution. The acetic or sulfuric acid generates the nitronium ion **2.42**, a good electrophile. [2.2]Paracyclophane attacks to generate the arenium ion intermediate **2.43**, from which the conjugate base of the initial acid abstracts a proton and aromaticity is restored (Scheme 2.27). We believe problems arise when over-nitration, oxidation or skeletal rearrangement of [2.2]paracyclophane occurs under these still harsh conditions.



SCHEME 2.27: Nitration of [2.2]paracyclophane.

Formylation

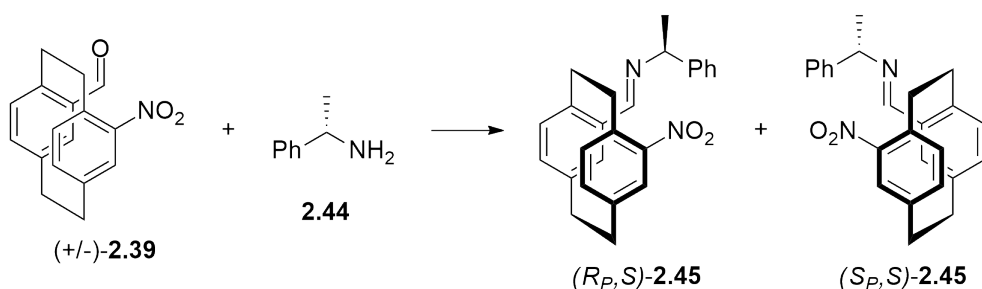
The Reiche formylation used in the oxime methodology was also employed with good results here. No optimisation was required. This reaction proceeded well on 4-nitro[2.2]paracyclophane **2.38** (Scheme 2.28) with yields averaging 80%. Even with the strongly electron withdrawing nitro group, [2.2]paracyclophane can still be considered a good nucleophile on the non-substituted deck. The product **2.39** was easily purified using column chromatography. These conditions are discussed in more detail in Section 2.3.2.



SCHEME 2.28: Formylation of 4-nitro[2.2]paracyclophane.

Resolution of 4-nitro-13-carboxy[2.2]paracyclophane

Reversible imine formation between a chiral amine and the 4-nitro-13-carboxy[2.2]-paracyclophane was investigated to determine the suitability for resolution of the R_P - and S_P - stereoisomers at this step in the synthesis. Imine formation between (*S*)-1-phenylethylamine **2.44** and the aldehyde group of 4-nitro-13-carboxy[2.2]paracyclophane **2.39** was easily performed and using (*S*)-1-phenylethylamine gave the product as a mixture of diastereomers, (R_P,S)-**2.45** and (S_P,S)-**2.45**, which if separated, could undergo imine hydrolysis to yield the title compound in enantiomerically pure form (Scheme 2.29). While the imine formation was successful and resolution by recrystallisation of the imine was proven possible, the recrystallisation was unreliable, and therefore this method of resolution was not used.

SCHEME 2.29: Synthesis of **2.45**.

[2.2]Paracyclophane compounds tend to readily solidify due to their limited solubility and rigid structure with strong ability for π - π interactions that encourage uniform packing. 1-Phenylethylamine has been used as a resolving agent in similar cases, such as the mono-aldehyde 4-carboxy[2.2]paracyclophane.^{51,197}

The best recrystallisation conditions for the imine were dissolving in hot toluene with slow cooling to -18°C ; however it did not produce crystals suitable for X-ray crystallography. [2.2]Paracyclophane derivatives tend to produce needles or long,

flat crystals that are difficult to examine with X-ray crystallography. All but the largest needle-shaped crystals are difficult to align in the X-ray beam.

One diastereomer of the product could be crystallised from the crude reaction material (Scheme 2.29). The mother liquor is enriched in the other diastereomer. This was seen in the proton NMR spectrum of imine **2.45** before crystallisation, and after: two peaks at 8.36 and 8.23 ppm are seen for the C(H)=N proton, each relating to one diastereomer, in the unresolved imine's spectrum; the crystals' spectrum shows only one peak. The mother liquor's ^1H NMR contains the two peaks but is enriched in the other peak (Fig. 2.30). Without X-ray crystallography data it proved impossible to determine which diastereomer is which.

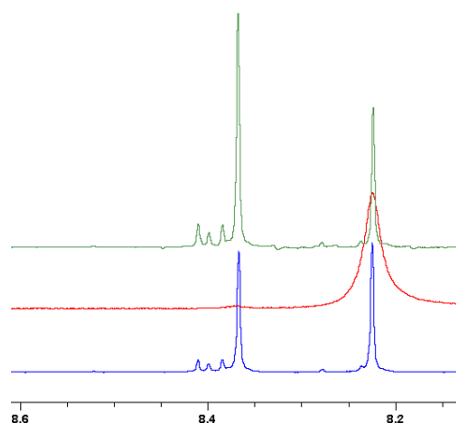


FIGURE 2.30: The C(H)=N peak region on the ^1H NMR spectrum of **2.45**. Bottom to top: unresolved mixture of diastereomers (blue); crystals of pure diastereomer (red); enriched mother liquor (green).

An additional problem was that ideal conditions that reliably produced crystals were difficult to deduce since the compound was equally likely to form an oil as a solid after work up. If there was too much solvent remaining in the oil, crystals would not form using any method. Trituration did not improve the outcome.

The crude imine product could not be purified using silica gel chromatography since the acidity of the silica was sufficient to cleave the imine. In fact, one method of cleaving the imine after resolution of the diastereomers used in this project was stirring the compound in a thin silica/ CH_2Cl_2 slurry. This method was devised after observing significant cleavage of the imine after attempted purification of **2.45** on a silica gel column and is also used in the literature.¹⁹⁷

Cleavage of the imine after separation of the diastereomers afforded enantiopure or enantioenriched (in the case of the diastereomer that remained in the mother liquor) (*R*_P)-**2.39** and (*S*_P)-**2.39**. These enantiomers are identical to most forms of analysis (NMR, mass spectrometry, IR); chiral HPLC on an OD-H column can distinguish between the enantiomers.

This method for resolving the enantiomers of the [2.2]paracyclophane derivative was not favourable since we could not find conditions to reliably crystallise the compound.

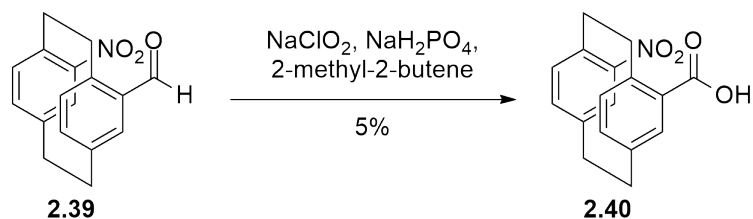
Aldehyde oxidation to carboxylic acid

There are a wealth of options for oxidation of an aldehyde to a carboxylic acid: from the reagents familiar from undergraduate chemistry courses, like Cr(IV) species (chromate or dichromate salts), Cu(II) salts (Benedict's and Fehling's reagents) and KMnO₄; to sodium chlorite and hypochlorite, orthoperiodic acid, potassium peroxymonosulfate, aerobic oxidation and others.^{198–203} While it is a textbook reaction, it is not necessarily that easy in practice, as was proven here.

Oxidation by potassium permanganate was initially avoided due to harsh conditions and problems other Rowlands group members had encountered. As the nitration had shown, [2.2]paracyclophane and the nitro derivative are not as robust as we expected under strongly oxidising conditions. Concerns about its interference with other functional groups were raised in similar [2.2]paracyclophane compounds as observed by an intern working in our group.²⁰⁴ For this reason, and since such a wealth of options exist for oxidising an aldehyde to a carboxylic acid, we screened a variety of other reagents first.

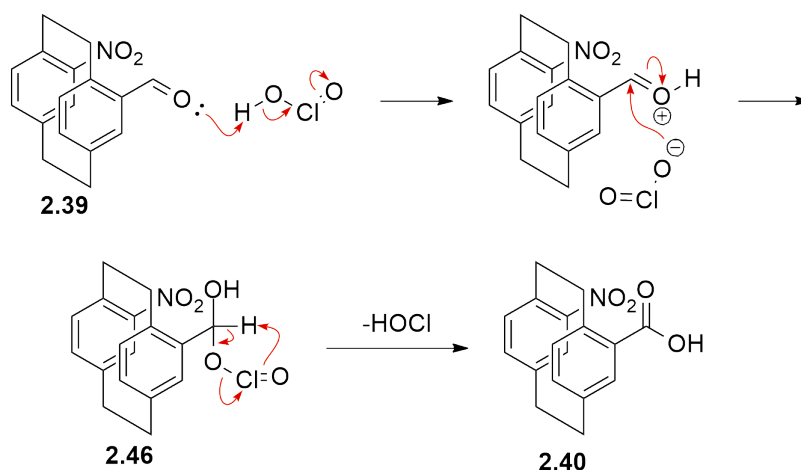
Pinnick oxidation conditions were chosen first, since it is a mild method that does not interact with other functional groups and is effective with sterically hindered compounds (Scheme 2.31).¹⁹⁸ These conditions met a small initial success, yielding approximately 5% (as measured by NMR spectroscopy) of the carboxylic acid. This was unrepeatable on following attempts with the same conditions, and no attempts at varying conditions were successful. Solvents tested were DMSO/H₂O, and also MeCN/H₂O which enabled the reaction to be run cooler than room temperature;

and increasing the equivalence of the reagents all resulted in no increase in conversion to the desired carboxylic acid.



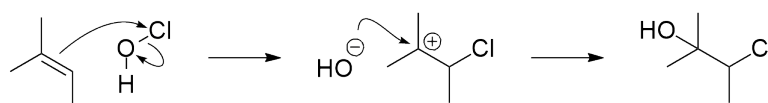
SCHEME 2.31: Pinnick oxidation of **2.39**.

The reaction mechanism is detailed in Scheme 2.32: First the aldehyde **2.39** is protonated and the chlorite attacks the aldehyde's carbonyl carbon. The tetrahedral intermediate rearranges **2.46** in a 5-membered transition state to oxidise the aldehyde to the carboxylic acid **2.40** and reduce the chlorine atom to hypochlorous acid.



SCHEME 2.32: Oxidation mechanism of aldehyde **2.39** using Pinnick conditions.

2-Methyl-2-butene is present in excess as a chlorine scavenger (Scheme 2.33): its C=C undergoes addition from the HOCl, removing the generated HOCl from the reaction mixture. This prevents hypochlorite from participating in side reactions with the chlorite that hinder the aldehyde oxidation.



SCHEME 2.33: 2-Methyl-2-butene as chlorine scavenger.

On the small scale this reaction was attempted (<100 mg) it is possible that measuring inaccuracy meant that less than the 1.75 molar equivalents necessary of 2-methyl-2-butene were present to halt the formation of the chlorine dioxide that impedes oxidation. The container of 2-methyl-2-butene present in the lab was also over 20 years old and may have degraded upon storage. As other oxidants, listed below, did not work it is possible that either the electron withdrawing nitro group hinders oxidation, or that the sterically challenging pseudo-*gem* aldehyde cannot be easily attacked and hence slows oxidation.

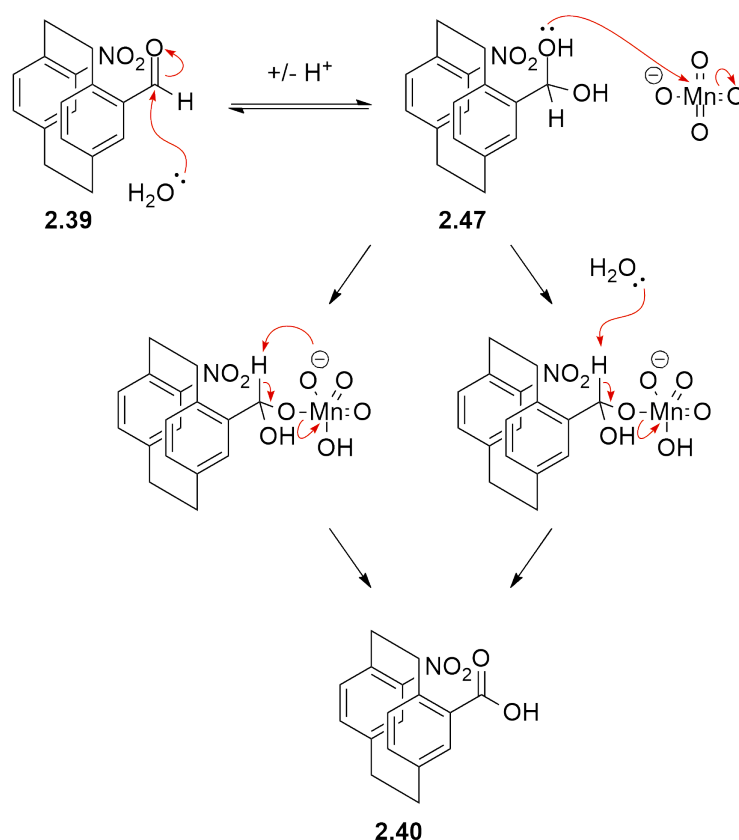
Nonetheless, alternative conditions for oxidation of the aldehyde by NaClO₂ were investigated, using TEMPO with NaClO as a catalyst.²⁰⁵ Although these conditions were designed for oxidising primary alcohols to the carboxylic acid, since they quickly convert the intermediate aldehyde to the carboxylic acid, they are commonly used for this oxidation and are suitable for the purpose of the required transformation.^{206,207} In a similar vein, NaClO oxidation catalysed by TEMPO and KBr was investigated, both in aqueous solvent and in a two-solvent system with phase-transfer catalyst (Starks' catalyst).²⁰⁸ These conditions all returned only starting material.

Potassium peroxymonosulfate (KHSO₅) in DMF, conditions previously shown to perform well with aromatic aldehydes with an electron withdrawing group,²⁰² were also used and found to be ineffective with 4-nitro-13-carboxy[2.2]paracyclophane. An oxidation of 4-acetyl[2.2]paracyclophane to the carboxylic acid reported by Richards *et al.*²⁰⁹ using hyperbromite was also ineffective. It appears that in the latter case, the nitro substituent interferes with the oxidation since Richards' oxidation was on the monosubstituted acetyl compound.

It was clear that the oxidation of **2.39** was more challenging than we had originally envisaged. Seeking further options, potassium permanganate was tested as an oxidant and found to be suitable in this case. Oxidation occurred to give **2.40** with 65% yield along with recovery of 30% starting material. This makes the yield 95% with respect to recovered starting material. We suspected that the incomplete reaction of the starting material could be due to either the reduced manganese reagent reacting with remaining KMnO₄; or that the acetone solvent was itself being oxidised by the KMnO₄. Evidence for the latter was the smell of acetic acid detected during work

up. Steps to counteract the incomplete reaction of the substrate included the addition of HCl to the reaction mixture to increase the oxidising potential; adding further equivalents of KMnO_4 part-way through the reaction time; and using *t*-BuOH as solvent instead of acetone. Unfortunately, these all proved ineffective. The best course of action was to collect the returned starting material and repeat the reaction.

The reaction mechanism is assumed to proceed in the usual manner for a KMnO_4 oxidation (Scheme 2.34).^{210,211} Water attacks the $\text{C}=\text{O}$ electrophile, giving the hydrate **2.47**. One oxygen atom attacks the permanganate, then proton transfer oxidises the tetrahedral carbon to give the carboxylic acid **2.40**.

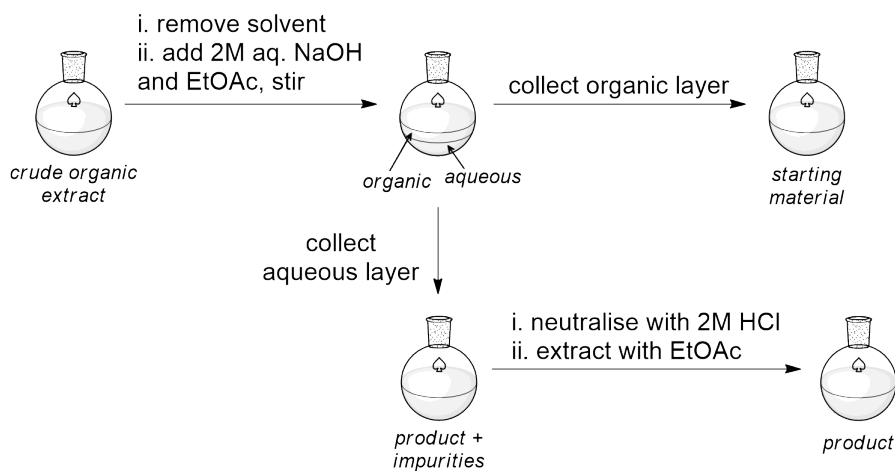


SCHEME 2.34: Oxidation of aldehyde **2.39** using KMnO_4 .

While this methodology gave the desired product, the work-up could be problematic with the metal waste causing turbidity which can disguise the aqueous/organic solvent interface. This could be minimised by filtering the crude reaction mixture to remove the solids. However, this decreased the yield of the product from approximately 60% to 30%, which was probably simply due to incomplete extraction of the product from the retained solids during filtration. A better alternative to expedite

work-up was using a straight-walled separating funnel, rather than a round shaped funnel, which allowed the layers to settle much faster. Addition of an acid to the reaction mixture at the start of the reaction did not increase conversion of the starting material to the product.

The inclusion of a carboxylic acid allows acid/base extraction protocol to remove any impurities, and isolate unreacted starting material. In fact, this step is so effective at delivering the pure compound that the previous two nitration and formylation steps can be completed without further purification, and the crude 4-nitro-13-formyl[2.2]paracyclophane may be used in this reaction. The acid/base work up delivers pure 4-nitro[2.2]paracyclophane-13-carboxylic acid with good yield (Scheme 2.35).



SCHEME 2.35: Acid/base work up procedure for aldehyde oxidation.

The purification involved the following steps: first the solvent is removed from the crude organic extract since it contains a large volume of acetone which can inhibit complete separation of the starting material and product in the next step. The solids, containing a mixture of the aldehyde starting material, the carboxylic acid, retained impurities from previous steps, and their side products, are partitioned between EtOAc and 2 M aqueous NaOH with vigorous stirring. The EtOAc layer contains the unreacted aldehyde starting material, and may be concentrated to recover it. The aqueous layer contains the sodium carboxylate salt of the desired product, which may be retrieved by acidifying the solution to around pH 2-3 with HCl. The carboxylic acid precipitates from solution and can be collected by filtration or organic

extraction of the aqueous phase. Filtration may give a slightly purer product than extraction but at the cost of lower yield.

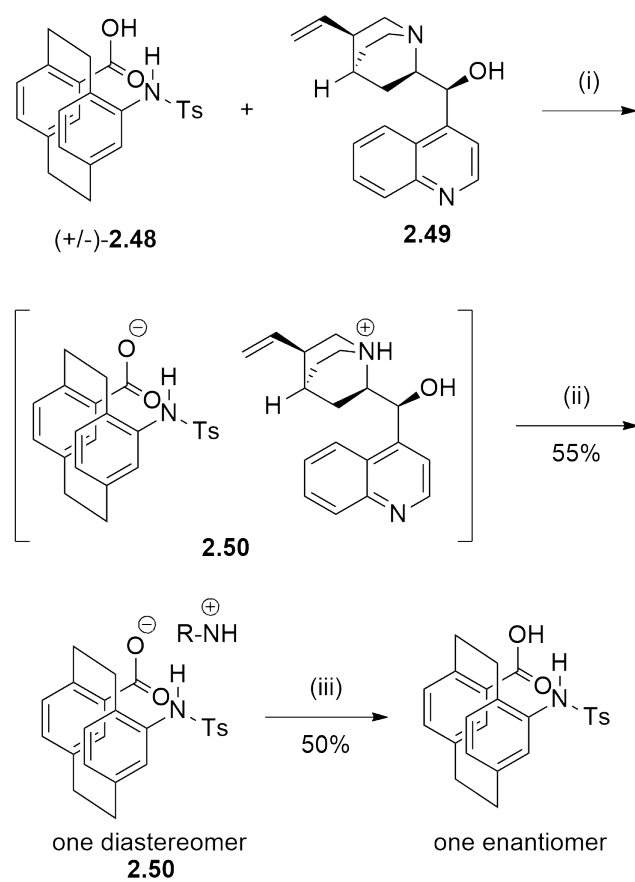
Resolution of 4-toluenesulfonylamido[2.2]paracyclophane-13-carboxylic acid

A possible method for resolution of [2.2]paracyclophane carboxylic acid derivatives that was considered was recrystallisation of diastereomeric salts. Due to difficulties recrystallising the desired compound discussed below, this method of resolution was not developed further.

Members of the Rowlands group used cinchonine **2.49** to form a salt with the carboxylic acid of *N*-tosyl Pca **2.48** (Scheme 2.36).^{20,212} Since tosylation of the amine was not part of the synthetic pathway, this method for resolution added an extra two steps: tosylation and then deprotection. There were also concerns about the ease of cleavage of the tosyl group from the nitrogen. Despite these apprehensions, resolution of *N*-tosyl Pca by recrystallisation of the cinchonine salt was trialled as a possibility, since this resolution would also act as a model for the Pca system. Recrystallisation conditions would be expected to be comparable between Pca and its *N*-tosyl derivative.

According to previous work in the Rowlands group, crystallisation of the salt was attempted using minimal hot acetone. The cinchonine in stock was not soluble in acetone, nor was the salt formed in these experiments. Using methanol instead of acetone produced satisfactory results. The salt **2.50** formed with high yield and purity and one diastereomer of the salt crystallised with hot methanol. The salt was neutralised with hydrochloric acid and the resultant 4-toluenesulfonylamido[2.2]paracyclophane-13-carboxylic acid was >99.9% enantiopure. The yield of this experiment is low but could be improved by optimisation of the protocol. The experiment was run at a small scale (100 mg), and the amount of transfer loss at this scale was significant. In the starting material the two enantiomers were present in 1:3 ratio due to use of previously enantioenriched material.

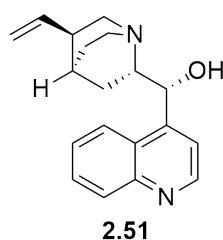
This result was confirmed by HPLC. Enantiomer A has a retention time of 13.232 minutes on an AD-H column running 80:20 hexane/*i*-PrOH @ 1 mL/min and enantiomer B has a retention time of 17.506 minutes. No crystal structure was obtained



SCHEME 2.36: Resolution of **2.48** by crystallisation of the cinchonine salt. i) MeOH. ii) crystallisation and collection of the crystals. iii) HCl.

so the absolute configuration of the enantiomers is not known.

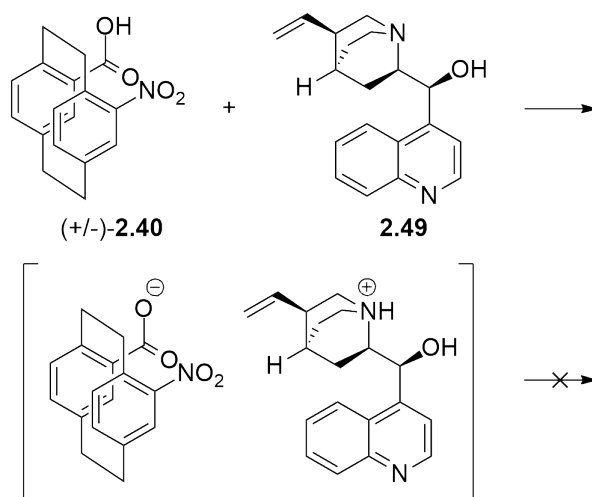
Successive crystallisations would produce an enriched mother liquor; however if both enantiomers of **2.50** were required perfectly enantiopure it might in theory be possible to achieve this by also running the same crystallisation method with the pseudo-enantiomer of cinchonine, cinchonidine **2.51** (Fig. 2.37). With the same stereochemistry in the piperidine cyclic system, the compound is often used to achieve resolution of the opposing enantiomer to cinchonine.



SCHEME 2.37: Cinchonidine.

Resolution of 4-nitro[2.2]paracyclophane-13-carboxylic acid

Following the success of using chiral alkaloids to separate the diastereomers of other [2.2]paracyclophane carboxylic acids, cinchonine was used as a resolving agent for 4-nitro[2.2]paracyclophane-13-carboxylic acid **2.40** (Scheme 2.38).



SCHEME 2.38: Attempted resolution of **2.40** with cinchonine.

However, no crystals of this compound could be formed from conditions tested: solvents tested were acetone and methanol, with both hot recrystallisation and slow evaporation tested for each. The pseudo-enantiomer of cinchonine, cinchonidine,

was also tested but no success was found in crystallising this salt either. Since few crystallisation conditions were tested, it is quite possible that this is a viable route. Resolution at this stage was abandoned since no progress was made after some time and we suspected after formation of pseudopeptides with Pca and natural amino acids, the diastereomeric compounds might be easier to resolve by column chromatography or recrystallisation.

Nitro reduction to amine

Aryl nitro reduction is another transformation that is documented with a large number of reagents described in the literature - to name just a few: catalytic hydrogenation (on Pd or Pt), hydrazine, Fe/H⁺, Sn(II) and Na₂S. The reduction has been described in the [2.2]paracyclophane literature, as well, with reagents employed including Adam's catalyst (Pt(IV) oxide) and Pd-C catalysed hydrogenations and Fe/HCl.^{173,196,213-217} However, none of the described methods have resulted in such an unusual compound that is both an electron rich aniline analogue or a bidentate aryl pseudoamino acid.

Previously, the Rowlands group has used iron with hydrochloric acid to reduce 4-bromo-13-nitro[2.2]paracyclophane, so these conditions were considered a good starting point for the reduction of 4-nitro[2.2]paracyclophane-13-carboxylic acid **2.40**.²¹⁵

While these conditions gave the desired product, the yield was an unattractive 50%. Worse, the reaction produced a mixture of amino acid and a significant amount (approximately 20%) of a side product: the methyl or ethyl ester of the carboxylic acid, depending on the alcoholic solvent used. The alcoholic solvent was required due to solubility issues. While the ester is easily hydrolysed using basic ester hydrolysis conditions, other concerns lead to a search for more appropriate means of reducing the nitro group to an amine. These concerns were that high pH raised safety concerns when the reaction was performed at larger scales, and made neutralisation time consuming and increased the volume of the aqueous phase; and that solubility of the product is low in most common laboratory solvents, which, combined with dilution of the aqueous phase, made extraction of the product from the bulk reaction mixture during work up laborious and inefficient.

Reduction using tin and hydrochloric acid had similar problems as the iron conditions; in addition, separation of the product from the residual tin was difficult. Thus, the product could not be analysed by NMR spectroscopy, due to the presence of the paramagnetic tin which causes peak broadening. The quality of the spectrum may have been further deteriorated by coordination of the ions to the [2.2]paracyclophane compound.

As a result we decided to screen other reductions. Reducing conditions with sodium borohydride and nickel(II) chloride produced no reaction.²¹⁸

Catalytic hydrogenation,²¹⁹ another method for the reduction of nitroarenes that uses palladium on charcoal also produced some initial success with traces of product but the yield could not be improved much. Addition of an acid, such as hydrochloric acid, to the reaction mixture increased the yield from 30%, since amines have the tendency to adsorb to the palladium catalyst. Acidification causes the lone pair on the nitrogen to be unavailable for adsorption. This method had the advantage of an easy work up: merely filtration over celite. However, the reaction was slow and took over 16 hours at 50 °C, which is much longer than usual for a catalytic hydrogenation. The extended reaction time resulted in the formation of side products that we suspect are cleavage of the ethylene bridges of [2.2]paracyclophane.

Zinc activated with ammonium chloride was found to be a milder reduction that produced less side product, giving <5% methyl ester.²²⁰ This zinc reduction proceeds by the following mechanism, where the ammonium chloride is the acid and zinc is the electron donor (Scheme 2.39).

A N-O- oxygen is protonated by ammonium chloride. Zinc donates two electrons, one at a time, to the positively charged nitrogen atom, creating a negative charge on the unprotonated oxygen, which is then protonated by another molecule of ammonium chloride. An oxygen is further protonated to the positively charged state, making a good leaving group. Expulsion of the water molecule creates the protonated nitroso compound **2.52**. Single electron transfer (from zinc) to the nitrogen gives the free radical **2.53**. This is quenched by a further single electron transfer

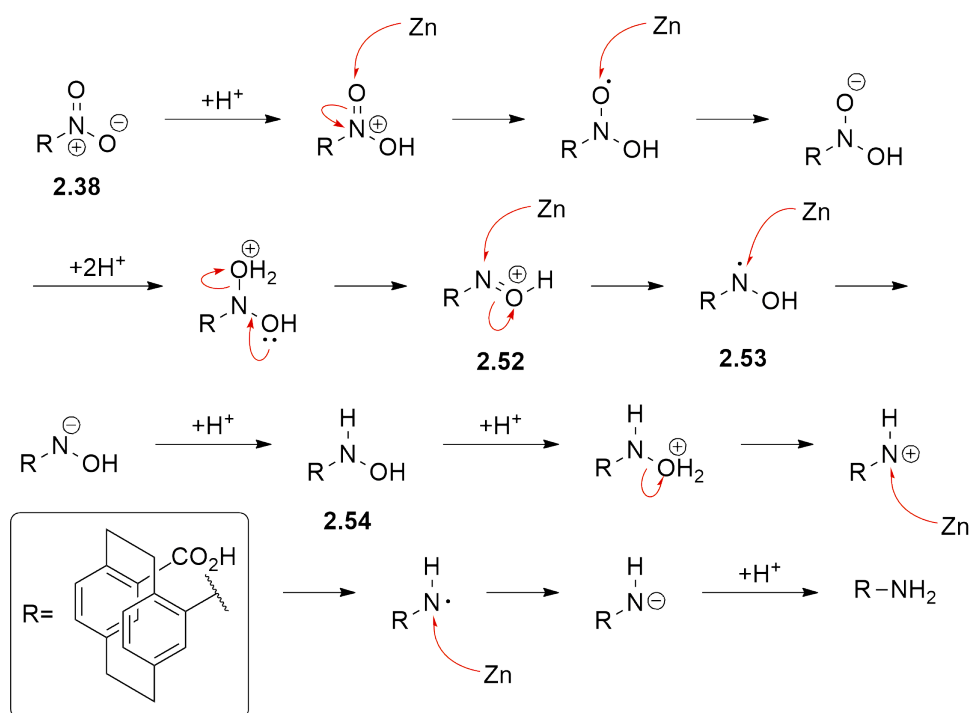


FIGURE 2.39: Reduction of the aryl nitro group to the amine with zinc and ammonium chloride.

and subsequent protonation of the nitrogen atom, giving the intermediate hydroxylamine **2.54**. Protonation of the -OH moiety allows water elimination. Two final single electron transfers and then nitrogen protonation forms the amine. The change in formal charge of the nitrogen from +4 to -2 requires 3 equivalents each of zinc and ammonium chloride.

These conditions were favourable compared to the conditions using iron and hydrochloric acid, or catalytic hydrogenation; the yield was acceptable at 65-80%, and very little side product formation occurs. The literature example of this reduction on 2-nitroazobenzene runs for only 2 hours, where reduction of nitro[2.2]paracyclophane derivatives required overnight heating. [2.2]Paracyclophane's slower reaction time could be due to its bulkiness and decreased reactivity of the nitrogen.

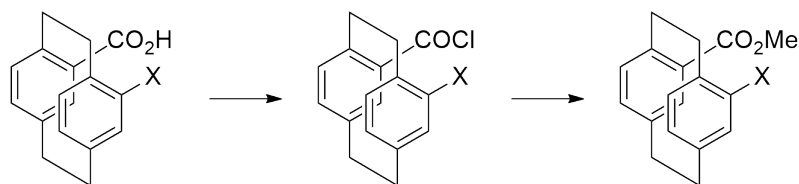
Filtration of the crude reaction mixture yields a mixture of the desired product and the remaining ammonium salts. This crude material matches the pure amine by TLC, ¹H NMR and mass spectrometry analysis; however the reaction yield is inflated to over 100%. The salt is easily removed by washing the crude solid with water.

The small amount of methyl ester side product was deemed acceptable, especially since amine derivatives of [2.2]paracyclophane make purification by chromatography difficult, with many compounds co-eluting despite retention factor gaps of greater than 0.3; they also tend to streak or even remain at the top of the silica. Since silica is acidic it can bond to the basic amines on the compound and inhibit their elution. In the case of 4-amino[2.2]paracyclophane-13-carboxylic acid, the compound may form a zwitterion that is highly attracted to silica and does not elute smoothly. It is also possible that the compounds exhibit intermolecular hydrogen bonding so are not cleanly separable. Additionally, removal of the methyl ester was often unnecessary since most synthetic pathways involved formation of the methyl ester.

Since the 4-amino[2.2]paracyclophane-13-carboxylic acid product is problematic to purify by column chromatography due to its tendency to adhere to the silica and streak down the column, attempts were made to purify at this step by recrystallisation. No suitable solvent system was found. This compound is remarkably insoluble in most solvents, with DMSO and DMF the only solvents which allow full dissolution.

Methyl ester protection of the carboxylic acid

As discussed above, methyl ester protection of the carboxylic acid can occur at several points in the synthesis of Pca. The most effective method is largely the same as in the oxime methodology: acyl chloride formation in neat thionyl chloride, then reaction with dry methanol (Scheme 2.40). Other ester protection methods that were trialled included acyl chloride formation with oxalyl chloride and an interesting set of conditions involving oxone (KHSO_5); these were not used since they gave less complete conversion to the ester or were more time-consuming.



SCHEME 2.40: Methyl ester protection of carboxylic acid *via* acyl chloride.

2.4 Conclusion

An updated route to 4-amino-13[2.2]paracyclophane-carboxylic acid (Pca) was developed and optimised (Scheme 2.41). The synthetic route comprises four steps with an overall yield of 50%. This compares with previous routes which had yields between 7% and 45% for 6 - 7 steps. The synthetic route is as follows: first, [2.2]paracyclophane is nitrated. Then, formylation gives the pseudo-*geminal* aldehyde. The aldehyde is oxidised, furnishing the carboxylic acid. The nitro group is reduced to the amine, giving Pca.

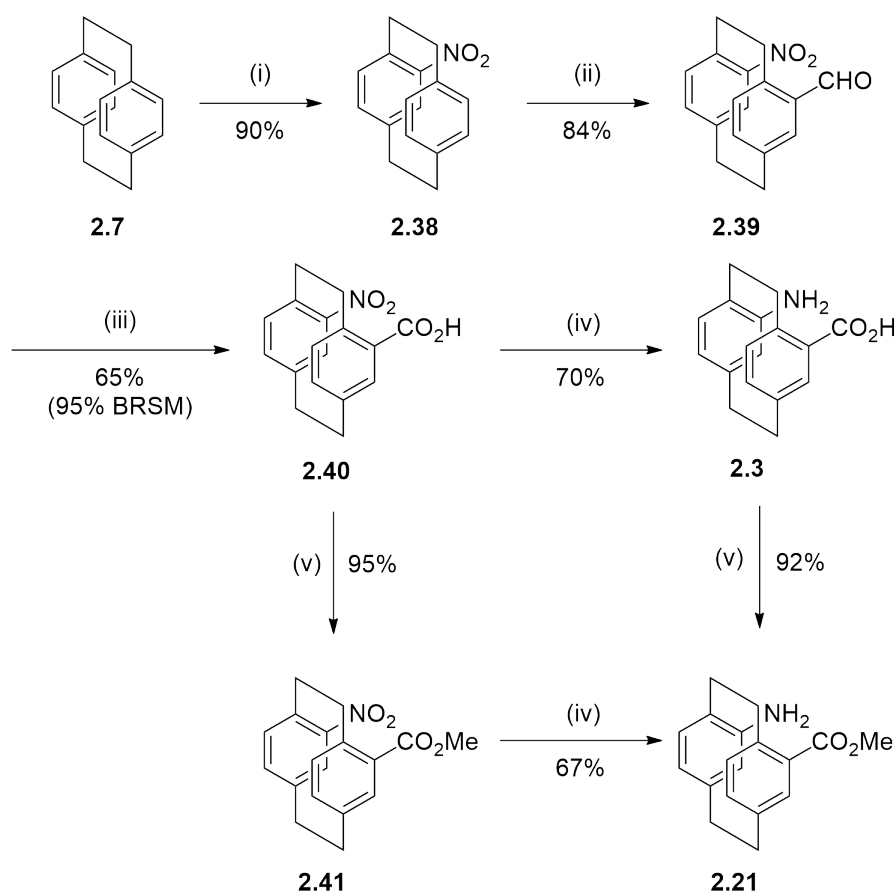


FIGURE 2.41: Optimised route for synthesis of Pca. i) HNO_3 , H_2SO_4 . ii) TiCl_4 , $\text{CH}_3\text{OCHCl}_2$. iii) KMnO_4 . iv) Zn , NH_4Cl . v) a. SOCl_2 b. MeOH .

Protection of the carboxylic acid is required for further elaboration of the N-terminus of Pca. The carboxylic acid may be protected with methyl ester formation either before, or after reduction of the nitro group to the amine, with little effect on the overall yield of the synthesis of Pca-OMe.

Resolution of the planar chiral enantiomers was attempted at two steps, with neither deemed satisfactory (Scheme 2.42). In both cases, recrystallisation of the formed diastereomeric compound or salt was problematic. Resolution of diastereomers was instead achieved for some compounds once coupled to natural amino acids: see Chapter 3.

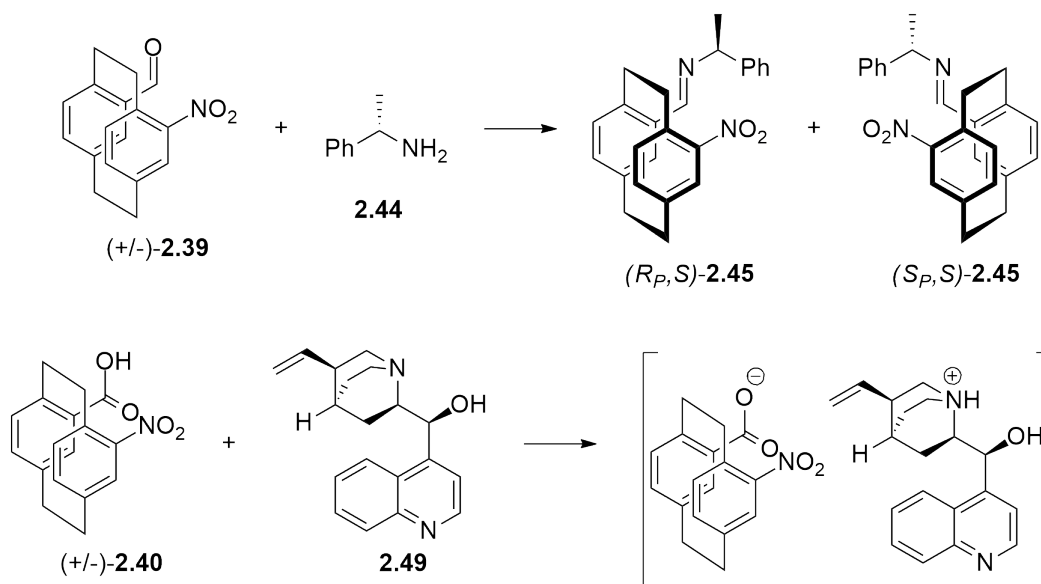


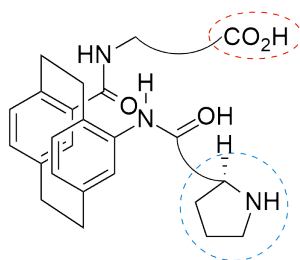
FIGURE 2.42: Diastereomer formations for attempted resolution by recrystallisation during Pca synthesis.

Chapter 3

Synthesis of 4-amino[2.2]paracyclophane-13-carboxylic acid pseudopeptides

3.1 Pseudopeptide design rationale

Pseudo-*geminal* Pca was selected as the isomer for the [2.2]paracyclophane-modified amino acid around which small peptides would be assembled (Fig. 3.1), since it was predicted to be the easiest to make (see Section 2.2).



3.1

FIGURE 3.1: Model peptide structure design.

At the N-terminus of the model Pca pseudopeptide **3.1** (outlined in blue in Fig. 3.1), we require a proline residue since its formation of a nucleophilic enamine from many aldehydes and ketones is a key factor in many organocatalytic reactions. The preference is for the proline residue to be directly coupled to the Pca residue so that we have increased control of the conformation through greater rigidity and less conformational freedom (**3.2**). A “linker” residue might also be included between these

two residues, in the sequence Pro-Xaa-Pca (3.3) (Fig. 3.2) but this might dilute the influence of the Pca.

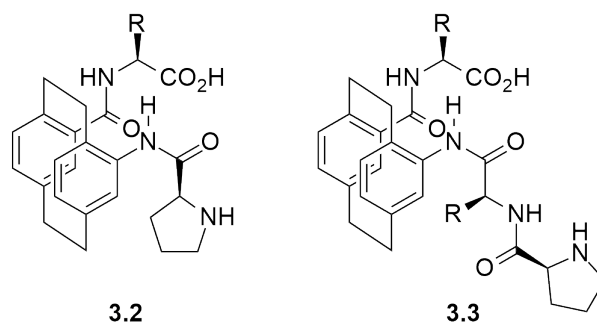


FIGURE 3.2: Examples of potential peptide structures with variations at the N-terminus.

The C-terminus' particular amino acid residue is less important (red outline in Fig. 3.1); we require a proton source for the catalysis mechanism and hope to hydrogen bond one or more components of the reaction. Any amino acid would suffice in providing a carboxylic acid for this purpose. This provides an opportunity to vary the residue at the C terminus to vary the spatial position of the carboxylic acid, the stereochemistry, and the bulk of the residue. Our goal was to alter these variables and study the difference in catalytic selectivity between carboxylic acid moieties at different lengths or orientations from the Pca scaffold.²²¹ This variation could be achieved by comparing Pca peptides with C-termini residues of, for instance, aspartic acid (3.4) and glutamic acid (3.5) (with their α -carboxylic acid groups protected); another amino acid with its α -carboxylic acid (in syntheses in this project, phenylalanine (3.6) and valine were extensively used for their ease of characterisation); and the carboxylic acid of Pca itself (3.7) (Fig. 3.3).

The two chains extending from the Pca residue's C- and N-termini should interact to control conformation - and effectively control secondary structure. They may also position reaction substrates. Our hypothesis was that [2.2]paracyclophane would provide an advantageous platform for controlling conformation of catalysts and studying the effects thereof in asymmetric organocatalysis. Effectively, it would be a β -turn mimic.

In the following sections each type of coupling reagent will be discussed as it is first mentioned, or where most relevant, with its mechanism of action. In other

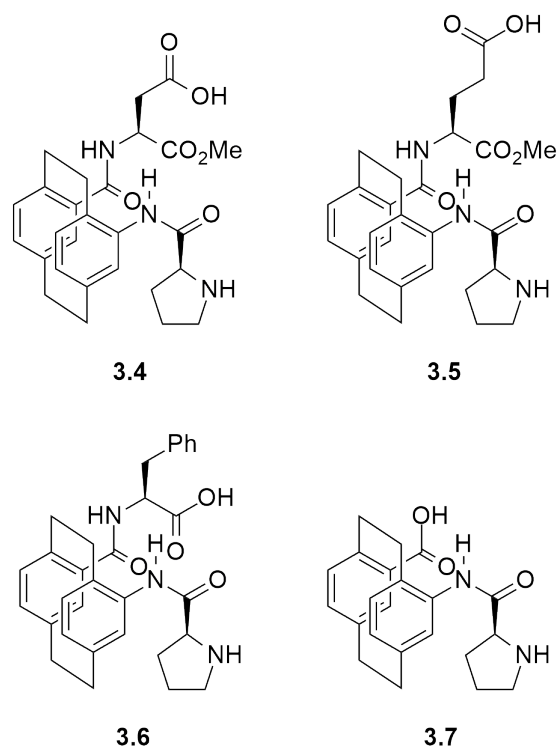


FIGURE 3.3: Examples of potential peptide structures with variations at the C-terminus.

synthetic routes it will be referenced briefly, with additional discussion focussing on particular information relevant to that substrate and any characteristics that may affect the coupling conditions. Interested readers are referred for further reading to an excellent review by Albericio and El-Faham, which covers the “letter soup” of peptide coupling reagents available to a chemist and influenced the choice of reagents.⁷⁸

3.2 Coupling studies with [2.2]paracyclophane analogues

Before synthesis of 4-amino[2.2]paracyclophane-13-carboxylic acid was complete, studies of amide couplings using analogues of the compound were conducted. The reason for this was we anticipated that couplings of aniline derivatives would be more challenging than alkyl amines due to delocalisation of the nitrogen lone pair and, in our case, the increased bulk of the Pca framework. Three analogues were studied: *o*-toluidine **3.8**, anthranilic acid **3.9**, 2,6-diaminotoluene **3.10** (Fig. 3.4). We anticipated this would aid in uncovering peptide coupling conditions for the

more complicated [2.2]paracyclophane system, and troubleshoot any initial problems found.

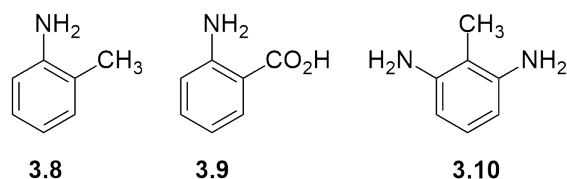


FIGURE 3.4: Pca analogues.

2,6-Diaminotoluene was included in this study both as an analogue of a [2.2]paracyclophane aniline for peptide coupling studies; and since resultant peptides might be further modified to become potential asymmetric organocatalysts themselves. 2,6-Diaminotoluene has two amine groups *ortho* to a methyl group. The presence of the methyl group simulates the steric and electronic effects of the ethylene bridges of [2.2]paracyclophane, creating an electron-rich and sterically hindered aryl ring. The two amines in close proximity to each other are obvious spots for functionalisation to create a binding pocket for organocatalysis. The central methyl group might be oxidised to a carboxylic acid, providing a chiral proton donor that would catalyse numerous useful reactions. Examples of this system were seen in papers by Pearson for aldol reactions, and Moriyama for Friedel-Crafts reactions.^{222,223} Two electron withdrawing amide functionalities on the 2,6-diaminotoluene scaffold assist to increase acidity of the benzoic acid in the catalyst but the main cause of the increased acidity is their hydrogen bonding with the carboxylic acid. A version with protected amino acids coupled instead of achiral elements would have the potential advantage of chirality, possibly permitting stereoselectivity (Fig. 3.5). We supposed that we could make a chiral version while learning about aromatic peptide coupling conditions.

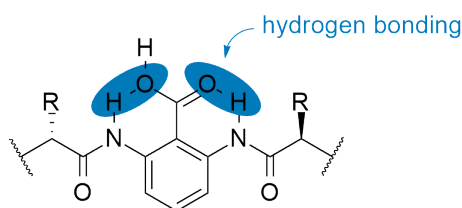


FIGURE 3.5: Example 2,6-diaminobenzoic acid peptide derivative of 2,6-diaminotoluene as Brønsted acid catalyst.

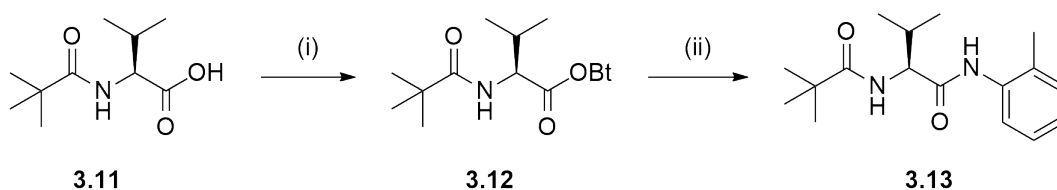
Except where noted, coupling tests were performed using N-protected valine as the

coupling partner, since the isopropyl unit is easy to spot in ^1H NMR. The -CH proton is split by the two -CH₃ groups to give a characteristic septet and the two methyl groups stand out from the other protons in our molecules.

3.2.1 Reactions of *o*-toluidine

The first couplings were performed on *o*-toluidine **3.8**, the mono-amine analogue of 2,6-diaminotoluene. Initial conditions involved attempted coupling *via* either the *N*-hydroxysuccinate ester or the acyl chloride but these were unsuccessful. *N*-Hydroxysuccinimide (NHS) along with dicyclohexylcarbodiimide (DCC) or diisopropylcarbodiimide (DIC) to make the *N*-hydroxysuccinimide ester of *N*-pivaloyl-protected valine was unsuccessful; so the coupling did not proceed in this case due to failed activation of the carboxylic acid.

Fortunately, the acid could be activated as the hydroxybenzotriazole ester which permitted coupling of *N*-pivaloyl valine **3.11** to *o*-toluidine **3.8**. 1-Ethyl-3-(3-dimethylaminopropyl)-carbodiimide (EDC) and hydroxybenzotriazole (HOBT) with 4-dimethylaminopyridine (DMAP) were used to form the activated ester **3.12** (Scheme 3.6). These conditions were successful, however the resultant amides **3.13** were not of interest for further study. A discussion of common carbodiimide coupling reagents, as trialled in this coupling, follows in section 3.2.2.



SCHEME 3.6: Coupling of *N*-pivaloyl valine to *o*-toluidine *via* benzotriazole ester. i) EDC, HOBT. ii) *o*-toluidine, DMAP.

The success of the latter set of coupling reagents suggested that we had found appropriate coupling conditions for Pca. This optimism was proven unfounded since they were not successful in other systems. This might be due to the electron-donating nature of the methyl substituent of *o*-toluidine increasing the reactivity of its aniline nitrogen enough to allow coupling where Pca-OMe's nitrogen is deactivated by the methyl ester and steric hindrance.

3.2.2 Coupling reagent: carbodiimides

A common set of coupling reagents (also discussed in Chapter 1, Section 1.2) for other unnatural amino acids are carbodiimides as dehydrating agents, alone or with HOBt, HOAt or analogues to promote coupling.²²⁴⁻²²⁶ Popular carbodiimide coupling reagents include *N,N'*-dicyclohexylcarbodiimide (DCC), *N,N'*-diisopropylcarbodiimide (DIC), and *N*-ethyl,*N'*-dimethylaminopropylcarbodiimide (EDC) (Fig. 3.7).

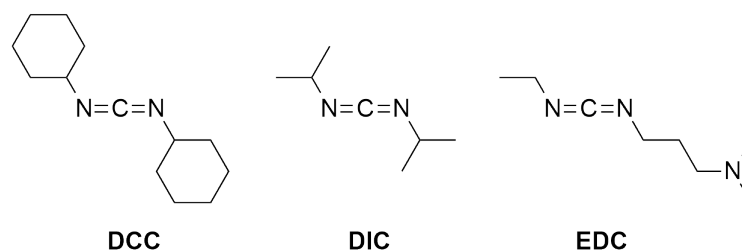


FIGURE 3.7: Carbodiimide coupling reagents, left to right: DCC, DIC, EDC.

Carbodiimides react with the carboxylic acid of an amino acid **3.14** to form the activated *O*-acylisourea species **3.15**. The coupling proceeds *via* several different intermediates (Scheme 3.8, from left to right): the formation of an anhydride **3.17** with a further molecule of amino acid R¹-CO₂H; direct coupling with the N-terminus of the new amino acid to form the desired product **3.18**; and, in the case of an activated carboxylic acid that is the C-terminus of a peptide chain of at least 2 amino acids, formation of an oxazolone **3.19**. The side product in each case is urea derivative **3.16**.

The oxazolone (**3.19**) route is undesirable since it will produce a racemic product under mildly basic conditions (Scheme 3.9) *via* the resonance-stabilised oxazolonium ion **3.20**.²²⁷

The *N*-hydroxybenzotriazole (HOBt) and similar benzotriazole derivatives (Fig. 3.10) function to prevent the unreactive *N*-acylurea **3.21** side product that may form from the *O*-acylisourea **3.15** (Scheme 3.11); an additional benefit is decreased racemisation of the amino acid by preventing intramolecular reaction forming the oxazolone.²²⁸

1-Hydroxy-7-azabenzotriazole (HOAt) and derivatives also gain from the interaction between the aza-N and the carbonyl of the coupled carboxylic acid, increasing reactivity (Fig. 3.12).

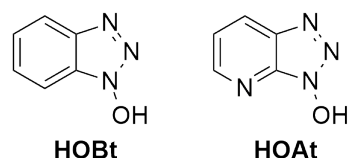
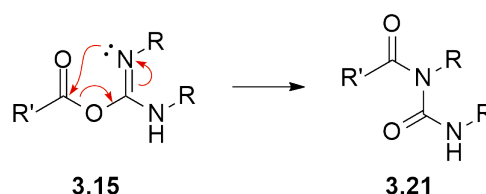


FIGURE 3.10: Example benzotriazole derivative additives. Left to right: 1-hydroxybenzotriazole (HOBt), 1-hydroxy-7-azabenzotriazole (HOAt).



SCHEME 3.11: Formation of *N*-acylurea isomer.

The *N*-hydroxy additives interact in the carbodiimide reaction by substituting with the *O*-acylisourea formed between the carboxylic acid and the carbodiimide reagent. The deprotonated *N*-hydroxy derivative attacks the carbonyl electrophile, substituting the urea derivative and forming the ester, which is slightly less reactive but less prone to isomer formation (Scheme 3.13). This reaction occurs more quickly than the *N*-acylurea formation.

3.2.3 Reactions of anthranilic acid

Anthranilic acid **3.9** was an interesting test subject since it was a single-ring mimic of the target centre compound of this project as it contained both an amine and a carboxylic acid group. The electron-withdrawing nature of the carboxylic acid in this molecule deactivates the aniline further which is relevant for peptide coupling to the *N*-terminus of Pca, since although the functional groups may be on different aromatic rings, transannular electronic communication between the rings still causes a similar effect. As such it was hypothesised that this compound would be a more

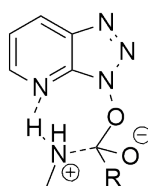
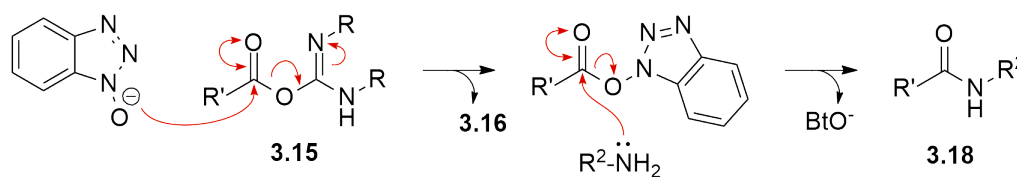


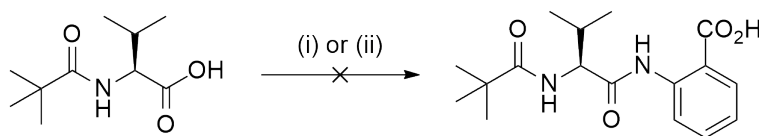
FIGURE 3.12: Neighbouring group effect in HOAt.



SCHEME 3.13: Benzotriazole additives in peptide coupling with carbodiimides.

accurate test compound for couplings before moving on to the more synthetically expensive Pca.

Attempts to repeat the successful EDC/HOBt conditions were met with little success. No reaction was observed. The next attempted conditions were acyl chloride formation with Et_3N which also failed (Scheme 3.14). It is suspected that anthranilic acid's carboxylic acid group interfered with the couplings. Ultimately, it was decided that the model studies were not helpful. Conditions are highly substrate specific so screening Pca itself seemed more efficient.



SCHEME 3.14: Attempted coupling conditions between *N*-pivaloyl valine and anthranilic acid's nitrogen atom. i) a. EDC, HOBt. b. anthranilic acid, DMAP; ii) a. DMF, $(\text{COCl})_2$. b. anthranilic acid, Et_3N .

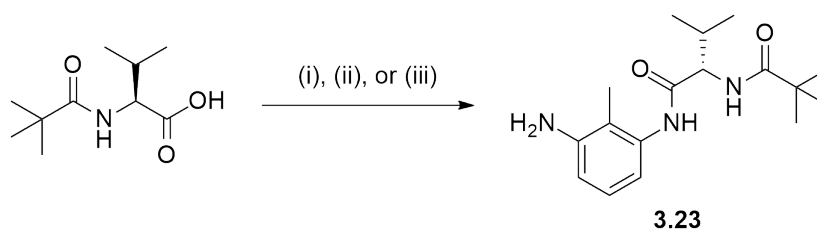
3.2.4 Reactions of 2,6-diaminotoluene

Several attempts were made at coupling amino acids to form a diamide **3.22** from 2,6-diaminotoluene **3.10**. Making a mixed anhydride with 2 equivalents each of ethyl chloroformate and either *N*-pivaloyl valine or Boc-valine, was unsuccessful, with not even mono-coupling occurring (Scheme 3.15). Increasing the stoichiometry of the *N*-pivaloyl valine or the Et_3N did not help.

Most amino acids were available in *N*-protected form if required; otherwise Boc protection was performed with Boc_2O (Scheme 3.16).

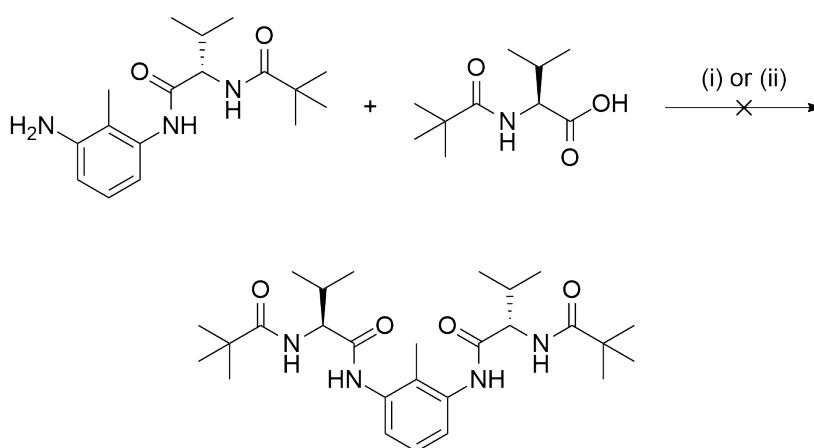
Acyl chloride formation with POCl_3 produced only trace amounts of the mono-coupled product **3.23**; most of the material was returned starting material (Scheme 3.17).

Using the successful peptide coupling conditions from the tests with *o*-toluidine (EDC, HOBt, DMAP), only mono-amide coupling occurred to give **3.23** in 50% yield; using microwave irradiation did not alter this. Other sets of reagents, combined with microwave irradiation, also only produced the mono-coupled product. These reagents included: TBTU, in concert with HOBt and DIPEA; and DCC with NHS and DMAP (Scheme 3.18). Aminium-uronium salts such as TBTU are discussed in the section to follow.



SCHEME 3.18: Attempted coupling between *N*-pivaloyl valine and 2,6-diaminotoluene with peptide coupling reagents. i) a. EDC, HOBt. b. anthranilic acid, DMAP; ii) a. TBTU, HOBt. b. anthranilic acid, DIPEA; iii) a. DCC, NHS. b. anthranilic acid, DMAP.

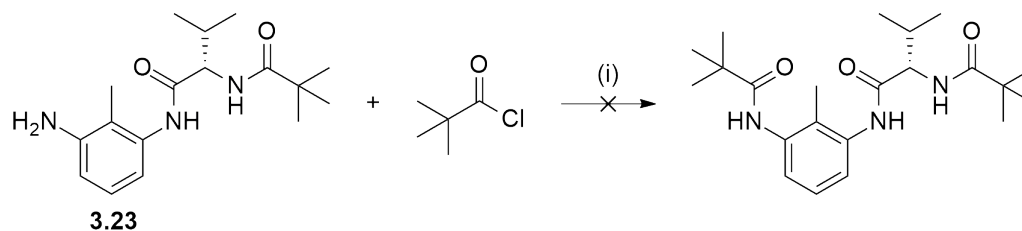
Attempts were made to couple an activated amino acid to the remaining aniline moiety on the purified product of single addition **3.23**. *N*-Pivaloyl valine activated by anhydride formation with ethyl chloroformate failed to give any reaction; neither did the previously successful conditions of EDC and HOBt with DMAP (Scheme 3.19).



SCHEME 3.19: Attempted coupling of *N*-pivaloyl valine to **3.23**. i) a. EtOCOCl. B. **3.23**, NMM; ii) a. EDC, HOBt. b. **3.23**, DMAP

Even coupling a simple acyl chloride in the form of *N*-pivaloyl chloride still gave no reaction (Scheme 3.20). This was worrying with regards to future pseudopeptide

coupling prospects.



SCHEME 3.20: Attempted coupling to *N*-pivaloyl chloride to **3.23**. i) NaOH.

Based on TLC and ^1H NMR and mass spectra evidence, coupling one amino acid was possible using standard peptide synthetic methods. They indicated consumption of the starting material **3.23**, and formation of a new amide product. However, forming the second peptide bond, either in concert with the first coupling, or as a separate step after successful mono-amide formation, was a more difficult task. Steric hindrance from the methyl group and bound amino acid undoubtedly inhibits this coupling. Additionally, the amide group is somewhat electron withdrawing and may lower reactivity of the second aniline such that a further peptide or amide coupling is no longer possible.

In the brief studies conducted on this subject, no successful route to the twice-coupled 2,6-diaminotoluene was found. 2,6-Diaminotoluene was used as a model for investigating coupling conditions for Pca, which has only one aniline group, so this was not necessarily a problem. However, a secondary aim of this strand of research was to develop the twice-coupled products themselves as catalysts, and in this respect, this strand of research was a failure. The continuing failure of the desired reaction is indicative of future problems that would be encountered in forming peptides with Pca.

3.2.5 Coupling reagent: aminium-uronium salts

Aminium-uronium salt reagents include TBTU and HATU, analogues of HOBT and HOAt, respectively (Fig. 3.21).

These reagents may be used independently, without other activating agents like carbodiimides (Scheme 3.22), but may have a tertiary base (such as DIPEA or Et_3N)

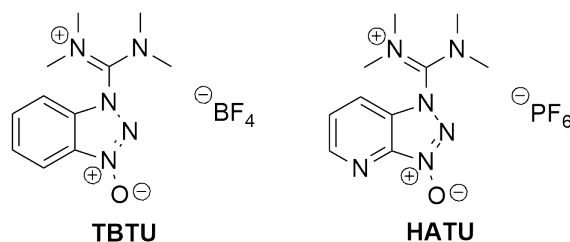
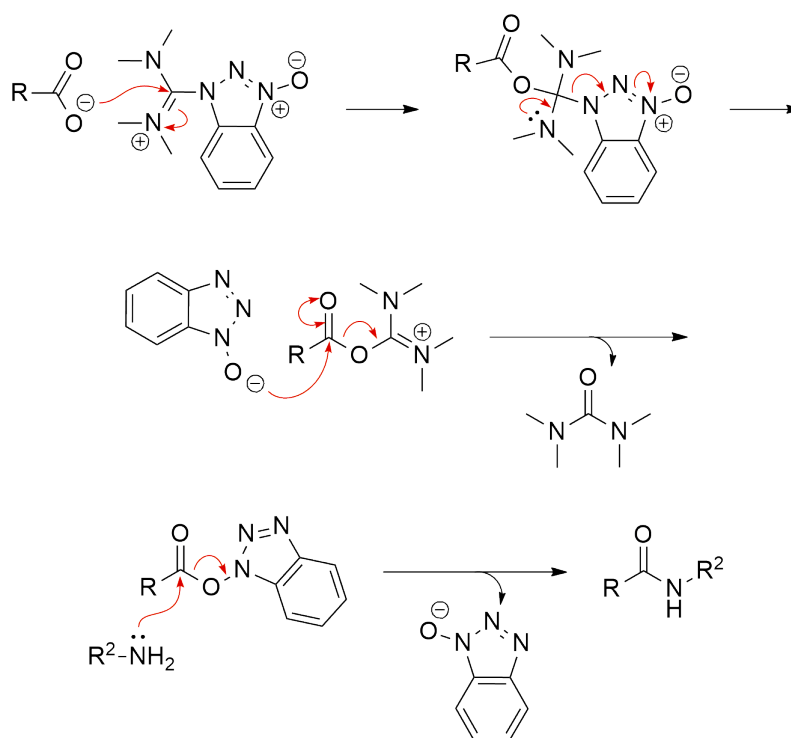


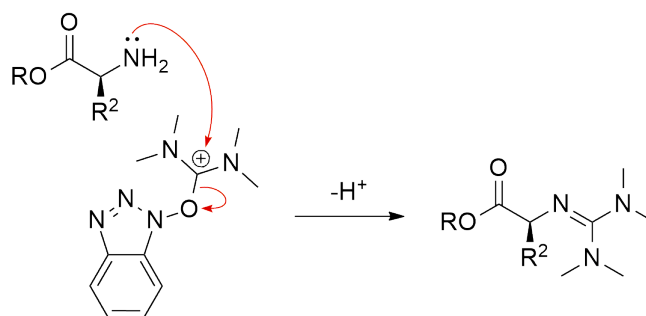
FIGURE 3.21: Aminium-uronium salt peptide coupling reagents. Left: *N*-[(1*H*-benzotriazol-1-yl)(dimethylamino)methylene]-*N*-methylmethanaminium tetrafluoroborate *N*-oxide (TBTU); right: *N*-[(dimethylamino)-1*H*-1,2,3-triazolo[4,5-*b*]pyridino-1-ylmethylene]-*N*-methylmethanaminium hexafluorophosphate (HATU).

present.



SCHEME 3.22: Peptide coupling mechanism with TBTU.

They are named aminium-uronium salt reagents because they may exist in either the uronium (O-linked) or aminium (*N*-linked) form: crystallographic data shows TBTU exists in the aminium isomeric form, which is slightly less reactive. A sub-stoichiometric quantity of these reagents is often used to avoid reaction of the uronium with the amine to form a guanidine, which caps the amino acid and prevents coupling with the appropriate carboxylic acid (Scheme 3.23).²²⁹

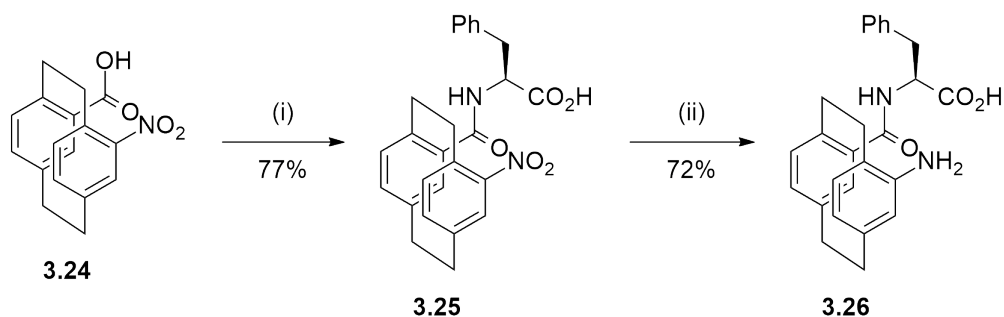


SCHEME 3.23: Undesirable guanidino derivative formation.

3.3 Coupling amino acids with 4-amino[2.2]paracyclophane-13-carboxylic acid

3.3.1 Synthesis of Pca-Phe

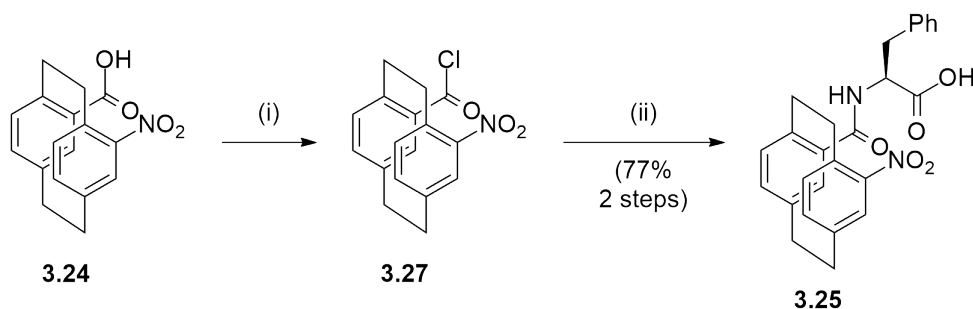
Couplings to the C-terminus of Pca were investigated first. The carboxylic acid is formed before the aniline group; and we expected coupling to the carboxylic acid would be facile. Phenylalanine was chosen as the amino acid that was coupled to Pca and the synthetic route to Pca-Phe **3.26** is summarised in Scheme 3.24.

SCHEME 3.24: Pca-Phe synthetic scheme. i) a. SOCl_2 . b. L-phenylalanine. ii) Zn , NH_4Cl .

Coupling L-phenylalanine with 4-nitro[2.2]paracyclophane-13-carboxylic acid **3.24**

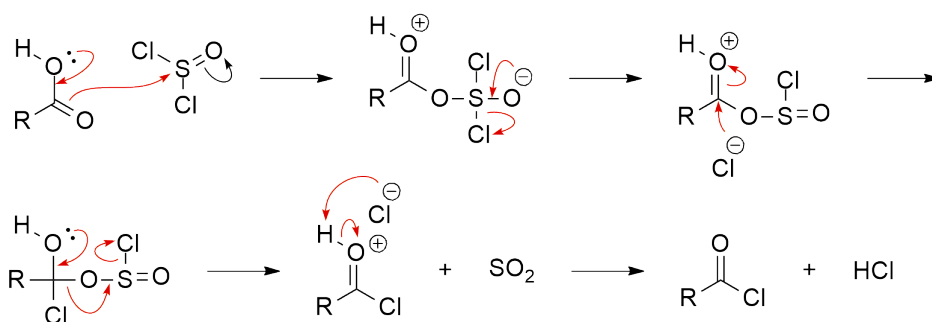
In the nitro methodology for Pca synthesis (Section 2.3.3), a convenient point to form a peptide bond at Pca's C-terminus is after oxidation to form the carboxylic acid, giving 4-nitro[2.2]paracyclophane-13-carboxylic acid **3.24**. Here, the nitro group is a masked amine, protecting the nitrogen from side reactions and avoiding the solubility problems associated with the amine.

Amide coupling between the carboxylic acid on [2.2]paracyclophane and a natural amino acid was achieved by activation of the carboxylic acid. An effective activation method was formation of an acyl chloride (Scheme 3.25). Thionyl chloride and oxalyl chloride were both effective means of activating the carboxylic acid and forming the subsequent peptide bond. Phenylalanine was used as the natural amino acid here due to its visibility on TLC plates with no requirement for a visualising agent.



SCHEME 3.25: Phenylalanine coupling to [2.2]paracyclophane carboxylic acid **3.24** via acyl chloride **3.27**. i) SOCl_2 or DMF, $(\text{COCl})_2$.
ii) L-phenylalanine, NaOH.

The acyl chloride formation with oxalyl chloride is akin to that detailed in Section 2.3.2. With thionyl chloride, the mechanism proceeds as follows: the nucleophilic carbonyl oxygen of the carboxylic acid attacks the sulfur of thionyl chloride. The $\text{S}=\text{O}$ bond is restored, ejecting the chloride ion. The chloride ion now attacks the carbonyl electrophile and then the chlorosulfite leaves, forming sulfur dioxide and chloride. The chloride deprotonates the carbonyl oxygen, leaving the acyl chloride and HCl (Scheme 3.26).



SCHEME 3.26: Acyl chloride formation mechanism with thionyl chloride.

Although acyl chloride formation is discouraged in peptide chemistry due to possibility of racemisation (see section 3.3.3), with Pca this is not a concern as there is

no stereocentre that can be racemised by deprotonation. Normal amino acids have a relatively acidic α -hydrogen that, in acyl chlorides, can be deprotonated to give a ketene with destruction of the stereocentre.

Other examples of coupling with a natural amino acid's amine *via* acyl chloride activation of the coupling partner's carboxylic acid suggest using high equivalents of the amino acid.²³⁰ This helps prevent side product formation by outcompeting other reactions that could occur such as quenching of the acyl chloride with water before it has a chance to react with the desired amine.

Resolution of diastereomers of Pca-peptides

Since peptide couplings were always performed with L-amino acids to racemic mixtures of the appropriate [2.2]paracyclophane compounds, the resultant peptides are diastereomers (Fig. 3.27). Since diastereomers no longer have essentially exactly the same physical behaviours such as solubility, and intramolecular hydrogen bonding, this allowed the possibility of separation by silica column chromatography without further modification. Recrystallisation is also a popular method of separation of diastereomers but was not achieved for these peptides in my hands.

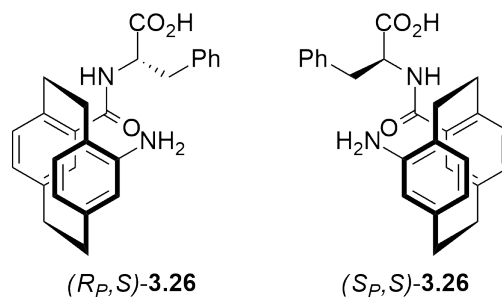
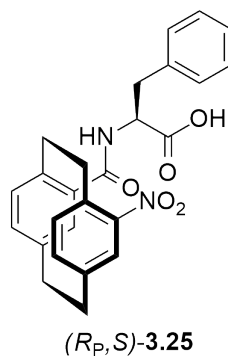


FIGURE 3.27: Diastereomers of Pca-containing dipeptide.

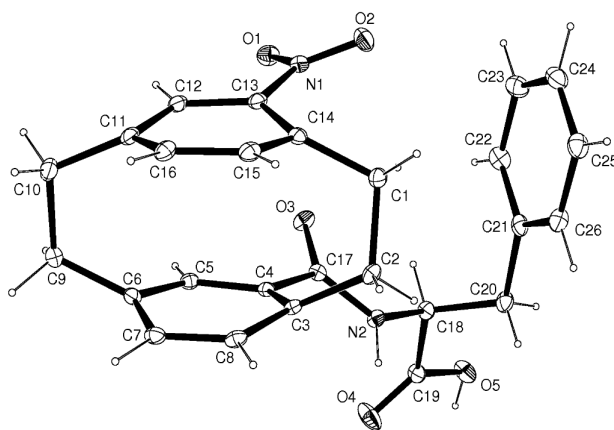
TLC analysis was a quick method of testing the compounds in different solvent systems to check for separation of diastereomers. With careful application of appropriate column chromatography technique, compounds with an R_f difference of as low as 0.05 may be at least partially separable. This usually involves measures such as increased column length and/or volume of silica gel; low eluent polarity; running the column very slowly as a gravity column; and taking very small fractions. This is time consuming but can deliver the desired compounds in small quantities.

Resolution of 4-nitro[2.2]paracyclophan-13-(amido-Phe)

Resolution of the two diastereomers could be achieved by column chromatography eluting with 1:1 hexane/EtOAc with 1% acetic acid. The separation was always incomplete, but fractions of each diastereomer could be isolated. In fact, in the more concentrated fractions of the slower-eluting diastereomer, crystals of (*R_P*,*S*)-**3.25** (Fig. 3.28) crashed out of solution.

FIGURE 3.28: (*R_P*,*S*)-**3.25**.

Crystals obtained were found to be enantiopure, assuming that the Phe stereocentre is fixed, and were of good enough quality to be X-rayed (Fig. 3.29).

FIGURE 3.29: X-ray crystal structure of (*R_P*,*S*)-**3.25**.

X-ray crystallography correlation to ¹H NMR spectra allowed for stereochemical attribution of the diastereomers using ¹H NMR spectra (Fig. 3.30). This could be achieved by looking at the NH-CO proton resonance, which appears as two doublets at 7.97 and 7.91 ppm in the mixture of diastereomers. A sample of **3.25** from

the same crystals that provided the X-ray crystal structure has only one of the doublets, at 7.97 ppm. Given the X-ray crystal structure shows this diastereomer to be (R_P,S)-**3.25**, the (R_P,S) diastereomer must have the amide proton peak at 7.71 ppm.

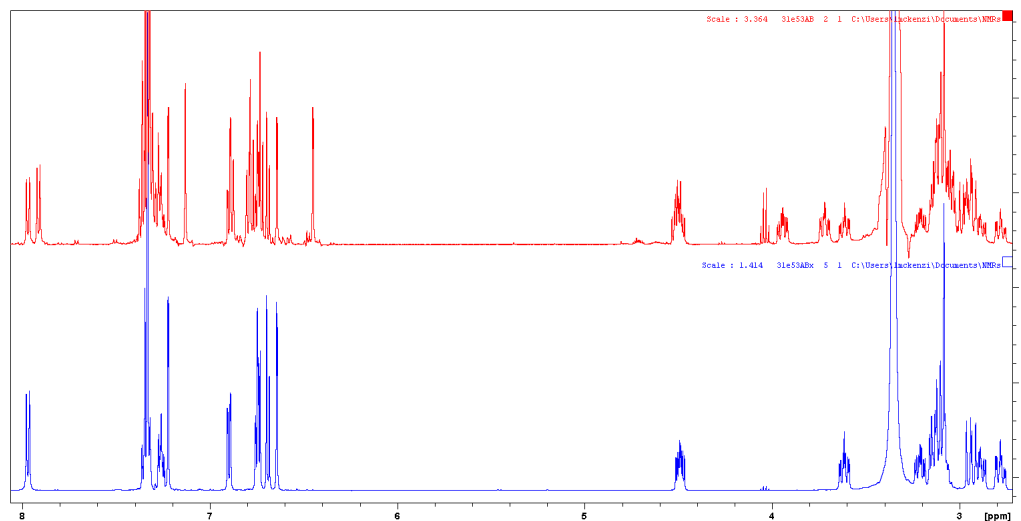


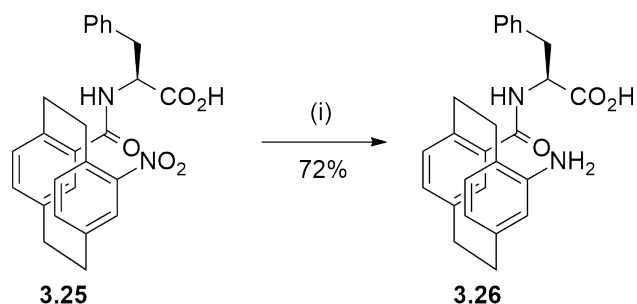
FIGURE 3.30: ^1H NMR spectra of **3.25**. Bottom (blue): (R_P,S)-**3.25**; top (red): mixture of diastereomers.

The full ^1H NMR spectrum shows many more sets of peaks exhibit shifted peaks between the diastereomers: for instance the [2.2]paracyclophanyl Ar-H at 7.22 and 7.13 ppm. The ^1H NMR spectrum of the mixture of diastereomers shows some peaks with integrals of around 0.5, indicating they are part of a pair of peaks, one for each diastereomer, and that the diastereomers are present in about 1:1 ratio.

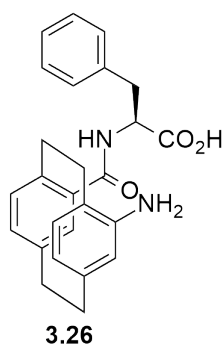
Nitro reduction to give Pca-Phe

As new conditions for reduction of the nitro group in 4-nitro[2.2]paracyclophane-13-carboxylic acid were optimised (see Section 2.3.3), they were applied to reduction of the phenylalanine amide **3.25**. The iron/hydrochloric acid and catalytic hydrogenation conditions for Pca synthesis both gave similar results for this reduction: moderate yields with problematic work up and/or side product formation. Providentially, the zinc/ammonium chloride conditions also gave good yield in high purity for the nitro reduction of **3.25** to furnish Pca-Phe **3.26** (Scheme 3.31).

Resolution of the reduced Pca-Phe pseudopeptide (Fig. 3.32) was also possible, however a larger proportion of the two diastereomers eluted concurrently, and the usual

SCHEME 3.31: Reduction of nitro group to give Pca-Phe. i) Zn, NH₄Cl

concerns with column chromatography of amines (see section 2.3.3) made this a more taxing column to run.

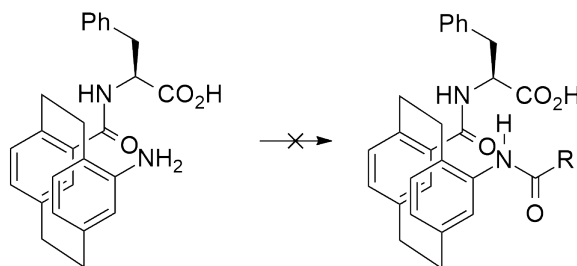
FIGURE 3.32: Pseudo-dipeptide **3.26**.

Amines are problematic in column chromatography and [2.2]paracyclophane amines tend to stick to the silica gel. We suspect either oxidation or polymerisation of the aniline is occurring.

Coupling to the N-terminus of Pca-Phe

The dipeptide was synthesised with good yield and was easily purified by column chromatography. The next step was to see if we could couple the dipeptide with an amino acid at Pca's N-terminus to furnish the first of our desired tripeptides (Scheme 3.33). It was anticipated to be a difficult endeavour, with the Phe residue and its peptide bond to Pca further decreasing the nucleophilicity of the Pca-N, and the additional steric bulk also hindering reactivity. No coupling conditions that were tested were successful in coupling an amino acid to the N-terminus of Pca-Phe.

Mixed anhydride formation was tested with two reagents: ethyl chloroformate and



SCHEME 3.33: Attempted coupling of amino acid to Pca-Phe's N-terminus. R = L-amino acid residue.

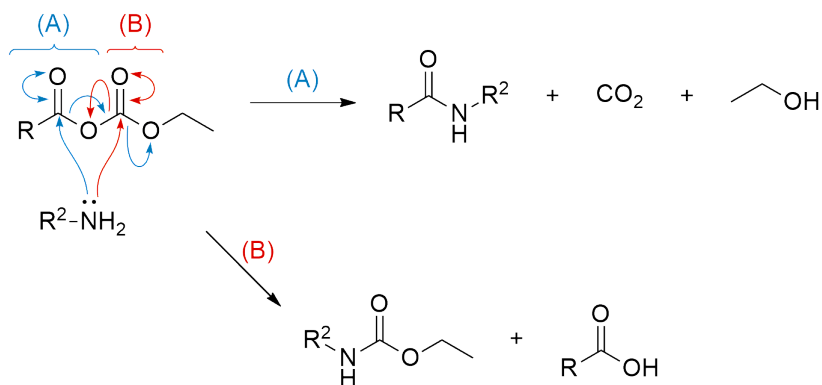
isobutyl chloroformate. Several base additives were trialed as well: Et_3N , *N*-methylmorpholine, and 1,8-diazabicyclo[5.4.0]undec-7-ene (DBU). The base is required in the formation of the activated mixed anhydride species, where it deprotonates the carboxylic acid. DBU was tested as it is a volatile amine base which allowed us to avoid water in the work up. We suspected that the product might be lost in an aqueous work up. This did not help the reaction succeed, and ultimately no combination of these reagents we tested successfully coupled Pca-Phe to Boc-L-proline. Mixed anhydride formation with chloroformate reagents is discussed below.

Another coupling condition that was trialed for this coupling was HOBt with TBTU and DIPEA. The final set of conditions used were DCC and NHS, which were also unsuccessful.

The route was terminated because we could not couple an amino acid to the N-terminus due to a combination of low reactivity and steric bulk, as well as possible interactions from the carboxylic acid on the C-terminus. Unfortunately no conditions were found for forming our desired tripeptide through this route so we moved on to testing coupling conditions to the Pca-N on Pca by itself.

Coupling reagent: chloroformates

For all the peptide coupling chemistry described in this chapter, the key is transforming the -OH into a leaving group. Every coupling, including making acyl chlorides, essentially varies only differs in how dehydration or the removal of OH is achieved. Thus, the mixed anhydride approach effectively allows us, in its desired route, to remove -OH in the form of CO_2 . In the undesired route it results in displacement of an acid and formation of a simple carbamate (Scheme 3.34).



SCHEME 3.34: Peptide bond formation (A) from mixed carbonic anhydrides and carbamate formed from side reaction (B).

Chloroformates such as ethyl chloroformate and isopropyl chloroformate (Fig. 3.35) are used in concert with a tertiary amine base to form a mixed anhydride (Scheme 3.36).

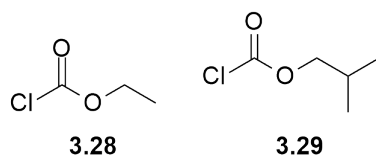
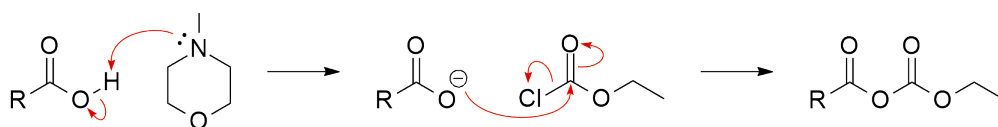


FIGURE 3.35: Chloroformate peptide coupling reagents. Left: ethyl chloroformate 3.28; right: isobutyl chloroformate 3.29.



SCHEME 3.36: Mixed anhydride formation mechanism with ethyl chloroformate and *N*-methylmorpholine.

Care must always be taken to avoid carbamate formation (Scheme 3.34).^{231,232} Precautions include keeping the reaction cool, using only one equivalent or a slight deficiency of chloroformate reagent, adding the amine coupling partner separately after anhydride formation, and increasing the steric bulk of the alkyl portion of the chloroformate reagent to slow attack at the wrong carbonyl.

3.3.2 Peptide coupling to the N-terminus of Pca

Natural amino acids being coupled by their carboxylic acid group to the aniline of Pca were *N*-protected in order to prevent side reactions. The most common protecting group used was *tert*-butoxycarbonyl (Boc), since it was easily and cleanly

removed under acidic conditions. The Boc group is compatible with most methods of amide couplings, and Boc-protected amino acids are readily commercially available.

While coupling to the C-terminus of Pca was facile, for couplings to the N-terminus, normal peptide and amide coupling conditions mostly proved unsuccessful, as will be discussed below. While anilines may successfully undergo amide and peptide couplings with several sets of conditions as detailed above and in the research of others,²³³ Pca displayed remarkable lack of reactivity and failed to couple under any of these conditions.

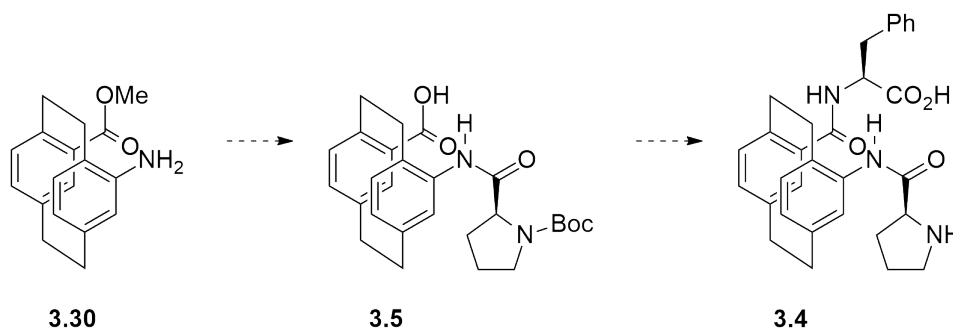
Common peptide coupling conditions tend to use a combination of reagents: one dehydrating and one that becomes an activated leaving group. Using the correct combination is vital. Most research groups tend to settle on one set of conditions that is most efficient for their application and in their hands. The highly substrate-dependent nature of peptide coupling conditions means that the combination required for one compound may be completely ineffective for similar compounds.

These common coupling reagents all act to convert the hydroxyl moiety into a leaving group which activates the carboxylic acid, increasing its reactivity. None activate the nitrogen. In Pca, the nitrogen is the issue. It is very poorly nucleophilic and only formed amide or peptide bonds in certain, strong conditions which may be unsuitable for use with natural amino acids. It would be interesting to see if in a different regioisomer of Pca, with a different relationship between the NH₂ and CO₂Me on [2.2]paracyclophane, the reaction would be any different.

It seems that with the Pca nitrogen, even with the most reactive activated carboxylic acids, is simply too unreactive for most peptide coupling conditions and requires either to be made more reactive itself, or an even harsher carboxylic acid activation that may not be suitable for use with natural amino acids since they are sensitive to racemisation.

3.3.3 Attempted synthesis of Pro-Pca

Since we could not find conditions for forming a tripeptide by coupling the N-terminus of Pca-Phe with a third amino acid, the next approach was to focus on the more problematic peptide coupling with the aniline nitrogen of Pca first. Then, after finding successful conditions for this challenging reaction, we could focus on the easier coupling to Pca's carboxylic acid (Scheme 3.37).



SCHEME 3.37: Proposed synthetic scheme for tripeptide synthesis starting with Pca-OMe.

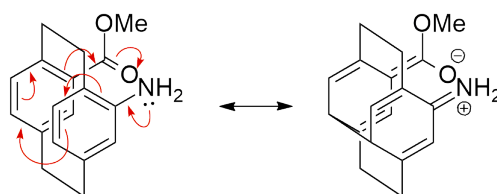
This route began with the synthesised Pca-OMe from the nitro methodology (see Section 2.3.3). The carboxylic acid of the [2.2]paracyclophane was protected with a methyl ester when coupling to amine of the paracyclophane in order to remove any influence the acid would have on the reaction.

Coupling Boc-L-proline to Pca-OMe

The first step for this pathway was to couple an amino acid to Pca-OMe. Before we discovered successful conditions, we investigated a number of other routes which returned only starting material due to the poorly-reactive aniline on Pca.

The aniline itself is unreactive because of the strong electron-withdrawing effect of the conjugated π -electron system. The nitrogens of aniline compounds tend to be unreactive; in [2.2]paracyclophane they are troublesomely so. The lone pair of the nitrogen is delocalised over the aryl ring it is bonded to, decreasing the nitrogen's nucleophilicity. In Pca the electrons are further withdrawn by the communication between the two rings of paracyclophane by the shared π system (Scheme 3.38). Since the two aromatic rings of [2.2]paracyclophane sit within each others' van der

Waals radii, the transannular electronic effect means that the lone pair on the nitrogen effectively can participate in resonance with two aryl rings and is less reactive.



SCHEME 3.38: Nitrogen lone pair participation in aromatic resonance in Pca-OMe.

The low reactivity is probably also further hindered by the steric effect of the nearby ethyl bridges joining the two rings, even though these groups would be electron-donating and in theory increase the nitrogen's reactivity; and by the lower deck. In addition, the steric hindrance is exacerbated by placing the ester or acid in the pseudo-*gem* position, directly beneath the amine. It is also possible that this enforces an interaction between the nitrogen lone pair and the π^* antibonding orbital of the ester, which would also decrease its reactivity (Fig. 3.39). This is similar to the secondary orbital effect which induces *endo* selectivity in Diels-Alder reactions.^{234,235} Figure 3.39 also shows the limited approach caused by the sterically congested system. It is not the case that the [2.2]paracyclophane-amine is the same as aniline; it behaves quite differently, as demonstrated in this thesis.

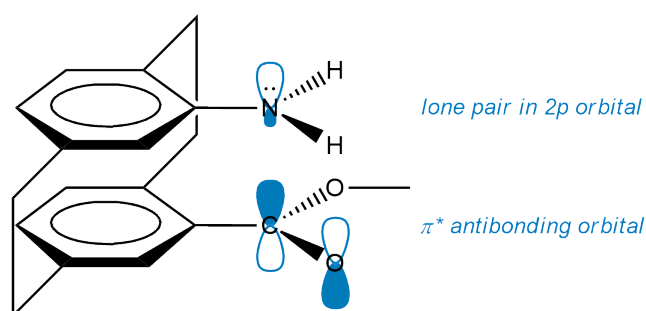
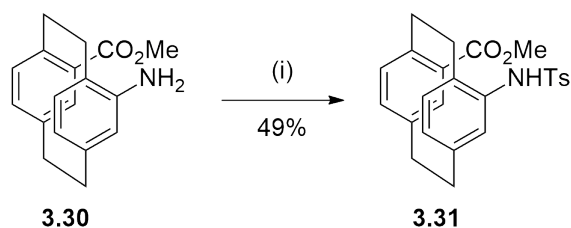


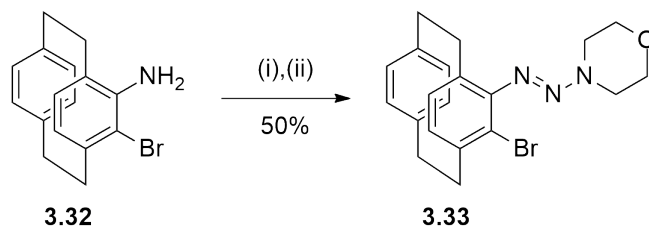
FIGURE 3.39: Orbital overlap in Pca-OMe.

Previous work by the Rowlands group has highlighted this component's poor reactivity;²⁰ for example, tosylation of methyl 4-amino[2.2]paracyclophane-13-carboxylate **3.30** occurs only in 49% yield, with the rest of the material being unreacted starting material, even with strong base (NaH) under reflux (Scheme 3.40). This usually uncomplicated procedure's difficulty here illustrates the low reactivity of this aniline.



SCHEME 3.40: Tosylation of methyl 4-amino[2.2]paracyclophane-13-carboxylate **3.30**. i) NaH, TsCl, reflux in THF.

The poorest reactivity in an amino[2.2]paracyclophane species our group has observed was in the *ortho*-bromo species, 4-amino-5-bromo[2.2]paracyclophane **3.32**.²⁰ Nearly all elaborations of the amine were fruitless, yielding only the starting material. These transformation attempts included various alkylations, reductive aminations, and acylations with anhydrides or acyl chlorides. Only one derivative was ever made and that involved formation of the diazonium salt with NaNO₂ then coupling with morpholine to give the triazene compound **3.33** (Scheme 3.41). The bromo group in the starting material withdraws electrons, further removing electron density from the already deactivated aniline nitrogen.



SCHEME 3.41: Synthesis of triazene **3.33**. i) HBF₄, NaNO₂. ii) morpholine.

Many peptide coupling conditions were tested in this coupling. The first was mixed anhydride formation, where the natural amino acid was either Boc-proline or *N*-pivaloyl valine; EtOCOCl was tested as the reagent with Et₃N as the base (discussed in Section 3.3.1). These conditions with both amino acids were unsuccessful, returning only starting material. We thought that the amino acid might be forming a carbamate with the ethyl chloroformate instead of the desired mixed anhydride, so we also tested the coupling of *N*-pivaloyl valine to Pca-OMe with *i*-BuOCOCl. Its increased bulk would hinder carbamate formation. However, this reagent was also ineffective. No carbamate was isolated.

The following sections discuss several peptide coupling conditions that were trialed in coupling Boc-Pro to Pca-OMe.

Coupling reagent: imidazoles

Carbonyldiimidazole (CDI, Fig. 3.42) is a useful reagent that forms from the acylimidazole active ester. It generates an imidazole molecule so that no additional base is required to form the peptide bond (Scheme 3.43).²³⁶

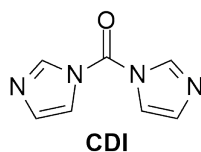
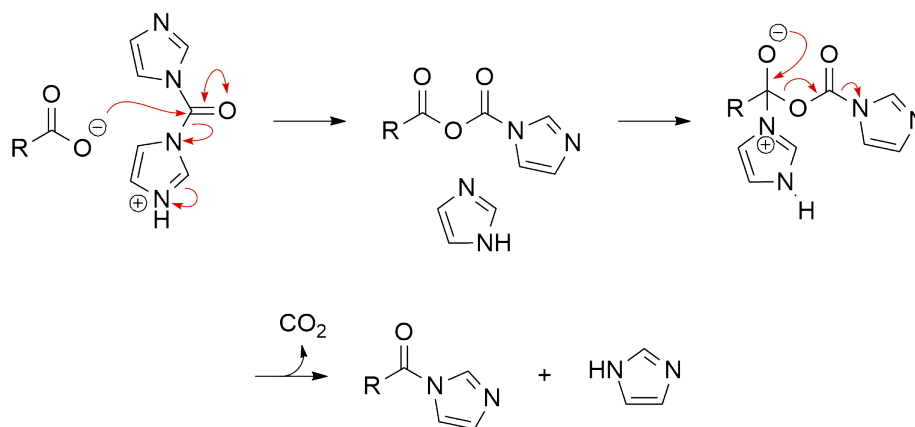


FIGURE 3.42: Carbonyldiimidazole.

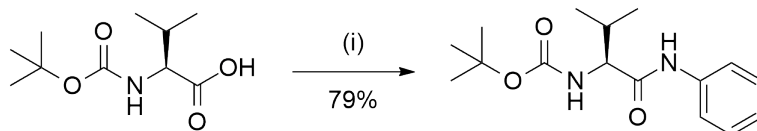


SCHEME 3.43: Active ester formation with CDI showing generation of an imidazole molecule.

We first separately formed the acylimidazole ester with Boc-valine to ensure that the active ester was being formed.²³⁷ This reaction was successful, so we moved on to the one-pot reaction with the active ester formed *in situ* and then, in theory, reacting with Pca-OMe.²³⁸ This was not successful, returning only the Pca-OMe starting material, even when the two steps were performed separately. The same conditions with Boc-proline as the amino acid also failed.

When no reaction was seen in couplings to Pca with CDI, external bases including K_2CO_3 , NaOH, and NaH were added to the reaction conditions, with no improvement in outcome. Additional tests were run coupling Boc-valine with proline to check the CDI reagent was still good; and with the amine on aniline with CDI to

test the efficacy of CDI with aromatic amines (Fig. 3.44). These couplings were successful, so the problem is with Pca's additional bulk and π electron participation of nitrogen's lone pair.



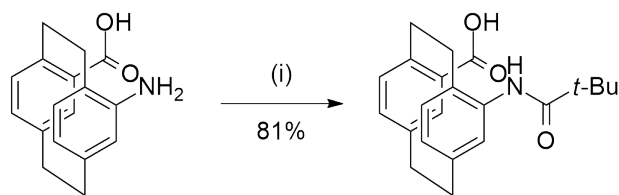
SCHEME 3.44: Boc-valine coupling with aniline. i) a. CDI. b. aniline.

Coupling reagent: acyl chlorides

In peptide synthesis, acyl chlorides tend to be avoided for their propensity to form numerous side products, including hydrolysis back to the parent acid and incompatibility with some protecting groups like Cbz, and racemisation at the α -carbon.^{239,240} Due to these severe limitations, acyl halide activation of chiral amino acids was found to be inappropriate. As discussed later in Section 3.3.7, we found that acyl chloride formation may be milder with respect to racemisation than the literature suggests. It is imperative that racemisation of incoming enantiopure amino acids does not occur in order to avoid introduction of another set of diastereomers. In any case, this does not change the fact that acyl chloride activation did not work for this amide formation, even with the inclusion of a base such as NaH.

Acyl chloride formation with oxalyl chloride and DMF on Fmoc-proline was looked into following conditions from Evindar and Batey.²³³ These conditions were not successful for Pca, with the desired product not forming, and the Fmoc carbamate additionally being cleaved. Cooling the reaction mixture to 0 °C for acyl chloride formation, then using NaH with the Pca-OMe and heating the reaction, did not aid this reaction.

One acyl chloride-activated amide coupling that was successful was between Pca and *N*-pivaloyl chloride in the presence of *n*-BuLi (Fig. 3.45).²⁴¹ These conditions were run to check that amide bond formation with Pca's nitrogen was possible at all. The combination of strong base and acyl chloride was necessary but these conditions did not translate to amino acid coupling. The acyl chloride of Boc-glycine did not couple to Pca in the same conditions.

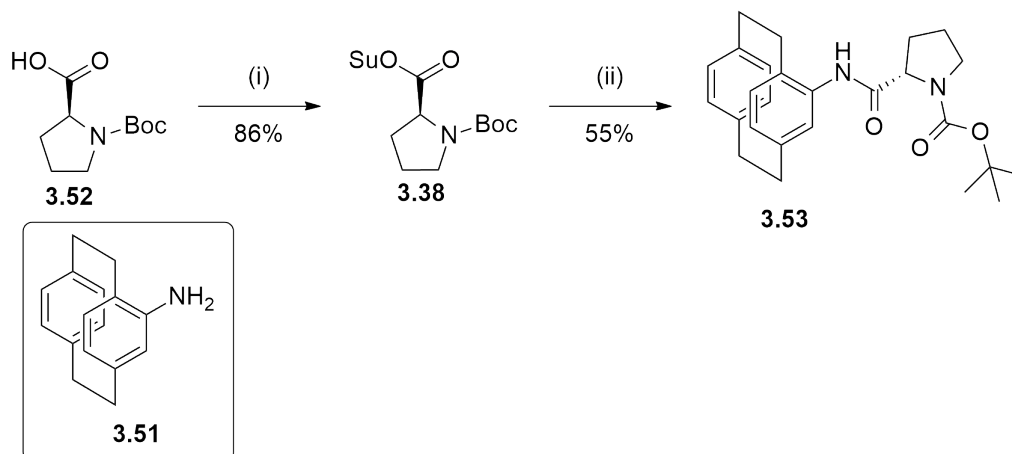


SCHEME 3.45: Pivaloyl amide formation with Pca. i) a. *n*-BuLi, -78 °C. b. *N*-pivaloyl chloride.

Fluorination was not tested for couplings in this project; however, given the poor results with acyl chloride activation, it is likely that the acyl fluoride would not have been a strong enough activator to couple an amino acid to the nitrogen of Pca.

Coupling reagent: *N*-hydroxysuccinimide in the synthesis of Pro-Pca

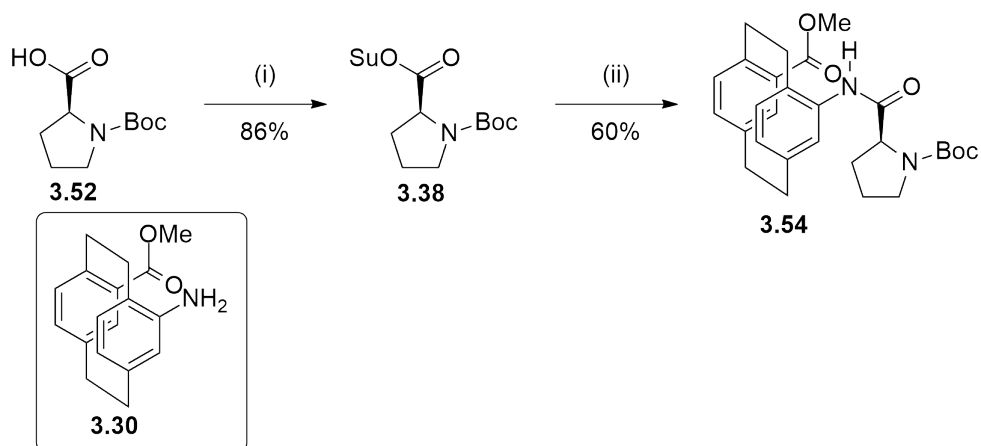
During this project it was observed by a colleague that coupling could be achieved in a simpler system, 4-amino[2.2]paracyclophane **3.51** (Scheme 3.46).



SCHEME 3.46: Amide coupling between Boc-proline **3.52** and 4-amino[2.2]paracyclophane **3.51**. i) DCC, NHS. ii) **3.51**.

This result was repeated and the discovery was carried forward to determine if the reaction would still proceed on Pca-OMe **3.30**. Small scale experiments confirmed its success and a small amount of Boc-Pro-Pca-OMe **3.54** was prepared (Scheme 3.47). This discovery was made toward the end of this project so the opportunity was not available to try it on other systems or with any other amino acids.

Active esters formed from reagents such as *N*-hydroxysuccinimide (Fig. 3.48), which generates a hydroxamic acid ester, act as all the other reagents described, to make the carbonyl carbon more susceptible to attack from the amine by turning to -OH



SCHEME 3.47: Peptide coupling between Boc-proline and Pca-OMe.
i) DCC, NHS. ii) 3.30.

into a good leaving group.²⁴² These activated esters have the advantage of being shelf-stable.

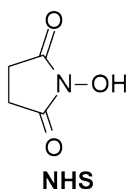


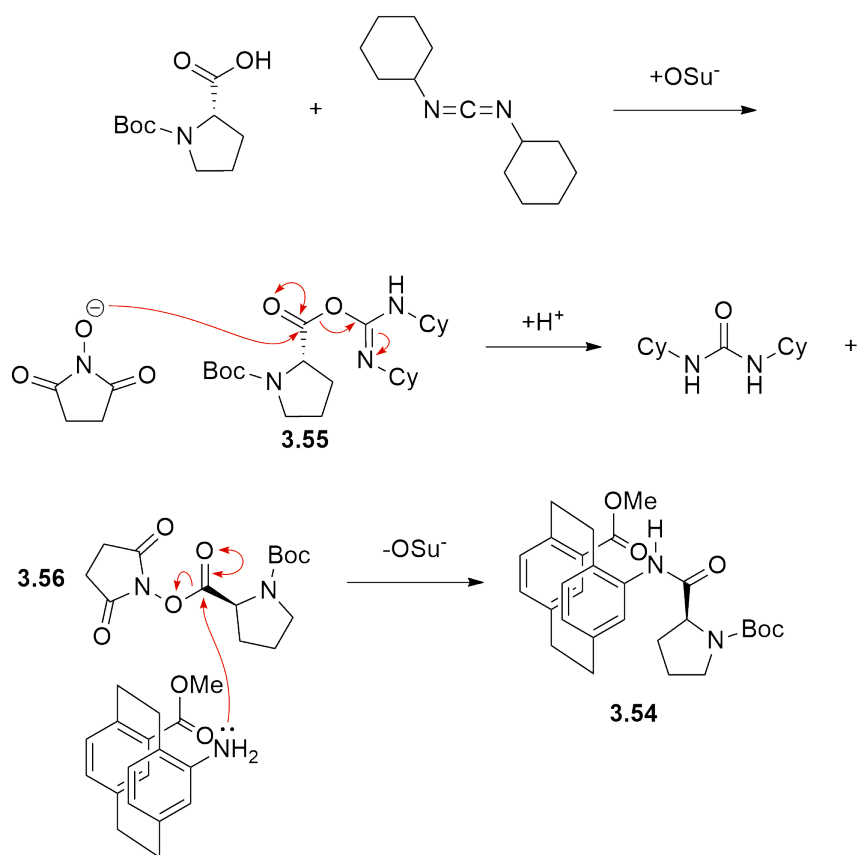
FIGURE 3.48: *N*-Hydroxysuccinimide (NHS).

Carbodiimides may be used as pre-activating reagents to aid in formation of these active esters; and NHS in combination with DCC was found to be an effective set of coupling conditions for peptide synthesis with Pca.

The coupling reaction with DCC and NHS proceeds as follows (Scheme 3.49). First the *O*-acylisourea 3.55 forms between the carboxylic acid on Boc-proline and DCC. The carboxylic acid protonates the carbodiimide and the carboxylate ion attacks the protonated carbodiimide giving the *O*-acylisourea.

The mechanism of the *O*-acylisourea formation can be seen in Section 3.2.2. DCC is a low-melting point solid and thus easily transferred by gently heating the container; and in winter, any glassware used handling it.

The NHS then substitutes to form the succinate ester 3.56. Formation of the urea is the driving force for this reaction. The urea derivative formed by the substitution is predictably insoluble and may be removed from the prepared succinate ester by



SCHEME 3.49: Peptide coupling mechanism between Boc-proline and Pca-OMe using DCC and NHS.

performing two or three successive recrystallisation steps, filtering off the solid dicyclohexylurea and concentrating the filtrate containing the active ester. When added to the reaction mixture, Pca's nitrogen forms the amide bond with nucleophilic attack to the succinate ester carbonyl, giving NHS and Boc-Pro-Pca-OMe **3.54**.

A literature search did not suggest that NHS with DCC are necessarily good conditions for peptide couplings with anilines. More common coupling conditions for these relatively unreactive nitrogens are HOBt and EDC or the host of other reagents we had tried with the Pca analogues (Section 3.2). NHS was not a common activating agent for these compounds. As to why these conditions are successful in Pca's case, one possibility is that the succinate is a comparatively small moiety compared to the benzotriazole derivatives and reduces steric hindrance on the coupling, occurring between two already quite bulky compounds. Perhaps the carbonyl groups on the succinate moiety participate in hydrogen bonding with the aniline and carboxylic acid hydrogens (Fig. 3.50), resulting in increased reactivity in something akin to the neighbouring group effect seen in azabenzotriazoles due to the spatial position of its 7-N.²²⁸

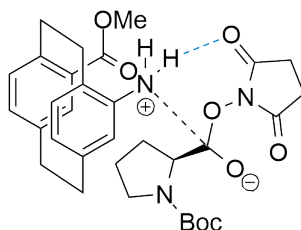


FIGURE 3.50: Possible neighbouring group effect between Pca-OMe and Boc-Pro-OSu.

Important for the success of this reaction are the exclusion of water from the solvent and atmosphere; DCC is a dehydrating agent so its presence in excess probably contributes to the success of these reaction conditions. Some variability was seen in the yield of this reaction, with the worst yield being from a large scale (3 g) coupling which only gave 200 mg of the product with the rest of the substrate being returned starting material and a mixture of side products. Possible reasons for this poor result could have been low solubility of the starting material leading to the starting material crashing out of solution; or incomplete exclusion of air and water from the reaction vessel. It was noted that the rubber septum used to cap the reaction vessel

was degraded and may have been leaky.

The success of this reaction can be confirmed by certain changes in the ^1H NMR of the compound: the peak at 5.26 ppm which was assigned to H-5 in the Pca-OMe (Fig. 3.51) starting material has shifted downfield, due to the presence of the amide compared to the aniline (Fig. 3.52). This proton is now more deshielded. The remaining aryl peaks also experience a downfield shift compared to the starting material. Of course, the presence of amide N-H protons for the peptide and Boc-group moieties as well as peaks corresponding to the proline alkyl groups at the appropriate intensities also indicate this successful coupling.

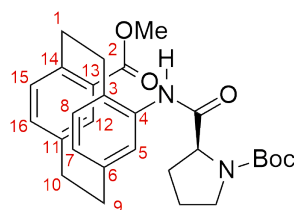


FIGURE 3.51: Boc-Pro-Pca-OMe, numbered.

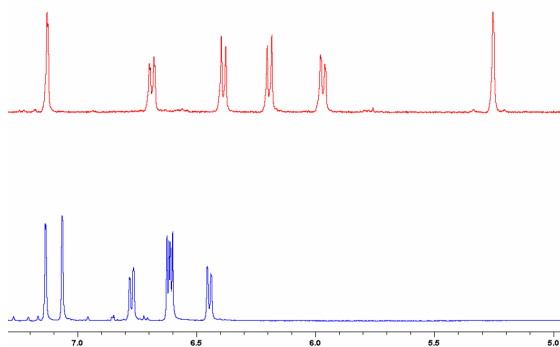
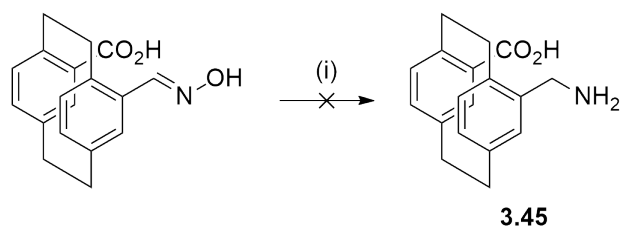


FIGURE 3.52: Proline coupling to Pca (blue, bottom) compared with the Pca starting material (red, top) aryl region.

3.3.4 Attempted synthesis of 4-methylamino[2.2]paracyclophane-13-carboxylic acid

During the course of research, alternatives to true peptide couplings between Pca and other amino acids were attempted. Reduction of the oxime to the methylamine substituent **3.45** might have been an acceptable compromise for the aryl amine, since

the aryl amine was so difficult to form and couple to other amino acids (Scheme 3.53).



SCHEME 3.53: Proposed oxime reduction to methylamine **3.45**. i) Zn, HCl.

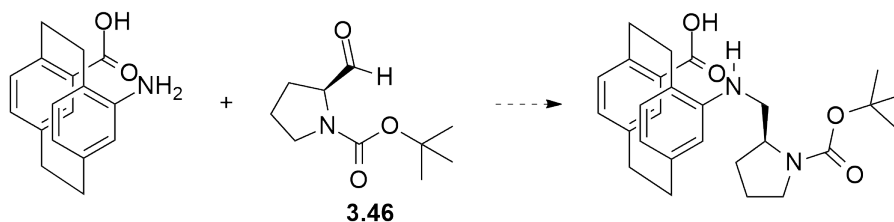
We hypothesised that part of the difficulty in forming the aryl amine was the lower electron density on the final nitrogen. Separating it from resonance with the aryl ring with a methylene group might have alleviated this issue and if the alkyl amine would couple better. The alkyl amine might be more nucleophilic, as seen in the glycine residue. However, oxime reduction with zinc and HCl was unsuccessful, and due to time constraints other chemoselective reductions were not attempted.

3.3.5 Attempted coupling of Boc-proline derivatives to Pca

Reductive amination

Following from the attempted oxime reduction to the primary amine, different types of bonds were explored. A small drawback is that these bonds would lack the structural and electronic properties of the amide bond.

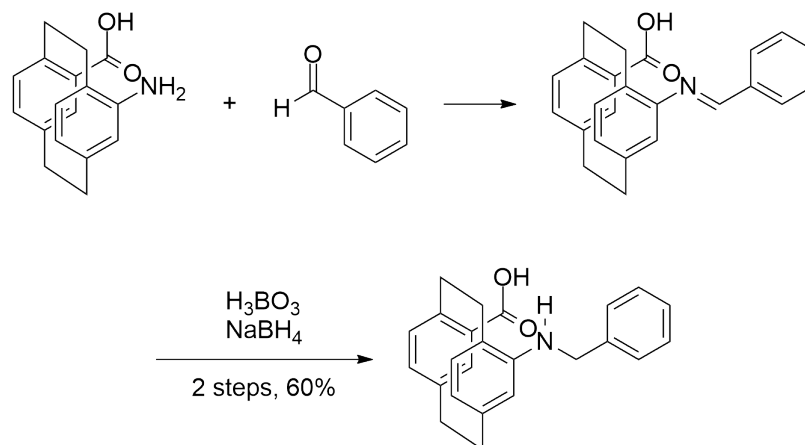
An alternative coupling method to produce a peptide analogue is reductive amination of the formyl carbonyl group of a reduced natural amino acid such as prolinal (**3.46**, Scheme 3.54).



SCHEME 3.54: Proposed reductive amination with Boc-prolinal **3.46**.

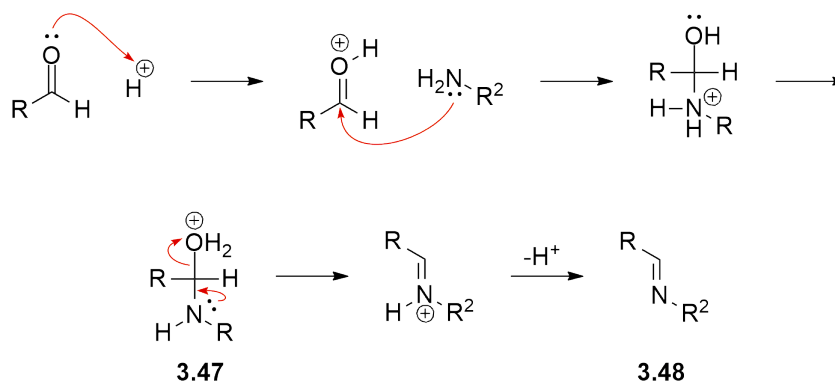
This route was attractive since imine formation at [2.2]paracyclophanyl amines has been performed in the Rowlands group before with benzaldehyde. Anilines are particularly susceptible to reductive amination. As mentioned, a drawback is that this compound would lack the amide functionality at the nitrogen of Pca. Loss of the carbonyl would affect conformation and hydrogen bonding potential of the compound. While we wanted the compounds to be as close to an amide as possible, considering how hard the amide coupling had been we were prepared to try alternative options to move the project forward.

As a test, we tried reductive amination with benzaldehyde which was high-yielding (Scheme 3.55). This reaction has the benefit of the product being highly crystalline and able to be isolated in high yield and purity by recrystallisation.



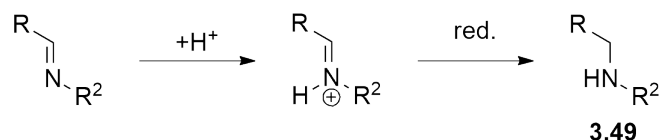
SCHEME 3.55: Reductive amination of Pca with benzaldehyde.

Reductive amination of an aldehyde proceeds by the following mechanism: first the imine or iminium is formed in a series of reversible reactions (Scheme 3.56).



SCHEME 3.56: Imine formation mechanism.

The carbonyl oxygen is protonated. Nucleophilic addition to the carbonyl by the amine nitrogen and loss and gain of a proton gives the hemiaminal intermediate **3.47**. Elimination of a water molecule gives the imine **3.48**. The imine may be isolated at this point. The protonated iminium species is reduced giving the secondary amine **3.49** (Scheme 3.57).



SCHEME 3.57: Reduction of the imine to complete reductive amination.

Initially, we believed the reaction between Pca and Boc-L-prolinal had been successful. Proton NMR of the crude reaction mixture revealed that the aldehyde proton of Boc-L-prolinal was greatly diminished in integration compared to the remaining prolinal peaks; small shifts in the aryl peaks of [2.2]paracyclophane also suggested the imine formation was successful. Unfortunately the NMR spectrum was not clear and attempts to purify the imine failed. The compound did not crystallise under similar conditions that resulted in the formation of benzaldehyde imine. Where the benzyl imine could be purified by recrystallisation by cooling to 4°C overnight; the prolinal imine was a liquid which could not be recrystallised in the same manner, even when cooling to -18°C. Column chromatography was impaired by imine cleavage under the mildly acidic environment of silica gel. Instead, the prolinal imine was prepared for reduction (or storage) by running the material through an alumina plug to remove any traces of acid or moisture which might cleave the imine, and imine reduction was attempted on the crude material.

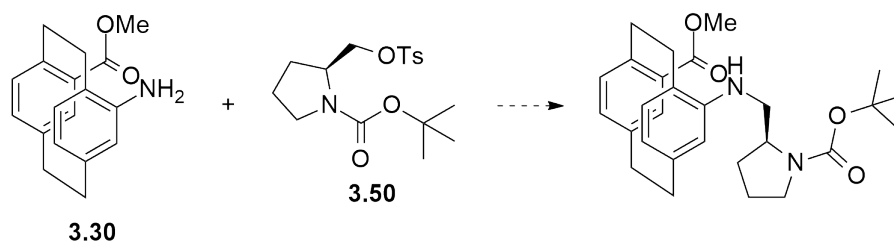
However this imine could not be reduced in the same manner. Other reduction conditions with catalytic hydrogenation or sodium cyanoborohydride were also unsuccessful. The issue with this transformation could have been either the Pca not reacting with Boc-L-prolinal to form the imine; or that the reduction was unsuccessful. The evidence for formation of the imine is somewhat tenuous, with the main data point backing this up being the disappearance of the CHO peak of prolinal. The two reaction steps were performed separately, confirming the presence of the

supposed imine intermediate before adding the reducing agent; this test was also unsuccessful, so the choice of reducing agent would not have interfered with imine formation: for instance, by being too strongly acidic and protonating the amine substrate, hindering imine formation.

It appears that imine formation was possible but that purification and reduction were the issue. Reduction of this imine might be problematic due to the differences in electronics and sterics between Boc-proline and benzaldehyde. Aryl amines are more stable to purification yet more reactive due to conjugation. Alkyl imines are electron-rich and thus cannot be reduced as readily because they are generally less stable, easily undergoing tautomerisation to an enamine. Boc-proline is also considerably more sterically demanding than the flat aromatic ring structure of benzaldehyde, which again decreases reactivity.

Substitution with prolinol derivatives

Another alternative that was *N*-alkylation with an appropriately activated derivative of Boc-prolinol (Scheme 3.58). While formation of the tosylate was possible it failed to react. Again the low reactivity of the Pca nitrogen was at fault. A further attempt with the bromide of prolinol failed; it was similarly unreactive in this substitution.



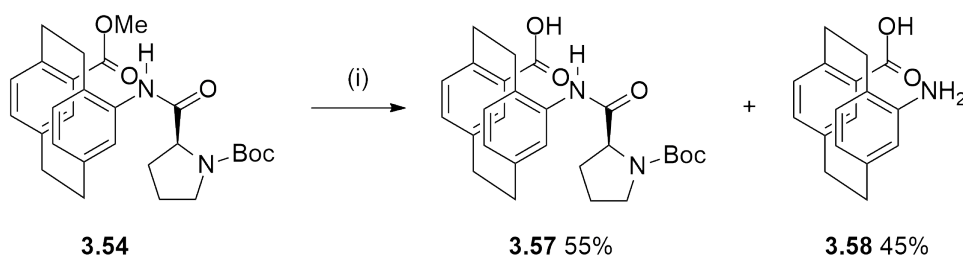
SCHEME 3.58: Proposed reaction between Boc-Pro-OTs 3.50 and Pca-OMe 3.30.

3.3.6 Deprotection of and attempted peptide coupling to Boc-Pro-Pca-OMe

Ester hydrolysis of the Boc-Pro-Pca-OMe dipeptide

After successful coupling of Boc-Pro to Pca-OMe using NHS and DCC, the next step was hydrolysis of the methyl ester. An alternative method was required for compounds that did not dissolve in mixtures of alcohol and water, in the conditions developed for the ester hydrolysis on Pca-OMe in the oxime methodology (see Section 2.3.2). Heating with 2 M ethanolic potassium hydroxide is a common method for ester hydrolysis and the protected pseudopeptide **3.54** dissolved in EtOH with heating.

Boc-Pro-Pca-OMe was very sensitive to these conditions, with both the methyl ester and the amide bond between Pro and Pca being hydrolysed, yielding Pca **3.58**; the same result was found with the reaction run at 50 °C. At room temperature, overnight approximately half the material was hydrolysed at the amide bond as well as the ester (Scheme 3.59). Due to time constraints, we were unable to explore milder conditions, such as conducting the reaction at lower temperature or attempting the reaction with a weaker base.



SCHEME 3.59: Methyl ester cleavage of Boc-Pro-Pca-OMe.

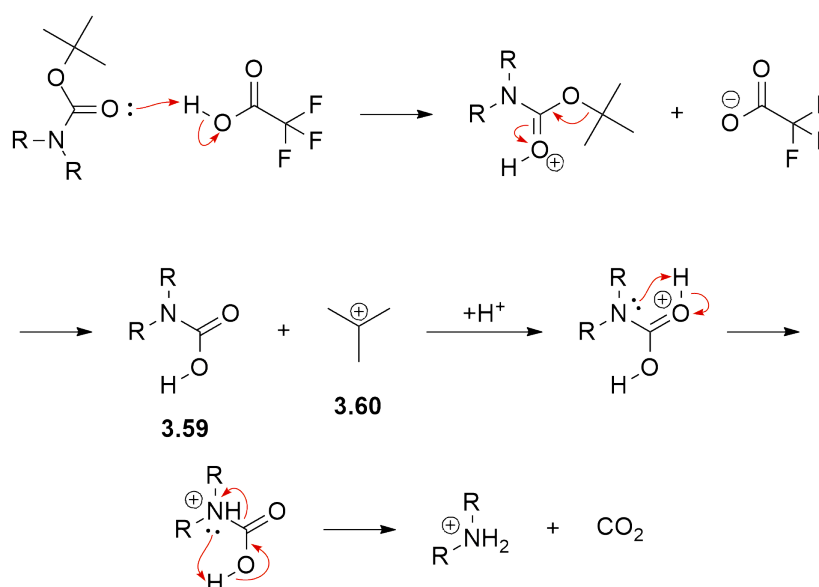
Coupling attempts to Boc-Pro-Pca's C-terminus

Due to time constraints only a limited number of conditions were attempted but we had hoped it would be easier considering the success described in Section 3.3.1. We chose first the mild and, to this point, most effective peptide coupling conditions we had found, activating the carboxylic acid with DCC and NHS. When this activation was unsuccessful we also tried mixed anhydride formation with EtOCOCl and NMM as the base. However, only starting material was returned.

Frustratingly, having made a dipeptide, Boc-Pro-Pca, it now proved impossible to add another amino acid to the C-terminus.

Boc cleavage of Boc-Pro-Pca

The Boc group of **3.57** was cleaved using 3:1 CH₂Cl₂/CF₃COOH at room temperature to give the deprotected pseudopeptide **3.7**.²⁴³ Acidic Boc cleavage occurs by the following mechanism:²⁴⁴ the first step is protonation of the carbamate. The *tert*-butyl cation **3.60** dissociates. The resulting carbamic acid **3.59** undergoes decarboxylation to give CO₂ and the free amine, which will be protonated due to the excess of acid in the reaction mixture (Scheme 3.60).



SCHEME 3.60: Mechanism of Boc cleavage with TFA.

Some Boc cleavage conditions include a trapping agent for the *tert*-butyl cation since it may react with the amine to produce unwanted side products, however in this case it was not found to be necessary.

Resolution of Pro-Pca

Analysis of 2D spectra of this compound **3.7** (Fig. 3.61) indicated that the obtained material was a single diastereomer, with L-proline and a single enantiomer of Pca.

It is not clear which of *R*_P- or *S*_P-Pca is present since a lack of crystals prevented confirmation of configuration, and the 2D NMR spectra are sufficiently complicated

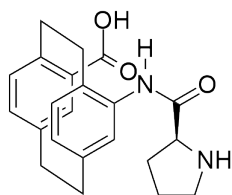
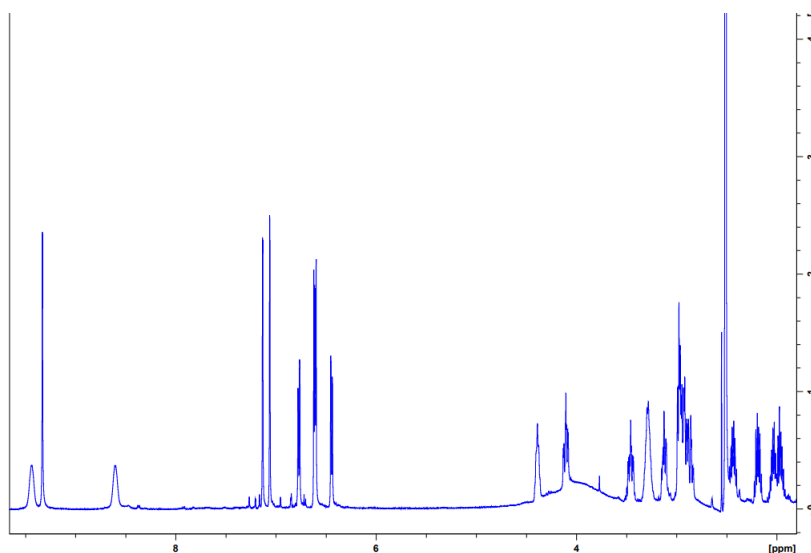


FIGURE 3.61: Pro-Pca 3.7.

to make them difficult to completely assign. As can be seen in ^1H NMR spectra of diastereomeric compounds where both diastereomers are present (see Section 3.3.1), often twin peaks are seen for certain protons (for instance, the amide protons at around 8-9 ppm). No evidence of these can be found in the proton spectrum of this compound (Fig. 3.62). Additionally, the split peaks normally seen in 2D spectra where diastereomers are present are not seen for this product.

FIGURE 3.62: ^1H NMR spectrum of 3.7.

The broad OH and NH peaks at 9.44 and 8.61 ppm indicate one (or more) of several things is occurring: chemical exchange with the solvent; hindered rotation of the molecule; and slow tumbling in the viscous solvent (DMSO).

It is not clear at which point in the compound's synthesis this accidental resolution occurred. There are many possibilities. The resolution could have occurred during a reaction, where one diastereomer was faster or more energetically favoured to form. It also could have occurred during work up if one diastereomer was more soluble than another and was either removed during washing, or not taken up during extraction. If there were a significant difference in R_f during column chromatography,

one diastereomer could have been lost during purification.

Looking at the yields of the reactions from the point where the diastereomers were formed, *i.e.* the coupling of Boc-L-proline, might illuminate where the resolution occurred.

The peptide coupling had a yield of 42%, which could mean that only one enantiomer of Pca-OMe reacted with Boc-Pro-OSu, or one of the diastereomeric products was lost during work up. It could also simply be a low yield due to the challenging nature of coupling to Pca's nitrogen.

The ester hydrolysis had a low yield of 39% of the desired carboxylic acid, which might have suggested that this is the step where resolution was occurring. However the low yield of this step was due to the poor optimisation of the reaction, which gave a mixture of starting material, desired product, and Pca. Thus it is not clear if the resolution occurred at this step due to more selective hydrolysis of the ester of one diastereomer; or if both diastereomers were equally poorly suited for these reaction conditions.

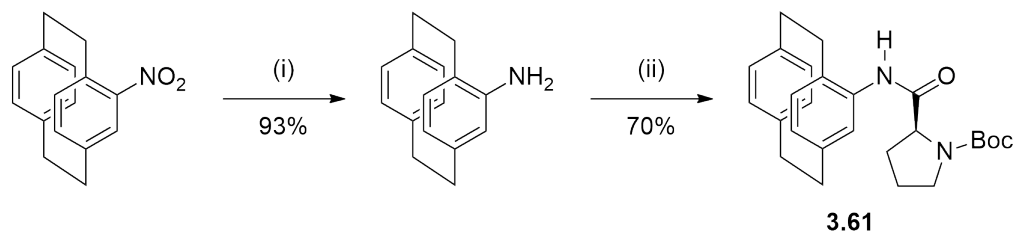
The Boc cleavage gave a good yield of over 90%, so the resolution did not occur in this step.

Synthesis of the mono-substituted 4-prolinamido[2.2]paracyclophane

The mono-substituted 4-prolinamido[2.2]paracyclophane was desired for our catalysis tests to see the effect of the carboxylic acid or its absence. The synthetic route was easily adapted from the nitro methodology, with nitration followed by reduction to the amine. Boc-L-proline was then coupled to the amine using the same conditions with DCC and NHS to yield the amide **3.61** (Scheme 3.63).

3.3.7 Synthesis of Pro-Gly-Pca

Since established peptide formations were demonstrated to be largely incompatible with the poor nucleophilicity of the Pca nitrogen, another method of constructing an amide bond to a short alkyl group was considered. The failure to react with anything except highly activated acyl chlorides and the concern about steric hindrance caused



SCHEME 3.63: Synthetic scheme for mono-substituted 4-prolinamido[2.2]paracyclophane from 4-nitro[2.2]paracyclophane. i) Zn, NH₄Cl. ii) DCC, NHS, Boc-L-proline.

by the [2.2]paracyclophane skeleton led us to consider adding a simple linker such as glycine (**3.34**, Fig. 3.64).

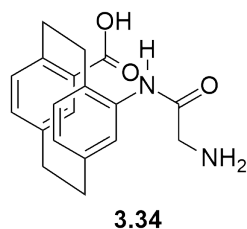


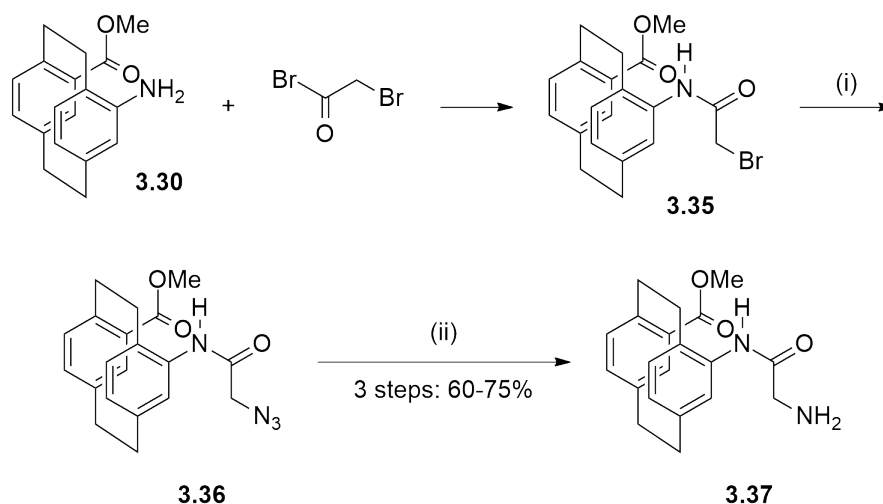
FIGURE 3.64: Gly-Pca-OH **3.34**, with its ethanamide moiety.

This would allow incorporation of a primary alkyl amine. This should be more nucleophilic than an aniline nitrogen and less sterically encumbered. Additionally, it would allow us to use much stronger electrophiles. Constructing a glycine residue starting with a strong electrophile that would be capable of reacting with the very poor nucleophile might be a way of circumventing Pca's poor reactivity at its aniline.

With this in mind, we looked at coupling Pca to bromoacetyl bromide, a highly electrophilic acylating reagent, that contains a handle for subsequent elaboration. The terminal bromide could be transformed to an amine **3.37** *via* an azide **3.36** (Scheme 3.65). This has the benefits of constructing an amino acid by synthetic chemistry where it was nigh impossible to couple one; and the resulting alkyl amine should be far more reactive than the aniline, allowing coupling of further amino acids.

Synthesis of bromide **3.35**

Bromoacetyl bromide was found to form an amide, coupling with the nitrogen of [2.2]paracyclophane (Scheme 3.66), with remarkable yield and purity, considering the previous difficulties in this amine's reactivity.^{245,246} The product precipitates on



SCHEME 3.65: Synthetic route to Gly-Pca-OMe. i) NaN_3 . ii) H_2 , 10% Pd/C.

addition of water to the reaction mixture and can be obtained as an essentially pure material by filtration.

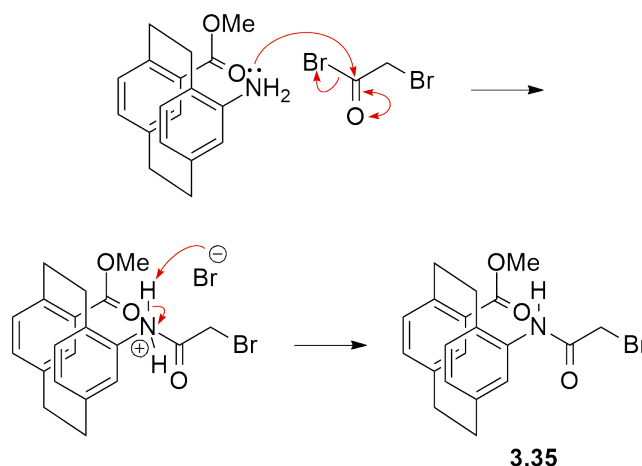


FIGURE 3.66: Mechanism of formation of **3.35**.

The acyl bromide amide formation proceeds by the nitrogen adding to the carbonyl group. The bromide is eliminated and may remove a proton from the nitrogen, giving the amide **3.35**. The success of this reaction where acyl chlorides of proline failed can be rationalised for two reasons: the bromide ion is a better leaving group than chloride, increasing impetus to form the amide; secondly, bromoacetyl bromide is a smaller, less sterically hindered compound compared to Boc-protected proline.

The α -carbonyl bromide is especially labile. The π^* orbital of $\text{C}=\text{O}$ and the σ^* orbital of $\text{C}-\text{Br}$ blend and this lowers the energy of the LUMO, making it more prone to

nucleophilic attack (Fig. 3.67).²⁴⁷ Since the bromide ion is a good leaving group, substitution readily occurs.

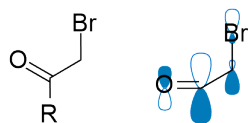
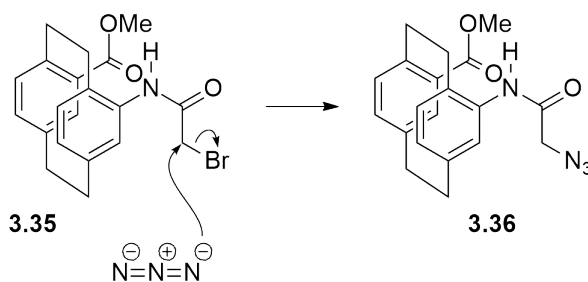


FIGURE 3.67: Orbital diagram of the α -carbonyl bromide of **3.35** demonstrating the orbital blending.

The compound could be used without further purification, which was valuable since the bromide was prone to degradation to the alcohol in the presence of any atmospheric water over time. It is stable to storage under inert atmosphere at -18°C for a short time (a few weeks).

Synthesis of azide **3.36**

Bromide **3.35** could be transformed to the azide **3.36** using sodium azide. It is a simple $\text{S}_{\text{N}}2$ substitution of the azide for the bromide (Scheme 3.68). Again the crude product could be used without purification, as the azide formation proceeded predictably without formation of any side product; any remaining sodium azide or sodium bromide did not hinder the next reaction.

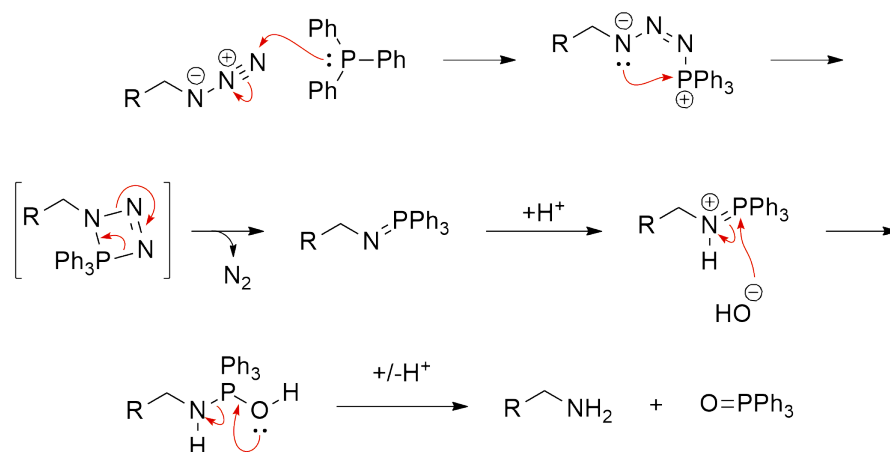


SCHEME 3.68: Transformation of bromide **3.35** to azide **3.36**.

Synthesis of amine **3.37**

The azide could be reduced to the amine using one of several reducing agents. Phosphines (triphenylphosphine, trioctylphosphine) efficiently reduced the azide however the resulting phosphine oxides were difficult to separate from the product.

Reduction using a phosphine follows the Staudinger reduction mechanism (Scheme 3.69).^{248,249}



SCHEME 3.69: Reduction with triphenylphosphine following the Staudinger mechanism.

It was considered that Staudinger ligation could be used at this step to form a tripeptide in the same step, however this method was not pursued for three reasons: the glycine residue formed from the azide reduction was a desired compound in itself; the required phosphinomethyl thiol was not readily available; and the phosphine oxide would still need to be removed from the crude product, which is a notoriously difficult operation.^{227,250,251}

Because of difficulties in purification, hydrogenation over 10% palladium on carbon was preferred (Scheme 3.70). The reaction proceeds to completion in less than an hour and the pure product is easily separated from the reaction mixture by filtration through celite.

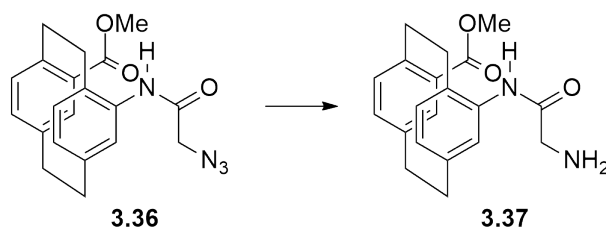


FIGURE 3.70: Reduction of the azide to the amine.

Attempted resolution of Gly-Pca

The Gly-Pca **3.34** was obtained by ester hydrolysis of **3.37** (Fig. 3.71).

Resolution of the racemic **3.34** was attempted by forming an imine with a chiral aldehyde such as camphor (Scheme 3.72), for subsequent resolution by recrystallisation.

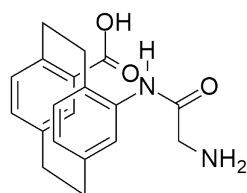
However, no available chiral aldehyde was found to form an imine with Gly-Pca - the reaction did not occur and only starting material was returned. Resolution by salt formation with cinchonine as with 4-toluenesulfonylamido[2.2]paracyclophane-13-carboxylic acid **2.48** (section 2.3.3) was also unsuccessful.

With the Gly-Pca dipeptide synthesised, the next step was to couple a more catalytically useful amino acid to the more reactive alkyl amine of the glycine residue. An L-amino acid would create two diastereomers which might be easier to resolve, as well.

Coupling of Pro to Gly-Pca

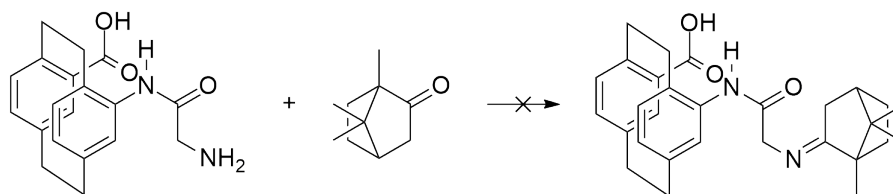
Our goal was to incorporate proline because of its role in catalysis for the reactions that will be tested in this project. The amine of proline was protected to avoid unwanted side couplings with the Boc group since this protecting group is readily removed using acid.

Using the mixed anhydride activation of Boc-proline's carboxylic acid with isobutyl chloroformate and DBU as the base successfully coupled the Boc-proline with Gly-Pca-OMe. However, the crude product retained a number of side products and reagents, which were difficult to remove during work up or using column chromatography, so better conditions were sought.



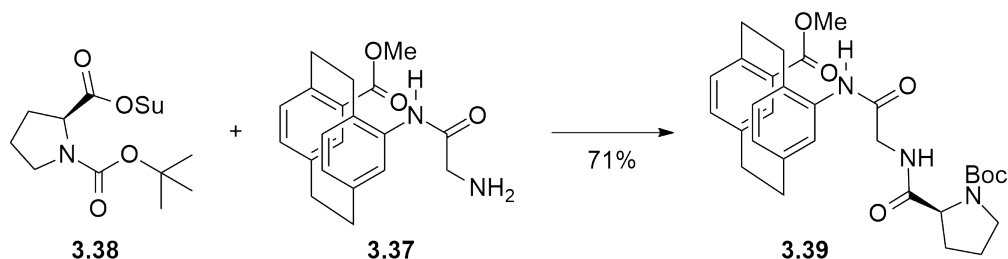
3.34

FIGURE 3.71: Gly-Pca **3.34**.



SCHEME 3.72: Attempted imine formation between Gly-Pca and camphor.

Since NHS and DCC were successful conditions for couplings with Boc-proline elsewhere in this project, these conditions were also tested. Boc-proline was coupled to Gly-Pca-OMe **3.37** using NHS and DCC as activating agents in good yield (Scheme 3.73). The mechanism of action of these reagents is discussed in Section 3.3.3.

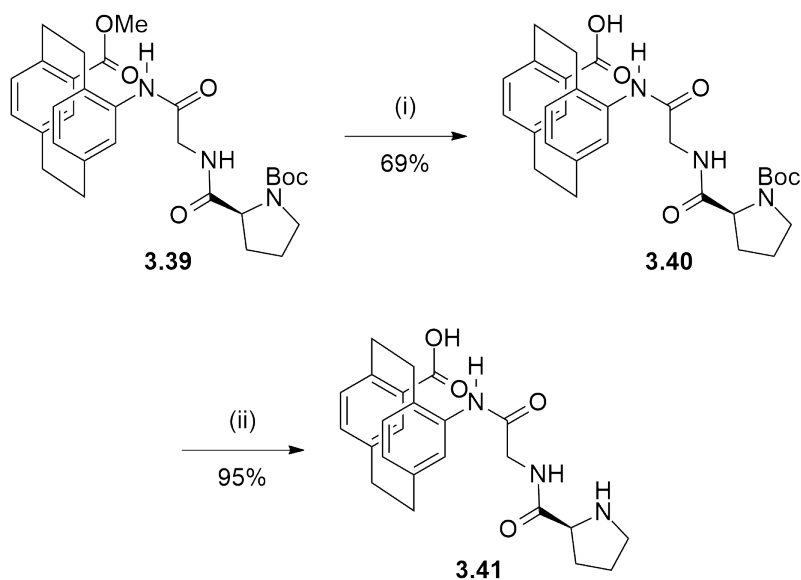


SCHEME 3.73: Coupling Boc-Pro-OSu **3.38** to Gly-Pca-OMe **3.39**.

Purification of the protected pseudopeptide product **3.39** was achieved by flash column chromatography and a MeOH/CH₂Cl₂ mixture as eluent.

Deprotection of the Boc-Pro-Gly-Pca-OMe tripeptide

Deprotection of the methyl ester and the Boc group were trivial (Scheme 3.74).



SCHEME 3.74: Deprotection of tripeptide **3.39**. i) KOH, heat. ii) TFA.

For hydrolysis of the methyl ester on the tripeptide **3.39**, reflux with 2 M ethanolic potassium hydroxide was too harsh; the ester was hydrolysed as well as the peptide bond between Gly and Pca. Repeating the conditions at 50°C, produced more favourable results with only the methyl ester being hydrolysed, albeit taking slightly

longer, requiring about 24 hours to go to completion with no formation of the ethyl ester from EtOH.

Other conditions resulted in a mixture of products containing the carboxylic acid and the ester corresponding to the solvent alcohol. The reaction proceeded best if the ester was dissolved in ethanol first, then ground KOH was added to the ester solution; otherwise, the substrate did not completely dissolve and reaction would not go to completion.

The ^1H NMR shows significant broadening of some, but not all, of the peaks (Fig. 3.75).

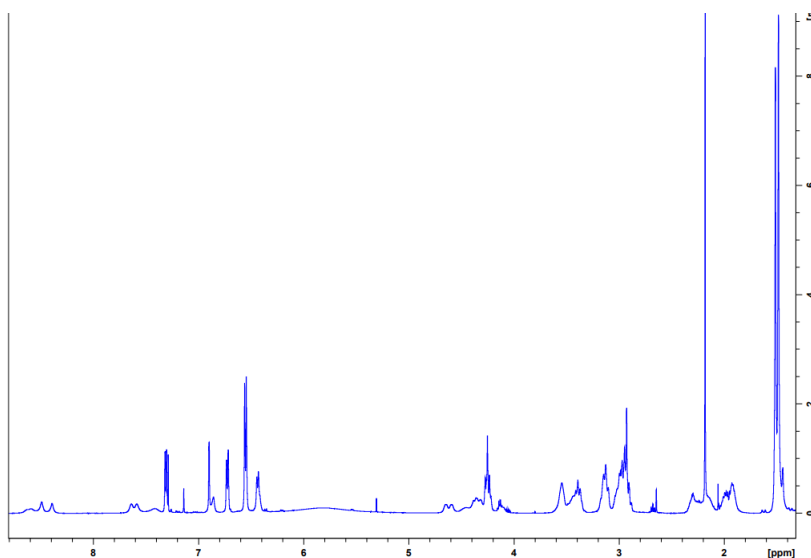


FIGURE 3.75: ^1H NMR of Boc-Pro-Gly-Pca.

The [2.2]paracyclophane aryl peaks, some alkyl peaks, and the Boc-group protons, are well-resolved; this is because these protons are not in local environments experiencing slow rotation about those bonds. The amide protons, as for Pro-Pca (Section 3.3.6), are subject to this effect (Figure 3.76), as are some protons in the glycine and proline residues.

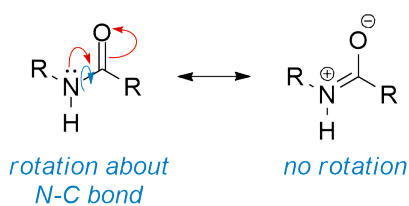
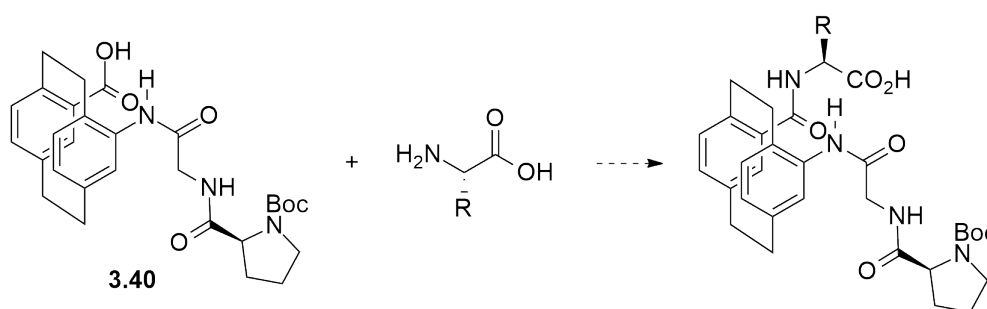


FIGURE 3.76: Delocalisation of nitrogen lone pair causing hindered rotation about the amide bond.

The broadening effect is further exacerbated by the presence of two diastereomers, which can make full interpretation of some pseudopeptide compounds difficult. Peak broadening due to poor sample preparation, for instance presence of paramagnetic ions, poorly-dissolved compound, or temperature or concentration gradients across the sample, can be ruled out since all peaks would be affected in this case.

Coupling attempts to Boc-Pro-Gly-Pca's C-terminus

After methyl ester deprotection, amino acid couplings to the C-terminus of the Pca were attempted (Scheme 3.77).



SCHEME 3.77: Attempted couplings between pseudo-tripeptide 3.40 and natural amino acids.

Since this compound was easier to synthesise than Pro-Pca, more coupling conditions could be tested. Attempts were made using the following sets of reagents: mixed anhydride formation with either ethyl chloroformate or isobutyl chloroformate and DIPEA; active ester formation with DCC and NHS; activation with EDC and HOBt; and finally acyl chloride formation using either cyanuric chloride or thionyl chloride. As before with Pro-Pca (Section 3.3.6), none were successful: they gave either returned starting material or a negligible amount of product - <3% as measured by ¹H NMR or mass spectrum peaks matching the product. On the small scales these experiments were run on (<20 mg), this product was impractical to obtain.

For many of the experiments it was unclear why no coupling was observed. But with the case of an attempted coupling between phenylalanine's N-terminus and Pca's C-terminus using ethyl chloroformate or isobutyl chloroformate, it was found that the corresponding Pca ester was formed instead of the desired mixed anhydride (Fig. 3.78).

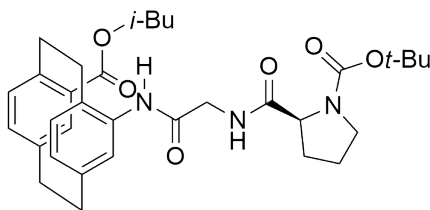


FIGURE 3.78: Isobutyl ester of Boc-Pro-Gly-Pca-OH.

The mass spectrum of the obtained product gave $m/z = 600$; the mass of this compound is 577, so the sodium adduct gives $577+23=600$. Additionally, the distinctive isobutyl $\text{CH}(\text{CH}_3)_2$ multiplet is visible in the proton NMR spectrum of the product. The isobutyl chloroformate may have decomposed and formed isobutanol, allowing ester formation to be favourable over the mixed anhydride.

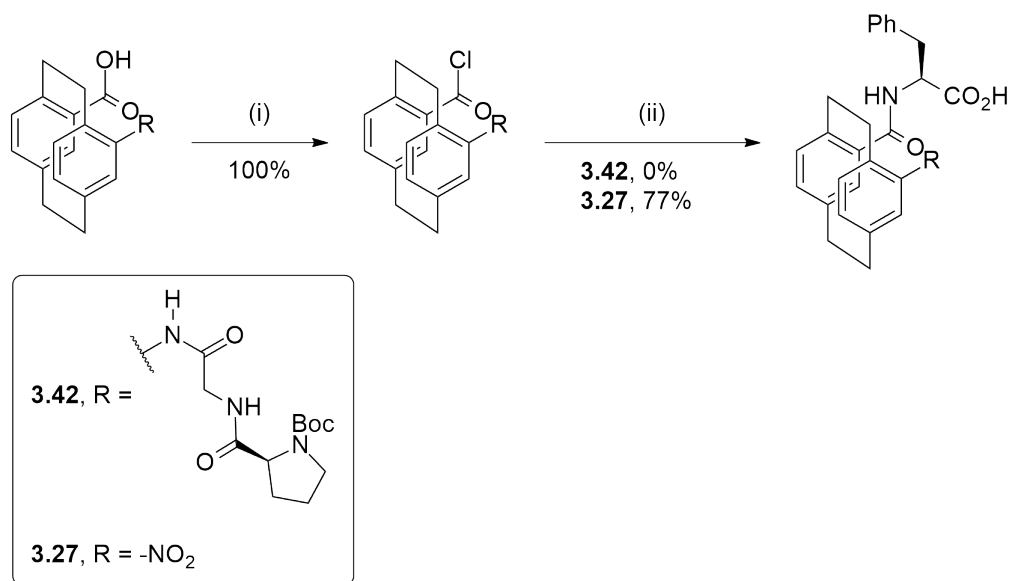
N-Hydroxy succinate ester activation of Boc-Pro-Gly-Pca's carboxylic acid was tested with its usual partner DCC. The active ester was isolated then added to phenylalanine. The presence of the active ester was confirmed by proton NMR and mass spectrum. There was no reaction between the active ester and phenylalanine.

A carbodiimide activation with EDC · HCl, stabilised by HOBT and including DMAP as an additional basic catalyst was also unsuccessful.

While initially, harsher coupling conditions were avoided, as a last attempt, carboxylic acid activation was attempted using thionyl chloride or cyanuric chloride (Scheme 3.79).

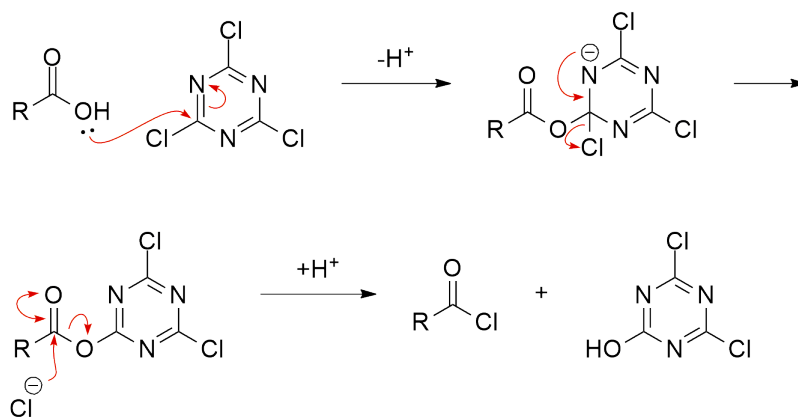
TLC analysis showed consumption of the starting material, however the amide product was never formed. At first it was suspected that, due to steric hindrance, the acyl chloride was slower to react and the presence of any water in the reaction mixture would simply form the starting carboxylic acid. These are the same conditions that worked in reasonable yield with 4-nitro[2.2]paracyclophane-12-carboxylic acid. However, the use of anhydrous conditions with nitrogenous bases instead of aqueous sodium hydroxide did not improve the result.

For the formation of an acyl chloride with cyanuric chloride in the presence of a base such as triethylamine, the mechanism begins with the displacement of a chloride ion by the carboxylic acid. The chloride ion then attacks the carbonyl carbon and



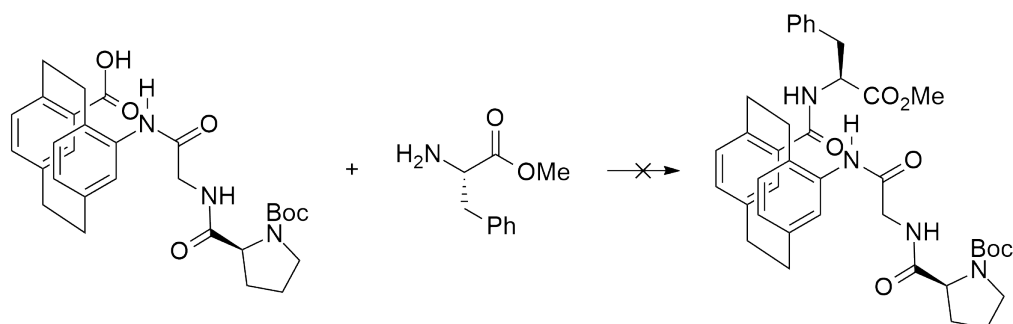
SCHEME 3.79: Coupling phenylalanine to the carboxylic acid of [2.2]paracyclophane derivatives *via* the acyl chloride. i) a. SOCl₂, b. MeOH. ii) L-phenylalanine, aq. NaOH.

ejects the alcohol byproduct, giving the acyl chloride (Scheme 3.80). Again, just the dehydrating or activating of the carboxylic acid part is changing.



SCHEME 3.80: Acyl chloride formation with cyanuric chloride.

Phenylalanine was used for these coupling attempts since we had already coupled this amino acid to the C-terminus of Pca (Scheme 3.81). When initial coupling attempts with phenylalanine failed, Phe-OMe was synthesised in order to prevent the carboxylic acid of Phe interfering with the coupling, and to increase solubility of the amino acid in solvents compatible with the Pca derivative. Phe-OMe was synthesised according to methods from Shibata *et al.* using thionyl chloride and methanol.²⁵²



SCHEME 3.81: Attempted coupling of Phe-OMe to Boc-Pro-Gly-Pca-OH.

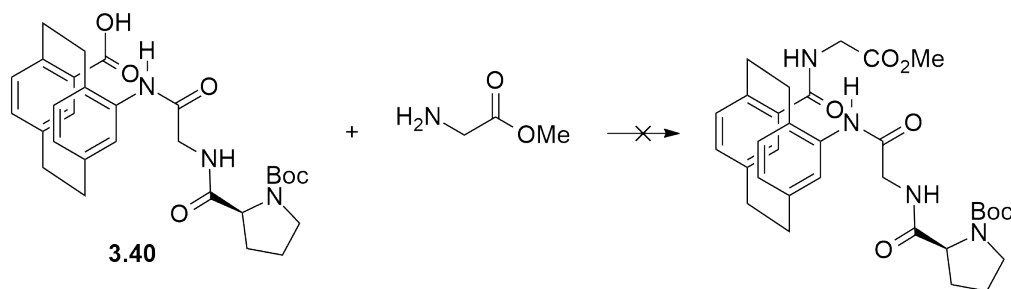
The enantiomeric purity of the obtained Phe-OMe was checked using circular dichroism (CD) spectrometry and found to be acceptable. Enantiomers give CD spectra with equal amplitude but opposite sign; therefore the CD spectra for a racemate would be flat. Since no reference CD spectrum was available for L-Phe-OMe, its CD spectrum was compared with the starting L-phenylalanine and found to be comparable in amplitude. This evidence suggests that even if a small portion of the material had racemised, the bulk of the material remained stereochemically unaltered.

Since these conditions were found to maintain stereochemistry, the use of thionyl chloride as a carboxylic acid activating reagent was used in other points of synthesis where stereochemistry was at risk. Protection of the carboxylic acid did not aid peptide coupling, even when using thionyl chloride as an activating reagent. Thionyl chloride under most circumstances is an efficient coupling reagent so would be expected to give a positive result if coupling on this compound were possible.

To see if the bulk of the nucleophile was the issue we attempted to couple glycine methyl ester (Scheme 3.82). When this was also unsuccessful we presumed that the problem resided with the Pca derivative considering 4-nitro[2.2]paracyclophane-13-carboxylic acid could be coupled under similar conditions (Section 3.3.1).

Boc cleavage of Boc-Pro-Gly-Pca

The Boc group was cleaved using 1:3 trifluoroacetic acid in dichloromethane at 0°C. With this pseudopeptide **3.41** fully deprotected, another pseudopeptide to be tested as a catalyst was prepared and ready for resolution of the diastereomers (Fig. 3.83).



SCHEME 3.82: Attempted coupling of glycine to Boc-Pro-Gly-Pca-OH 3.40.

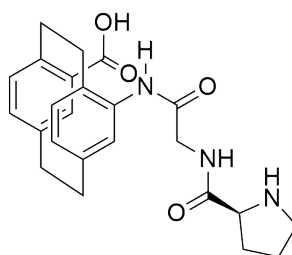


FIGURE 3.83: Pseudopeptide 3.41.

The proton NMR of the pseudopeptide product displays some interesting effects of the compound's structure. Variable temperature ^1H NMR shows how the N-H peaks of this compound start as several well-defined peaks and coalesce to an averaged peak as the temperature increases (Fig. 3.84).

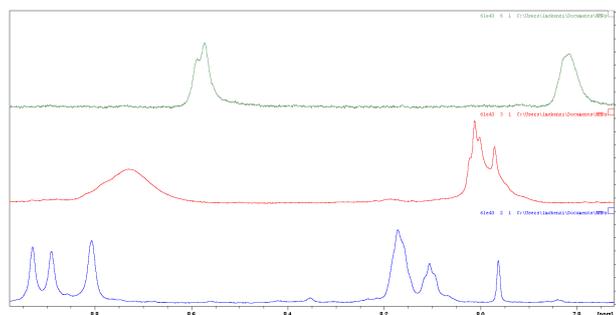


FIGURE 3.84: N-H region of the Pro-Gly-Pca spectrum in variable temperature ^1H NMR. Bottom to top: 298 K (blue), 328 K (red), 373 K (green).

This is due to the faster tumbling of the amide bonds with the increased kinetic energy. It may also be affected by a decrease in intramolecular hydrogen bonding as temperature increases, which would explain their shift upfield due to less deshielding.

Resolution of Pro-Gly-Pca

TLC analysis of the fully deprotected pseudopeptide **3.41** (Fig. 3.83) eluting with 5% methanol in dichloromethane, when run twice gave two spots with an R_f difference of 0.07 (0.32 and 0.39). Standard flash column chromatography failed to resolve the diastereomers, but a gravity silica column partially separated the two with the bulk of the product inseparable. A small quantity of each diastereomer was separable before and after the main bulk of the material. Using a smaller particle size of silica (25-40 μm instead of the standard 60 μm) also aided this separation. Finer silica may clog the pores of a glass frit in a column and prevent eluent flow; this may be avoided by first adding a layer of a material like sand or glass wool to the bottom of the column.

The two diastereomers were separated, with some central overlap as above for the Pca-Phe precursor **3.25**. However, it was not possible to grow crystals of adequate quality for X-ray crystallography; NMR data was not sufficient for elucidation of absolute configuration of the two diastereomers. Thus, they are referred to as **3.41-A** and **3.41-B**; A is the diastereomer with the higher R_f . The flexibility of the central glycine unit causes problems for both recrystallisation and analysis of the NMR.

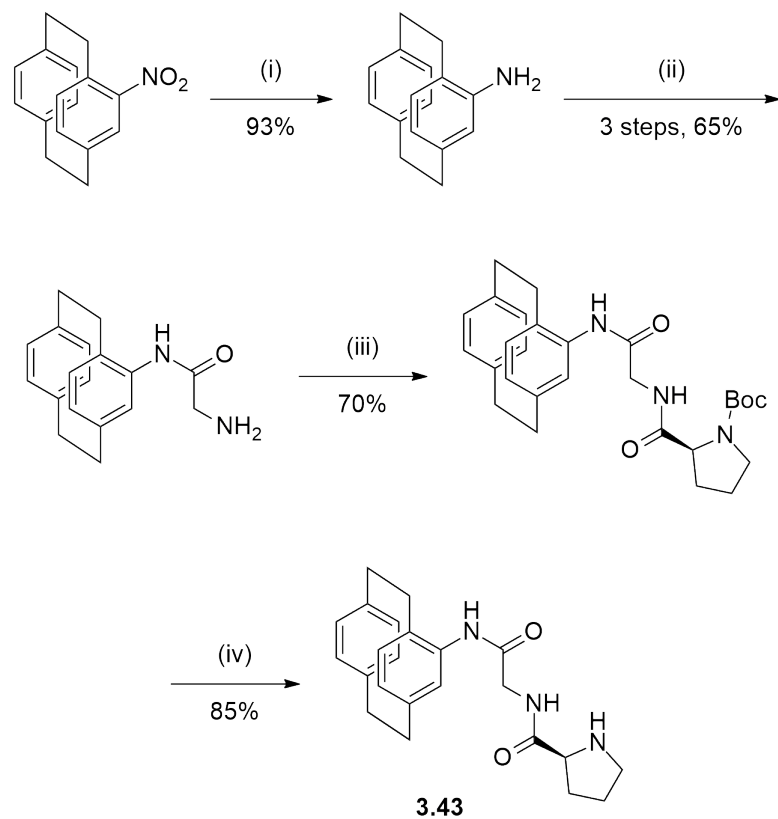
Synthesis of the mono-substituted 4-Pro-glycinamido[2.2]paracyclophane

As for Pro-Pca (Section 3.3.6), the mono-substituted version of Pro-Gly-Pca was synthesised in the same manner, starting with 4-amino[2.2]paracyclophane, affording the diamide **3.43** (Scheme 3.85).

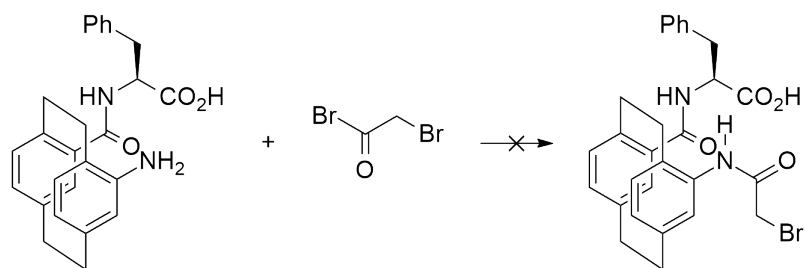
Attempted synthesis of the glycine residue on Pca-Phe

With conditions for synthesis of the glycine residue in hand, we also looked at using the same strategy to form a tripeptide with Pca as the central residue. Starting with the previously synthesised Pca-Phe, the same synthesis to Gly-Pca-Phe was attempted (Scheme 3.86). The first reaction, amide formation with bromoacetyl bromide, was unsuccessful.

Initially, we believed that the free carboxylic acid of the phenylalanine residue was the cause. To test this, the acid was protected with a methyl ester giving **3.44**.

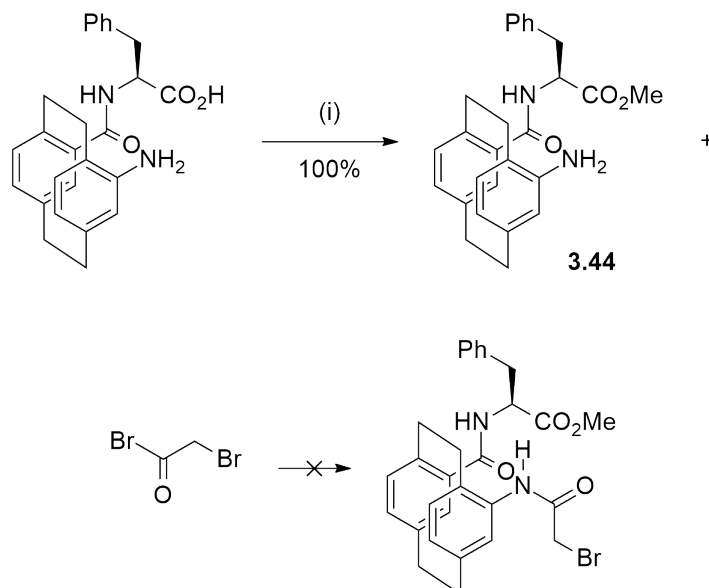


SCHEME 3.85: Synthesis of the mono 4-Pro-Gly-amido[2.2]paracyclophane. i) Zn, NH₄Cl ii) a. bromoacetyl bromide, b. NaN₃, c. H₂, Pd/C iii) Boc-Pro-Osu iv) CF₃COOH



SCHEME 3.86: Attempted synthesis of Gly-Pca-Phe.

The methyl ester was formed with thionyl chloride and methanol. The amide coupling with bromoacetyl bromide was attempted again and it was still unsuccessful (Scheme 3.87).



SCHEME 3.87: Attempted amide coupling between Pca-Phe-OMe **3.44** and bromoacetyl bromide. i) SOCl₂, MeOH.

Including Et₃N as a base to manage the acidity did not make the coupling work.²⁵³ Enhancing solubility by changing the solvent to acetonitrile or acetone was not helpful.

Another cause of the failure of this coupling is considered to be the increased steric hindrance from the phenylalanine residue. The organisation of the 22PC-amine and the phenylalanine residue on the opposite deck of the [2.2]paracyclophane scaffold would seem to allow hydrogen bonding between the two substituents, decreasing the nitrogen's propensity to react.

3.4 Outcome of peptide syntheses

Figure 3.88 shows the compounds that were synthesised. Not all were tested as catalysts in this project: Pca-Phe **3.44** was not used since it did not contain the active proline moiety. Resolution of **3.7**, **3.41** and **3.44** was achieved. With these in hand we could turn our attention to catalyst studies.

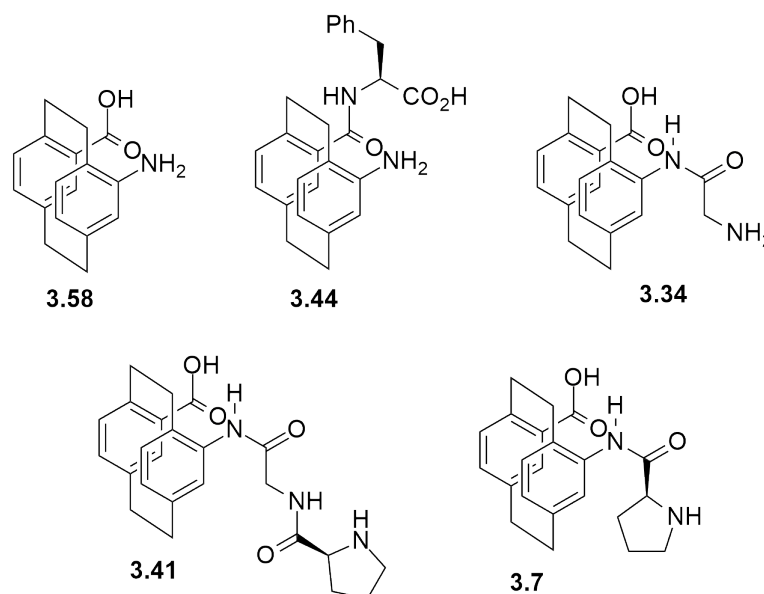


FIGURE 3.88: Pca derivatives synthesised and tested in this project. **3.58**: Pca; **3.44**: Pca-Phe; **3.34**: Gly-Pca; **3.41**: Pro-Gly-Pca; **3.7**: Pro-Pca.

Synthesis of new peptides containing Pca was hindered by poor reactivity but conditions for peptide couplings with Pca were obtained with some success. For couplings to the Pca carboxylic acid, acyl chloride formation is an effective yield giving good yield and high purity. For peptide couplings to the unreactive Pca aniline, *N*-hydroxysuccinate ester activation of the amino acid gave acceptable results. Also developed was the synthesis of a glycine residue directly on the Pca aniline.

Four new Pca-containing peptides were described: Pro-Pca **3.7**, Gly-Pca **3.34**, Pro-Gly-Pca **3.41**, and Pca-Phe **3.44**.

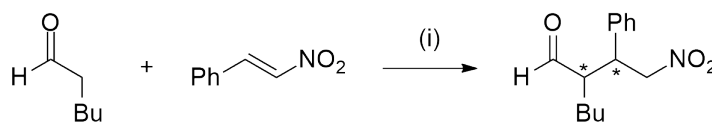
The combination of the above work sets the stage for development of interesting new planar chiral compounds with diverse chemistry.

Chapter 4

Asymmetric organocatalysed Michael addition with planar chiral amine derivatives

With the peptide synthesis complete, a catalytic screening was necessary to investigate the potential and differences of the [2.2]paracyclophane-centred peptides as catalysts. The Michael addition was chosen since it is a useful asymmetric carbon-carbon bond forming reaction that many proline-derived catalysts have been developed for.

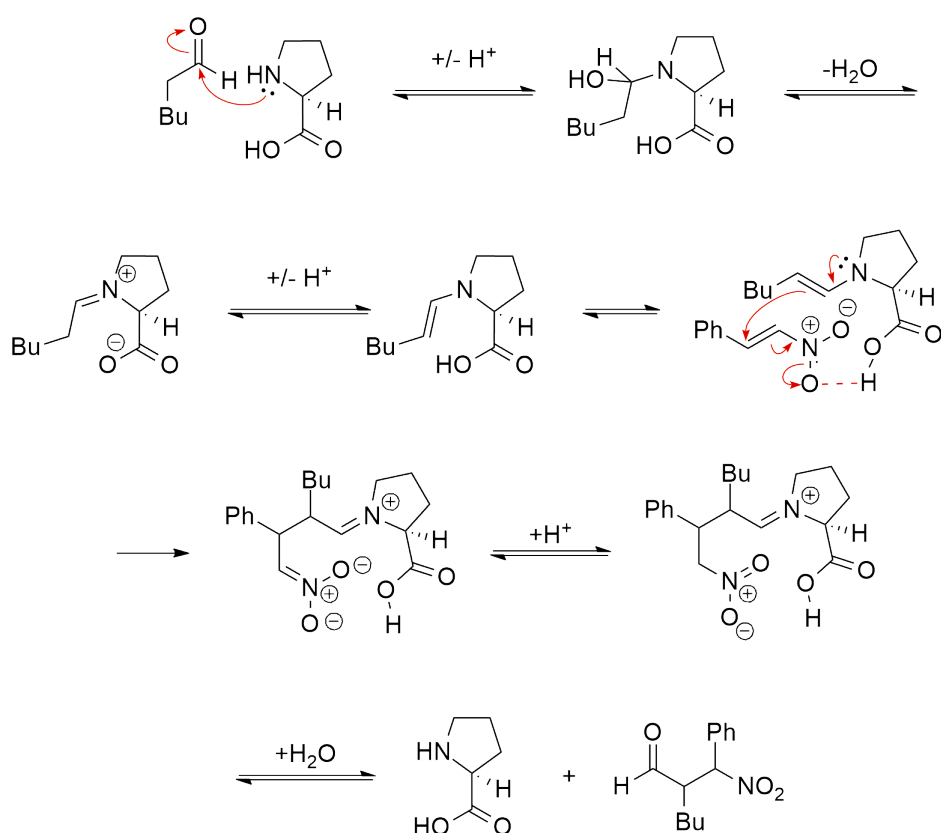
Michael addition of hexanal to *trans*- β -nitrostyrene (Scheme 4.1) was chosen as the test reaction system for asymmetric catalysis by the small library of pseudopeptides synthesised.



SCHEME 4.1: Asymmetric Michael addition between *trans*- β -nitrostyrene and hexanal. i) 5-20 mol % catalyst, 5-10 mol % NMM.

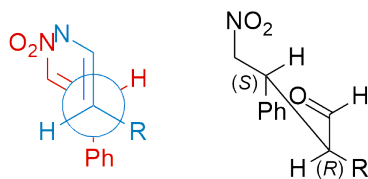
4.1 Michael addition between *trans*- β -nitrostyrene and hexanal

Michael addition of an alkyl aldehyde to *trans*- β -nitrostyrene (Scheme 4.2) has attracted attention from groups designing asymmetric organocatalysts. Two stereocentres are installed; the *syn* ((*R,S*) or (*S,R*)) configuration is usually the major diastereomer pair formed when asymmetric catalysts are employed. It has been reported that the carboxylic acid at the C-terminus of the peptide stabilises the intermediate and this influences stereochemistry of the product.²⁵⁴



SCHEME 4.2: Mechanism of Michael addition between *trans*- β -nitrostyrene and hexanal catalysed by proline.

Syn addition is favoured because of the shape of the reaction intermediate. Figure 4.3 shows the orientation of the approach of the two molecules in the C-C bond forming step according to Seebach's topological model.²⁵⁵ The existing substituents are staggered. The N donor will be gauche and overlapped with the acceptor NO₂; this minimises charge separation and forms a *quasi*-chair conformation. This gives the *syn* product in our Michael addition.

FIGURE 4.3: *Syn* product formation.

4.1.1 Initial reaction condition screening

Since this reaction has been studied extensively conditions and results could be compared to other groups'. Hexanal was chosen as the substrate from those which had been presented in the literature. Butanal, pentanal, 3-methylbutanal and hexanal were trialled and the cleanest reaction was observed with hexanal.

DL-Proline and L-proline were the first catalysts tested in the Michael reaction. This was for several reasons:

- to determine appropriate reaction conditions with this system,
- to compare results with other groups' results with a standard catalyst, since proline is a common catalyst to test with Michael addition of *trans*- β -nitrostyrene and aldehydes, which ensured our results are standard, and
- to provide a control reaction.

These reactions also provided racemic material to standardise the HPLC analysis.

The initial reactions employed conditions used in previous studies. This helped both ensure our results can be compared with literature, and furthermore using known conditions decreased the amount of troubleshooting required to find a suitable set of conditions for catalyst testing. Initial tests used 9:1 chloroform/isopropanol as the solvent mixture. It was found that even with proline as the catalyst, it would not fully dissolve in the reaction mixture and required the addition of a small amount (10-15%) of methanol into the solvent mixture. With increasing catalyst size, methanol was no longer sufficient to dissolve the compounds. For optimal catalyst solubility the reaction solvent system must contain a small amount of DMSO. Thus further control reactions were run with the final solvent mixture of 9:1:1.6 chloroform/isopropanol/DMSO. Compounds containing [2.2]paracyclophane tend to

have low solubility; the amount of intramolecular hydrogen bonding and the size of the molecules make the Pca peptide catalysts particularly poor examples.

Wennemers *et al.* tested the reaction of butanal with *trans*- β -nitrostyrene with their tripeptide catalysts in different solvents and found a mixture of 9:1 chloroform/isopropanol to give the best combination of conversion, diastereoselectivity and enantioselectivity.²⁵⁶ NMM is used as a base additive to the peptide catalyst which is added as the hydrochloride salt. Using DMSO as solvent increased conversion but gave lower selectivity. Pearson *et al.* tested the reaction of *p*-nitrobenzaldehyde with cyclohexanone with various solvents and acidic additives.²²² DMSO was found to be the best solvent for their system; running the reaction at low temperatures with low boiling point solvents was found to be undesirable due to the pseudopeptide catalysts crashing out of solution at temperatures below room temperature. Acidic additives are not appropriate for our experiments since we want the carboxylic acid of the catalyst to be active in the reaction.

We first ran a series of control reactions involving just proline as the catalyst, which completed the reaction within hours. The next step was to investigate the influence of our catalysts. The reactions with our peptides were slower. A number of times and temperatures were trialled and the most effective was running the reaction at room temperature for 2 days, then at 60°C for 2 days (Entries 9-11 in Table 4.1), so the screening tests were standardised to this schedule.

Since the screening reactions were always taken to completion, as measured by TLC analysis and confirmed by the absence of starting material in ¹H NMR, % yield is an irrelevant metric; and since the reactions were run on 10 mg scale, measuring the yield was somewhat impractical, so this figure will not be quoted. Instead, the catalysts' effectivenesses are measured using two metrics: diastereoselectivity (the ratio of *syn* addition vs. *anti*); and enantioselectivity (of the *syn* product, how much of the major (*S,R*) enantiomer was made vs. the minor enantiomer (*R,S*)).

The former is measured using the ¹H NMR spectrum, where several key protons in the diastereomers have identifiable peaks that are separate enough to measure the ratio between them (Fig. 4.4). The latter is measured using HPLC, where using the

correct chiral column and conditions, we can measure the ratio of major and minor enantiomers' peaks (Fig. 4.5).

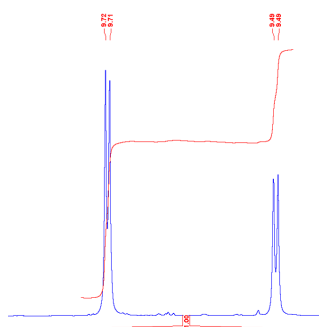


FIGURE 4.4: Aldehyde proton peak for the *syn* (9.72 ppm) and *anti* (9.49 ppm) diastereomers of 2-butyl-4-nitro-3-phenylbutanal.

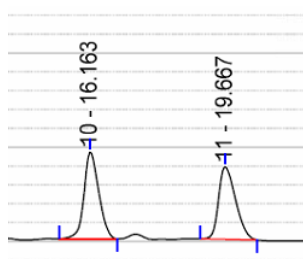


FIGURE 4.5: Major (*S,R*, 16.2 min) and minor (*R,S*, 19.7 min) *syn* product HPLC peaks (OD-H column, 9:1 hexane/*i*-PrOH), 1 mL/min.

HPLC conditions were chosen so that literature values could be used to identify the correct peaks. Several authors have published HPLC data on the compounds with different conditions, with the most common conditions using the OD-H column with between 3% and 20% *i*-PrOH in hexane.^{256–262} Thus, tests were run using these column conditions and 20% *i*-PrOH in hexane was chosen as the solvent ratio since it gave faster elution while retaining separation. The Michael product peaks were found in agreement with literature.

4.2 Catalysis screening results

The amino acids and pseudopeptides presented in Figure 4.6 were tested in the standardised Michael reaction between *trans*- β -nitrostyrene and hexanal (Fig. 4.1).

Notably, the Pca-Phe dipeptide that was synthesised in this project was not tested as a catalyst since it did not contain the proline residue that was desired for catalytic

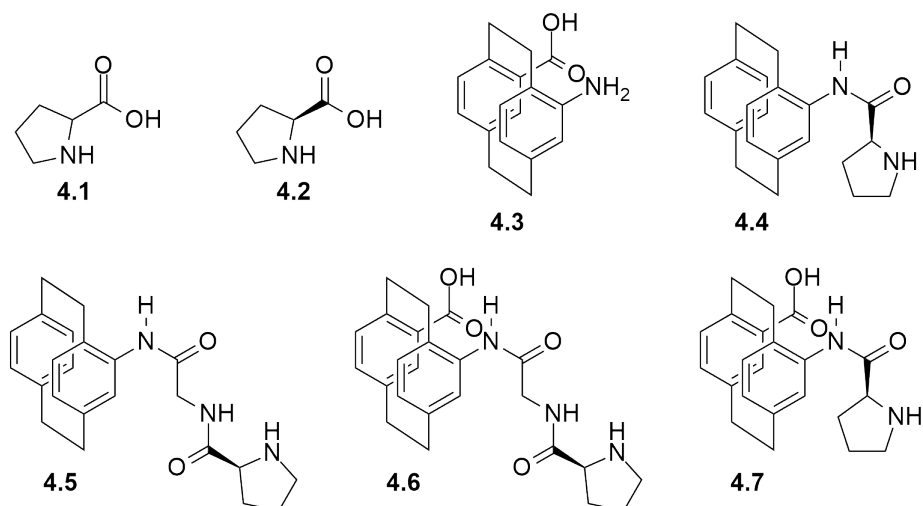


FIGURE 4.6: Catalysts tested in asymmetric organocatalysed Michael addition. **4.1:** DL-proline; **4.2:** L-proline; **4.3:** Pca; **4.4:** Pro-PC; **4.5:** Pro-Gly-PC; **4.6:** Pro-Gly-Pca; **4.7:** Pro-Pca.

activity in this reaction. Since the results obtained from this tested were not as explicable as expected, as explained in the discussions to follow, it might have been interesting to include Pca-Phe in the catalyst screening.

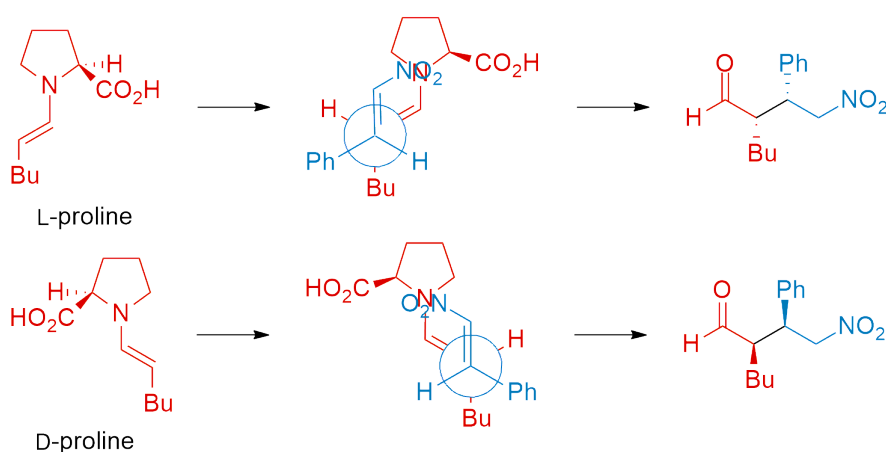
Entry	Catalyst	Time & temperature alterations	<i>dr</i> , <i>anti:syn</i>	<i>er</i> , <i>(R,S):(S,R)</i>
1	4.1	1 day RT	5:95	50:50
2	4.2	1 day RT	4:96	43:57
3	4.3 , racemate	-	33:67	50:50
4	4.4 -A and B	-	35:65	48:52
5	4.5 -A and B	-	23:77	42:58
6	4.6 -A and B	-	32:68	37:63
7	4.6 -A	-	32:68	39:61
8	4.6 -B	-	33:67	38:62
9	4.6 -B	9 days RT	42:58	39:61
10	4.6 -B	2 days 60°C	37:63	49:51
11	4.6 -B	2 days RT then 4 days 60°C	33:67	42:58
12	4.7 , single diastereomer	-	29:71	30:70

TABLE 4.1: Results of asymmetric Michael addition between *trans*- β -nitrostyrene and hexanal catalysed by peptides. Conditions: solvent - 9:1:1.4 CHCl₃/*i*-PrOH/DMSO; 2 days RT then 2 days 60°C; 5 mol % catalyst, 10 mol % NMM.

Where possible, all tests were performed in triplicate (or more) to confirm the results were within agreement. Figures stated in Table 4.1 are mean values.

4.2.1 Proline 4.1 and 4.2

A control study with L-proline was found to be in agreement with literature results, and showed L-proline gave *dr* (*anti:syn*) of 4:96, and *er* [(*R,S*):(*S,R*)] of 43:57.²⁶³ Predictably, DL-proline does not select for the (*R,S*) or (*S,R*) enantiomers at all. It exhibits diastereoselectivity because of its control over the transition state as shown in Figure 4.3 which preferentially forms the *s-trans* intermediate, in which the enamine bond and attached groups are arranged with the R group of the aldehyde away from proline's carboxylic acid; but cannot differentiate between the diastereomers of the *syn* product since it is racemic (Figure 4.7).



SCHEME 4.7: Newman projections of Michael addition with DL-proline catalyst.

These tests were only run at room temperature with no heating phase, unlike most other screens, since the reaction went to completion within one day.

Proline has quite a low enantioselectivity but when combined with a co-catalyst or included as a larger peptide it gave superior enantioselectivity of 80-90% *ee*.^{256,264,265} As Wennemers found this is probably due to the more optimal distance between the enamine-forming nitrogen and the carboxylic acid.¹⁴⁷ We hoped this would mean our Pca catalysts would give good results.

4.2.2 Tests for importance of stereochemical resolution of catalysts

Since most Pca pseudo-peptides were difficult to resolve, a set of tests was devised to test the importance of enantiomeric or diastereomeric purity. Pro-Gly-Pca was able to be resolved into its diastereomers so each diastereomer was screened separately,

along with a mixture of the two diastereomers. Comparing these tests shows that the diastereomeric purity of this catalyst was not an important factor for the stereochemical outcome of the reaction. Entries 6-8 in Table 4.1 show each of these tests gave similar *dr* and *er* within the range of normal variation. It was a disappointing result since we hoped that the [2.2]paracyclophane backbone would influence the stereochemical outcome of the reaction.

We concluded that the rest of the tests could be run with the unresolved Pca catalysts. We assumed that using mixtures of diastereomers or enantiomers of the catalysts would have negligible effect on their stereoselectivity, but we are aware that this may not be the case. Each pseudopeptide or pseudoamino acid may behave differently due to the different relative positioning of each functional group.

The lack of influence of the Pca moiety on the selectivity of the tripeptide is probably the result of the flexible nature of the Gly residue. It would be illuminating to test this by replacing glycine with an alternative residue, either a natural amino acid with an R group that could decrease the conformational freedom or another unnatural amino acid that makes this section more rigid. The results might suggest that the carboxylic acid is not involved in this reaction and it would have been useful to test this theory by using the ester as a catalyst.

Unfortunately, the more rigid system Pro-Pca was only available as a single diastereomer so it is impossible to know if the Pca moiety played a more important role. With more time the other diastereomer could have been synthesised. While it is dangerous to make assumptions, the fact that **4.4** (Entry 4 in Table 4.1), without the acid functionality, gave a lower enantioselectivity suggests this group is important in Pro-Pca's catalysis mechanism. This could be because for Pro-Pca, the carboxylic acid moiety is closer to the proline residue.

4.2.3 Tests for effect of time and temperature

The effects of varying the time and temperature the reaction is run for are shown in Entries 9 - 11 in Table 4.1. Running the reaction only for two days at 60°C decreases the enantioselectivity of the reaction. This could be due to the increased flexibility of the glycine-proline chain at high temperature.

Longer reaction times decreasing the diastereoselectivity of the reaction might be due to an equilibrium existing between the diastereomers, as suggested by other groups studying the same reaction.²⁶⁶ If the catalyst is able to form the enamine with the product it can interconvert between the *anti* and *syn* products.²⁶⁷ Thus, the slow rate of reaction with the Pca catalysts might to their quite low diastereoselectivity. Since the reactions take about 4 days to run to completion, finishing them as soon as the starting material is consumed, and before equilibration between the diastereomers begins, is difficult.

4.2.4 Pca 4.3

A mixture of enantiomers of Pca gave a 33:67 mixture of *anti/syn* diastereomers of the Michael product. We know from previous experiments (Section 3.3.5) that imine formation at the Pca N is possible so Pca can act as a catalyst here - although the reaction proceeds slowly, as with all the [2.2]paracyclophane-containing catalysts tested. As with DL-proline, we see no enantioselectivity since this material was racemic.

All the Pca-containing catalysts show a reversal of stereoselectivity towards the *anti* product. Recently the Wennemers group also found that altering the active proline moiety to introduce steric inhibition of the formation of the *Si/Si* intermediate could influence the diastereoselectivity of the reaction (Figure 4.8).²⁶⁸ Wennemers' group showed that including bulky groups on the δ -C of the catalytic proline residue of their tripeptide catalysts caused reversal of the usual *syn* diastereoselectivity of amine-catalysed Michael reactions of nitroolefins. Their dimethylproline residue caused preferential formation of the *s-cis* enamine intermediate since this configuration was sterically favoured. When the nitroolefin attacks, it is still held in *Si* alignment by the carboxylic acid of the catalyst, giving a larger proportion of the *anti S,R* major product.

A reversal of diastereoselectivity is also seen in the Pca catalysts tested here. A similar effect may be occurring, where the bulky [2.2]paracyclophane backbone is having an inhibitory effect on the *s-trans* enamine, changing the equilibrium of the transition state in favour of the *s-cis* configuration.

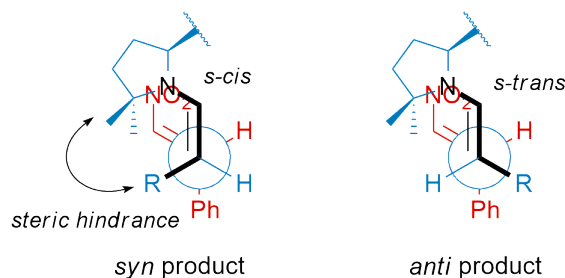


FIGURE 4.8: *Syn* and *anti* transition states in Wennemers' *anti*-selective Michael addition.

4.2.5 Pro-NH-22PC 4.4

The monosubstituted Pro-NH-22PC gave similar *dr* and *er* to Pca. A mixture of diastereomers, stereochemically pure at the Pro moiety but unresolved at Pca gave an essentially racemic product.

Compared to the results for L-proline, in this catalyst proline is coupled through an amide bond to 4-amino[2.2]paracyclophane. This prevents its carboxylic acid from interacting in the reaction and increases steric bulk. Compared to L-proline, this catalyst showed a slight reversal of diastereoselectivity (4:96 *anti*/*syn* for L-proline vs 35:65 for 22PC-NHPro). Regardless of chiral orientation at 22PC, since this was a mixture of diastereomers, the 22PC component exhibits a greater tendency to produce the *anti* product, as seen with Pca. Without the carboxylic acid, the incoming nitrostyrene is not spatially directed as strongly, so there is very little enantioselectivity.

4.2.6 Pro-Gly-NH-22PC 4.5

With this catalyst as a mixture of diastereomers, we see minimal enantioselectivity (42:58 minor/major); and a higher ratio of *syn* product compared to Pro-NH-22PC, *i.e.* less reversal of diastereoselectivity toward the *anti* product. The glycine residue increases flexibility of the molecule and distance from the 22PC moiety. These combine to decrease the influence of the 22PC compared to the catalytic centre of the proline residue. By separating the proline residue from the [2.2]paracyclophane backbone the *dr* starts to return to that of L-proline, compared to the mono Pro-NH-22PC. Figure 4.9 shows the possible configurations that would lead to the *anti* and *syn* diastereomers. When Pca is directly coupled to proline the [2.2]paracyclophane

backbone is closer to the catalytic centre and by interaction with the nitro group influences diastereoselectivity. Again, without the carboxylic acid on the opposing deck of [2.2]paracyclophane, this mono-substituted amide gives very low enantioselectivity.

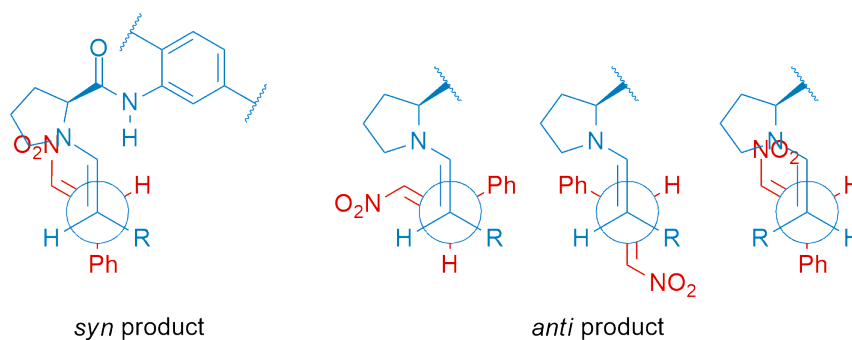


FIGURE 4.9: Possible configurations of the enamine intermediate.

4.2.7 Pro-Gly-Pca 4.6

Three tests were performed with this catalyst: each diastereomer individually, then a 1:1 mixture of diastereomers. The tests show insignificant difference between the two diastereomers, and the mixture thereof. This suggests the stereochemistry at Pca is not important for enantioselectivity and that Pca's effect is mainly due to its steric bulk and possibly the geometric arrangement of the -COOH and the -NH-Gly-Pro peptide chain pseudo-*gem* from each other. We know from comparing 4.4 and 4.5 that distance between the Pca and Pro residues diminishes [2.2]paracyclophane's effect on *dr*.

Entries 5 & 6 in Table 4.1 compare the Pro-Gly chain with and without the carboxylic acid on the opposing face of [2.2]paracyclophane. For the Pca derivative 4.6, *dr* decreases but the *er* increases.

DFT calculations of the peptide ground states were carried out by Tyson Dais, using the ω B97XD functional. The ω B97XD functional is range-separated, which makes it suitable for [2.2]paracyclophane, with its ring-to-ring interactions. Models of the ground state Pro-Gly-Pca show a difference between diastereomers in the conformation of the Pro-Gly chain due to hydrogen bonding. These are the lowest energy conformers.

As seen in Figures 4.10 and 4.11 the S_P -diastereomer contains a hydrogen bond contact where the R_P -diastereomer does not: between the Pro-Gly amide C=O and the O-H of the [2.2]paracyclophanyl carboxylic acid.

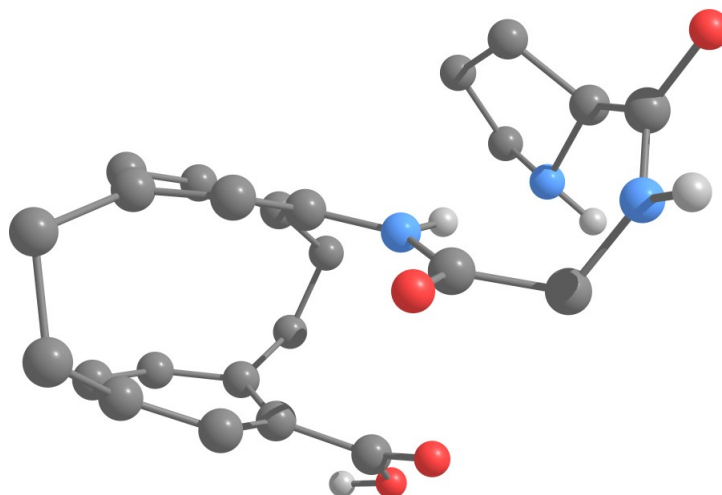


FIGURE 4.10: Computational model of R_P,S -Pro-Gly-Pca.

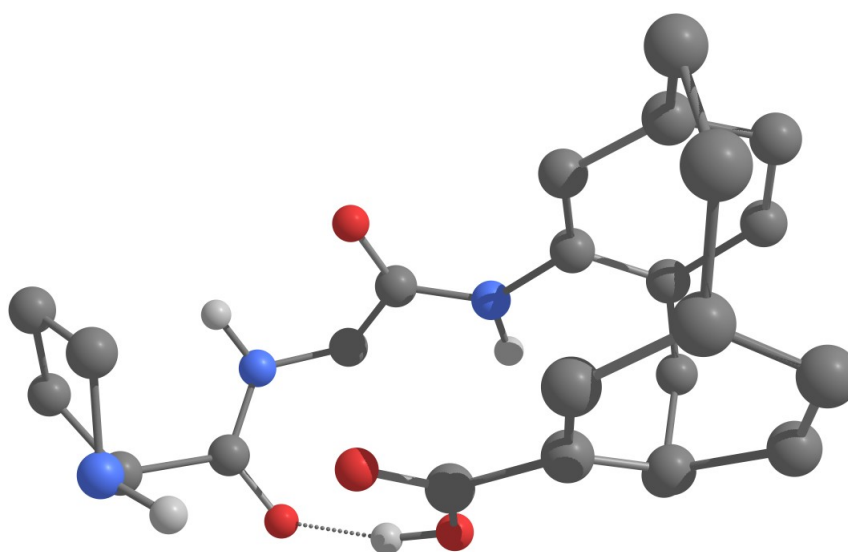


FIGURE 4.11: Computational model of S_P,S -Pro-Gly-Pca.

We might expect the R_P,S -diastereomer to give better stereoselectivity since the orientation of the proline N directs the substrate towards the centre of the catalyst molecule as well as its active carboxylic acid on the opposing [2.2]paracyclophane aryl deck. However, no difference in stereoselectivity was seen between the two diastereomers, which suggests that there is too much conformational flexibility in the molecule for stereochemical information to be transmitted from the [2.2]paracyclophane moiety.

4.2.8 Pro-Pca 4.7

This catalyst showed the best *er* of any catalysts tested (30:70). With proline directly coupled to Pca the enantioselectivity is increased. Crystals of this molecule could not be produced and thus stereochemistry at the Pca residue is not known, nor is its conformation; but computer modelling suggests the following conformation of the compound (Fig. 4.12 and 4.13). According to this model, there is little conformational flexibility in this molecule with the amide bond between Pca and Pro being rigid. The amide C-N bond is intermediate in length between a C-N single bond and double bond, indicating partial double bond character, giving it limited rotation. The ^1H NMR spectrum, with its broad N-H peak supports this. Thus the proline-N and Pca-COOH are held in quite static position.

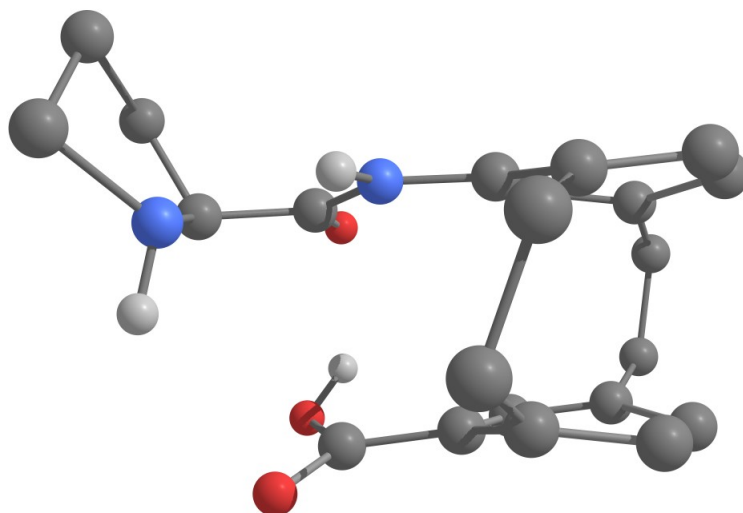
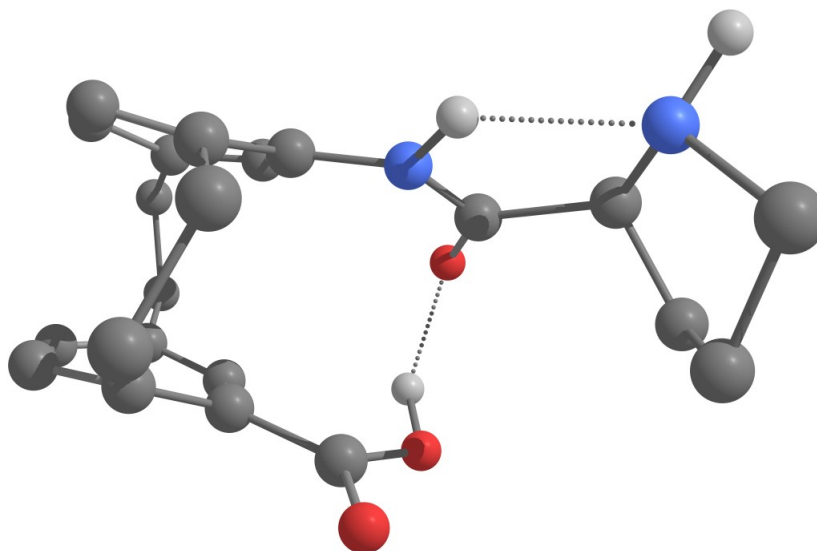


FIGURE 4.12: Computational model of R_P,S -Pro-Pca.

As discussed in Section 3.3.6, the Pro-Pca synthesised was found to be a single diastereomer. In computational models of the two diastereomers of 4.7, the R_P,S - and S_P,S - diastereomers of Pro-Pca could have different relative shapes, with R_P,S -4.7 looking like it might lead to a more sterically congested enamine, due to the presence of intramolecular hydrogen bonding only in the S_P,S diastereomer. This orients the pyrrolidine ring inwards with the N pointing away from the rest of the molecule, whereas the pyrrolidine ring in R_P,S -4.7 points outwards with the N pointing inwards towards the opposite [2.2]paracyclophane deck. In either case there is limited conformational freedom about the Pro-Pca amide bond, which is probably the

FIGURE 4.13: Computational model of S_P,S-Pro-Pca.

cause of the increased stereoselectivity compared to Pro-Gly-Pca. Given more time it would have been ideal to make the other diastereomer and identify how the shapes of these two diastereomers affected stereoselectivity.

The hydrogen bonding seen in S_P,S-4.7 might also be the cause of only one diastereomer being found in the synthesised product: the compound with intramolecular hydrogen bonds has fewer atoms involved in intermolecular hydrogen bonding. This would decrease its solubility in aqueous solutions whereas the other diastereomer might be lost to aqueous washes due to its increased solubility in water.

Comparing the results of Pro-NH-22PC and Pro-Pca (Entries 4 & 12 respectively), and Pro-Gly-NH-22PC and Pro-Gly-Pca (Entries 5 & 6 respectively), we can see that diastereoselectivity increases when incorporating Pca instead of 4-amino[2.2]-paracyclophane with Pro; and that it decreases when incorporating Pca instead of amino[2.2]paracyclophane with Gly-Pro. This suggests the combination of distance and lower rigidity puts the carboxylic acid in a less ideal position in Pro-Gly-Pca.

4.3 Conclusion

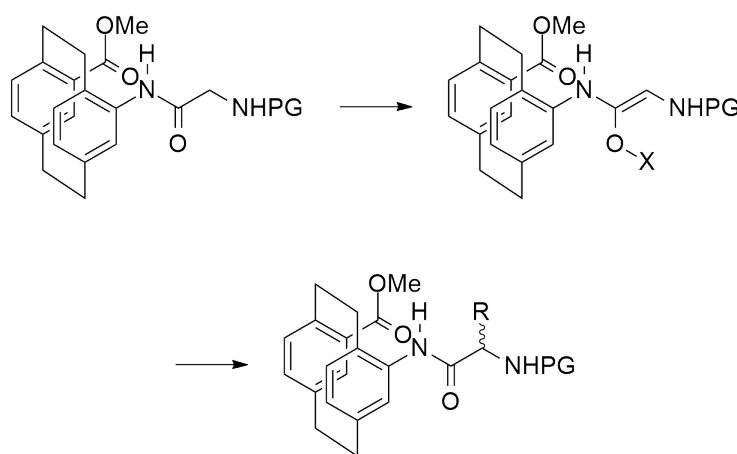
Pca and two Pca-containing pseudopeptides were studied as asymmetric organocatalysts in Michael addition between *trans*- β -nitrostyrene and hexanal and were compared to proline, a known catalyst for this reaction. These tests were performed to

probe the relationship between relative conformation between the carboxylic acid and amine moieties of the catalyst, and the catalyst's stereoselectivity. There are some promising preliminary results. Pca exhibited a moderate reversal of the usual strongly *syn*-directing catalysis, which is in contrast to the bulk of the literature on this Michael addition. Direct coupling of Pro to Pca gave better enantioselectivity than coupling Pro-Gly to Pca, indicating that decreasing conformational flexibility is important for stereoselectivity.

4.4 Future directions

4.4.1 R group functionalisation

'R group' functionalisation of the glycine residue would be interesting (Scheme 4.14). The [2.2]paracyclophane backbone might allow control of diastereoselectivity when adding the R-group. The R-group could introduce further functionality for catalysis, solubility, stability and so forth, and also might decrease rotational freedom about that α -carbon. Since that rotational freedom is thought to lower stereoselectivity of the Michael reaction, this could help increase stereoselectivity of the catalyst.



SCHEME 4.14: R-group functionalisation of glycine.

4.4.2 N-alkylation

A problem encountered with the Pca catalyst was its poor solubility in aqueous and many organic solvents. Wennemers' work with alkylated peptide catalysts showed that this simple modification can increase the solubility of poorly-soluble catalysts and thus increased catalyst efficiency.¹⁴⁸ It could be worth looking into similar modifications of Pca-peptides. Figure 4.15 shows possible N-alkylation in Pca peptides.

4.4.3 Synthesis of further peptides

This work, at its outset, intended to synthesise a wider array of peptides in order to probe the spatial relationship between the carboxylic acid and proline moieties in the catalyst for Michael addition. Due to time-consuming difficulties encountered in the synthesis of Pca and Pca-centred peptides, the range of peptides synthesised was

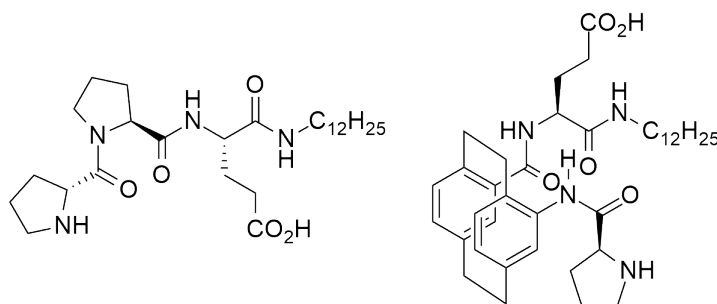


FIGURE 4.15: Wennemers' *N*-alkylated tripeptide (left) and a Pca analogue (right).

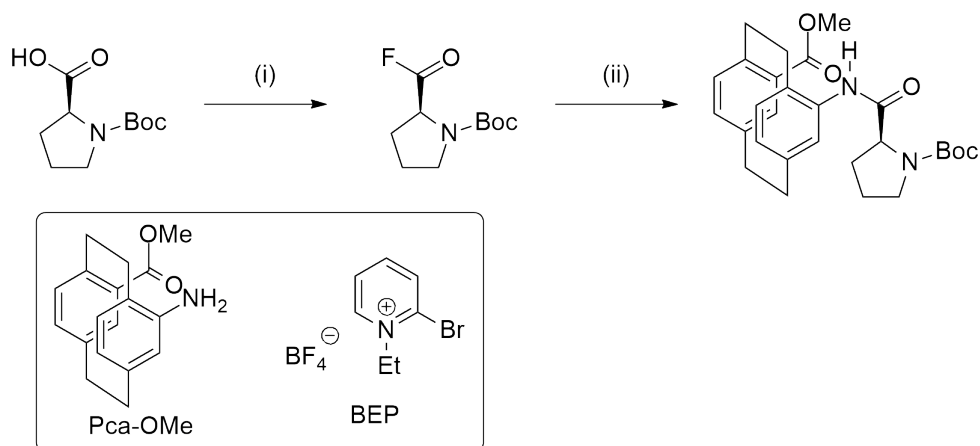
narrowed. Since the problems with these syntheses were largely overcome through optimisation in this project, the next step would be to test a larger range of catalysts in the Michael reaction. This would include tripeptides of the type Pro-Pca-Xaa, where Xaa is a natural amino acid with a carboxylic acid at varying lengths from its α carbon.

4.4.4 Acyl fluoride activation

Some peptide coupling conditions were untested because the required reagents were inaccessible. A promising avenue is acyl fluoride activation. Fluorinating agents are popular for their higher reactivity, increased stability to hydrolysis and high retention of stereochemistry compared to acyl chlorides. They may be used with protecting groups that are sensitive to acyl chloride activation. Common fluorinating agents are cyanuric fluoride and 2-fluoro-1-ethyl pyridinium tetrafluoroborate (BEP) (Scheme 4.16).²⁶⁹ In this project acyl chlorides were not successful when coupling natural amino acids to the aniline of Pca, but an acyl bromide (bromoacetyl bromide) was found to be reactive enough to form an amide bond with Pca (section 3.3.7).

4.4.5 Resolution of catalysts

Resolution of diastereomers of Pca peptides, as well as synthesis of the diastereomer of Pro-Pca not obtained in this project, would help complete this data set and give a more complete picture of the mechanisms at work behind the stereoselectivities exhibited by the peptides tested.

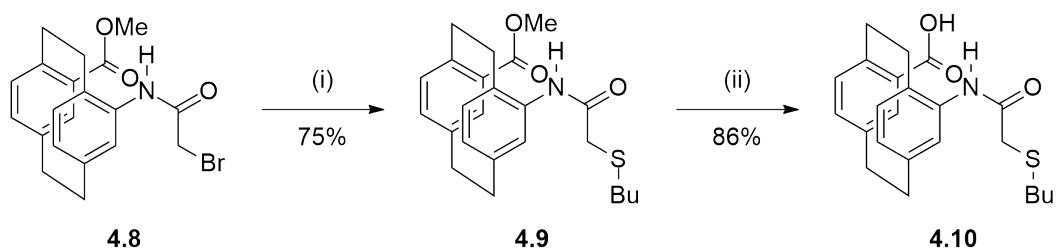


SCHEME 4.16: Acyl fluoride activation for peptide coupling with Pca-OMe. i. 2-Fluoro-1-ethyl pyridinium tetrafluoroborate. ii. Pca-OMe.

4.4.6 Potential thioether catalyst

During the course of this research, the successful synthesis of bromide **4.8** allowed branching of the synthetic route to target a range of interesting and useful compounds for different kinds of catalysis. As a brief proof of concept, formation of the thioether catalysts for bromolactonisation was explored as another potential catalyst target.

From the previously synthesised methyl 4-[(3-bromo-1-oxoethyl)amino][2.2]paracyclophane-13-carboxylate **4.8**, the butyl thioether was synthesised using 1-butanethiol,²⁷⁰ by S_N2 substitution (Scheme 4.17). The bromide again exhibited good reactivity and the reaction proceeded in high yield and purity.

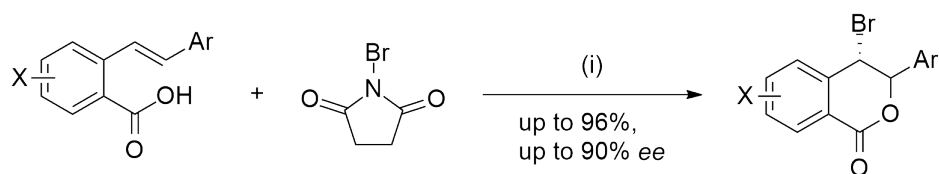


SCHEME 4.17: Synthesis of thioether **4.10**. i) K_2CO_3 , BuSH. ii) KOH.

1-Butanethiol is a hazardous and malodorous compound and as such should always be handled in a fume cupboard. Glassware used with this compound was soaked in a dilute bleach bath to remove odour before cleaning. The resulting sulfide compound retained a slight allium/brassica smell even after purification to remove residual butanethiol.

The methyl ester **4.9** may be cleaved with base in the usual method in 2 M ethanolic KOH.

While this branch of catalysts could perform interesting and useful reactions such as bromolactonisation reactions (Fig. 4.18),²⁷¹⁻²⁷⁴ it is beyond the scope of the current work and may be explored by future members of the Rowlands group.



SCHEME 4.18: Exemplar sulfide-catalysed asymmetric bromolactonisation. i) 10 mol % chiral sulfide catalyst.

Chapter 5

Methods and Materials

5.1 General information

All starting compounds and solvents were used as received from commercial sources without further purification unless otherwise noted. Solvents were dried using the following methods: diethyl ether and THF were heated at reflux over fresh sodium wire in the presence of benzophenone indicator. Toluene and DMF were stored over 4 Å molecular sieves. Dioxane was stored over sodium wire. Triethylamine was freshly distilled over sodium hydroxide pellets.

TLC analysis was performed using aluminium-backed silica gel plates, visualised using UV light (254 nm), and stained with ninhydrin, iodine, cerium ammonium molybdate, or KMnO_4 where applicable.

NMR spectra were recorded using Bruker 400 MHz or 500 MHz Avance instruments and processed using Topspin. 2D spectra were recorded on a Bruker 700 MHz Avance instrument by Dr Pat J. Edwards. Chemical shifts are in ppm and referenced to the NMR solvent. Multiplicities are described as follows: *s* = singlet, *d* = doublet, *t* = triplet, *q* = quartet, *dd* = double doublet, *ddd* = double double doublet, *dt* = double triplet, *td* = triple doublet, *m* = multiplet, *br* = broad.

For mass spectra, where data are quoted to two dp, they were recorded on a Bruker HPLC-MS for ESI spectra. High resolution mass spectra were recorded on a ThermoScientific Q Exactive Focus Hybrid Quadrupole-Orbitrap Mass Spectrometer by

David J. Lun. Analytical chiral HPLC was performed on a Bruker HPLC-MS with a Daicel Chiralcel OD-H HPLC column (25 cm) with UV detection at 254 nm.

IR spectra were collected using a Perkin-Elmer 1600 Fourier Transform spectrometer as either thin film (CH_2Cl_2) or solid, as ATR spectra.

Melting points were recorded on a Gallenkamp melting point apparatus and are uncorrected.

Optical rotation was recorded on a Perkin Elmer 241 polarimeter using a sodium lamp, emitting at 589 nm. All samples were measured in a 10 cm cell and are an average of 10 readings. Average temperature was 25°C.

CD spectra were recorded using a Chirascan CD spectrophotometer (150 W Xe arc) from Applied Photophysics with a Quantum Northwest TC125 temperature controller. CD spectra (average of at least 3 scans) were recorded between 210 and 350 nm with 1 nm intervals, 120 nm/min scan rate followed by subtraction of a background spectrum (solvent only).

X-ray crystallography was performed by Prof Martyn P. Coles. Crystals were covered in Fomblin and suitable single crystals were selected under a microscope and mounted on a Kappa CCD diffractometer. The structures were refined with SHELXL-97.

Column chromatography was performed using flash silica column chromatography or a Buchi automatic chromatography system, with silica size 40-63 μm (230-400 mesh) except where noted. The Buchi automatic chromatography system uses silica cartridges and provides automated solvent mixing allowing gradient methods to be used. Compound detection is accessible using up to 4 different UV wavelengths. Flow rate, gradient profile, and collection conditions may be customised for the design of a suitable separation.

DFT calculations were performed by Tyson Dais using Gaussian 09, with the ωB97XD functional and the 6-311g(d,p) basis set.

Where data is stated to be of insufficient quality for further analysis, either:

- The compound had poor solubility in solvents for NMR or mass spectrometry;

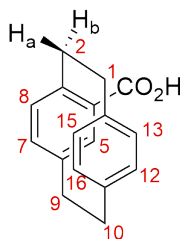
- The material could not be purified sufficiently for full analysis; or
- There was insufficient material for full analysis.

More analysis to obtain these data was not completed due to restrictions during the COVID-19 pandemic.

5.2 Synthetic methods

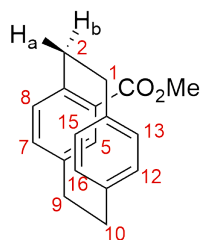
5.2.1 Synthesis of Pca, oxime methodology

[2.2]Paracyclophane-4-carboxylic acid 2.12

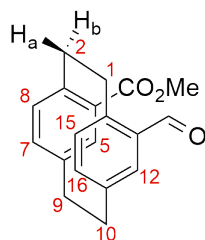


AlCl_3 (2.25 g, 16.82 mmol, 1.75 eq.) was dissolved in CH_2Cl_2 (48 mL, 0.2 M) under inert atmosphere and cooled to $-10\text{ }^\circ\text{C}$ in an ice/acetone bath. $(\text{COCl})_2$ (1.44 mL, 16.82 mmol, 1.75 eq) was added and the mixture was stirred at $-10\text{ }^\circ\text{C}$ for 30 minutes. [2.2]Paracyclophane (2.0 g, 9.61 mmol, 1.0 eq.) was added and the mixture was stirred at $-10\text{ }^\circ\text{C}$ for a further 10 minutes. The reaction was quenched by slowly adding water (30 mL). The aqueous layer was extracted with CH_2Cl_2 (3 x 50 mL). Combined organics were dried (MgSO_4) and the solvent was removed under reduced pressure, affording the intermediate oxo-acyl chloride as a white powder.

Chlorobenzene (20 mL) was added to dissolve the intermediate product and this solution was heated at reflux overnight. Water (20 mL) was added and the mixture was heated at reflux for a further three hours. After cooling, the aqueous layer was extracted with CH_2Cl_2 (2 x 50 mL), dried (MgSO_4) and the solvent removed under reduced pressure. The crude material was dissolved in EtOAc (50 mL) and extracted with 2 M aq. NaOH (3 x 80 mL). The aqueous layer was neutralised with 2 M aq. HCl and the resulting precipitate was collected with suction filtration, affording [2.2]paracyclophane-4-carboxylic acid as a white powder (0.73 g, 2.89 mmol, 30%). R_f (1:1 hexane:EtOAc) 0.22. ^1H NMR (500 MHz, CDCl_3): δ 7.26 (1H, d, $J = 1.5$ Hz, H-5), 6.60 (1H, d, $J = 7.5$ Hz, H-13), 6.53 (1H, d, $J = 7.5$ Hz, H-7), 6.48 (3H, m, H-8, H-12, H-15), 6.38 (1H, d, $J = 7.5$ Hz, H-16), 4.08 (1H, t, $J = 10.5$ Hz, H-2_b), 3.53-2.93 (6H, m, H-1, H-9, H-10), 2.76 (1H, dt, $J = 3.5, 1.5$ Hz, H-2_a). Data comparable to that reported in the literature.²⁰⁹

Methyl [2.2]paracyclophane-4-carboxylate 2.13

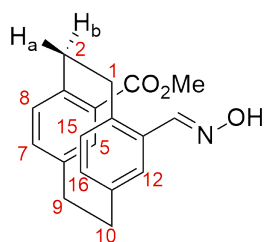
To a suspension of [2.2]paracyclophane-4-carboxylic acid (0.73 g, 2.90 mmol, 1.0 eq.) in dry CH_2Cl_2 (14.5 mL, 0.2 M) at $-10\text{ }^\circ\text{C}$ under inert atmosphere was added $(\text{COCl})_2$ (0.30 mL, 3.48 mmol, 1.2 eq.). A catalytic amount of DMF (one drop of a solution of one drop DMF in 5 mL CH_2Cl_2) was added and the reaction mixture was stirred at room temperature until bubbling ceased, about 30 minutes. Solvent was removed under reduced pressure. Dry CH_2Cl_2 (7.5 mL) and dry MeOH (7.5 mL) were added to dissolve the material and the solution was heated at reflux overnight. The solvent was removed affording methyl [2.2]paracyclophane-4-carboxylate as a white powder (0.70 g, 2.63 mmol, 91%). MP $129\text{--}131\text{ }^\circ\text{C}$. R_f (4:1 hexane:EtOAc) 0.42. ^1H NMR (500 MHz, CDCl_3): δ 7.16 (1H, d, $J = 1.9$ Hz, H-5), 6.68 (1H, dd, $J = 7.9, 1.9$ Hz, H-13), 6.59-6.56 (2H, m, H-7, H-12), 6.54-6.46 (3H, m, H-8, H-15, H-16) 4.11 (1H, ddd, $J = 12.1, 10.7, 1.5$ Hz, H-2_b), 3.94 (3H, s, CH_3) 3.23-3.01 (6H, m, H-1, H-9, H-10), 2.89 (1H, ddd, $J = 12.8, 10.1, 6.9$ Hz, H-2_a). Data comparable to that reported in the literature.²⁷⁵

Methyl 13-formyl[2.2]paracyclophane-4-carboxylate 2.19

To a stirred solution of methyl [2.2]paracyclophane-4-carboxylate (0.70 g, 2.63 mmol, 1.0 eq.) in dry CH_2Cl_2 (9 mL, 0.3M) under inert atmosphere at $-10\text{ }^\circ\text{C}$ was added 1,1-dichlorodimethyl ether (0.26 mL, 2.89 mmol, 1.1 eq.) and TiCl_4 (0.58 mL, 5.26

mmol, 2.0 eq.). The reaction mixture was allowed to slowly come to room temperature overnight. Ice was added and once the colour changed from opaque dark red to clear yellow, the aqueous and organic layers were separated. The aqueous layer was extracted with CH_2Cl_2 (3 x 20 mL). Combined organics were washed successively with saturated NaHCO_3 , water, and brine (30 mL each), then dried (MgSO_4) and the solvent removed under reduced pressure affording methyl 13-formyl[2.2]paracyclophane-4-carboxylate as a white powder (0.50 g, 1.69 mmol, 65%). R_f (4:1 hexane:EtOAc) 0.65. $^1\text{H NMR}$ (500 MHz, CDCl_3): δ 9.91 (1H, s, CHO), 7.07 (2H, t, $J = 2.4$ Hz, H-5, H-12), 6.73 (2H, ddd, $J = 7.8, 5.9, 2.0$ Hz, H-7, H-16), 6.66 (1H, d, $J = 8.0$ Hz, H-15), 6.63 (1H, d, $J = 8.0$ Hz, H-8), 4.20-4.11 (2H, m, H-1_b, H-2_b), 3.84 (3H, s, CH_3), 3.18-3.11 (5H, m, H-2_a, H-9, H-10), 3.03 (1H, ddd, $J = 12.3, 10.3, 4.4$ Hz, H-2_a). Data comparable to that reported in the literature.¹⁸⁶

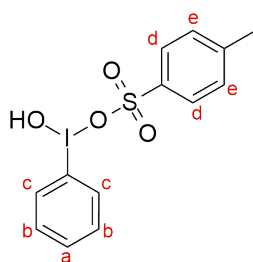
Methyl 13-hydroxylimino[2.2]paracyclophane-4-carboxylate 2.20



Methyl 13-formyl[2.2]paracyclophane-4-carboxylate (1.03 g, 3.4 mmol, 1.0 eq.) and NaOAc (1.39 g, 17.0 mmol, 5.0 eq.) were suspended in EtOH (30 mL, 0.2 M) and heated to reflux. $\text{NH}_2\text{OH} \cdot \text{HCl}$ (1.07 g, 13.6 mmol, 4.0 eq.) was added and the mixture was heated at reflux overnight. The solvent was removed under reduced pressure and water (25 mL) was added. This aqueous residue was extracted with EtOAc (3 x 30 mL). Combined organics were dried (MgSO_4) and the solvent removed under reduced pressure to afford methyl 13-hydroxylimino[2.2]paracyclophane-4-carboxylate as a light yellow solid (0.81 g, 2.6 mmol, 77%). MP 160 °C (decomposes). R_f (4:1 hexane:EtOAc) 0.43. $^1\text{H NMR}$ (500 MHz, CDCl_3): δ 8.14 (1H, s, $\text{CH}=\text{N}$), 7.26 (1H, d, $J = 1.9$ Hz, H-5), 6.87 (1H, d, $J = 1.3$ Hz, H-12), 6.72 (1H, dd, $J = 7.8, 1.9$ Hz, H-7), 6.63 (1H, d, $J = 7.8$ Hz, H-16), 6.61-6.58 (2H, m, H-8, H-15), 4.33-4.36 (1H, m, H-2_b), 3.92 (3H, s, CH_3), 3.72-3.67 (1H, m, H-1_b), 3.20-3.00 (6H, m, H-1_a, H-2_a, H-9,

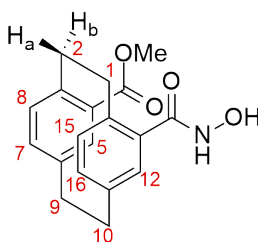
H-10). ^{13}C NMR (125 MHz, CDCl_3): δ 167.1 (C=O), 149.2 (C=N), 142.7 (CH), 139.8 (CH), 139.6 (C), 139.5 (C), 136.5 (C), 136.3 (C), 135.1 (C), 134.5 (C), 134.3 (CH), 132.2 (CH), 130.5 (CH), 129.5 (CH), 51.9 (CH_3), 34.9 (CH_2), 34.8 (CH_2), 34.8 (CH_2), 32.4 (CH_2). HRMS (ESI) found: $[\text{M} + \text{Na}]^+$ 332.1260. $\text{C}_{19}\text{H}_{19}\text{N}_1\text{O}_3\text{Na}$ requires $[\text{M} + \text{Na}]^+$ 332.1257.

Hydroxyl(tosyloxy)iodobenzene 2.31



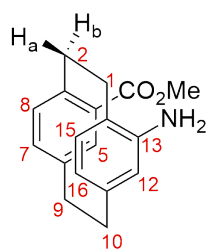
p-Toluenesulfonic acid monohydrate (5.0 g, 26.32 mmol, 2.0 eq.) was dissolved in a minimum quantity of MeCN and added to a suspension of iodobenzene diacetate (4.24 g, 13.16 mmol, 1.0 eq.) in MeCN (33 mL, 0.4 M). The reaction mixture was left to stand without stirring for one hour. The resulting white precipitate was filtered and washed with acetone then petroleum ether (BP 40-60°C), affording hydroxyl(tosyloxy)iodobenzene as fine white needles (4.60 g, 11.7 mmol, 89%). MP 132-134 °C. ^1H NMR (400 MHz, $\text{DMSO}-d_6$): δ 9.76 (1H, s, br, OH), 8.17 (2H, d, $J = 6.4$ Hz, H-d), 7.57 (2H, d, $J = 6.4$ Hz, H-c), 7.54-7.52 (1H, m, H-a), 7.47 (2H, d, $J = 7.2$ Hz, H-e), 7.11 (2H, d, $J = 6.4$ Hz, H-b), 2.29 (3H, s, CH_3). Data comparable to that reported in the literature.²⁷⁶

Methyl 4-(*N*-hydroxyamido)[2.2]paracyclophane-13-carboxylate 2.34



Methyl 13-hydroxylimino[2.2]paracyclophane-4-carboxylate (0.80 g, 2.61 mmol, 1.0 eq.) and hydroxyl(tosyloxy)iodobenzene (1.13 g, 2.87 mmol, 1.1 eq.) were dissolved in DMSO (30 mL, 0.1 M) and heated at 90 °C overnight. The reaction mixture was cooled and water (30 mL) was added. The aqueous layer was extracted with EtOAc (3 x 20 mL). Combined organics were dried (MgSO₄) and the solvent removed under reduced pressure. The resulting residue was separated by column chromatography eluting a gradient of hexane:EtOAc 10:1 to 0:1 to afford methyl 4-(*N*-hydroxyformamido)-[2.2]paracyclophane-13-carboxylate as a yellow oil (0.43 g, 1.32 mmol, 51%). *R*_f (1:1 hexane:EtOAc) 0.20. ¹H NMR (500 MHz, CDCl₃): δ 10.39 (1H, s, OH), 8.71 (1H, s, NH), 7.13 (1H, d, *J* = 1.7 Hz, H-5), 6.78 (1H, dd, *J* = 7.7, 1.9 Hz, H-16), 6.71-6.67 (2H, m, H-12, H-7), 6.65-6.63 (2H, m, H-8, H-15), 4.06-4.01 (1H, m, H-2_b), 3.76 (3H, s, CH₃), 3.65 (1H, ddd, *J* = 12.5, 9.9, 5.2 Hz, H-1_b), 3.10-2.97 (5H, m, H-1_a, H-9, H-10), 2.90 (1H, ddd, *J* = 12.2, 10.0, 5.3 Hz, H-2_a). ¹³C NMR (125 MHz, CDCl₃): δ 166.4 (C=O), 165.3 (C=O), 142.6 (C), 139.8 (C), 139.6 (C), 139.4 (CH), 136.5 (CH), 136.4 (C), 135.8 (C), 135.3 (C), 134.4 (CH), 133.4 (CH), 130.8 (CH), 130.0 (CH), 51.9 (CH₃), 35.6 (CH₂), 34.6 (CH₂), 34.5 (CH₂), 33.5 (CH₂). HRMS (ESI) found: [M + H]⁺ 326.1314. C₁₉H₁₉N₁O₃Na requires [M + H]⁺ 326.1310.

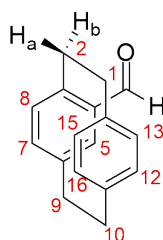
Methyl 13-amino[2.2]paracyclophane-4-carboxylate 2.21



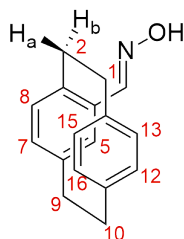
Methyl 13-hydroxylimino[2.2]paracyclophane-4-carboxylate (0.90 g, 2.91 mmol, 1.0 eq.) and hydroxyl(tosyloxy)iodobenzene (1.25 g, 3.20 mmol, 1.1 eq.) were dissolved in DMSO (30 mL, 0.1 M) and heated at 110 °C overnight. NaOH pellets (0.25 g, 6.34 mmol, 1.8 eq) were ground to a powder and added. This mixture was heated at 110 °C for a further four hours. After cooling, water (25 mL) was added and the crude product extracted with EtOAc (4x50 mL). Combined organics were dried (MgSO₄) and the solvent was removed under reduced pressure affording the crude product as

a dark orange oil. The resulting residue was separated by column chromatography and elution with 4:1 hexane:EtOAc, affording methyl 13-amino[2.2]paracyclophane-4-carboxylate as a pale yellow-brown solid (0.15 g, 0.53 mmol, 18%). MP 165 °C (decomposes). R_f (4:1 hexane:EtOAc) 0.39. $^1\text{H NMR}$ (400 MHz, CDCl_3): δ 7.25 (1H, s, H-5), 6.69 (1H, dd, $J = 7.8, 1.9$ Hz, H-7), 6.42 (1H, d, $J = 7.6$ Hz, H-8), 6.34 (1H, d, $J = 7.6$ Hz, H-15), 6.17 (1H, dd, $J = 7.8, 1.9$ Hz, H-16), 5.44 (1H, d, $J = 1.5$ Hz, H-12), 4.40-4.25 (1H, m, H-2_b), 3.89 (3H, s, CH_3), 3.15 (1H, ddd, $J = 13.0, 9.8, 2.8$ Hz, H-1_b), 3.05-2.90 (5H, m, H-1_a, H-9, H-10), 2.73 (1H, ddd, $J = 13.9, 10.7, 5.2$ Hz, H-2_a). Data comparable to that reported in the literature.¹⁸¹

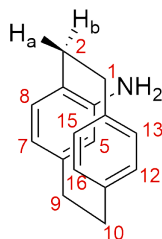
4-Carboxyl[2.2]paracyclophane 5.1



To a stirred solution of [2.2]paracyclophane (0.96 g, 4.81 mmol, 1.0 eq.) in dry CH_2Cl_2 (16 mL, 0.3 M) were added TiCl_4 (1.06 mL, 9.62 mmol, 2.0 eq.) and $\text{CH}_3\text{OCHCl}_2$ (0.48 mL, 5.29 mmol, 1.1 eq.) at -10 °C under Ar. This solution was allowed to slowly come to room temperature overnight. Ice (50 mL) was added and once it was melted the aqueous layer was extracted with CH_2Cl_2 (3 x 50 mL). Combined organics were washed once each with saturated NaHCO_3 , water, and brine (40 mL each), then dried (MgSO_4) and the solvent removed under reduced pressure, affording 4-carboxyl[2.2]paracyclophane as a pale yellow solid (0.98 g, 4.14 mmol, 86%). MP (149-151 °C). R_f (4:1 hexane:EtOAc) 0.39. $^1\text{H NMR}$ (400 MHz, CDCl_3): δ 9.96 (1H, s, CHO), 7.03 (1H, d, $J = 2.0$ Hz, H-5), 6.74 (1H, dd, $J = 7.7, 2.0$ Hz, H-13), 6.63-6.53 (2H, m, H-15, H-16), 6.51 (1H, d, $J = 8.4$ Hz, H-7), 6.44 (1H, dd, $J = 7.8, 1.8$ Hz, H-8), 6.39 (1H, dd, $J = 7.8, 1.8$ Hz, H-12) 4.14-4.08 (1H, m, H-2_b), 3.31-2.93 (7H, m, H-1, H-2_a, H-9, H-10). Data comparable to that reported in the literature.⁵¹

4-Hydroxylimino[2.2]paracyclophane 5.2

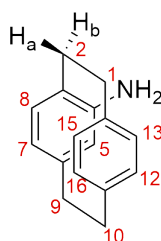
4-Carboxyl[2.2]paracyclophane (0.98 g, 4.15 mmol, 1.0 eq.) and NaOAc (1.70 g, 20.75 mmol, 5.0 eq.) were suspended in EtOH (20 mL, 0.2 M) and heated to reflux. $\text{NH}_2\text{OH} \cdot \text{HCl}$ (1.30 g, 16.60 mmol, 4.0 eq.) was added portionwise and this suspension was heated at reflux for two hours. The solvent was removed under reduced pressure and the crude product was redissolved in EtOAc (20 mL). The organic layer was washed with water (3 x 30 mL), then dried (MgSO_4) and the solvent removed under reduced pressure affording 4-hydroxylimino[2.2]paracyclophane as a pale yellow solid (0.88 g, 3.50 mmol, 84%). R_f (4:1 hexane:EtOAc) 0.45. ^1H NMR (500 MHz, CDCl_3): δ 8.20 (1H, s, $\text{CH}=\text{N}$), 6.79 (1H, d, $J = 1.2$ Hz, H-5), 6.63 (1H, d, $J = 8.0$ Hz, H-8), 6.60 (1H, dd, $J = 8.0, 1.7$ Hz, H-7), 6.53-6.47 (4H, m, H-12, H-13, H-15, H-16), 3.62-3.58 (1H, m, H-2_b), 3.20-2.88 (7H, m, H-1, H-2_a, H-9, H-10). ^{13}C NMR (125 MHz, CDCl_3): δ 150.1 (C=N), 140.5 (C), 139.8 (C), 139.7 (C), 135.5 (C), 134.5 (C), 133.6 (CH), 133.0 (CH), 132.2 (CH), 131.9 (CH), 131.8 (CH), 131.3 (2 CH), 35.5 (CH_2), 35.0 (CH_2), 35.0 (CH_2), 33.6 (CH_2). Data comparable to that reported in the literature.¹⁸⁶

4-Amino[2.2]paracyclophane 5.3

4-Hydroxylimino[2.2]paracyclophane (2.50 g, 9.96 mmol, 1.0 eq.) and hydroxyl-(tosyloxy)iodobenzene (4.30 g, 10.96 mmol, 1.1 eq.) were heated at 90 °C in DMSO (15 mL, 0.1 M) overnight. NaOH pellets (0.72 g, 17.93 mmol, 1.8 eq.) were ground to a powder and added, and the reaction mixture was heated for a further two hours.

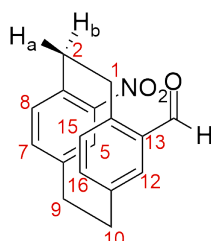
= 13.3, 9.5, 1.9 Hz, H-2_b), 3.26-3.06 (6H, m, H-1_a, H-2_a, H-9, H-10), 2.92 (1H, ddd, *J* = 13.3, 10.0, 7.2 Hz, H-1_b). ¹³C NMR (125 MHz, CDCl₃): δ 150.5 (C), 143.2 (C), 140.6 (C), 140.3 (C), 138.8 (CH), 138.4 (CH), 137.5 (C), 134.3 (2 C, CH), 133.5 (CH), 131.0 (CH), 130.6 (CH), 37.1 (CH₂), 36.0 (CH₂), 35.9 (CH₂), 35.6 (CH₂). Data comparable to that reported in the literature.¹⁹⁶

4-Amino[2.2]paracyclophane 5.3



4-Nitro[2.2]paracyclophane (3.10 g, 12.2 mmol, 1.0 eq.) was dissolved in MeOH (62 mL, 0.2 M) and heated to 80 °C. To this solution was added Zn powder (2.40 g, 36.7 mmol, 3.0 eq.) and NH₄Cl (1.96 g, 36.7 mmol, 3.0 eq.) and this mixture was stirred at 80 °C overnight, then allowed to cool. The mixture was filtered through qualitative filter paper and the solid washed with MeOH (2 x 40 mL). The filtrate and washings were combined and the solvent removed under reduced pressure. The residue was suspended in water and stirred for 30 minutes, then the remaining solids collected by filtration, affording the 4-amino[2.2]paracyclophane as a green-brown powder (2.53 g, 11.33 mmol, 93%). Data as reported earlier.

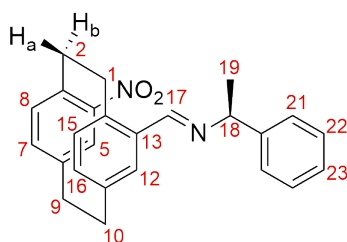
4-Nitro-13-formyl[2.2]paracyclophane 2.39



To a solution of 4-nitro[2.2]paracyclophane (4.54 g, 17.94 mmol, 1.0 eq) in dry CH₂Cl₂ (90 mL) under inert atmosphere at -10 °C was added 1,1-dichlorodimethyl ether

(1.79 mL, 19.73 mmol, 1.1 eq) and TiCl_4 (3.94 mL, 35.88 mmol, 2.0 eq). The mixture was stirred overnight, coming to room temperature. The mixture was poured onto ice (100 mL) and stirred until ice melted. The aqueous layer was extracted with CH_2Cl_2 (3 x 80 mL). Combined organics were washed with water, dried (MgSO_4) and the solvent removed under reduced pressure affording the crude product as an orange-brown solid. The crude product was purified using silica gel column chromatography using a gradient of 9:1 to 1:1 hexane:EtOAc affording the pure product as an orange-yellow solid (3.44 g, 12.2 mmol, 68%). MP 160 °C (decomposes). R_f (4:1 Hex/EtOAc) 0.20. ^1H NMR (500 MHz, CDCl_3): δ 9.96 (1H, s, CHO) 7.17 (1H, d, $J = 1.8$ Hz, H-5), 7.12 (1H, d, $J = 2.0$ Hz, H-12), 6.85 (1H, dd, $J = 7.8, 1.9$ Hz, H-7), 6.80 (1H, dd, $J = 7.8, 2.0$ Hz, H-16), 6.75 (1H, d, $J = 7.8$ Hz, H-8), 6.70 (1H, d, $J = 7.8$ Hz, H-15), 4.24-4.18 (1H, m, H-1_b), 4.08-3.99 (1H, m, H-2_b), 3.26-3.08 (6H, m, H-1_a, H-2_a, H-9, H-10). ^{13}C NMR (125 MHz, CDCl_3): δ 190.4 (CHO), 149.5 (C), 142.6 (C), 141.9 (C), 140.1 (C), 137.8 (C), 137.4 (CH), 137.4 (CH), 136.3 (CH), 136.1 (CH), 135.6 (C), 134.7 (CH), 128.3 (CH), 34.5 (CH_2), 34.4 (CH_2), 34.2 (CH_2), 31.7 (CH_2). HRMS (ESI) found: $[\text{M} + \text{H}]^+$ 282.1131. $\text{C}_{17}\text{H}_{16}\text{NO}_3$ requires $[\text{M} + \text{H}]^+$ 282.1125.

4-Nitro-13-[N-(1-phenylethyl)][2.2]paracyclophanyl methanimine 2.45



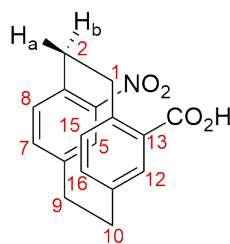
A solution of 4-nitro-13-formyl[2.2]paracyclophane (2.55 g, 9.1 mmol, 1.0 eq) and (S)-1-phenylethylamine (1.23 mL, 9.5 mmol, 1.05 eq) in CH_2Cl_2 (45 mL, 0.2 M) was stirred at room temperature overnight. Solvent was removed under reduced pressure affording the crude product as a brown oil. The crude product was recrystallised from a minimum amount of hot toluene affording pale yellow crystals. The crystals were collected using suction filtration and washed successively with cold

toluene and cold acetone affording {single diastereomer}-4-nitro-13-[N-(1-phenylethyl)][2.2]paracyclophanyl methanimine (0.64 g, 1.66 mmol, 18%) labelled A. **2.45-A** MP 155 °C (decomposes). R_f (4:1 Hex/EtOAc) 0.50. $^1\text{H NMR}$ (500 MHz, CDCl_3): δ 8.22 (1H, s, H-17), 7.42 (2H, dd, $J = 8.0, 1.2$ Hz, H-21), 7.37 (2H, td, $J = 6.8, 1.8$ Hz, H-22), 7.28 (1H, d, $J = 1.9$ Hz, H-5), 7.25 (1H, tt, $J = 7.3, 1.3$ Hz, H-23), 6.87 (1H, s, H-12), 6.80 (1H, dd, $J = 8.7, 1.8$ Hz, H-7), 6.73 (1H, d, $J = 7.9$ Hz, H-8), 6.64 (1H, d, $J = 7.8$ Hz, H-15), 6.62 (1H, dd, $J = 7.8, 1.8$ Hz, H-16), 4.48 (1H, q, $J = 6.6$ Hz, H-18), 4.33 (1H, ddd, $J = 13.0, 9.7, 3.5$ Hz, H-2_b), 4.09 (1H, ddd, $J = 13.6, 9.7, 4.2$ Hz, H-1_b), 3.19-3.11 (5H, m, H-1_a, H-9, H-10), 3.05 (1H, ddd, $J = 12.9, 10.0, 4.3$ Hz, H-2_a), 1.65 (3H, d, $J = 6.7$ Hz, H-19). $^{13}\text{C NMR}$ (125 MHz, CDCl_3): δ 216.7 (C), 158.6 (C(H)=N), 149.4 (C), 145.1 (C), 141.5 (C), 140.0 (C), 139.3 (C), 137.8 (CH), 137.3 (CH), 136.8 (CH), 136.5 (CH), 135.6 (C), 134.2 (CH), 134.0 (CH), 129.1 (C), 128.3 (CH), 128.0 (CH), 126.8 (CH), 126.7 (CH), 109.7 (CH), 70.0 (CH), 34.6 (CH_2), 33.6 (CH_2), 33.5 (CH_2), 23.6 (CH_3). HRMS (ESI) found: $[\text{M} + \text{H}]^+$ 385.1914. $\text{C}_{25}\text{H}_{24}\text{N}_2\text{O}_2$ requires $[\text{M} + \text{H}]^+$ 385.1911. $[\alpha]_D^{20}$ -0.010° (CH_2Cl_2 , 0.006 g/mL)

4-Nitro-13-formyl[2.2]paracyclophane (resolved) 2.39

A mixture of {single enantiomer}-4-nitro-13-[N-(1-phenylethyl)][2.2]paracyclophanyl methanimine (0.64 g, 1.6 mmol, 1.0 eq) and glacial acetic acid (0.092 mL, 1.6 mmol, 1.0 eq) in CH_2Cl_2 (20 mL) was stirred at room temperature for two hours. The organics were washed with water (20 mL), dried (MgSO_4), and the solvent was removed under reduced pressure affording the {single enantiomer}-4-nitro-13-formyl[2.2]paracyclophane as a dark yellow solid (0.44 g, 1.57 mmol, 97%). Data as reported earlier.

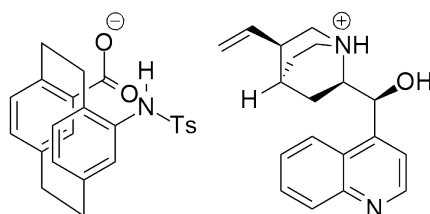
4-Nitro[2.2]paracyclophane-13-carboxylic acid 2.40



To a stirred solution of 4-nitro-13-formyl[2.2]paracyclophane (0.52 g, 1.8 mmol, 1.0 eq) in acetone (36 mL) was added a solution of KMnO_4 (0.44 g, 2.8 mmol, 1.5 eq) in water (14 mL) slowly over 10 minutes. The mixture was stirred overnight at room temperature then acidified to pH 2-3 (2 M HCl) and filtered through filter paper. The aqueous layer was extracted with EtOAc (3 x 40 mL). Combined organics were washed once each with water and brine, dried (MgSO_4), and the solvent was removed under reduced pressure. The crude solid was partitioned into 2 M NaOH and EtOAc (50 mL each). The organic layer was separated, dried (MgSO_4), and the solvent was removed under reduced pressure. The yellow solid obtained is the starting material (0.18 g, 35% RSM). The aqueous layer was neutralised (conc. HCl) and extracted with EtOAc (3 x 50 mL). The solvent was removed from the combined extracts under reduced pressure affording the product as a pale yellow solid (0.32 g, 1.08 mmol, 60%). R_f (4:1 Hex/EtOAc) 0.12. ^1H NMR (500 MHz, $\text{DMSO}-d_6$): δ 7.26 (1H, d, $J = 1.8$ Hz, H-5), 7.10 (1H, d, $J = 1.9$ Hz, H-12), 6.95 (1H, dd, $J = 7.7, 1.8$ Hz, H-7), 6.88 (1H, d, $J = 7.8$ Hz, H-8), 6.83 (1H, dd, $J = 7.7, 1.9$ Hz, H-12), 6.76 (1H, d, $J = 7.8$ Hz, H-15), 4.05 (1H, ddd, $J = 12.7, 9.7, 3.3$ Hz, H-2_b), 3.84 (1H, ddd, $J = 13.4, 9.7, 4.0$ Hz, H-1_b), 3.19-3.10 (5H, m, H-1_a, H-9, H-10), 3.03 (1H, ddd, $J = 12.5, 10.1, 4.1$ Hz, H-2_a). HRMS (ESI) found: $[\text{M} + \text{Na}]^+$ 320.0897. $\text{C}_{17}\text{H}_{15}\text{NO}_4\text{Na}$ requires $[\text{M} + \text{Na}]^+$ 320.0893.

Resolution of 4-(*p*-Toluenesulfonamido)[2.2]paracyclophane-13-carboxylic acid

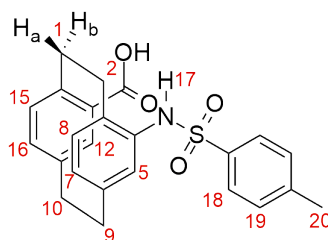
2.50



To a solution of 4-(*p*-toluenesulfonamido)[2.2]paracyclophane-13-carboxylic acid (0.10 g, 0.24 mmol, 1.0 eq.) in acetone (0.6 mL, 0.4 M) was added dropwise a solution of cinchonine (63 mg, 0.21 mmol, 0.9 eq.) in a minimum amount of MeOH (2 mL). The resulting mixture was stirred for one hour then left to stand for one hour. The resulting white crystals were filtered affording the first diastereomeric salt (95 mg,

0.13 mmol, 56%). The solvent was removed from the filtrate to afford the second diastereomeric salt as a pale brown solid (65 mg, 27%). ^1H NMR (400 MHz, CDCl_3): δ 9.14 (1H, s), 8.97 (1H, d, $J = 4.4$ Hz), 8.34 (1H, d, $J = 8.4$ Hz), 8.17 (1H, d, $J = 8.3$ Hz), 7.82 (1H, d, $J = 4.4$ Hz), 7.75 (1H, t, $J = 7.4$ Hz), 7.67 (1H, d, $J = 7.8$ Hz), 7.34 (2H, d, $J = 8.2$ Hz), 7.06 (2H, d, $J = 8.1$ Hz), 6.98 (1H, d, $J = 1.7$ Hz), 6.66 (1H, s), 6.57 (1H, d, $J = 7.8$ Hz), 6.48 (1H, dd, $J = 7.6, 1.5$ Hz), 6.44 (1H, dd, $J = 7.7, 1.5$ Hz), 6.40 (1H, d, $J = 7.7$ Hz), 6.09 (1H, ddd, $J = 17.2, 10.3, 7.0$ Hz), 5.90 (1H, d, $J = 1.2$ Hz), 5.33 (1H, d, $J = 12.8$ Hz), 5.30 (1H, d, $J = 5.9$ Hz), 4.54 (1H, ddd, $J = 12.8, 9.0, 1.9$ Hz), 4.05 (1H, ddd, $J = 13.1, 9.9, 3.5$ Hz), 3.73-3.57 (4H, m), 3.30 (1H, ddd, $J = 12.1, 9.6, 9.6$ Hz), 3.10-3.04 (1H, m), 2.99-2.87 (4H, m), 2.75-2.63 (2H, m), 2.37-2.33 (2H, m), 2.02 (1H, s), 1.96 (1H, t, $J = 11.0$ Hz), 1.87-1.73 (2H, m), 1.27 (1H, s), 1.02-0.99 (1H, t, $J = 7.2$ Hz).

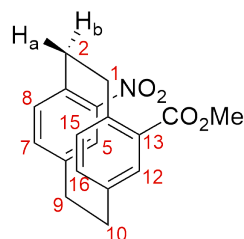
2.48



The resolved diastereomeric salt (95 mg, 0.133 mmol) was suspended in MeOH (1.3 mL, 0.1 M) and 2 M HCl (3 mL) was added. The resulting mixture was agitated by sonication for 5 minutes. The mixture was left to stand for one hour and the resulting solid was filtered and washed with MeOH (3 x 3 mL) affording the resolved 4-(*p*-toluenesulfonamido)[2.2]paracyclophane-13-carboxylic acid as a white powder (28 mg, 0.07 mmol, 50%). R_f (19:1 $\text{CH}_2\text{Cl}_2/\text{MeOH}$) 0.27. ^1H NMR (400 MHz, CDCl_3): δ 7.68 (1H, s, H-17), 7.52 (2H, d, $J = 8.1$ Hz, H-18), 7.13 (1H, d, $J = 1.8$ Hz, H-12), 7.10 (2H, d, $J = 8.0$ Hz, H-19), 6.75 (1H, dd, $J = 7.5, 1.8$ Hz, H-15), 6.62 (1H, d, $J = 7.8$ Hz, H-16), 6.53 (1H, d, $J = 7.8$ Hz, H-8), 6.39 (1H, dd, $J = 7.8, 1.9$ Hz, H-7), 6.31 (1H, d, $J = 1.8$ Hz, H-5), 4.39 (1H, t, $J = 10.7$ Hz, H-1_b), 3.80-3.75 (1H, m, H-2_b), 3.19- 2.87 (6H, m, H-1_a, H-2_a, H-9, H-10), 2.32 (3H, s, H-20). ^{13}C NMR (100 MHz, CDCl_3): δ 173.2 (C=O), 144.8 (C), 144.3 (C), 141.5 (C), 139.9 (C), 137.9 (CH), 137.5 (CH), 137.3 (CH),

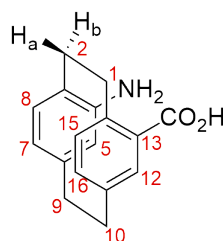
137.0 (CH), 136.9 (C), 136.4 (CH), 135.0 (C), 132.2 (CH), 130.2 (C), 129.2 (2 CH), 129.0 (C), 128.3 (2 CH), 37.0 (CH₂), 35.6 (CH₂), 35.6 (CH₂), 32.1 (CH₂), 22.6 (CH₃).

Methyl 4-nitro[2.2]paracyclophane-13-carboxylate 2.41



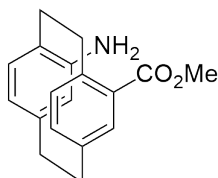
4-Nitro[2.2]paracyclophane-13-carboxylic acid (0.20 g, 0.67 mmol, 1.0 eq) was dissolved in SOCl₂ (3.4 mL, 0.2 M) under inert atmosphere and heated at reflux overnight. The solvent was removed by vacuum distillation. The crude acyl chloride was dissolved in dry MeOH under inert atmosphere (3.4 mL, 0.2 M) and stirred at room temperature overnight. The solvent was evaporated under reduced pressure affording methyl 4-nitro[2.2]paracyclophane-13-carboxylate as a yellow solid (0.20 g, 0.64 mmol, 97%). MP 160 °C (decomposes). ¹H NMR (500 MHz, CDCl₃): δ 7.24 (1H, d, *J* = 1.3 Hz, H-5), 7.11 (1H, d, *J* = 1.5 Hz, H-12), 6.96 (1H, dd, *J* = 7.8, 1.3 Hz, H-7), 6.88 (2H, d, *J* = 7.7 Hz, H-8, H-15), 6.80 (1H, d, *J* = 7.5 Hz, H-16), 3.97 (1H, ddd, *J* = 12.7, 9.9, 3.1 Hz), 3.88 (1H, d, *J* = 1.8 Hz), 3.78 (1H, ddd, *J* = 13.3, 9.7, 3.9 Hz), 3.72 (3H, s, CH₃), 3.19-3.05 (6H, m, H-1_a, H-2_a, H-9, H-10). ¹³C NMR (125 MHz, DMSO-*d*₆): δ 166.9 (C=O), 149.1 (C), 142.5 (C), 141.8 (C), 140.4 (CH), 138.9 (CH), 137.9 (C), 137.1 (C), 136.8 (CH), 135.8 (CH), 134.1 (C), 129.5 (CH), 127.8 (CH), 52.0 (CH₃), 34.3 (2 CH₂), 34.0 (CH₂), 33.1 (CH₂).

4-Amino[2.2]paracyclophane-13-carboxylic acid 2.3



To a solution of 4-nitro[2.2]paracyclophane-13-carboxylic acid (0.20 g, 0.67 mmol, 1.0 eq) in MeOH (3.0 mL, 0.2 M) was added NH_4Cl (0.108 g, 2.02 mmol, 3.0 eq) and Zn powder (0.132 g, 2.02 mmol, 3.0 eq), and heated at 80 °C overnight. The mixture was filtered through a sintered glass funnel connected to a Büchner apparatus. The solid was washed with MeOH (3 x 10 mL) and the combined filtrate was concentrated under reduced pressure. The reduced filtrate was suspended in water (15 mL) and stirred for 30 minutes at room temperature. The solids were collected by filtration and dried under vacuum. The residue was purified by a silica plug and elution with 5% MeOH in CH_2Cl_2 afforded 4-amino[2.2]paracyclophane-13-carboxylic acid as a pale brown solid (0.15 g, 0.56 mmol, 81%). R_f (9:1 $\text{CH}_2\text{Cl}_2/\text{MeOH}$) 0.63. mp 165 °C (decomposes). ^1H NMR (500 MHz, $\text{DMSO}-d_6$): δ 7.11 (1H, d, $J = 1.7$ Hz, H-12), 6.65 (1H, dd, $J = 7.3, 1.7$ Hz, H-16), 6.35 (1H, d, $J = 7.7$ Hz, H-15), 6.21 (1H, d, $J = 7.6$ Hz, H-8), 5.99 (1H, dd, $J = 7.4, 1.5$ Hz, H-7), 5.27 (1H, d, $J = 1.5$ Hz, H-5), 4.29 (1H, ddd, $J = 13.3, 9.7, 6.0$ Hz, H-1_b), 3.28-3.23 (1H, m, H-2_b), 2.98-2.75 (5H, m, H-2_a, H-9, H-10), 2.50-2.55 (1H, m, H-1_a). Data comparable to that reported in the literature.¹⁷⁷

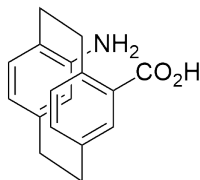
Methyl 4-amino[2.2]paracyclophane-13-carboxylate 2.21



To a solution of methyl 4-nitro[2.2]paracyclophane-13-carboxylate (0.210 g, 0.68 mmol, 1.0 eq) in MeOH (3.4 mL, 0.2 M) was added NH_4Cl (0.11 g, 2.02 mmol, 3.0 eq) and Zn powder (0.13 g, 2.02 mmol, 3.0 eq), and heated at 80 °C overnight. The mixture was filtered through a sintered glass funnel connected to a Büchner apparatus. The reduced filtrate was washed with MeOH (3 x 10 mL) and the combined filtrate was concentrated under reduced pressure. The solids were suspended in water (20 mL) and stirred for 30 minutes. The solids were collected by filtration and dried under vacuum, affording the crude product as a brown solid. The residue was purified by a silica plug and elution with 5% MeOH in CH_2Cl_2 afforded the methyl 4-amino[2.2]paracyclophane-13-carboxylate as a pale brown solid (0.15 g, 79%). Data

as reported earlier.

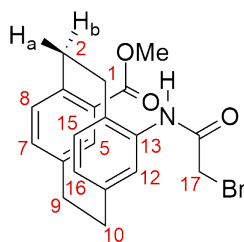
4-Amino[2.2]paracyclophane-13-carboxylic acid, ester hydrolysis 2.3



To a solution of methyl 4-amino[2.2]paracyclophane-13-carboxylate (0.107 g, 0.38 mmol, 1.0 eq) in 3:1 EtOH/H₂O (5.7 mL) was added ground KOH (0.104 g, 1.85 mmol, 4.9 eq). This mixture was heated at 50 °C overnight then cooled to room temperature. The mixture was adjusted to pH 6 with conc. H₂SO₄ and the EtOH removed under reduced pressure. The remaining aqueous mixture was extracted with EtOAc (3 x 15 mL). Combined extracts were dried (MgSO₄) and the solvent removed under reduced pressure affording 4-amino[2.2]paracyclophane-13-carboxylic acid as a yellow solid (0.060 g, 0.22 mmol, 59%). Data as reported earlier.

5.2.3 Synthesis of Gly-Pca

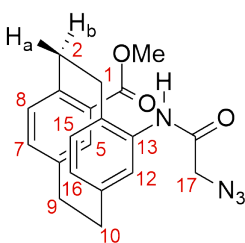
Methyl 4-[(2-bromo-1-oxoethyl)amino][2.2]paracyclophane-13-carboxylate 3.35



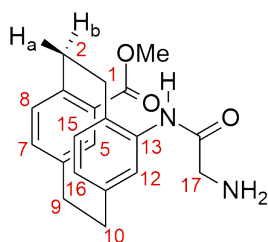
To a solution of methyl 4-amino[2.2]paracyclophane-13-carboxylate (50 mg, 0.18 mmol, 1.0 eq) in 1:1 dry DMF/dioxane (2.2 mL, 0.1 M) under inert atmosphere at -10 °C was added dropwise bromoacetyl bromide (20 μ L, 1.3 eq). The reaction mixture was stirred overnight, coming to room temperature. Water (5 mL) was added and the mixture stirred for 30 minutes. The light brown precipitate was collected by filtration through filter paper on a Büchner apparatus. The solid was washed with water (3 x mL) and dried under vacuum, affording the product as a light brown solid (45

mg, 0.11 mmol, 62%). R_f (2:1 hexane:EtOAc) 0.48. $^1\text{H NMR}$ (500 MHz, $\text{DMSO-}d_6$): δ 9.27 (1H, s, NH), 7.12 (1H, d, $J = 1.2$ Hz, H-5), 6.79-6.76 (2H, m, H-7, H-12), 6.63 (1H, d, $J = 7.8$ Hz, H-8), 6.58 (1H, d, $J = 7.8$ Hz, H-15), 6.43 (1H, dd, $J = 7.7, 1.3$ Hz, H-16), 4.15 (1H, d, $J = 11.1$ Hz, H-17_a), 4.04-3.98 (2H, m, H-17_b, H-2_b), 3.79 (3H, s, CH_3), 3.29 (1H, ddd, $J = 9.8, 6.0, 4.2$ Hz, H-1_b), 3.11-2.87 (1H, m, H-2_a), 3.03-2.81 (5H, m, H-1_a, H-9, H-10). HRMS (ESI) found: $[\text{M} + \text{Na}]^+$ 424.0508, 426.0489. $\text{C}_{20}\text{H}_{20}\text{BrNO}_3\text{Na}$ requires $[\text{M} + \text{Na}]^+$ 424.0519, 426.0499. The material was used as is due to the compound's rapid decomposition.

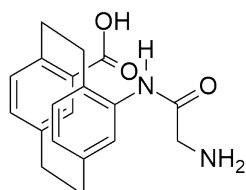
Methyl 4-[(2-azido-1-oxoethyl)amino][2.2]paracyclophane-13-carboxylate 3.36



To a stirred solution of methyl 4-[(3-bromo-1-oxoethyl)amino][2.2]paracyclophane-13-carboxylate (0.10 g, 0.25 mmol, 1.0 eq) in DMF (1.2 mL, 0.2 M) was added NaN_3 (65 mg, 4.0 eq) and the mixture was heated at 80 °C overnight. The solvent was removed under reduced pressure affording methyl 4-[(2-azido-1-oxoethyl)amino]-[2.2]paracyclophane-13-carboxylate as a pale yellow solid (38 mg, 0.10 mmol, 42%). Note: taking this mixture to dryness is not advisable on a large scale due to the risk of explosion by the azide present. R_f (2:1 hexane:EtOAc) 0.48. $^1\text{H NMR}$ (500 MHz, $\text{DMSO-}d_6$): δ 8.03 (1H, s, br, NH), 7.21 (1H, s, H-5), 6.80 (1H, s, H-12), 6.73 (1H, d, $J = 7.8$ Hz, H-7), 6.60 (1H, d, $J = 7.8$ Hz, H-8), 6.57 (1H, d, $J = 7.8$ Hz, H-15), 6.49 (1H, d, $J = 7.8$ Hz, H-16), 4.19-4.11 (1H, m, H-2_b), 4.11 (2H, s, H-17), 3.91 (3H, s, CH_3), 3.32-3.28 (1H, m, H-1_b), 3.19-3.00 (6H, m, H-1_a, H-2_a, H-9, H-10). $^{13}\text{C NMR}$ (125 MHz, $\text{DMSO-}d_6$): δ 168.8 (C=O), 164.2 (C=O), 141.7 (C), 140.7 (C), 139.6 (C), 136.7 (C), 136.1 (C), 135.8 (CH), 134.9 (CH), 134.0 (CH), 131.0 (CH), 130.0 (C), 128.4 (CH), 126.3 (CH), 53.2 (CH_3), 51.9 (CH_2), 34.8 (2 CH_2), 33.3 (CH_2), 31.7 (CH_2). HRMS (ESI) found: $[\text{M} + \text{H}]^+$ 387.1609. $\text{C}_{20}\text{H}_{21}\text{N}_4\text{O}_3$ requires $[\text{M} + \text{H}]^+$ 365.1608.

Methyl 4-[(2-amino-1-oxoethyl)amino][2.2]paracyclophane-13-carboxylate 3.37

To a solution of methyl 4-[(2-azido-1-oxoethyl)amino][2.2]paracyclophane-13-carboxylate (50 mg, 0.14 mmol, 1.0 eq) in dry MeOH was added 10% Pd/C (5 mg, 10 wt%). The suspension was put under H₂ atmosphere and stirred at room temperature until TLC analysis indicated the starting material had been consumed; about 30 minutes. The suspension was filtered through filter paper and the solid was washed with MeOH (3 x 3 mL). Combined filtrate and washings were concentrated under reduced pressure. The crude solid was purified by flash column chromatography and elution with 1:1 hexane:EtOAc affording methyl 4-[(2-amino-1-oxoethyl)amino]-[2.2]paracyclophane-13-carboxylate as a light yellow solid (34 mg, 0.10 mmol, 73%). *R_f* (2:1 hexane:EtOAc) 0.03. ¹H NMR (500 MHz, DMSO-*d*₆): δ 7.15 (1H, d, *J* = 1.7 Hz, H-5), 6.95 (1H, d, *J* = 1.5 Hz, H-12), 6.76 (1H, dd, *J* = 7.5, 1.7 Hz, H-7), 6.59 (1H, d, *J* = 7.7 Hz, H-8), 6.57 (1H, d, *J* = 7.8 Hz, H-15), 6.42 (1H, dd, *J* = 7.7, 1.5 Hz, H-16), 4.09 (1H, ddd, *J* = 13.4, 9.4, 4.3 Hz, H-2_b), 3.77 (3H, s, CH₃), 3.25-3.17 (3H, m, H-1_b, H-17), 3.10-2.85 (5H, m, H-2_a, H-9, H-10), 4.09 (1H, ddd, *J* = 13.4, 9.4, 4.3 Hz, H-1_a). ¹³C NMR (125 MHz, DMSO-*d*₆): δ 165.9 (C=O), 162.2 (C=O), 137.4 (C), 135.4 (C), 134.4 (C), 132.5 (CH), 131.8 (C), 131.5 (C), 130.0 (CH), 129.0 (CH), 124.4 (CH), 123.2 (C), 122.8 (CH), 119.3 (CH), 46.9 (CH₃), 40.5 (CH₂), 29.7 (CH₂), 29.5 (CH₂), 27.6 (CH₂), 26.8 (CH₂). HRMS (ESI) found: [M + H]⁺ 339.1699. C₂₀H₂₃N₂O₃ requires [M + H]⁺ 339.1703.

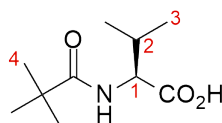
4-[(2-Amino-1-oxoethyl)amino][2.2]paracyclophane-13-carboxylic acid 3.38

To a stirred solution of methyl 4-[(2-amino-1-oxoethyl)amino][2.2]paracyclophane-13-carboxylate (0.56 g, 1.65 mmol, 1.0 eq.) in EtOH (7.2 mL, 0.2 M) was added ground KOH (1.61 g, 33.1 mmol, 20 eq.). The mixture was stirred at room temperature overnight. The mixture was neutralised with 2 M HCl (approx. 8 mL). The aqueous layer was extracted with EtOAc (3 x 15 mL). Combined organics were dried (MgSO₄) and the solvent was removed under reduced pressure, affording the product as an oily yellow solid (0.47 g, 1.45 mmol, 88%). HRMS (ESI) found: [M + H]⁺ 323.1390. C₁₉H₁₉N₂O₃ requires [M + H]⁺ 323.1401. Material could not be purified for further characterisation.

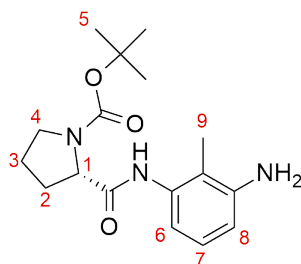
5.2.4 Peptide couplings & transformations

Pivaloyl-L-valine 5.4

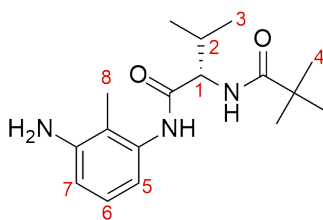
Prepared according to literature procedure.²⁷⁸



To a solution of L-valine (0.20 g, 1.71 mmol, 1.0 eq.) in 1:1 MeOH/1 M aq. NaOH (3.4 mL, 0.5 M) at 0 °C was added pivaloyl chloride (0.21 mL, 1.71 mmol, 1.0 eq.) and the mixture was stirred overnight with no further cooling. The reaction mixture was washed with EtOAc (10 mL) and the aqueous layer was acidified to pH 2-3 with 1 M HCl, then extracted with EtOAc (3 x 10 mL). The combined organic extracts were dried (MgSO₄) and the solvent removed under reduced pressure affording pivaloyl-L-valine (0.20 g, 0.99 mmol, 58%). *R*_f (1:1 hexane:EtOAc) 0.63. ¹H NMR (500 MHz, CDCl₃): 10.18 (1H, s, CO₂H), 6.15 (1H, d, *J* = 8.0 Hz, NH), 4.54 (1H, dd, *J* = 8.3, 5.0 Hz, H-1), 2.29 (1H, td, *J* = 6.9, 5.0 Hz, H-2), 1.26 (9H, s, H-4), 1.00 (6H, dd, *J* = 15.0, 6.9 Hz, H-3). Data comparable to that reported in the literature.²⁷⁸

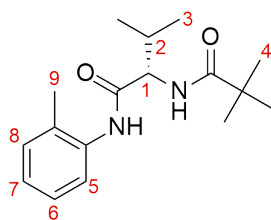
2-(Boc-prolinamido)-6-aminotoluene 5.5

To a stirred solution of *N*-methylmorpholine (0.36 mL, 3.28 mmol, 2.0 eq.) and EtO-COCl (0.31 mL, 3.28 mmol, 2.0 eq.) in CH₂Cl₂ (6.5 mL, 0.25 M) at 0 °C was added portionwise Boc-L-proline (0.70 g, 3.28 mmol, 2.0 eq.), followed by 2,6-diaminotoluene (0.20 g, 1.64 mmol, 1.0 eq.). The reaction mixture was stirred overnight, coming to room temperature. Water (10 mL) was added and the aqueous layer extracted with CH₂Cl₂ (3 x 10 mL). Combined organics were washed once each with 2 M HCl then sat. aq. NaHCO₃ (20 mL), then dried (MgSO₄) and the solvent removed under reduced pressure. The reaction was intended to couple a Boc-proline moiety to both amino groups of 2,6-diaminotoluene, however only singly substituted diaminotoluene was found, which was purified by column chromatography and elution with hexane:EtOAc 1:1 affording 2-(Boc-prolinamido)-6-aminotoluene as a pale yellow solid (0.38 g, 1.19 mmol, 73%). MP 162 °C (decomposes). *R*_f (1:1 hexane:EtOAc) 0.23. ¹H NMR (500 MHz, CDCl₃) δ 8.89 (1H, s, NH), 7.70-7.67 (2H, m, H-6, H-8), 7.21 (1H, d, *J* = 7.5, 7.4 Hz, H-7), 4.51 (2H, s, NH₂), 3.45 (3H, s, H-9), 2.57 (2H, s, H-4), 2.09-1.98 (5H, m, H-1, H-2, H-3), 1.51 (9H, s, H-5). MS (ESI) found: 320.1971. C₁₇H₂₆N₃O₃ requires [M + H]⁺ 320.1969. Material was of insufficient quality for further analysis.

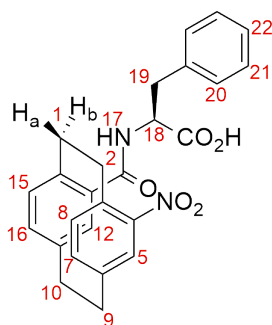
2-(Pivaloyl-L-valinamido)-6-aminotoluene 3.23

To a solution of pivaloyl-L-valine (0.37 g, 1.86 mmol, 2.0 eq.) in MeCN (10 mL, 0.2 M) at 0 °C was added 2,6-diaminotoluene (0.20 g, 0.93 mmol, 1.0 eq.), DMAP (0.23 g, 1.86 mmol, 2.0 eq.), HOBT (0.37 g, 2.42 mmol, 2.6 eq.), and EDC · HCl (0.46 g, 2.42 mmol, 2.6 eq.). The reaction mixture was stirred overnight at room temperature. Water (10 mL) was added, the layers separated and the aqueous layer was extracted with CH₂Cl₂ (3 × 10 mL). Combined organics were dried (MgSO₄) and the solvent was removed under reduced pressure. The crude product was purified on a silica column eluting 1:1 hexane:EtOAc affording 2-(pivaloyl-L-valinamido)-6-aminotoluene as a white solid (0.25 g, 0.82 mmol, 88%). *R_f* (1:1 hexane:EtOAc) 0.72. ¹H NMR (500 MHz, DMSO-*d*₆): 9.19 (1H, s, NH₂), 6.88-6.80 (2H, m, NH), 6.76 (1H, d, *J* = 8.5 Hz, H-6), 6.50-6.44 (2H, m, H-5, H-7), 3.91 (1H, dd, *J* = 8.0, 6.0 Hz, H-1), 2.10-2.03 (1H, m, H-2), 1.89 (3H, s, H-8), 1.41 (9H, s, H-4), 0.94 (6H, dd, 10.0, 6.5 Hz, H-3). Material was of insufficient quality for further analysis.

2-(Pivaloyl-L-valinamido)toluene 3.13



To a solution of pivaloyl-L-valine (0.20 g, 1.0 mmol, 1.0 eq.) in MeCN (5.0 mL, 0.2 M) at 0 °C was added *o*-toluidine (0.10 g, 1.0 mmol, 1.0 eq.), DMAP (0.12 g, 1.0 mmol, 1.0 eq.), HOBT (0.20 g, 1.29 mmol, 1.3 eq.), and EDC · HCl (0.25 g, 1.29 mmol, 1.3 eq.). The reaction mixture was stirred overnight at room temperature. Water (5 mL) was added and the aqueous layer was extracted with CH₂Cl₂ (3 × 5 mL). Combined organics were dried (MgSO₄) and the solvent was removed under reduced pressure affording a white solid containing crude 2-(pivaloyl-L-valinamido)toluene in a mixture of compounds. The compound was not purified further. *R_f* (1:1 hexane:EtOAc) 0.45. ¹H NMR (500 MHz, DMSO-*d*₆): δ 7.82 (2H, d, *J* = 8.2 Hz, NH), 7.23-7.17 (2H, m, H-5, H-7), 7.09 (1H, dd, *J* = 8.0, 7.8 Hz, H-6), 5.18 (1H, d, *J* = 13.4 Hz, H-8), 4.07 (1H, dd, *J* = 8.4, 6.5 Hz, H-1), 2.39-2.31 (1H, m, H-2), 2.27 (3H, s, H-9), 1.48 (9H, s, H-4), 1.04 (6H, d, *J* = 7.0 Hz, H-3). Material was of insufficient quality for further analysis.

4-Nitro[2.2]paracyclophan-13-(amido-Phe) 3.25

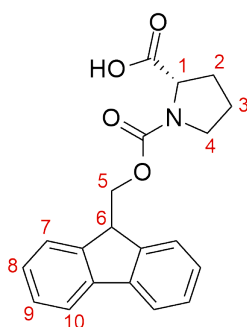
4-Nitro[2.2]paracyclophane-13-carboxylic acid (0.57 g, 1.0 mmol, 1.0 eq) was heated at reflux in SOCl_2 (10 mL) overnight under inert atmosphere. The solvent was removed under reduced pressure and the acyl chloride dissolved in dry THF (3 mL) was added dropwise over 20 minutes to a stirred solution of L-phenylalanine (0.63 g, 3.84 mmol, 2.0 eq) in 1 M aqueous NaOH (3.8 mL, 1 M) at 0 °C. The mixture was stirred for two hours at 0 °C then acidified to pH 2-3 (1 M HCl) and extracted with EtOAc (3 x 10 mL). Combined organics were washed with brine (20 mL), dried (MgSO_4) and the solvent removed under reduced pressure affording the crude product as a pale yellow solid. The crude product was purified using column chromatography eluting 1:1 hexane:EtOAc with 1% AcOH affording partial separation of the two diastereomers (*S_P,S*)-**3.25** 0.043 g, (*R_P,S*)-**3.25** 0.075 g, mixture of diastereomers 0.25 g, total 0.37 g, 0.83 mmol, 43%).

(*S_P,S*)-**3.25**: R_f (1:1 hexane:EtOAc + 1% AcOH) 0.45. ^1H NMR (500 MHz, $\text{DMSO}-d_6$): δ 12.40 (1H, s, br, OH), 7.92 (1H, d, $J = 7.8$ Hz, H-17), 7.38-7.25 (5H, m, H-20, H-21, H-22), 7.12 (1H, s, H-5), 6.88 (1H, d, $J = 7.6$ Hz, H-7), 6.80-6.76 (2H, m, H-8, H-16), 6.72 (1H, d, $J = 7.7$ Hz, H-15), 6.44 (1H, s, H-12), 4.50 (1H, dd, $J = 14.1, 8.3$ Hz, H-2_b), 3.94 (1H, ddd, $J = 11.2, 9.8, 3.5$ Hz, H-1_b), 3.73-3.69 (1H, m, H-2_a), 3.13-2.90 (8H, m, H-1_a, H-9, H-10, H-18, H-19). Note: this sample/spectrum was of insufficient quality to define all multiplets and J couplings. Many doublets with small J couplings (<2) are not resolved and are characterised here as singlets or multiplets. ^{13}C NMR (125 MHz, $\text{DMSO}-d_6$): δ 173.5 (C=O), 172.5 (C=O), 168.0 (C), 148.0 (C), 142.0 (CH), 139.6 (C), 138.8 (C), 138.5 (CH), 138.4 (C), 137.8 (CH), 136.2 (C), 135.8 (CH), 134.5 (CH), 131.9 (CH), 129.5 (C), 129.1 (CH), 128.6 (CH), 127.8 (2 CH), 126.8 (CH), 54.5 (CH),

pale yellow solid (36 mg, 0.087 mmol, 65%). R_f (19:1 CH_2Cl_2 :MeOH) 0.19. ^1H NMR (500 MHz, $\text{DMSO}-d_6$, mixture of rotamers): δ 7.74 (1H, t, $J = 7.6$ Hz, H-17), 7.34-7.25 (4H, m, H-20, H-21), 7.18 (1H, d, $J = 6.7$ Hz, H-22), 6.80 (1H, s, H-12), 6.53 (1H, t, $J = 7.5$ Hz, H-16), 6.33 (1H, d, $J = 7.3$ Hz, H-15), 6.22 (1H, t, $J = 8.4$ Hz, H-7), 6.00 and 5.98 (1H, d, $J = 7.8$ Hz, H-8), 5.41 and 5.30 (1H, s, H-5), 4.71-4.61 (1H, m, H-1_b), 4.38-4.18 (1H, m, H-2_b), 4.10 (1H, q, $J = 5.3$ Hz, H-18), 3.14-2.74 (8H, m, H-1_a, H-2_a, H-9, H-10, H-19). MS (ESI) $[\text{M} + 3\text{H}]^+$ 139.03.

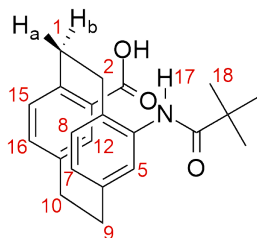
Fmoc-L-proline 5.6

Prepared according to literature procedure.²⁷⁹

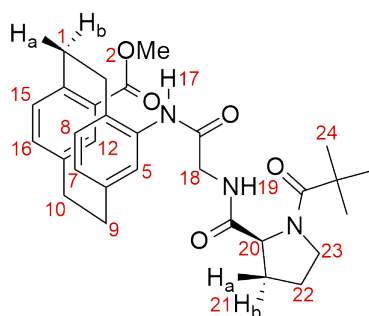


To a stirred solution of L-proline (0.93 g, 8.12 mmol, 1.05 eq.) and K_2CO_3 (2.78 g, 20.10 mmol, 2.6 eq.) in a 10:3 mixture of water/dioxane (150 mL, 0.05 M) at 0 °C was added Fmoc chloride (2.00 g, 7.73 mmol, 1.0 eq.). The resulting mixture was stirred overnight without further cooling. The reaction mixture was washed with Et_2O (2 x 100 mL). The aqueous layer was acidified to pH 1 with 1 M HCl and extracted with CH_2Cl_2 (3 x 100 mL). Combined organics were dried (MgSO_4) and the solvent was removed under reduced pressure affording Fmoc-L-proline as a yellow solid (2.33 g, 6.90 mmol, 85%). MP 137 °C (decomposes). ^1H NMR (500 MHz, CDCl_3): δ 7.82 (2H, d, $J = 1.0$ Hz), 7.64 (2H, d, $J = 1.0$ Hz), 7.36 (2H, dd, $J = 2.0, 1.0$ Hz), 7.31-7.26 (2H, m), 4.42 (2H, d, $J = 7.0$ Hz), 4.38-4.29 (2H, m), 3.59-3.51 (2H, m), 2.39-2.32 (1H, m), 2.02-1.98 (3H, m). Data comparable to that reported in the literature.²⁷⁹

4-Pivalamido[2.2]paracyclophane-13-carboxylic acid 5.7



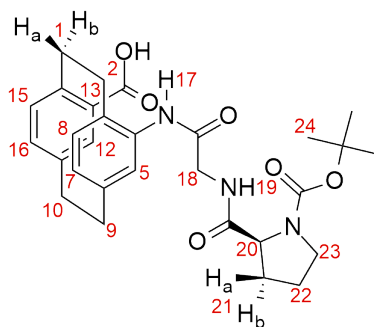
To a stirred solution of 4-amino[2.2]paracyclophane-13-carboxylic acid (50 mg, 0.19 mmol, 1.0 eq.) in THF (0.4 mL, 0.5 M) under inert atmosphere at $-80\text{ }^{\circ}\text{C}$ was added *n*-BuLi in hexane (1.7 M, 0.28 mL, 4.68 mmol, 2.5 eq.) dropwise over 8 minutes and the reaction mixture maintained at $-80\text{ }^{\circ}\text{C}$ for 20 minutes. Pivaloyl chloride (28 μL , 0.22 mmol, 1.2 eq.) was added and the reaction mixture was stirred overnight, allowing to come to room temperature. Water (1 mL) and EtOAc (1 mL) were added with vigorous stirring, then the layers were separated and the organic layer washed successively with water (1 mL) and brine (1 mL). The organic layer was dried (MgSO_4) and the solvent removed under reduced pressure. The resulting residue was purified by column chromatography and elution with a gradient of hexane:EtOAc 7:1 to 4:1 to afford 4-(pivalamido)[2.2]paracyclophane-13-carboxylic acid as a dark yellow oil (48 mg, 0.14 mmol, 72%). R_f (4:1 hexane:EtOAc) 0.30. ^1H NMR (500 MHz, $\text{DMSO-}d_6$): δ 12.66 (1H, s, br), 7.98 (1H, s), 7.15 (1H, s), 6.73 (1H, s), 6.57 (2H, d), 6.43 (2H, s), 3.89 (1H, s), 3.10-2.88 (5H, m), 2.78 (1H, s), 1.24 (9H, s). Note: this spectrum was not well-resolved so *J*-couplings are not reported and multiplets with smaller *J*-couplings are not apparent). ^{13}C NMR (125 MHz, $\text{DMSO-}d_6$): δ 175.4 (C=O), 169.2 (C=O), 142.2 (C), 139.8 (C), 139.3 (C), 137.2 (C), 136.5 (CH), 136.4 (CH) 136.3 (CH), 134.8 (CH), 134.3 (C), 134.2 (CH), 130.2 (C), 127.1 (CH), 39.1 (C), 34.7 (CH_2), 34.6 (CH_2), 33.9 (CH_2), 32.5 (CH_2), 27.6 (CH_3).

Boc-Pro-Gly-Pca-OMe 3.39

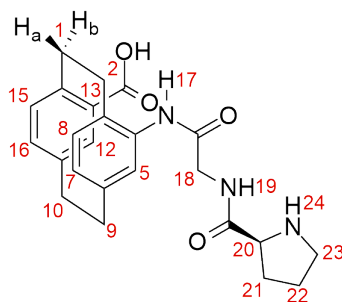
To a stirred solution of NHS (0.048 g, 0.414 mmol, 1.0 eq) and Boc-L-proline (0.089 g, 0.414 mmol, 1.0 eq) in THF (2.1 mL, 0.2 M) was added DCC (0.085 g, 0.414 mmol, 1.0 eq) and the mixture stirred for 30 minutes. The precipitate was removed by filtration and washed with THF (3 x 1 mL). The combined filtrate and washings were added to a stirred solution of methyl 4-[(3-amino-1-oxopropyl)amino]-[2.2]paracyclophane-13-carboxylate (0.140 g, 0.414 mmol, 1.0 eq) in DMF (5.0 mL, 0.1 M) followed by DMAP (0.005 g, 0.041 mmol, 0.1 eq). The resulting solution was stirred at room temperature overnight. Water (5 mL) was added and the aqueous layer was extracted with EtOAc (3 x 10 mL). The combined organic layers were washed once each with water and brine (20 mL), dried (MgSO₄) and the solvent removed under reduced pressure. The crude product was purified on a silica column eluting 19:1 CH₂Cl₂/MeOH affording the desired product as a light yellow solid (0.144 g, 0.27 mmol, 65%). *R_f* (19:1 CH₂Cl₂/MeOH) 0.06. MP 170 °C (decomposes). ¹H NMR (500 MHz, CDCl₃): δ 8.08-7.93 (1H, m, H-17), 7.56-7.45 (1H, m, H-19), 7.19 (1H, br s, H-12), 6.86-6.75 (1H, m, H-5), 6.70 (1H, d, *J* = 7.0 Hz, H-15), 6.58 (1H, dd, *J* = 7.7, 3.9 Hz, H-16), 6.54 (1H, dd, *J* = 7.7, 2.2 Hz, H-7), 6.47-6.49 (1H, m, H-8), 4.49-4.30 (1H, m, H-20), 4.17-4.14 (1H, m, H-2_b), 4.07-3.99 (2H, m, H-18), 3.91 (3H, d, *J* = 10.4 Hz, CH₃), 3.52 and 3.42 (2H, two br s without baseline separation, H-23), 3.28 (1H, ddd, *J* = 13.5, 9.9, 3.7 Hz, H-1_b), 3.18-3.10 (2H, m, H-9), 3.07-2.95 (4H, m, H-1_a, H-2_a, H-10), 2.43-2.38 (1H, m, H-21_a), 2.05-2.00 (2H, m, H-22), 1.94-1.93 (1H, m, H-21_b), 1.51 and 1.46 (9H, two s without baseline separation, H-24). Note: many peaks are broad, undefined and/or twinned due to slow tumbling of the compound in the solvent, as well as the presence of two diastereomers. ¹³C NMR (125 MHz, DMSO-*d*₆): δ 173.6 (C=O), 173.2 (C=O), 167.3 (C=O), 154.2 (C=O), 142.8 (C), 142.9 (C), 140.1 (C),

139.4 (CH), 137.7 (C), 136.4 (CH), 135.2 (CH), 134.2 (CH), 130.5 (CH), 128.8 (C), 128.0 (CH), 124.5 (CH), 79.1 (C), 60.1 (C), 51.9 (CH₃), 47.2 (CH₂), 43.3 (CH₂), 33.8 (CH₂), 33.3 (CH₂), 32.2 (CH₂), 31.5 (CH₂), 30.4 (CH₂), 25.8 (CH₂), 23.7 (3 CH₃). HRMS (ESI) found: [M + Na]⁺ 558.2570. C₃₀H₃₇N₃NaO₆ requires [M + Na]⁺ 558.2575.

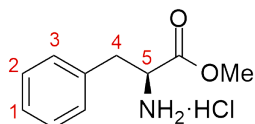
Boc-Pro-Gly-Pca 3.40



Boc-Pro-Gly-Pca-OMe (1.7 g, 3.17 mmol, 1.0 eq.) was dissolved in EtOH (32 mL, 0.1 M) then ground KOH (3.56 g, 63.5 mmol, 40 eq.) was added and the solution was stirred overnight at room temperature. 2 M HCl (approx. 30 mL) was added to neutralise the mixture. The aqueous layer was extracted with EtOAc (3 x 50 mL), affording the product as an oily yellow solid (0.94 g, 1.81 mmol, 57%). *R_f* (19:1 CH₂Cl₂/MeOH) 0.26. ¹H NMR (500 MHz, CDCl₃): δ 8.59-8.39 (1H, m, NH), 7.64-7.59 (1H, m, NH), 7.31 (1H, dd, *J* = 7.1, 1.4 Hz, H-12), 6.90-6.86 (1H, m, H-5), 6.72 (1H, d, *J* = 7.7 Hz, H-16), 6.55 (2H, d, *J* = 7.7 Hz, H-8, H-15), 6.44-6.42 (1H, m, H-8), 4.64-4.59 (1H, m, H-20), 4.36-4.32 (1H, m, H-2_b), 4.27-4.21 (2H, m, H-18), 3.57-3.52 (1H, m, H-1_b), 3.41-3.37 (2H, m, H-23), 3.14-3.10 (2H, m, H-9), 3.00-2.89 (4H, m, H-1_a, H-2_a, H-10), 2.31-2.30 (1H, m, H-21_a), 2.12-2.06 (1H, m, H-21_b), 2.04-1.93 (2H, m, H-22), 1.45 (9H, two s without baseline separation, H-24). Note: many peaks are broad, undefined and/or twinned due to slow tumbling of the compound in the solvent, as well as the presence of two diastereomers. ¹³C NMR (125 MHz, CDCl₃): δ 174.0 (C=O), 171.2 (C=O), 170.2 (C=O), 166.9 (C=O), 143.0 (C), 143.0 (C), 140.4 (C), 140.4 (C), 139.5 (C), 136.7 (CH), 136.3 (CH), 135.1 (CH), 134.8 (CH), 129.5 (CH), 128.4 (C), 125.8 (CH), 81.2 (C), 60.5 (CH), 47.4 (CH₂), 44.4 (CH₂), 34.2 (CH₂), 34.0 (CH₂), 31.6 (CH₂), 31.4 (CH₂), 29.2 (CH₂), 28.4 (3 CH₃), 24.5 (CH₂). HRMS (ESI) found: [M + H]⁺ 520.2440. C₂₉H₃₄N₃O₆ requires [M + H]⁺ 520.2453.

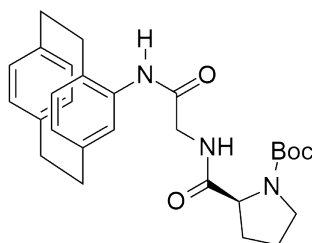
Pro-Gly-Pca 3.41

Boc-Pro-Gly-Pca-OH (0.35 g, 0.67 mmol, 1.0 eq) was dissolved in 6.7 mL 3:1 TFA/CH₂Cl₂ at 0 °C. The solution was stirred for 30 minutes then the solvent was removed under reduced pressure affording an orange oil. The crude material was purified by autocolumn chromatography (silica gel, 0-10% MeOH in CH₂Cl₂ as eluent) affording the desired product as a mixture of diastereomers in an oily yellow solid (0.26 g, 0.62 mmol, 92%). Separation of the diastereomers was achieved by gravity column (silica gel, 10% MeOH in CH₂Cl₂ as eluent) affording three fractions: diastereomer A, A+B, and diastereomer B. ¹H NMR (500 MHz, DMSO-*d*₆): δ 9.84 (1H, s, NH), 9.07 (1H, t, *J* = 6.1 Hz, NH), 6.67 (1H, s, H-12), 6.52 (1H, d, *J* = 7.8 Hz, H-15), 6.45 (2H, d, *J* = 7.7 Hz, H-7, H-16), 6.43 (1H, d, *J* = 7.7 Hz, H-8), 6.11 (1H, s, H-5), 4.43 (1H, t, *J* = 7.7 Hz, H-20), 3.95-3.90 (1H, m, *J* = 6.7 Hz, H-2_b), 3.63 (1H, ddd, *J* = 12.4, 9.4, 4.2 Hz, H-1_b), 3.52 (2H, dd, *J* = 17.2, 5.5 Hz, H-18), 3.13-3.07 (2H, m, H-23), 3.02-2.89 (4H, m, H-9, H-10), 2.76 (1H, ddd, *J* = 12.9, 10.1, 3.2 Hz, H-1_a), 2.65 (1H, ddd, *J* = 12.6, 10.8, 3.8 Hz, H-2_a), 2.22-2.15 (1H, m, H-21_a), 2.07-2.03 (1H, m, H-21_b), 2.00-1.92 (2H, m, H-22). ¹³C NMR (125 MHz, CDCl₃): δ 174.0 (C=O), 170.2 (C=O), 166.9 (C=O), 141.9 (C), 140.9 (C), 139.5 (C), 139.4 (C), 135.5 (C), 133.8 (CH), 133.7 (CH), 132.2 (CH), 130.7 (CH), 128.7 (CH), 128.5 (C), 126.23 (CH), 62.3 (CH), 47.2 (CH₂), 45.7 (CH₂), 35.2 (CH₂), 35.0 (CH₂), 32.9 (CH₂), 30.0 (CH₂), 27.1 (CH₂), 25.2 (CH₂). HRMS (ESI) found: [M + H]⁺ 422.2081. C₂₄H₂₈N₃O₄ requires [M + H]⁺ 422.2075.

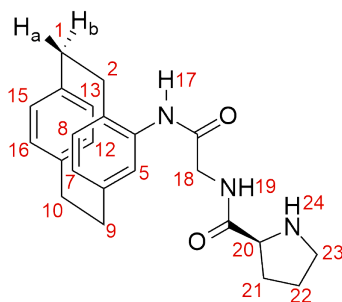
L-Phenylalanine, methyl ester hydrochloride 5.8

To a stirred solution of L-phenylalanine (0.202 g, 1.21 mmol, 1.0 eq.) in dry MeOH (6.0 mL, 0.2 M) under inert atmosphere at 0 °C was added SOCl₂ (0.35 mL, 4.84 mmol, 4.0 eq.). This mixture was stirred, coming to room temperature, overnight. The solvent was removed by vacuum distillation affording (S)-methyl 2-amino-3-phenylpropanoate as the hydrochloride salt (0.243 g, 1.13 mmol, 93%). *R*_f (9:1 CH₂Cl₂/MeOH) 0.74. ¹H NMR (500 MHz, D₂O): δ 7.33 (2H, t, *J* = 7.3 Hz, H-2), 7.30 (1H, t, *J* = 7.0 Hz, H-1), 7.25 (2H, d, *J* = 7.3 Hz, H-3), 4.25 (1H, t, *J* = 6.5 Hz, H-5), 3.34 (3H, s, CH₃), 3.20 (1H, dd, *J* = 14.0, 5.7 Hz, H-4_a), 3.10 (1H, dd, *J* = 14.0, 7.4 Hz, H-4_b). Data comparable to that reported in the literature.²⁸⁰

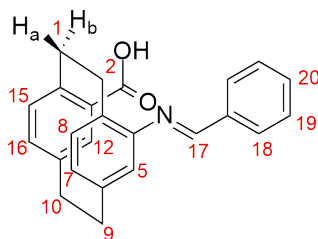
(4-*N*-Boc-Pro-Gly-amino)[2.2]paracyclophane 5.9



To a stirred solution of *N*-hydroxysuccinimide (0.45 g, 3.92 mmol, 1.0 eq) and Boc-L-proline (0.85 g, 3.92 mmol, 1.0 eq) in THF (20 mL, 0.2 M) was added dicyclohexylcarbodiimide (0.81 g, 3.92 mmol, 1.0 eq) and further stirred for 30 minutes. The precipitate was removed by filtration and washed with THF (3 × 10 mL). The combined filtrate and washings were added to a stirred solution of 4-[(3-amino-1-oxopropyl)amino]-[2.2]paracyclophane (1.10 g, 3.92 mmol, 1.0 eq) in DMF (40 mL, 0.1 M) followed by DMAP (48 mg, 0.39 mmol, 0.1 eq). The resulting solution was stirred at 60 °C overnight. The solvent was removed under reduced pressure and the crude product was purified on a silica column eluting 19:1 CH₂Cl₂/MeOH affording (4-*N*-Boc-Pro-Gly-amino)[2.2]paracyclophane as a light yellow solid (1.06 g, 2.22 mmol, 57%). *R*_f (19:1 CH₂Cl₂/MeOH) 0.23. MP 168 °C (decomposes). MS (ESI) found: [M + Na]⁺ 500.10. C₂₈H₃₅N₃O₄Na requires [M + Na]⁺ 520.25. The compound was not fully characterised until the Boc protecting group was removed. Rotamers made it impossible to assign spectra until removal of the Boc group.

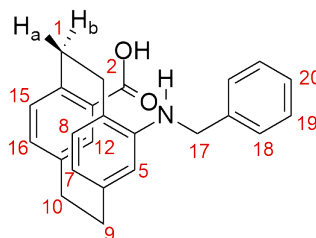
(4-*N*-Pro-Gly-amino)[2.2]paracyclophane 3.43

(4-*N*-Boc-Pro-Gly-amino)[2.2]paracyclophane (1.06 g, 2.22 mmol, 1.0 eq) was dissolved in CH₂Cl₂ (16.5 mL) at 0 °C and TFA was added (5.5 mL, 0.2 M total). The mixture was stirred at 0 °C for one hour then the solvent was removed under reduced pressure. The residue was purified by flash column eluting 9:1 CH₂Cl₂/MeOH to afford (4-*N*-Pro-Gly-amino)[2.2]paracyclophane as an oily yellow solid (0.50 g, 1.32 mmol, 60%). *R*_f (CH₂Cl₂/MeOH) 0.23. ¹H NMR (500 MHz, DMSO-*d*₆): δ 9.36 (1H, d, *J* = 6.1 Hz, H-24), 8.89 (1H, t, *J* = 5.5 Hz, H-19), 8.61 (1H, s, H-17), 6.76 (1H, d, *J* = 7.7 Hz, H-8), 6.56 (1H, d, *J* = 1.5 Hz, H-5), 6.52 (1H, dd, *J* = 7.7, 1.6 Hz, H-7), 6.44 (2H, dd, *J* = 8.0, 2.0 Hz, H-12, H-13), 6.41-6.39 (2H, m, H-15, H-16), 4.29-4.27 (1H, m, H-20), 4.19-4.08 (2H, m, H-18), 3.33-3.22 (3H, m, H-2_b, H-23), 3.01-2.86 (6H, m, H-1, H-9, H-10), 2.68-2.63 (1H, m, H-2_a), 2.37-2.33 (1H, m, H-21_a), 1.97-1.89 (3H, m, H-21_b, H-22). ¹³C NMR (125 MHz, DMSO-*d*₆): δ 169.2 and 169.2 (C=O), 166.6 (C=O), 140.4 (C), 139.6 (C), 139.1 (C), 137.0 (C), 135.5 (CH), 133.3 (CH), 133.3 (CH), 132.7 (CH), 132.6 (CH), 129.4 (C), 129.4 (C), 127.3 (C), 59.5 (CH), 46.2, 43.1 (CH₂), 35.2 (CH₂), 35.0 (CH₂), 33.7 (CH₂), 30.1 (CH₂), 30.1 (CH₂), 24.0 (CH₂). MS (ESI) found: [M + H]⁺ 378.13. C₂₃H₂₈N₃O₂ requires [M + H]⁺ 378.22.

4-(*N*-benzylidene)-[2.2]paracyclophane-13-carboxylic acid 5.10

To a stirred solution of 4-amino-[2.2]paracyclophane-13-carboxylic acid (15 mg, 0.07 mmol, 1.0 eq.) in dry EtOH (0.7 mL, 0.1 M) at 60 °C was added benzaldehyde (0.015 mL, 0.15 mmol, 2.0 eq.). The mixture was stirred for two hours at 60 °C then cooled slowly to 4 °C and left undisturbed overnight. The precipitated solid was collected by filtration and washed with cold dry EtOH. The filtrate was recrystallised from dry EtOH and the solid was collected again in the same manner, affording 4-(*N*-benzylidene)-[2.2]paracyclophane-13-carboxylic acid (7 mg, 0.02 mmol, 28%). R_f (4:1 hexane:EtOAc) 0.17. The material's identity is confirmed by the characterisation of the following compound.

4-(*N*-benzylamino)-[2.2]paracyclophane-13-carboxylic acid 5.11

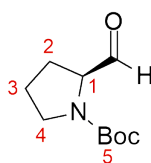


To a stirred suspension of 4-(*N*-benzylidene)-[2.2]paracyclophane-13-carboxylic acid (7 mg, 0.02 mmol, 1.0 eq.) in dry MeOH (0.5 mL, 0.05 M) at 60 °C was added H_3BO_3 (1.3 mg, 0.02 mmol, 1.1 eq.). $NaBH_4$ was added in small portions until bubbling upon addition ceased. Water (1 mL) was added and the mixture was extracted with CH_2Cl_2 (3 x 1 mL). Combined organics were dried ($MgSO_4$) and the solvent evaporated under reduced pressure affording 4-(*N*-benzylamino)-[2.2]paracyclophane-13-carboxylic acid as an off-white solid. (5 mg, 0.01 mmol, 70%). MP 160 °C (decomposes). R_f (4:1 hexane:EtOAc) 0.10. 1H NMR (500 MHz, $CDCl_3$): δ 7.36 (1H, d, $J = 1.5$ Hz, H-20), 7.32 (2H, d, $J = 7.4$ Hz, H-19), 7.20 (2H, t, $J = 7.4$ Hz, H-18), 7.18-7.13 (1H, m, Hz, H-12) 6.81 (1H, d, $J = 7.7, 1.4$ Hz, H-16), 6.47 (1H, d, $J = 7.7$ Hz, H-15), 6.40 (1H, d, $J = 7.6$ Hz, H-7), 6.23 (1H, dd, $J = 7.6, 1.5$ Hz, H-8), 5.42 (1H, s, H-5), 4.38 (1H, ddd, $J = 13.8, 9.4, 5.3$ Hz, H-1_a), 4.22 (1H, d, $J = 13.1$ Hz, H-17_a), 3.94 (1H, d, $J = 13.1$ Hz, H-17_b), 3.17-2.97 (6H, m), 2.80 (1H, ddd, $J = 14.1, 10.7, 5.4$ Hz, H-2_b). ^{13}C NMR (125 MHz, $CDCl_3$): δ 172.3 (C=O), 147.2 (C), 142.7 (C), 141.0 (C), 139.0 (C), 138.7 (CH), 136.3 (CH), 135.7 (C), 134.5 (C), 133.9 (C), 128.6 (2 CH), 127.2 (2 CH),

126.0 (CH), 124.3 (2 CH), 120.9 (CH), 116.0 (CH), 48.1 (CH₂), 35.0 (CH₂), 34.8 (CH₂), 31.2 (CH₂), 29.7 (CH₂).

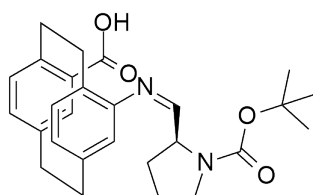
(S)-N-(*tert*-butoxycarbonyl)prolinal 3.46

Prepared according to literature procedure.^{281,282}



To a stirred solution of (COCl)₂ (0.10 mL, 1.19 mmol, 1.2 eq.) in CH₂Cl₂ (2.6 mL, 0.4 M) at -40 °C was added dropwise over 10 minutes a solution of DMSO (0.16 mL, 2.19 mmol, 2.2 eq.) in CH₂Cl₂ (0.6 mL, 4 M). This mixture was stirred for a further 10 minutes, then (*S*)-N-(*tert*-butoxycarbonyl)prolinol (0.20 g, 1.0 mmol, 1.0 eq.) in CH₂Cl₂ (10 mL, 0.1 M) was added dropwise over 10 minutes. The reaction mixture was stirred for 30 minutes, maintaining the temperature of the reaction vessel below -40 °C. DIPEA (0.69 mL, 3.97 mmol, 4.0 eq.) was added and the reaction mixture was stirred for a further 30 minutes. The mixture was washed successively with 2 M HCl (2 x 10 mL), water (2 x 10 mL), and brine (1 x 10 mL), then dried (MgSO₄) and the solvent removed under reduced pressure. The resulting residue was separated by column chromatography and elution with hexane:EtOAc 2:1 to afford (*S*)-N-(*tert*-butoxycarbonyl)prolinal as an off-white oil (130 mg, 0.65 mmol, 65%). IR (KBr) cm⁻¹ 2975 (C-H), 1732 (C=O), 1691 (C=O). ¹H NMR (500 MHz, CDCl₃, mixture of rotamers) δ 9.58 and 9.48 (1H, s, CHO), 4.23 and 4.07 (1H, ddd, *J* = 8.4, 6.0, 2.6 Hz, H-1), 3.55-3.40 (2H, m, H-4) 2.20-1.81 (4H, m, H-2, H-3), 1.49 and 1.45 (9H, s, H-5). Data comparable to that reported in the literature.²⁸³

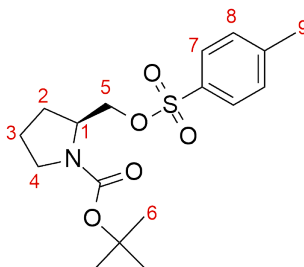
Imine 5.12



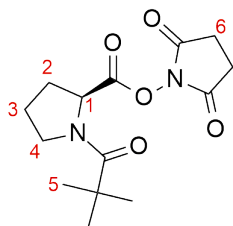
To a stirred solution of 4-amino-[2.2]paracyclophane-13-carboxylic acid (30 mg, 0.11 mmol, 1.0 eq.) in dry EtOH (1.1 mL, 0.1 M) at 60 °C was added Boc-L-prolinal (45 mg, 0.22 mmol, 2.0 eq.). The mixture was stirred for three hours at 60 °C then the solvent was removed under reduced pressure affording the imine **5.12** as a yellow-brown oily solid. R_f (7:1 hexane:EtOAc) 0.74. The material was of insufficient quality for full characterisation.

tert*-Butyl (2*S*)-2-[(*p*-toluenesulfonyloxy)methyl]pyrrolidine-1-carboxylate **3.50*

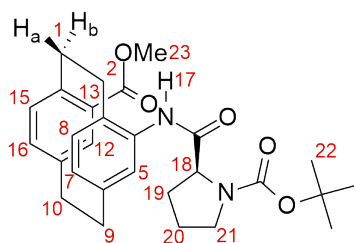
Prepared according to literature procedure.²⁸⁴



To a solution of (*S*)-1-Boc-2-pyrrolidinemethanol (0.20 g, 1.0 mmol, 1.0 eq) in pyridine (0.6 mL) and CH₂Cl₂ (1.9 mL) at 0 °C was added *p*-toluenesulfonyl chloride (0.24 g, 1.24 mmol, 1.25 eq) and the mixture was stirred for 24 hours at room temperature. The mixture was diluted with 3 mL CH₂Cl₂ and washed successively with 5 mL each of water, 1 M HCl, sat. aq. NaHCO₃, and brine, then dried (MgSO₄) and concentrated under reduced pressure affording the crude product as a colourless oil. The crude product was purified by flash column chromatography through silica eluting with 4:1 hexane:EtOAc affording the product as a colourless oil (0.18 g, 0.51 mmol, 51%). ¹H NMR (500 MHz, CDCl₃): δ 7.80 (2H, d, J = 8.2 Hz, H-7), 7.37 (2H, m, H-8), 4.11 (1H, dd, J = 9.0, 2.8 Hz, H-1), 3.99-3.92 (2H, m, H-5), 3.36-3.31 (2H, m, H-4), 2.47 (3H, s, H-9), 1.94-1.81 (4H, m, H-2, H-3), 1.43 and 1.39 (9H, two s without baseline separation, H-6). Data comparable to that reported in the literature.²⁷⁹

Boc-L-proline, *N*-hydroxysuccinimide ester 3.38

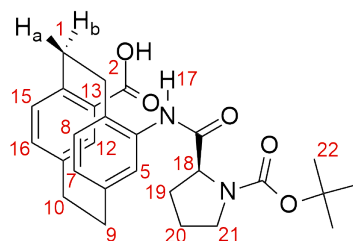
To a stirred solution of Boc-L-proline (0.38 g, 1.74 mmol, 1.0 eq.) and *N*-hydroxysuccinimide (0.20 g, 1.74 mmol, 1.0 eq.) in CH₂Cl₂ (17 mL, 0.1 M) under inert atmosphere at 0 °C was added DCC (0.36 g, 1.74 mmol, 1.0 eq.). The mixture was stirred, coming to room temperature, overnight. The mixture was filtered to remove the white precipitate and the filtrate was concentrated to a volume of 5 mL under reduced pressure. The filtrate was cooled to 4 °C for three hours. The resulting white precipitate was again removed by filtration. The filtrate was evaporated to dryness under reduced pressure affording Boc-L-proline *N*-hydroxysuccinimide ester as a white powder (0.36 g, 1.15 mmol, 66%). MP 134-136 °C. ¹H NMR (500 MHz, DMSO-*d*₆): δ 4.58 (1H, dd, *J* = 8.9, 3.6 Hz, H-1), 3.43-3.37 (1H, m, H-4_a), 3.36-3.34 (1H, m, H-4_b), 2.83-2.77 (4H, m, H-6), 2.45-2.37 (1H, m, H-2_a), 2.09-2.04 (1H, m, H-2_b), 1.95-1.84 (2H, m, H-3), 1.40 (9H, two s without baseline separation, H-6).

Boc-Pro-Pca-OMe 3.54

A stirred solution of 4-amino[2.2]paracyclophane (85 mg, 0.30 mmol, 1.0 eq.) and Boc-L-proline *N*-hydroxysuccinimide ester (104 mg, 0.33 mmol, 1.1 eq.) in CH₂Cl₂ (12 mL, 0.025 M) under inert atmosphere was heated at reflux for 3 days. The solvent was removed under reduced pressure. The residue was purified by column chromatography and elution with a gradient of hexane:EtOAc 10:1 to 3:1 affording the Boc-Pro-Pca-OMe as a pale yellow oily solid (87 mg, 0.18 mmol, 60%). *R*_f (2:1

hexane:EtOAc) 0.37. ^1H NMR (500 MHz, CDCl_3): δ 7.31-7.29 (1H, m, H-12), 7.23 (1H, d, $J = 1.9$ Hz, H-5), 6.71 (1H, dd, $J = 7.7, 1.9$ Hz, H-16), 6.45 (1H, d, $J = 7.7$ Hz, H-15), 6.39 (1H, d, $J = 7.7$ Hz, H-8), 6.23 (1H, dd, $J = 7.7, 1.6$ Hz, H-7), 4.51-4.36 (2H, m, H-21) 4.27 (1H, ddd, $J = 13.5, 9.8, 5.1$ Hz, H-1_b), 3.91 (3H, s, H-23), 3.22 (2H, ddd, $J = 13.7, 10.2, 3.2$ Hz, H-1_a, H-2_b), 3.08-2.98 (5H, m, H-9, H-10, H-18), 2.95 (2H, dd, $J = 7.9, 6.4$ Hz, H-19), 2.83 (2H, ddd, $J = 14.0, 10.7, 5.1$ Hz, H-2_a), 1.52 (9H, s, H-22), 1.28 (2H, dd, $J = 8.2, 6.6$ Hz, H-20). ^{13}C NMR (125 MHz, CDCl_3): δ 169.4 (C=O), 164.5 (C=O), 163.5 (C=O), 141.8 (C), 140.7 (C), 138.9 (C), 136.2 (CH), 136.0 (C), 135.5 (CH), 134.9 (CH), 133.6 (CH), 127.6 (C), 125.4 (C), 123.6 (CH), 121.7 (CH), 80.6 (C), 60.4 (CH), 51.8 (CH_3), 47.0 (CH_2), 34.8 (CH_2), 34.7 (CH_2), 34.7 (CH_2), 32.1 (CH_2), 31.7 (CH_2), 31.5 (CH_2), 28.5 (3 CH_3). HRMS (ESI) found: $[\text{M} + \text{H}]^+$ 479.2537. $\text{C}_{28}\text{H}_{35}\text{N}_2\text{O}_5$ requires $[\text{M} + \text{H}]^+$ 479.2540.

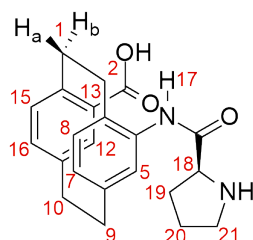
Boc-Pro-Pca 3.57



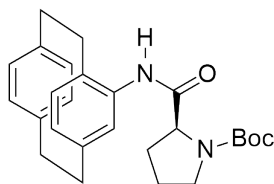
Boc-Pro-Pca-OMe (0.13 g, 0.27 mmol, 1.0 eq.) was dissolved in EtOH (2.5 mL, 0.1 M) then ground KOH (0.61 g, 10.8 mmol, 40 eq.) was added and the solution was stirred overnight at room temperature. The mixture was neutralised with 2 M HCl (approx. 3 mL). The aqueous layer was extracted with EtOAc (3 x 5 mL). The combined organics were dried (MgSO_4), and the solvent was removed under reduced pressure. The residue was purified by column chromatography and elution with 19:1 $\text{CH}_2\text{Cl}_2/\text{MeOH}$ affording the product as an oily yellow solid (70 mg, 0.15 mmol, 55%). R_f (19:1 $\text{CH}_2\text{Cl}_2/\text{MeOH}$) 0.23. ^1H NMR (500 MHz, $\text{DMSO}-d_6$): δ 8.81 and 8.40 (1H, s, H-17), 7.11 (1H, s, H-12), 6.91 and 6.76 (1H, s, H-5), 6.72-6.70 (1H, m, H-16), 6.58-6.51 (2H, m, H-15, H-8), 6.41 (1H, dd, $J = 7.7, 1.1$ Hz, H-7), 4.54-4.50 (1H, m, H-18), 4.39-4.35 (1H, m, H-2_b), 3.51-3.47 (1H, m, H-2_a), 3.08-3.06 (2H, m, H-21), 2.97-2.94 (5H, m, H-1_b, H-9, H-10), 2.81-2.77 (2H, m, H-19), 2.25-2.20 (1H, m, H-1_a), 1.92-1.82

(2H, m, H-20), 1.45 (9H, s, H-22). ^{13}C NMR (125 MHz, CDCl_3): δ 170.4 (C=O), 169.6 (C=O), 156.7 (C=O), 143.2 (C), 140.7 (C), 140.4 (C), 137.3 (C), 136.7 (CH), 136.4 (CH), 135.8 (CH), 134.6 (CH), 134.5 (C), 129.2 (CH), 127.8 (C), 125.5 (CH), 81.3 (C), 61.2 (CH), 47.3 (CH) 39.0 (CH), 34.6 (CH), 31.0 (CH), 30.9 (CH), 29.8 (CH), 28.7 (CH), 25.3 (3 CH_3), 24.5. As described above for other amide bond-containing compounds (e.g. for Boc-Pro-Gly-Pca), this compound exhibits peak broadening in the ^1H NMR spectrum that disguises certain J-couplings as well as twinned peaks for certain protons. HRMS (ESI) found: $[\text{M} + \text{H}]^+$ 463.2236. $\text{C}_{27}\text{H}_{31}\text{N}_2\text{O}_5$ requires $[\text{M} + \text{H}]^+$ 463.2227.

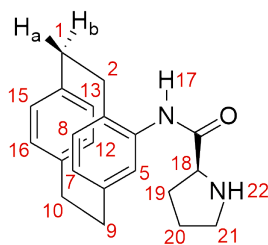
Pro-Pca 3.7



To a stirred solution of Boc-Pro-Pca (25 mg, 0.054 mmol, 1.0 eq.) in CH_2Cl_2 (0.75 mL) at 0 °C was added TFA (0.25 mL, 0.2 M total). The mixture was stirred at 0 °C for 90 minutes then the solvent was removed under reduced pressure affording Pro-Pca as an oily yellow solid (18 mg, 0.049 mmol, 91%). R_f (19:1 $\text{CH}_2\text{Cl}_2/\text{MeOH}$) 0.13. ^1H NMR (500 MHz, $\text{DMSO}-d_6$): δ 9.44 (1H, s, br, NH), 9.33 (1H, s, OH), 8.61 (1H, s, br, H-17), 7.13 (1H, d, $J = 1.4$ Hz, H-12), 7.06 (1H, d, $J = 1.1$ Hz, H-5), 6.77 (1H, dd, $J = 7.6, 1.3$ Hz, H-16), 6.62 (1H, d, $J = 4.2$ Hz, H-15), 6.60 (1H, d, $J = 4.3$ Hz, H-8), 6.44 (1H, dd, $J = 7.7, 1.1$ Hz, H-7), 4.41-4.36 (1H, m, H-18), 4.10 (1H, ddd, $J = 12.4, 9.4, 2.9$ Hz, H-2_b), 3.48-3.43 (1H, m, H-1_b), 3.31-3.26 (2H, m, H-21), 3.15-3.10 (1H, m, H-2_a), 2.99-2.83 (5H, m, H-1_a, H-9, H-10), 2.47-2.40 (1H, m, H-19_a), 2.19 (1H, sextet, $J = 7.1$ Hz, H-19_b), 2.03 (1H, sextet, $J = 6.4$ Hz, H-20_a), 1.99-1.92 (1H, m, H-20_b). ^{13}C NMR (125 MHz, $\text{DMSO}-d_6$): δ 168.4 (C=O), 166.6 (C=O), 142.6 (C), 140.3 (C), 139.3 (C), 137.1 (C), 136.7 (CH), 136.4 (CH), 135.3 (CH), 134.6 (CH), 130.2 (CH), 129.6 (C), 128.9 (C), 124.7 (CH), 60.2 (CH), 46.2 (CH_2), 34.9 (CH_2), 34.7 (CH_2), 33.9 (CH_2), 31.7 (CH_2), 29.5 (CH_2), 24.2 (CH_2). HRMS (ESI) found: $[\text{M} + \text{H}]^+$ 365.1852. $\text{C}_{22}\text{H}_{25}\text{N}_2\text{O}_3$ requires $[\text{M} + \text{H}]^+$ 365.1860.

4-*N*-Boc-Pro-amino[2.2]paracyclophane 3.53

A stirred solution of 4-amino[2.2]paracyclophane (0.27 g, 1.21 mmol, 1.0 eq.) and Boc-L-proline *N*-hydroxysuccinimide ester (0.42 g, 1.33 mmol, 1.1 eq.) in CH₂Cl₂ (48 mL, 0.025 M) was heated at reflux for 3 days under inert atmosphere. The solvent was removed under reduced pressure. The residue was purified by column chromatography and elution with CH₂Cl₂ affording the 4-*N*-Boc-Pro-amino[2.2]paracyclophane as a pale yellow solid (0.39 g, 0.93 mmol, 70%). *R*_f (19:1 CH₂Cl₂/MeOH) 0.77. MS (ESI) found: [M + H]⁺ 419.21. C₂₆H₃₃N₂O₃ requires [M + H]⁺ 419.26. Further data was not available as the NMR spectra are too complicated to interpret. The material's identity is confirmed by the characterisation of the following compound.

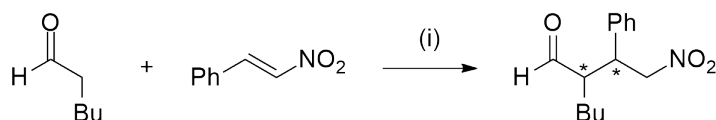
4-*N*-Pro-amino[2.2]paracyclophane 3.61

To a stirred solution of 4-*N*-Boc-Pro-amino[2.2]paracyclophane (0.244 g, 0.58 mmol, 1.0 eq.) in CH₂Cl₂ (4.35 mL) at 0 °C was added TFA (1.45 mL, 0.2 M total). The mixture was stirred at 0 °C for two hours then the solvent removed under reduced pressure. The residue was purified by flash column eluting 19:1 CH₂Cl₂/MeOH affording 4-*N*-Pro-amino[2.2]paracyclophane as an oily yellow solid (0.13 g, 0.41 mmol, 70%). *R*_f (19:1 CH₂Cl₂/MeOH) 0.17. ¹H NMR (500 MHz, DMSO-*d*₆): δ 9.93 and 9.83 (1H, s, H-17), 6.85-6.84 (1H, m, H-8), 6.69 and 6.66 (1H, dd, *J* = 7.8, 1.6 Hz, H-7), 6.53 and 6.52 (1H, d, *J* = 2.2 Hz, H-5), 6.45-6.38 (4H, m, H-12, H-13, H-15, H-16), 4.06-4.03 (1H, m, H-18), 3.92 (1h, ddd, *J* = 14.7, 8.9, 5.7 Hz, H-2_b), 3.37-3.28 (3H, m,

H-21, H-20_a), 3.15-3.09 (1H, m, H-20_b), 2.99-2.98 (2H, m, H-9), 2.92-2.83 (2H, m, H-10), 2.77-2.74 (1H, m, H-2_a), 2.24-2.12 (1H, m, H-19_a), 1.87-1.77 (3H, m, H-1, H-19_b). As described above for other amide bond-containing compounds (e.g. for Boc-Pro-Gly-Pca), this compound exhibits peak broadening in the ¹H NMR spectrum that disguises certain *J*-couplings as well as twinned peaks for certain protons. Twinned peaks are also present in the ¹³C NMR spectrum. ¹³C NMR (125 MHz, DMSO-*d*₆): δ 174.87 and 174.48 (C=O), 153.96 and 153.59 (C), 140.81 and 140.79 (C), 139.31 and 139.24 (C), 139.11 and 138.99 (C), 135.37 and 135.32 (CH), 133.56 and 133.53 (CH), 133.43 and 133.40 (CH), 132.35 and 132.31 (CH), 130.55 and 130.49 (CH), 128.71 and 128.65 (C), 128.49 and 128.45 (CH), 126.30 and 126.24 (CH), 70.25 (CH), 61.05 and 60.90 (CH₂), 47.08 and 47.02 (CH₂), 35.17 and 34.98 (CH₂), 33.71 and 33.53 (CH₂), 29.87 (CH₂), 25.96 (CH₂), 24.33 (CH₂). MS (ESI) found: [M + H]⁺ 321.24. C₂₁H₂₅N₂O requires [M + H]⁺ 321.20.

5.2.5 Michael addition

Protocol for Michael reaction of *trans*-β-nitrostyrene and hexanal

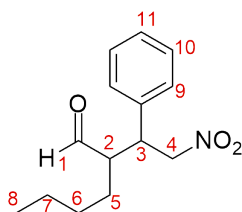


A stock solution was prepared with *trans*-β-nitrostyrene (0.746 g, 5.0 mmol, 1.0 eq) and NMM (0.051 g, 0.50 mmol, 0.1 eq) in 9:1 CH₃Cl/*i*-PrOH (10 mL, 0.5 M). In a typical experiment, 0.2 mL stock solution was added to a 1.5 mL vial, along with 1.5 eq. hexanal (18 μL, 0.15 mmol) and 28 μL of a solution of the chosen catalyst (0.37 M, 0.05 eq, 5 μM) in DMSO. The mixture was allowed to stand at room temperature for 48 hours, then at 60 °C for 48 hours. The reaction mixture was quenched by the addition of 0.2 mL water. The layers were separated, and the aqueous layer was extracted twice with EtOAc. Combined organics were dried (MgSO₄) and the solvent was removed under reduced pressure. The crude product was analysed without further purification.

For HPLC analysis, 2 mg of the residue was dissolved in 1 mL of 4:1 hexane/*i*-PrOH in a 1.5 mL glass vial with screw-lid cap fitted with a rubber septum. HPLC was

performed on an OD-H 25 cm column eluting 4:1 hexane/*i*-PrOH at 1 mL/min at 25 °C for 30 minutes.

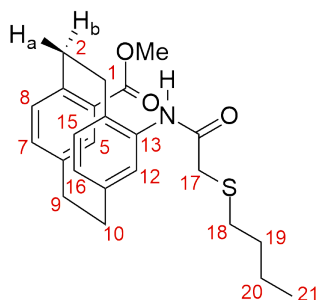
5.2.6 2-Butyl-4-nitro-3-phenylbutanal 5.13



This compound was prepared according to the general procedure described above. The residue was separated by column chromatography and elution with 9:1 hexane:EtOAc affording the (2*S*,3*R*)-2-butyl-4-nitro-3-phenylbutanal as an oily yellow solid. R_f (7:1 hexane:EtOAc) 0.35. ^1H NMR (500 MHz, CDCl_3): δ 9.72 (1H, d, J = 2.8 Hz, H-1), 7.38-7.29 (3H, m, H-9, H-11), 7.20-7.19 (2H, m, H-10), 4.73 (1H, dd, J = 12.8, 5.1 Hz, H-4), 4.66 (1H, dd, J = 12.8, 9.7 Hz, H-3), 3.80 (1H, ddd, J = 9.7, 9.7, 4.9 Hz, H-2), 2.72 (1H, tdd, J = 3.5, 9.4, 3.1 Hz, H-5), 1.35-1.11 (4H, m, H-6, H-7), 0.80 (3H, dt, J = 7.0 Hz, H-8). ^{13}C NMR (125 MHz, CDCl_3): δ 203.39 (C=O), 136.84 (C), 129.10 (2 CH), 128.24 (2 CH), 128.13 (CH), 78.45 (CH_2), 53.88 (CH), 43.12 (CH), 28.51 (CH_2), 25.25 (CH_2), 22.48 (CH_2), 13.63 (CH_3). HRMS (ESI) found: $[\text{M} - \text{H}]^-$ 248.1423. $\text{C}_{14}\text{H}_{18}\text{NO}_3$ requires $[\text{M} - \text{H}]^-$ 248.1287.

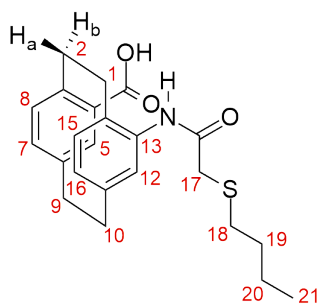
The diastereomeric ratio was determined by ^1H NMR. δ 9.72 (*syn*), 9.49 (*anti*) (CHO). The enantiomeric ratio was determined by HPLC with an OD-H column eluting 4:1 hexane/*i*-PrOH at 25 °C at 1 ml/min, UV detection at 254 nm. R_t (*syn*, major) = 10.8 min, (*syn*, minor) 13.2 min. Data comparable to that reported in the literature.^{221,285}

Sulfide 4.9, methyl ester



To a stirred solution of methyl 4-[(3-bromo-1-oxoethyl)amino][2.2]paracyclophane-13-carboxylate (0.19 g, 0.46 mmol, 1.0 eq.) in DMF (1.5 mL, 0.3 M) under inert atmosphere was added K_2CO_3 (0.13 g, 2.0 eq.) and BuSH (60 μ L, 0.55 mmol, 1.2 eq.), and the mixture was stirred at 60 °C overnight. The mixture was allowed to cool to room temperature then EtOAc (25 mL) was added. The organic layer was washed successively with water (2 x 25 mL), brine (25 mL), and sat. aq. Na_2CO_3 , then dried ($MgSO_4$) and the solvent removed under reduced pressure. The resulting residue was separated by column chromatography eluting a gradient of hexane:EtOAc 4:1 to 1:1 to afford the sulfide **4.9** as a pale yellow solid (0.10 mg, 0.24 mmol, 48%). R_f (4:1 hexane:EtOAc) 0.14. 1H NMR (500 MHz, $CDCl_3$): δ 8.59 (1H, s, NH), 7.23 (1H, d, $J = 1.5$ Hz, H-5), 6.81 (1H, s, H-12), 6.70 (1H, dd, $J = 7.6, 1.3$ Hz, H-7), 6.58 (1H, d, $J = 7.8$ Hz, H-8), 6.54 (1H, d, $J = 7.8$ Hz, H-15), 6.46 (1H, dd, $J = 7.8, 1.3$ Hz, H-16), 4.16 (1H, ddd, $J = 13.3, 9.7, 3.8$ Hz, H-2_b), 3.88 (3H, s, CH_3), 3.68 (2H, s, H-17), 3.16-2.90 (7H, m, H-1, H-2_a, H-9, H-10), 2.67-2.61 (2H, m, H-18), 1.67-1.60 (2H, m, H-19), 1.48-1.40 (2H, m, H-20), 0.93 (3H, $J = 7.4$ Hz, H-21). HRMS (ESI) found: $[M+H]^+$ 412.1898. $C_{24}H_{30}NO_3S$ requires $[M+H]^+$ 412.1941. Material was of insufficient quality for further characterisation.

Sulfide 4.10



To a stirred solution of sulfide **4.9** (0.17 g, 0.41 mmol, 1.0 eq.) in EtOH (2 mL, 0.2 M) was added ground KOH (0.22 g, 8.6 mmol, 20 eq) and the solution was stirred overnight at room temperature. The mixture was neutralised with 2 M HCl (approx. 3 mL). The aqueous layer was extracted with EtOAc (3 x 5 mL). The combined organics were washed with brine (15 mL), then dried ($MgSO_4$) and the solvent removed under reduced pressure affording the sulfide **4.10** as a yellow solid (0.13 g,

0.33 mmol, 80%). R_f (19:1 $\text{CH}_2\text{Cl}_2/\text{MeOH}$) 0.42. ^1H NMR (500 MHz, CDCl_3): δ 8.82 (1H, s, NH), 7.38 (1H, d, $J = 1.2$ Hz, H-5), 6.90 (1H, s, H-12), 6.77 (1H, dd, $J = 7.8, 1.4$ Hz, H-7), 6.60 (1H, d, $J = 7.7$ Hz, H-8), 6.58 (1H, d, $J = 8.0$ Hz, H-15), 6.49 (1H, dd, $J = 7.8, 1.1$ Hz, H-16), 4.32 (1H, ddd, $J = 13.0, 9.8, 3.3$ Hz, H-2_b), 3.18-2.98 (2H, m, H-17), 3.20-3.02 (6H, m, H-1, H-9, H-10), 2.76-2.72 (2H, m, H-18), 2.57 (1H, t, $J = 7.4$ Hz, H-2_a), 1.57 (2H, quint., $J = 7.4$ Hz, H-19), 1.38 (2H, sextet, 7.4 Hz, H-20), 0.89 (3H, t, $J = 7.3$ Hz, H-21). HRMS (ESI) found: $[\text{M} + \text{H}]^+$ 398.1782. $\text{C}_{23}\text{H}_{28}\text{NO}_3\text{S}$ requires $[\text{M} + \text{H}]^+$ 398.1785. Material was of insufficient quality for further characterisation.

Bibliography

- (1) Xie, F.; Deng, X.; Kratzer, D.; Cheng, K. C. K.; Friedmann, C.; Qi, S.; Solorio, L.; Lahann, J. Backbone-Degradable Polymers Prepared by Chemical Vapor Deposition. *Angewandte Chemie International Edition* **2017**, *56*, 203–207.
- (2) Morisaki, Y.; Gon, M.; Chujo, Y. Conjugated microporous polymers consisting of tetrasubstituted [2.2]Paracyclophane junctions. *Journal of Polymer Science Part A: Polymer Chemistry* **2013**, *51*, 2311–2316.
- (3) Elacqua, E.; Friščić, T.; MacGillivray, L. R. [2.2]Paracyclophane as a Target of the Organic Solid State: Emergent Properties via Supramolecular Construction. *Israel Journal of Chemistry* **2012**, *52*, 53–59.
- (4) Hasegawa, M.; Kobayakawa, K.; Matsuzawa, H.; Nishinaga, T.; Hirose, T.; Sako, K.; Mazaki, Y. Macrocyclic Oligothiophene with Stereogenic [2.2]Paracyclophane Scaffolds: Chiroptical Properties from π -Transannular Interactions. *Chemistry – A European Journal* **2017**, *23*, 3267–3271.
- (5) Salhi, F.; Collard, D. π -Stacked Conjugated Polymers: The Influence of Paracyclophane π -Stacks on the Redox and Optical Properties of a New Class of Broken Conjugated Polythiophenes. *Advanced Materials* **2003**, *15*, 81–85.
- (6) Morisaki, Y.; Ishida, T.; Chujo, Y. Synthesis and Properties of Novel Through-Space π -Conjugated Polymers Based on Poly(p-phenylenevinylene)s Having a [2.2]Paracyclophane Skeleton in the Main Chain. *Macromolecules* **2002**, *35*, 7872–7877.
- (7) Hassan, Z.; Spuling, E.; Knoll, D. M.; Lahann, J.; Bräse, S. Planar chiral [2.2]-paracyclophanes: from synthetic curiosity to applications in asymmetric synthesis and materials. *Chemical Society Reviews* **2018**, *47*, 6947–6963.

- (8) Wang, Y.; Zhao, C.-Y.; Wang, Y.-P.; Zheng, W.-H. Enantioselective Intramolecular Dearomative Lactonization of Naphthols Catalyzed by Planar Chiral Iodoarene. *Synthesis* **2019**, *51*, 3675–3682.
- (9) Xie, E.; Huang, S.; Lin, X. Design of Planar Chiral Phosphoric Acids with a [2.2]Paracyclophanyl Backbone as Organocatalysts for the Highly Enantioselective Aza-Friedel–Crafts Reaction. *Organic Letters* **2019**, *21*, 3682–3686.
- (10) Hopf, H. [2.2]Paracyclophanes in Polymer Chemistry and Materials Science. *Angewandte Chemie International Edition* **2008**, *47*, 9808–9812.
- (11) Veselá, D.; Marek, R.; Ubik, K.; Lunerová, K.; Sklenář, V.; Suchý, V. Draco-phane, a metacyclophane derivative from the resin of *Dracaena cinnabari* Balf. *Phytochemistry* **2002**, *61*, 967–970.
- (12) Cram, D. J.; Cram, J. M. Cyclophane chemistry: bent and battered benzene rings. *Accounts of Chemical Research* **1971**, *4*, 204–213.
- (13) Brown, C. J.; Farthing, A. C. Preparation and Structure of Di-p-Xylylene. *Nature* **1949**, *164*, 915–916.
- (14) Dodziuk, H.; Szymanski, S.; Jazwinski, J.; Ostrowski, M.; Demissie, T. B.; Ruud, K.; Kus, P.; Hopf, H.; Lin, S.-T. Structure and NMR spectra of some [2.2] paracyclophanes. The dilemma of [2.2] paracyclophane symmetry. *Journal of Physical Chemistry A* **2011**, *115*, 10638–10649.
- (15) Dyson, P. J.; Humphrey, D. G.; McGrady, J. E.; Mingos, D. M. P.; Wilson, D. J. Comparison of the reactivity of [2.2]paracyclophane and p-xylene. *Journal of the Chemical Society, Dalton Transactions* **1995**, 4039–4043.
- (16) Hassan, Z.; Spuling, E.; Knoll, D. M.; Bräse, S. Regioselective Functionalization of [2.2]Paracyclophanes: Recent Synthetic Progress and Perspectives. *Angewandte Chemie International Edition* **2020**, *59*, 2156–2170.
- (17) Reich, H. J.; Cram, D. J. Macro rings. XXXV. Transannular directive influences in electrophilic substitution of monosubstituted [2.2] paracyclophanes. *Journal of the American Chemical Society* **1969**, *91*, 3505–3516.
- (18) Mourad, A.-f. E.; Hassan, A. E.-D. A.; Dannheim, J. Molecular Complexes of Cyclophanes. XV. Charge-Transfer Complexes of Sterically Hindered [2.2]-metapara- and [2.2]paracyclophanes with π -Acceptors. *Bulletin of the Chemical Society of Japan* **1989**, *62*, 1379–1381.

- (19) Van Lindert, H. C.; Koeberg-Telder, A.; Cerfontain, H. Sulfonation of [2.2]paracyclophane; structures and modes of formation of the products. *Recueil des Travaux Chimiques des Pays-Bas* **1992**, *111*, 379–388.
- (20) Jayasundera, K. P.; Kusmus, D. N. M.; Deuilhé, L.; Etheridge, L.; Farrow, Z.; Lun, D. J.; Kaur, G.; Rowlands, G. J. The synthesis of substituted amino[2.2]-paracyclophanes. *Organic & Biomolecular Chemistry* **2016**, *14*, 10848–10860.
- (21) Wang, X.; Chen, Z.; Duan, W.; Song, C.; Ma, Y. Synthesis of [2.2]paracyclophane-based bidentate oxazoline–carbene ligands for the asymmetric 1,2-silylation of N-tosylaldimines. *Tetrahedron: Asymmetry* **2017**, *28*, 783–790.
- (22) Pye, P. J.; Rossen, K.; Reamer, R. A.; Tsou, N. N.; Volante, R. P.; Reider, P. J. A New Planar Chiral Bisphosphine Ligand for Asymmetric Catalysis: Highly Enantioselective Hydrogenations under Mild Conditions. *Journal of the American Chemical Society* **1997**, *119*, 6207–6208.
- (23) Rowlands, G. J. Planar Chiral Phosphines Derived from [2.2]Paracyclophane. *Israel Journal of Chemistry* **2012**, *52*, 60–75.
- (24) Cram, D. J.; Steinberg, H. Macro Rings. I. Preparation and Spectra of the Paracyclophanes. *Journal of the American Chemical Society* **1951**, *73*, 5691–5704.
- (25) Winberg, H. E.; Fawcett, F. S.; Mochel, W. E.; Theobald, C. W. Dimethylenedihydroheteroaromatic Compounds and Heterocyclophanes by 1,6-Hofmann Elimination Reactions. *Journal of the American Chemical Society* **1960**, *82*, 1428–1435.
- (26) Boekelheide, V.; Reingold, I. D.; Tuttle, M. Syntheses of cyclophanes by photochemical extrusion of sulphur. *Journal of the Chemical Society, Chemical Communications* **1973**, 406–407.
- (27) Chow, H.-F.; Low, K.-H.; Wong, K. Y. An Improved Method for the Regiospecific Synthesis of Polysubstituted [2.2]Paracyclophanes. *Synlett* **2005**, *2005*, 2130–2134.
- (28) Chen, H.-Y.; Lahann, J. Designable Biointerfaces Using Vapor-Based Reactive Polymers. *Langmuir* **2011**, *27*, 34–48.
- (29) IUPAC, *Compendium of Chemical Terminology (the "Gold Book")*. 2nd ed.; Blackwell Scientific Publications: Oxford, 1997; Vol. 2019.

- (30) Plevová, K.; Mudráková, B.; Rakovský, E.; Šebesta, R. Diastereoselective Pd-Catalyzed C–H Arylation of Ferrocenylmethanamines with Arylboronic Acids or Pinacol Esters. *Journal of Organic Chemistry* **2019**, *84*, 7312–7319.
- (31) Gibson, S. E.; Knight, J. D. [2.2]Paracyclophane derivatives in asymmetric catalysis. *Organic & Biomolecular Chemistry* **2003**, *1*, 1256–1269.
- (32) Astruc, D. Why is Ferrocene so Exceptional? *European Journal of Inorganic Chemistry* **2017**, 6–29.
- (33) Yoshida, K.; Yasue, R. Planar-Chiral Ferrocene-Based N-Heterocyclic Carbene Ligands. *Chemistry – A European Journal* **2018**, *24*, 18575–18586.
- (34) Bolm, C.; Wenz, K.; Raabe, G. Regioselective palladation of 2-oxazoliny[2.2]-paracyclophanes.: Synthesis of planar-chiral phosphines. *Journal of Organometallic Chemistry* **2002**, *662*, 23–33.
- (35) Kreis, M.; Nieger, M.; Bräse, S. Synthesis of novel planar-chiral [2.2]paracyclophane derivatives as potential ligands for asymmetric catalysis. *Journal of Organometallic Chemistry* **2006**, *691*, 2171–2181.
- (36) Dahmen, S.; Bräse, S. Planar and central chiral [2.2]paracyclophane-based N,O-ligands as highly active catalysts in the diethylzinc addition to aldehydes. *Chemical Communications* **2002**, 26–27.
- (37) Wu, X.-W.; Hou, X.-L.; Dai, L.-X.; Tao, J.; Cao, B.-X.; Sun, J. Synthesis of novel N,O-planar chiral [2,2]paracyclophane ligands and their application as catalysts in the addition of diethylzinc to aldehydes. *Tetrahedron: Asymmetry* **2001**, *12*, 529–532.
- (38) Viozquez, S. F.; Banon-Caballero, A.; Guillena, G.; Najera, C.; Gomez-Bengoa, E. Enantioselective direct aldol reaction of [small alpha]-keto esters catalyzed by (Sa)-binam-d-prolinamide under quasi solvent-free conditions. *Organic & Biomolecular Chemistry* **2012**, *10*, 4029–4035.
- (39) Hayashi, T.; Ohno, A.; Lu, S.-j.; Matsumoto, Y.; Fukuyo, E.; Yanagi, K. Optically Active Ruthenocenylobis(phosphines): New Efficient Chiral Phosphine Ligands for Catalytic Asymmetric Reactions. *Journal of the American Chemical Society* **1994**, *116*, 4221–4226.

- (40) Jarvo, E. R.; Copeland, G. T.; Papaioannou, N.; Bonitatebus, P. J.; Miller, S. J. A Biomimetic Approach to Asymmetric Acyl Transfer Catalysis. *Journal of the American Chemical Society* **1999**, *121*, 11638–11643.
- (41) Katsuki, T.; Sharpless, K. B. The first practical method for asymmetric epoxidation. *Journal of the American Chemical Society* **1980**, *102*, 5974–5976.
- (42) Bellemin-Laponnaz, S.; Tweddell, J.; Ruble, J. C.; Breitling, F. M.; Fu, G. C. The kinetic resolution of allylic alcohols by a non-enzymatic acylation catalyst; application to natural product synthesis. *Chemical Communications* **2000**, 1009–1010.
- (43) Hrdina, R.; Müller, C. E.; Wende, R. C.; Wanka, L.; Schreiner, P. R. Enantiomerically enriched trans-diols from alkenes in one pot: a multicatalyst approach. *Chemical Communications* **2012**, *48*, 2498–2500.
- (44) Alachraf, M. W.; Wende, R. C.; Schuler, S. M. M.; Schreiner, P. R.; Schrader, W. Functionality, Effectiveness, and Mechanistic Evaluation of a Multicatalyst-Promoted Reaction Sequence by Electrospray Ionization Mass Spectrometry. *Chemistry – A European Journal* **2015**, *21*, 16203–16208.
- (45) Hoveyda, A. H.; Schrock, R. R. Catalytic Asymmetric Olefin Metathesis. *Chemistry – A European Journal* **2001**, *7*, 945–950.
- (46) Rossen, K.; Pye, P. J.; Maliakal, A.; Volante, R. P. Kinetic Resolution of rac-4,12-Dibromo[2.2]paracyclophane in a Palladium [2.2]PHANEPHOS Catalyzed Amination. *Journal of Organic Chemistry* **1997**, *62*, 6462–6463.
- (47) Rowlands, G. J. The synthesis of enantiomerically pure [2.2]paracyclophane derivatives. *Organic & Biomolecular Chemistry* **2008**, *6*, 1527–1534.
- (48) Pamperin, D.; Schulz, C.; Hopf, H.; Syldatk, C.; Pietzsch, M. Chemoenzymatic Synthesis of Optically Pure Planar Chiral (S)-(–)-5-Formyl-4-hydroxy-[2.2]paracyclophane. *European Journal of Organic Chemistry* **1998**, 1441–1445.
- (49) Pamperin, D.; Ohse, B.; Hopf, H.; Pietzsch, M. Synthesis of planar-chiral [2.2]-para-cyclophanes by biotransformations: screening for hydrolase activity for the kinetic resolution of 4-acetoxy-[2.2]paracyclophane. *Journal of Molecular Catalysis B: Enzymatic* **1998**, *5*, 317–319.
- (50) Cipiciani, A.; Fringuelli, F.; Mancini, V.; Piermatti, O.; Scappini, A. M.; Ruzzi-coni, R. Enzymatic kinetic resolution of (±)-4-acetoxy[2.2]paracyclophane by

- Candida cylindracea lipase. An efficient route for the preparation of (+)-R-4-hydroxy- and (+)-S-4-acetoxy[2.2]paracyclophane. *Tetrahedron* **1997**, *53*, 11853–11858.
- (51) Friedmann, C. J.; Ay, S.; Bräse, S. Improved Synthesis of Enantiopure 4-Hydroxy[2.2]paracyclophane. *Journal of Organic Chemistry* **2010**, *75*, 4612–4614.
- (52) Masterson, D. S.; Shirley, C.; Glatzhofer, D. T. N-(4-[2.2]paracyclophanyl)-2'-hydroxyacetophenone imine: An effective paracyclophane Schiff-base ligand for use in catalytic asymmetric cyclopropanation reactions. *Journal of Molecular Catalysis A: Chemical* **2012**, *361-362*, 111–115.
- (53) Nozaki, H.; Moriuti, S.; Takaya, H.; Noyori, R. Asymmetric induction in carbonyl reaction by means of a dissymmetric copper chelate. *Tetrahedron Letters* **1966**, *7*, 5239–5244.
- (54) Dougherty, D. A. Unnatural amino acids as probes of protein structure and function. *Current Opinion in Chemical Biology* **2000**, *4*, 645–652.
- (55) Paul, P. K. C.; Sukumar, M.; Bardi, R.; Piazzesi, A. M.; Valle, G.; Toniolo, C.; Balaram, P. Stereochemically constrained peptides. Theoretical and experimental studies on the conformations of peptides containing 1-aminocyclohexanecarboxylic acid. *Journal of the American Chemical Society* **1986**, *108*, 6363–6370.
- (56) Tanda, K.; Eto, R.; Kato, K.; Oba, M.; Ueda, A.; Suemune, H.; Doi, M.; Demizu, Y.; Kurihara, M.; Tanaka, M. Peptide foldamers composed of six-membered ring α,α -disubstituted α -amino acids with two changeable chiral acetal moieties. *Tetrahedron* **2015**, *71*, 3909–3914.
- (57) Prasad, S.; Rao, R. B.; Balaram, P. Contrasting solution conformations of peptides containing α,α -dialkylated residues with linear and cyclic side chains. *Biopolymers* **1995**, *35*, 11–20.
- (58) Aboul-Enein, M. N.; El-Azzouny, A. A. S.; Saleh, O. A.; Amin, K. M.; Maklad, Y. A.; Hassan, R. M. Synthesis and Anticonvulsant Activity of Substituted-1,3-diazaspiro[4.5]decan-4-ones. *Archiv der Pharmazie* **2015**, *348*, 575–588.
- (59) Ishihara, K.; Hamamoto, H.; Matsugi, M.; Shioiri, T. SN2 displacement at the quaternary carbon center: a novel entry to the synthesis of α,α -disubstituted α -amino acids. *Tetrahedron Letters* **2015**, *56*, 3169–3171.

- (60) Drauz, K.; Grayson, I.; Kleemann, A.; Krimmer, H.; Leuchtenberger, W.; Weckbecker, C. In *Ullmann's Encyclopedia of Industrial Chemistry*, Ullmann, F., Ed.; Wiley: New York, 2007.
- (61) Erb, W.; Levanen, G.; Roisnel, T.; Dorcet, V. Application of the Curtius rearrangement to the synthesis of 1'-aminoferrocene-1-carboxylic acid derivatives. *New Journal of Chemistry* **2018**, *42*, 3808–3818.
- (62) Herrick, R. S.; Jarret, R. M.; Curran, T. P.; Dragoli, D. R.; Flaherty, M. B.; Lindyberg, S. E.; Slate, R. A.; Thornton, L. C. Ordered conformations in bis(amino acid) derivatives of 1,1'-ferrocenedicarboxylic acid. *Tetrahedron Letters* **1996**, *37*, 5289–5292.
- (63) Barišić, L.; Dropučić, M.; Rapić, V.; Pritzkow, H.; Kirin, S. I.; Metzler-Nolte, N. The first oligopeptide derivative of 1'-aminoferrocene-1-carboxylic acid shows helical chirality with antiparallel strands. *Chemical Communications* **2004**, 2004–2005.
- (64) Heinze, K.; Schlenker, M. Main Chain Ferrocenyl Amides from 1-Aminoferrocene-1'-carboxylic Acid. *European Journal of Inorganic Chemistry* **2004**, 2974–2988.
- (65) Butler, I. R.; Quayle, S. C. The synthesis and characterisation of heterosubstituted aminoferrocenes. *Journal of Organometallic Chemistry* **1998**, *552*, 63–68.
- (66) Okamura, T.-a.; Sakauye, K.; Ueyama, N.; Nakamura, A. An Amide-Linked Ferrocene Dimer: Formation of Inter- and Intramolecular NH...OC Hydrogen Bonds. *Inorganic Chemistry* **1998**, *37*, 6731–6736.
- (67) Bildstein, B.; Malaun, M.; Kopacka, H.; Wurst, K.; Mitterböck, M.; Ongania, K.-H.; Opromolla, G.; Zanello, P. N,N'-Diferrocenyl-N-heterocyclic Carbenes and Their Derivatives. *Organometallics* **1999**, *18*, 4325–4336.
- (68) Semenčić, M.; Siebler, D.; Heinze, K.; Rapić, V. Bis- and Trisamides Derived From 1'-Aminoferrocene-1-carboxylic Acid and α -Amino Acids: Synthesis and Conformational Analysis. *Organometallics* **2009**, *28*, 2028–2037.
- (69) Barišić, L.; Kovačević, M.; Mamić, M.; Kodrin, I.; Mihalić, Z.; Rapić, V. Synthesis and Conformational Analysis of Methyl N-Alanyl-1'-aminoferrocene-1-carboxylate. *European Journal of Inorganic Chemistry* **2012**, *2012*, 1810–1822.

- (70) Kovačević, M.; Molčanov, K.; Radošević, K.; Srček, V. G.; Roca, S.; Čače, A.; Barišić, L. Conjugates of 1'-Aminoferrocene-1-carboxylic Acid and Proline: Synthesis, Conformational Analysis and Biological Evaluation. *Molecules* **2014**, *19*, 12852–12880.
- (71) Khan, M. A. K.; Long, Y.-T.; Schatte, G.; Kraatz, H.-B. Surface Studies of Aminoferrocene Derivatives on Gold: Electrochemical Sensors for Chemical Warfare Agents. *Analytical Chemistry* **2007**, *79*, 2877–2884.
- (72) Siebler, D.; Förster, C.; Heinze, K. Molecular Multi-Wavelength Optical Anion Sensors. *European Journal of Inorganic Chemistry* **2010**, *2010*, 523–527.
- (73) Barišić, L.; Čakić, M.; Mahmoud, K. A.; Liu, Y.-n.; Kraatz, H.-B.; Pritzkow, H.; Kirin, S. I.; Metzler-Nolte, N.; Rapić, V. Helically Chiral Ferrocene Peptides Containing 1'-Aminoferrocene-1-Carboxylic Acid Subunits as Turn Inducers. *Chemistry – A European Journal* **2006**, *12*, 4965–4980.
- (74) Mahmoud, K. A.; Kraatz, H.-B. Synthesis and Electrochemical Investigation of Oligomeric and Polymeric Ferrocenyl-Amides having Cyclohexyl, Phenylene, and Lysyl Spacers. *Journal of Inorganic and Organometallic Polymers and Materials* **2008**, *18*, 69–80.
- (75) Heinze, K.; Siebler, D. Oligonuclear Amide-bridged Ferrocenes from N-Fmoc Protected 1-Amino-1'-fluorocarbonyl Ferrocene. *Zeitschrift für Anorganische und Allgemeine Chemie* **2007**, *633*, 2223–2233.
- (76) Barišić, L.; Rapić, V.; Metzler-Nolte, N. Incorporation of the Unnatural Organometallic Amino Acid 1'-Aminoferrocene-1-carboxylic Acid (Fca) into Oligopeptides by a Combination of Fmoc and Boc Solid-Phase Synthetic Methods. *European Journal of Inorganic Chemistry* **2006**, 4019–4021.
- (77) Heinze, K.; Wild, U.; Beckmann, M. Solid-Phase Synthesis of Chiral Modular Ferrocene-Based Peptides. *European Journal of Inorganic Chemistry* **2007**, 617–623.
- (78) El-Faham, A.; Albericio, F. Peptide Coupling Reagents, More than a Letter Soup. *Chemical Reviews* **2011**, *111*, 6557–6602.
- (79) Kovač, V.; Radolović, K.; Habuš, I.; Siebler, D.; Heinze, K.; Rapić, V. Conformational Analysis of β -Lactam-Containing Ferrocene Peptides. *European Journal of Inorganic Chemistry* **2009**, 389–399.

- (80) Förster, C.; Kovačević, M.; Barišić, L.; Rapić, V.; Heinze, K. Ferrocenyl-Labeled Sugar Amino Acids: Conformation and Properties. *Organometallics* **2012**, *31*, 3683–3694.
- (81) Siebler, D.; Linseis, M.; Gasi, T.; Carrella, L. M.; Winter, R. F.; Förster, C.; Heinze, K. Oligonuclear Ferrocene Amides: Mixed-Valent Peptides and Potential Redox-Switchable Foldamers. *Chemistry – A European Journal* **2011**, *17*, 4540–4551.
- (82) Mahmoud, K.; Long, Y.-T.; Schatte, G.; Kraatz, H.-B. Electronic communication through the ureylene bridge: spectroscopy, structure and electrochemistry of dimethyl 1',1'-ureylenedi(1-ferrocenecarboxylate). *Journal of Organometallic Chemistry* **2004**, *689*, 2250–2255.
- (83) Chowdhury, S.; Schatte, G.; Kraatz, H.-B. Rational Design of Bioorganometallic Foldamers: A Potential Model for Parallel β -Helical Peptides. *Angewandte Chemie International Edition* **2006**, *45*, 6882–6884.
- (84) Mahmoud, K. A.; Kraatz, H.-B. A Bioorganometallic Approach for the Electrochemical Detection of Proteins: A Study on the Interaction of Ferrocene-Peptide Conjugates with Papain in Solution and on Au Surfaces. *Chemistry – A European Journal* **2007**, *13*, 5885–5895.
- (85) Scholtissek, C.; Quack, G.; Klenk, H. D.; Webster, R. G. How to overcome resistance of influenza A viruses against adamantane derivatives. *Antiviral Research* **1998**, *37*, 83–95.
- (86) Weller, M.; Finiels-Marlier, F.; Paul, S. M. NMDA receptor-mediated glutamate toxicity of cultured cerebellar, cortical and mesencephalic neurons: neuroprotective properties of amantadine and memantine. *Brain Research* **1993**, *613*, 143–148.
- (87) Wanka, L.; Cabrele, C.; Vanejews, M.; Schreiner, P. R. γ -Aminoadamantane-carboxylic Acids Through Direct C–H Bond Amidations. *European Journal of Organic Chemistry* **2007**, *2007*, 1474–1490.
- (88) Miller, S. J. In Search of Peptide-Based Catalysts for Asymmetric Organic Synthesis. *Accounts of Chemical Research* **2004**, *37*, 601–610.
- (89) Formaggio, F.; Barazza, A.; Bertocco, A.; Toniolo, C.; Broxterman, Q. B.; Kaptein, B.; Brasola, E.; Pengo, P.; Pasquato, L.; Scrimin, P. Role of Secondary Structure

- in the Asymmetric Acylation Reaction Catalyzed by Peptides Based on Chiral C α -Tetrasubstituted α -Amino Acids. *Journal of Organic Chemistry* **2004**, *69*, 3849–3856.
- (90) Kapoerchan, V. V.; Knijnenburg, A. D.; Niamat, M.; Spalburg, E.; de Neeling, A. J.; Nibbering, P. H.; Mars-Groenendijk, R. H.; Noort, D.; Otero, J. M.; Llamas-Saiz, A. L.; van Raaij, M. J.; van der Marel, G. A.; Overkleeft, H. S.; Overhand, M. An Adamantyl Amino Acid Containing Gramicidin S Analogue with Broad Spectrum Antibacterial Activity and Reduced Hemolytic Activity. *Chemistry – A European Journal* **2010**, *16*, 12174–12181.
- (91) Müller, J.; Kirschner, R. A.; Berndt, J.-P.; Wulsdorf, T.; Metz, A.; Hrdina, R.; Schreiner, P. R.; Geyer, A.; Klebe, G. Diamondoid Amino Acid-Based Peptide Kinase A Inhibitor Analogues. *ChemMedChem* **2019**, *14*, 663–672.
- (92) Ritter, J. J.; Minieri, P. P. A New Reaction of Nitriles. I. Amides from Alkenes and Mononitriles¹. *Journal of the American Chemical Society* **1948**, *70*, 4045–4048.
- (93) Maison, W.; Frangioni, J. V.; Pannier, N. Synthesis of Rigid Multivalent Scaffolds Based on Adamantane. *Organic Letters* **2004**, *6*, 4567–4569.
- (94) Khilchevskii, A.; Baklan, V.; Kukhar, V. Interaction of adamantane, carboxylic acids of adamantane and bicyclo [3.3. 1] nonane series with acetonitrile in liquid bromine. *Zhurnal Organicheskoi Khimii* **1996**, *32*, 1022–1024.
- (95) Olah, G. A.; Gupta, B. G. B.; Narang, S. C. Synthetic Methods and Reactions; 661. Nitrosonium Ion Induced Preparation of Amides from Alkyl (Arylalkyl) Halides with Nitriles, a Mild and Selective Ritter-Type Reaction. *Synthesis* **1979**, *4*, 274–276.
- (96) Fokin, A. A.; Schreiner, P. R. Selective Alkane Transformations via Radicals and Radical Cations: Insights into the Activation Step from Experiment and Theory. *Chemical Reviews* **2002**, *102*, 1551–1594.
- (97) Müller, C. E.; Wanka, L.; Jewell, K.; Schreiner, P. R. Enantioselective Kinetic Resolution of trans-Cycloalkane-1,2-diols. *Angewandte Chemie International Edition* **2008**, *47*, 6180–6183.

- (98) Müller, C. E.; Hrdina, R.; Wende, R. C.; Schreiner, P. R. A Multicatalyst System for the One-Pot Desymmetrization/Oxidation of meso-1,2-Alkane Diols. *Chemistry – A European Journal* **2011**, *17*, 6309–6314.
- (99) Xu, S.; Held, I.; Kempf, B.; Mayr, H.; Steglich, W.; Zipse, H. The DMAP-Catalyzed Acetylation of Alcohols: A Mechanistic Study. *Chemistry – A European Journal* **2005**, *11*, 4751–4757.
- (100) Dalessandro, E. V.; Collin, H. P.; Guimarães, L. G. L.; Valle, M. S.; Pliego, J. R. Mechanism of the Piperidine-Catalyzed Knoevenagel Condensation Reaction in Methanol: The Role of Iminium and Enolate Ions. *Journal of Physical Chemistry B* **2017**, *121*, 5300–5307.
- (101) Hajos, Z. G.; Parrish, D. R. Asymmetric synthesis of bicyclic intermediates of natural product chemistry. *Journal of Organic Chemistry* **1974**, *39*, 1615–1621.
- (102) Hoang, L.; Bahmanyar, S.; Houk, K. N.; List, B. Kinetic and Stereochemical Evidence for the Involvement of Only One Proline Molecule in the Transition States of Proline-Catalyzed Intra- and Intermolecular Aldol Reactions. *Journal of the American Chemical Society* **2003**, *125*, 16–17.
- (103) Taylor, M. S.; Jacobsen, E. N. Asymmetric Catalysis by Chiral Hydrogen-Bond Donors. *Angewandte Chemie International Edition* **2006**, *45*, 1520–1543.
- (104) Schreiner, P. R. Metal-free organocatalysis through explicit hydrogen bonding interactions. *Chemical Society Reviews* **2003**, *32*, 289–296.
- (105) Seayad, J.; List, B. Asymmetric organocatalysis. *Organic & Biomolecular Chemistry* **2005**, *3*, 719–724.
- (106) Dalko, P. I.; Moisan, L. In the Golden Age of Organocatalysis. *Angewandte Chemie International Edition* **2004**, *43*, 5138–5175.
- (107) List, B.; Yang, J. W. The Organic Approach to Asymmetric Catalysis. *Science* **2006**, *313*, 1584–1586.
- (108) Vachal, P.; Jacobsen, E. N. Structure-Based Analysis and Optimization of a Highly Enantioselective Catalyst for the Strecker Reaction. *Journal of the American Chemical Society* **2002**, *124*, 10012–10014.
- (109) Sigman, M. S.; Jacobsen, E. N. Schiff Base Catalysts for the Asymmetric Strecker Reaction Identified and Optimized from Parallel Synthetic Libraries. *Journal of the American Chemical Society* **1998**, *120*, 4901–4902.

- (110) Denmark, S. E.; Stavenger, R. A.; Wong, K.-T.; Su, X. Chiral Phosphoramidate-Catalyzed Aldol Additions of Ketone Enolates. Preparative Aspects. *Journal of the American Chemical Society* **1999**, *121*, 4982–4991.
- (111) Kim, S. M.; Jin, M. Y.; Kim, M. J.; Cui, Y.; Kim, Y. S.; Zhang, L.; Song, C. E.; Ryu, D. H.; Yang, J. W. N-Heterocyclic carbene-catalysed intermolecular Stetter reactions of acetaldehyde. *Organic & Biomolecular Chemistry* **2011**, *9*, 2069–2071.
- (112) Ahrendt, K. A.; Borths, C. J.; MacMillan, D. W. C. New Strategies for Organic Catalysis: The First Highly Enantioselective Organocatalytic Diels-Alder Reaction. *Journal of the American Chemical Society* **2000**, *122*, 4243–4244.
- (113) Paras, N. A.; MacMillan, D. W. C. New Strategies in Organic Catalysis: The First Enantioselective Organocatalytic Friedel-Crafts Alkylation. *Journal of the American Chemical Society* **2001**, *123*, 4370–4371.
- (114) Brochu, M. P.; Brown, S. P.; MacMillan, D. W. C. Direct and Enantioselective Organocatalytic α -Chlorination of Aldehydes. *Journal of the American Chemical Society* **2004**, *126*, 4108–4109.
- (115) Brochu, M. P.; Brown, S. P.; MacMillan, D. W. C. Direct and Enantioselective Organocatalytic α -Chlorination of Aldehydes. *Journal of the American Chemical Society* **2004**, *126*, 4108–4109.
- (116) Hechavarria Fonseca, M. T.; List, B. Catalytic Asymmetric Intramolecular Michael Reaction of Aldehydes. *Angewandte Chemie International Edition* **2004**, *43*, 3958–3960.
- (117) Brown, S. P.; Goodwin, N. C.; MacMillan, D. W. C. The First Enantioselective Organocatalytic Mukaiyama-Michael Reaction: A Direct Method for the Synthesis of Enantioenriched γ -Butenolide Architecture. *Journal of the American Chemical Society* **2003**, *125*, 1192–1194.
- (118) Reyes-Rodríguez, G. J.; Rezayee, N. M.; Vidal-Albalat, A.; Jørgensen, K. A. Prevalence of Diarylprolinol Silyl Ethers as Catalysts in Total Synthesis and Patents. *Chemical Reviews* **2019**, *119*, 4221–4260.
- (119) Franzén, J.; Marigo, M.; Fielenbach, D.; Wabnitz, T. C.; Kjærsgaard, A.; Jørgensen, K. A. A General Organocatalyst for Direct α -Functionalization of Aldehydes: Stereoselective C-C, C-N, C-F, C-Br, and C-S Bond-Forming Reactions. Scope

- and Mechanistic Insights. *Journal of the American Chemical Society* **2005**, *127*, 18296–18304.
- (120) Marigo, M.; Franzén, J.; Poulsen, T. B.; Zhuang, W.; Jørgensen, K. A. Asymmetric Organocatalytic Epoxidation of α,β -Unsaturated Aldehydes with Hydrogen Peroxide. *Journal of the American Chemical Society* **2005**, *127*, 6964–6965.
- (121) Hayashi, Y.; Gotoh, H.; Hayashi, T.; Shoji, M. Diphenylprolinol Silyl Ethers as Efficient Organocatalysts for the Asymmetric Michael Reaction of Aldehydes and Nitroalkenes. *Angewandte Chemie International Edition* **2005**, *44*, 4212–4215.
- (122) Carlson, E. C.; Rathbone, L. K.; Yang, H.; Collett, N. D.; Carter, R. G. Improved Protocol for Asymmetric, Intramolecular Heteroatom Michael Addition Using Organocatalysis: Enantioselective Syntheses of Homoproline, Pelletierine, and Homopiperic Acid. *Journal of Organic Chemistry* **2008**, *73*, 5155–5158.
- (123) Hong, B.-C.; Kotame, P.; Tsai, C.-W.; Liao, J.-H. Enantioselective Total Synthesis of (+)-Conicol via Cascade Three-Component Organocatalysis. *Organic Letters* **2010**, *12*, 776–779.
- (124) Mukherjee, S.; Yang, J. W.; Hoffmann, S.; List, B. Asymmetric Enamine Catalysis. *Chemical Reviews* **2007**, *107*, 5471–5569.
- (125) Prieto, A.; Halland, N.; Jørgensen, K. A. Novel Imidazolidine-Tetrazole Organocatalyst for Asymmetric Conjugate Addition of Nitroalkanes. *Organic Letters* **2005**, *7*, 3897–3900.
- (126) Hanessian, S.; Shao, Z.; Warrier, J. S. Optimization of the Catalytic Asymmetric Addition of Nitroalkanes to Cyclic Enones with *trans*-4,5-Methano-l-proline. *Organic Letters* **2006**, *8*, 4787–4790.
- (127) List, B.; Lerner, R. A.; Barbas, C. F. Proline-Catalyzed Direct Asymmetric Aldol Reactions. *Journal of the American Chemical Society* **2000**, *122*, 2395–2396.
- (128) Northrup, A. B.; MacMillan, D. W. C. The First Direct and Enantioselective Cross-Aldol Reaction of Aldehydes. *Journal of the American Chemical Society* **2002**, *124*, 6798–6799.
- (129) Notz, W.; Tanaka, F.; Watanabe, S.-i.; Chowdari, N. S.; Turner, J. M.; Thayumanavan, R.; Barbas, C. F. The Direct Organocatalytic Asymmetric Mannich

- Reaction: Unmodified Aldehydes as Nucleophiles. *Journal of Organic Chemistry* **2003**, *68*, 9624–9634.
- (130) Enders, D.; Seki, A. Proline-Catalyzed Enantioselective Michael Additions of Ketones to Nitrostyrene. *Synlett* **2002**, 26–28.
- (131) Orsini, F.; Pelizzoni, F.; Forte, M.; Destro, R.; Gariboldi, P. 1,3 Dipolar cycloadditions of azomethine ylides with aromatic aldehydes. syntheses of 1-oxapyrrolizidines and 1,3-oxazolidines. *Tetrahedron* **1988**, *44*, 519–541.
- (132) Rizzi, G. P. Evidence for an azomethine ylide intermediate in the carbonyl-assisted decarboxylation of sarcosine. Novel synthesis of dl-phenylephrine hydrochloride. *Journal of Organic Chemistry* **1970**, *35*, 2069–2072.
- (133) Juliá, S.; Masana, J.; Vega, J. C. "Synthetic Enzymes". Highly Stereoselective Epoxidation of Chalcone in a Triphasic Toluene-Water-Poly[(S)-alanine] System. *Angewandte Chemie International Edition in English* **1980**, *19*, 929–931.
- (134) Mohr, P.; Waespe-Šarčević, N.; Tamm, C.; Gawronska, K.; Gawronski, J. K. A Study of Stereoselective Hydrolysis of Symmetrical Diesters with Pig Liver Esterase. *Helvetica Chimica Acta* **1983**, *66*, 2501–2511.
- (135) Ohno, M.; Otsuka, M. In *Organic Reactions*; John Wiley and Sons, Inc.: 2004, pp 1–55.
- (136) Richter, J. P.; Goroncy, A. K.; Ronimus, R. S.; Sutherland-Smith, A. J. The Structural and Functional Characterization of Mammalian ADP-dependent Glucokinase. *J Biol Chem* **2016**, *291*, 3694–704.
- (137) Chen, F.-F.; Cosgrove, S. C.; Birmingham, W. R.; Mangas-Sanchez, J.; Citoler, J.; Thompson, M. P.; Zheng, G.-W.; Xu, J.-H.; Turner, N. J. Enantioselective Synthesis of Chiral Vicinal Amino Alcohols Using Amine Dehydrogenases. *ACS Catalysis* **2019**, *9*, 11813–11818.
- (138) Thorpe, T. W.; France, S. P.; Hussain, S.; Marshall, J. R.; Zawodny, W.; Mangas-Sanchez, J.; Montgomery, S. L.; Howard, R. M.; Daniels, D. S. B.; Kumar, R.; Parmeggiani, F.; Turner, N. J. One-Pot Biocatalytic Cascade Reduction of Cyclic Enamines for the Preparation of Diastereomerically Enriched N-Heterocycles. *Journal of the American Chemical Society* **2019**, *141*, 19208–19213.

- (139) Lewis, C. A.; Sculimbrene, B. R.; Xu, Y.; Miller, S. J. Desymmetrization of Glycerol Derivatives with Peptide-Based Acylation Catalysts. *Organic Letters* **2005**, *7*, 3021–3023.
- (140) Copeland, G. T.; Miller, S. J. Selection of Enantioselective Acyl Transfer Catalysts from a Pooled Peptide Library through a Fluorescence-Based Activity Assay: An Approach to Kinetic Resolution of Secondary Alcohols of Broad Structural Scope. *Journal of the American Chemical Society* **2001**, *123*, 6496–6502.
- (141) Abascal, N. C.; Lichtor, P. A.; Giuliano, M. W.; Miller, S. J. Function-oriented investigations of a peptide-based catalyst that mediates enantioselective allylic alcohol epoxidation. *Chemical Science* **2014**, *5*, 4504–4511.
- (142) Henbest, H. B.; Wilson, R. A. L. 376. Aspects of stereochemistry. Part I. Stereospecificity in formation of epoxides from cyclic allylic alcohols. *Journal of the Chemical Society (Resumed)* **1957**, 1958–1965.
- (143) Bach, R. D.; Estévez, C. M.; Winter, J. E.; Glukhovtsev, M. N. On the Origin of Substrate Directing Effects in the Epoxidation of Allyl Alcohols with Peroxyformic Acid. *Journal of the American Chemical Society* **1998**, *120*, 680–685.
- (144) Adam, W.; Bach, R. D.; Dmitrenko, O.; Saha-Möller, C. R. A Computational Study of the Hydroxy-Group Directivity in the Peroxyformic Acid Epoxidation of the Chiral Allylic Alcohol (Z)-3-Methyl-3-penten-2-ol: Control of Threo Diastereoselectivity through Allylic Strain and Hydrogen Bonding. *Journal of Organic Chemistry* **2000**, *65*, 6715–6728.
- (145) Duschmalé, J.; Wennemers, H. Adapting to Substrate Challenges: Peptides as Catalysts for Conjugate Addition Reactions of Aldehydes to α,β -Disubstituted Nitroolefins. *Chemistry – A European Journal* **2012**, *18*, 1111–1120.
- (146) Schnitzer, T.; Wiesner, M.; Krattiger, P.; Revell, J. D.; Wennemers, H. Is more better? A comparison of tri- and tetrapeptidic catalysts. *Organic & Biomolecular Chemistry* **2017**, *15*, 5877–5881.
- (147) Rigling, C.; Kisunzu, J. K.; Duschmalé, J.; Häussinger, D.; Wiesner, M.; Ebert, M.-O.; Wennemers, H. Conformational Properties of a Peptidic Catalyst: Insights from NMR Spectroscopic Studies. *Journal of the American Chemical Society* **2018**, *140*, 10829–10838.

- (148) Duschmale, J.; Kohrt, S.; Wennemers, H. Peptide catalysis in aqueous emulsions. *Chemical Communications* **2014**, *50*, 8109–8112.
- (149) Darbre, T.; Reymond, J.-L. Peptide Dendrimers as Artificial Enzymes, Receptors, and Drug-Delivery Agents. *Accounts of Chemical Research* **2006**, *39*, 925–934.
- (150) Douat-Casassus, C.; Darbre, T.; Reymond, J.-L. Selective Catalysis with Peptide Dendrimers. *Journal of the American Chemical Society* **2004**, *126*, 7817–7826.
- (151) Wende, R. C.; Seitz, A.; Niedek, D.; Schuler, S. M. M.; Hofmann, C.; Becker, J.; Schreiner, P. R. The Enantioselective Dakin–West Reaction. *Angewandte Chemie International Edition* **2016**, *55*, 2719–2723.
- (152) Müller, C. E.; Zell, D.; Hrdina, R.; Wende, R. C.; Wanka, L.; Schuler, S. M. M.; Schreiner, P. R. Lipophilic Oligopeptides for Chemo- and Enantioselective Acyl Transfer Reactions onto Alcohols. *Journal of Organic Chemistry* **2013**, *78*, 8465–8484.
- (153) Hrdina, R.; Müller, C. E.; Schreiner, P. R. Kinetic resolution of trans-cycloalkane-1,2-diols via Steglich esterification. *Chemical Communications* **2010**, *46*, 2689–2690.
- (154) Dalla-Vechia, L.; Santos, V. G.; Godoi, M. N.; Cantillo, D.; Kappe, C. O.; Eberlin, M. N.; de Souza, R. O. M. A.; Miranda, L. S. M. On the mechanism of the Dakin–West reaction. *Organic & Biomolecular Chemistry* **2012**, *10*, 9013–9020.
- (155) Hofmann, C.; Schuler, S. M. M.; Wende, R. C.; Schreiner, P. R. En route to multicycatalysis: kinetic resolution of trans-cycloalkane-1,2-diols via oxidative esterification. *Chemical Communications* **2014**, *50*, 1221–1223.
- (156) Moles, F. J. N.; Guillena, G.; Nájera, C. Aqueous organocatalyzed aldol reaction of glyoxylic acid for the enantioselective synthesis of α -hydroxy- γ -keto acids. *RSC Advances* **2014**, *4*, 9963–9966.
- (157) Nishibayashi, Y.; Takei, I.; Uemura, S.; Hidai, M. Extremely High Enantioselective Redox Reaction of Ketones and Alcohols Catalyzed by RuCl₂(PPh₃)-(oxazolinylferrocenylphosphine). *Organometallics* **1999**, *18*, 2291–2293.
- (158) Takasu, K.; Maiti, S.; Ihara, M. Asymmetric Intramolecular Aza-Michael Reaction Using Environmentally Friendly Organocatalysis. *Heterocycles* **2003**, *59*, 51–55.

- (159) Humphrey, G. R.; Dalby, S. M.; Andreani, T.; Xiang, B.; Luzung, M. R.; Song, Z. J.; Shevlin, M.; Christensen, M.; Belyk, K. M.; Tschaen, D. M. Asymmetric Synthesis of Letemovir Using a Novel Phase-Transfer-Catalyzed Azamichael Reaction. *Organic Process Research & Development* **2016**, *20*, 1097–1103.
- (160) Shaw, S.; White, J. D. Regioselective and Enantioselective Addition of Sulfur Nucleophiles to Acyclic $\alpha,\beta,\gamma,\delta$ -Unsaturated Dienones Catalyzed by an Iron(III)–Salen Complex. *Organic Letters* **2015**, *17*, 4564–4567.
- (161) Wadhwa, P.; Kharbanda, A.; Sharma, A. Thia-Michael Addition: An Emerging Strategy in Organic Synthesis. *Asian Journal of Organic Chemistry* **2018**, *7*, 634–661.
- (162) Kaplan, W.; Khatri, H. R.; Nagorny, P. Concise Enantioselective Total Synthesis of Cardiotonic Steroids 19-Hydroxysarmentogenin and Trewianin Aglycone. *Journal of the American Chemical Society* **2016**, *138*, 7194–7198.
- (163) Zhang, L.-D.; Zhong, L.-R.; Xi, J.; Yang, X.-L.; Yao, Z.-J. Enantioselective Total Synthesis of Lycoposerramine-Z Using Chiral Phosphoric Acid Catalyzed Intramolecular Michael Addition. *Journal of Organic Chemistry* **2016**, *81*, 1899–1904.
- (164) Ohshima, T.; Xu, Y.; Takita, R.; Shimizu, S.; Zhong, D.; Shibasaki, M. Enantioselective Total Synthesis of (-)-Strychnine Using the Catalytic Asymmetric Michael Reaction and Tandem Cyclization. *Journal of the American Chemical Society* **2002**, *124*, 14546–14547.
- (165) Raheem, I. T.; Goodman, S. N.; Jacobsen, E. N. Catalytic Asymmetric Total Syntheses of Quinine and Quinidine. *Journal of the American Chemical Society* **2004**, *126*, 706–707.
- (166) Mitsunuma, H.; Shibasaki, M.; Kanai, M.; Matsunaga, S. Catalytic Asymmetric Total Synthesis of Chimonanthine, Folicanthine, and Calycanthine through Double Michael Reaction of Bisoxindole. *Angewandte Chemie International Edition* **2012**, *51*, 5217–5221.
- (167) Ouchi, H.; Asahina, A.; Asakawa, T.; Inai, M.; Hamashima, Y.; Kan, T. Practical Total Syntheses of Acromelic Acids A and B. *Organic Letters* **2014**, *16*, 1980–1983.

- (168) Sun, Z.; Zhou, M.; Li, X.; Meng, X.; Peng, F.; Zhang, H.; Shao, Z. Catalytic Asymmetric Assembly of Octahydroindolones: Divergent Synthesis of Lycorine-type Amaryllidaceae Alkaloids (+)- α -Lycorane and (+)-Lycorine. *Chemistry – A European Journal* **2014**, *20*, 6112–6119.
- (169) Li, L.; Yang, Q.; Wang, Y.; Jia, Y. Catalytic Asymmetric Total Synthesis of (-)-Galanthamine and (-)-Lycoramine. *Angewandte Chemie International Edition* **2015**, *54*, 6255–6259.
- (170) Mondal, A.; Bhowmick, S.; Ghosh, A.; Chanda, T.; Bhowmick, K. C. Advances on asymmetric organocatalytic 1,4-conjugate addition reactions in aqueous and semi-aqueous media. *Tetrahedron: Asymmetry* **2017**, *28*, 849–875.
- (171) Pearson, A. J.; Panda, S. N-Prolinylanthranilamide Pseudopeptides as Bifunctional Organocatalysts for Asymmetric Aldol Reactions. *Organic Letters* **2011**, *13*, 5548–5551.
- (172) Davie, E. A. C.; Mennen, S. M.; Xu, Y.; Miller, S. J. Asymmetric Catalysis Mediated by Synthetic Peptides. *Chemical Reviews* **2007**, *107*, 5759–5812.
- (173) Pelter, A.; Crump, R. A. N. C.; Kidwell, H. Chiral [2.2]paracyclophanes—III. The preparation of unique homochiral amino-acids derived from [2.2]paracyclophane. *Tetrahedron: Asymmetry* **1997**, *8*, 3873–3880.
- (174) Hitchcock, P. B.; Hodgson, A. C. C.; Rowlands, G. J. The First Examples of Planar Chiral Organic Benzimidazole Derivatives. *Synlett* **2006**, *16*, 2625–2628.
- (175) Kitagaki, S.; Ueda, T.; Mukai, C. Planar chiral [2.2]paracyclophane-based bis-(thiourea) catalyst: application to asymmetric Henry reaction. *Chemical Communications* **2013**, *49*, 4030–4032.
- (176) Takenaga, N.; Adachi, S.; Furusawa, A.; Nakamura, K.; Suzuki, N.; Ohta, Y.; Komizu, M.; Mukai, C.; Kitagaki, S. Planar chiral [2.2]paracyclophane-based phosphine-phenol catalysts: application to the aza-Morita-Baylis-Hillman reaction of N-sulfonated imines with various vinyl ketones. *Tetrahedron* **2016**, *72*, 6892–6897.
- (177) Hong, B.; Ma, Y.; Zhao, L.; Duan, W.; He, F.; Song, C. Synthesis of planar chiral imidazo[1,5-a]pyridinium salts based on [2.2]paracyclophane for asymmetric β -borylation of enones. *Tetrahedron: Asymmetry* **2011**, *22*, 1055–1062.

- (178) Whelligan, D. K.; Bolm, C. Synthesis of Pseudo-geminal-, Pseudo-ortho-, and ortho-Phosphinyl-oxazoliny[2.2]paracyclophanes for Use as Ligands in Asymmetric Catalysis. *Journal of Organic Chemistry* **2006**, *71*, 4609–4618.
- (179) Cram, D. J.; Allinger, N. L. Macro Rings. XII. Stereochemical Consequences of Steric Compression in the Smallest Paracyclophane. *Journal of the American Chemical Society* **1955**, *77*, 6289–6294.
- (180) Pelter, A.; Crump, R. A. N. C.; Kidwell, H. Chiral [2.2]paracyclophanes.1.: Synthesis and characterisation of unique homochiral amino-acids derived from [2.2]paracyclophane. *Tetrahedron Letters* **1996**, *37*, 1273–1276.
- (181) Marchand, A.; Maxwell, A.; Mootoo, B.; Pelter, A.; Reid, A. Oxazoline Mediated Routes to a Unique Amino-acid, 4-Amino-13-carboxy[2.2]paracyclophane, of Planar Chirality. *Tetrahedron* **2000**, *56*, 7331–7338.
- (182) Ghosh, H.; Patel, B. K. Hypervalent iodine(iii)-mediated oxidation of aldoximes to N-acetoxy or N-hydroxy amides. *Organic & Biomolecular Chemistry* **2010**, *8*, 384–390.
- (183) Hoshino, Y.; Okuno, M.; Kawamura, E.; Honda, K.; Inoue, S. Base-mediated rearrangement of free aromatic hydroxamic acids (ArCO-NHOH) to anilines. *Chemical Communications* **2009**, 2281–2283.
- (184) Patel, B. K.; Ghosh, H.; Banerjee, A.; Rout, S. K. A convenient one-pot synthesis of amines from aldoximes mediated by Koser's reagent. *Archive for Organic Chemistry* **2011**, *2*, 209–216.
- (185) Psiorz, M.; Schmid, R. Cyclophane, I. Ein einfacher Zugang zu funktionalisierten [2.2]Paracyclophanen. *Chemische Berichte* **1987**, *120*, 1825–1828.
- (186) Zitt, H.; Dix, I.; Hopf, H.; Jones, P. 4,15-Diamino[2.2]paracyclophane, a Reusable Template for Topochemical Reaction Control in Solution. *European Journal of Organic Chemistry* **2002**, *2002*, 2298–2307.
- (187) Rieche, A.; Gross, H.; Höft, E. Über α -Halogenäther, IV. Synthesen aromatischer Aldehyde mit Dichlormethyl-alkyläthern. *Chemische Berichte* **1960**, *93*, 88–94.
- (188) Hopf, H.; Raulfs, F.-W. Cyclophanes, XXIII [1] [2.2] Indenophanes — Building Blocks for Novel Multilayered Organoiron Complexes. *Israel Journal of Chemistry* **1985**, *25*, 210–216.

- (189) Ramm, S. M.; Hopf, H.; Jones, P. G.; Bubenitschek, P.; Ahrens, B.; Ernst, L. Annulation of Seven-Membered Rings to [2.2]Paracyclophane. *European Journal of Organic Chemistry* **2008**, *2008*, 2948–2959.
- (190) Eltamany, S. H.; Hopf, H. Cyclophane, XIV : darstellung polymethylierter [2.2]paracyclophane. *Tetrahedron Letters* **1980**, *21*, 4901–4904.
- (191) Busch, M.; Cayir, M.; Nieger, M.; Thiel, W. R.; Bräse, S. Roadmap towards N-Heterocyclic [2.2]Paracyclophanes and Their Application in Asymmetric Catalysis. *European Journal of Organic Chemistry* **2013**, *2013*, 6108–6123.
- (192) Garcia, O.; Nicolás, E.; Albericio, F. o-Formylation of electron-rich phenols with dichloromethyl methyl ether and TiCl₄. *Tetrahedron Letters* **2003**, *44*, 4961–4963.
- (193) De Luca, L.; Giacomelli, G.; Porcheddu, A. Beckmann Rearrangement of Oximes under Very Mild Conditions. *Journal of Organic Chemistry* **2002**, *67*, 6272–6274.
- (194) Das, B.; Holla, H.; Mahender, G.; Banerjee, J.; Ravinder Reddy, M. Hypervalent iodine-mediated interaction of aldoximes with activated alkenes including Baylis–Hillman adducts: a new and efficient method for the preparation of nitrile oxides from aldoximes. *Tetrahedron Letters* **2004**, *45*, 7347–7350.
- (195) Koradin, C.; Dohle, W.; Rodriguez, A. L.; Schmid, B.; Knochel, P. Synthesis of polyfunctional indoles and related heterocycles mediated by cesium and potassium bases. *Tetrahedron* **2003**, *59*, 1571–1587.
- (196) Schneider, J. F.; Fröhlich, R.; Paradies, J. Synthesis of Enantiopure Planar-Chiral Thiourea Derivatives. *Synthesis* **2010**, 3486–3492.
- (197) Banfi, S.; Manfredi, A.; Montanari, F.; Pozzi, G.; Quici, S. Synthesis of chiral Mn(III)-meso-tetrakis-[2.2]-p-cyclophanyl-porphyrin: a new catalyst for enantioselective epoxidation. *Journal of Molecular Catalysis A: Chemical* **1996**, *113*, 77–86.
- (198) Bal, B. S.; Childers, W. E.; Pinnick, H. W. Oxidation of α,β -unsaturated aldehydes. *Tetrahedron* **1981**, *37*, 2091–2096.
- (199) Zhao, M.; Li, J.; Mano, E.; Song, Z.; Tschaen, D. M.; Grabowski, E. J. J.; Reider, P. J. Oxidation of Primary Alcohols to Carboxylic Acids with Sodium Chlorite

- Catalyzed by TEMPO and Bleach. *Journal of Organic Chemistry* **1999**, *64*, 2564–2566.
- (200) Shibuya, M.; Sato, T.; Tomizawa, M.; Iwabuchi, Y. Oxoammonium salt/NaClO₂: an expedient, catalytic system for one-pot oxidation of primary alcohols to carboxylic acids with broad substrate applicability. *Chemical Communications* **2009**, 1739–1741.
- (201) Hunsen, M. Carboxylic Acids from Primary Alcohols and Aldehydes by a Pyridinium Chlorochromate Catalyzed Oxidation. *Synthesis* **2005**, 2487–2490.
- (202) Travis, B. R.; Sivakumar, M.; Hollist, G. O.; Borhan, B. Facile Oxidation of Aldehydes to Acids and Esters with Oxone. *Organic Letters* **2003**, *5*, 1031–1034.
- (203) Zhang, Y.; Cheng, Y.; Cai, H.; He, S.; Shan, Q.; Zhao, H.; Chen, Y.; Wang, B. Catalyst-free aerobic oxidation of aldehydes into acids in water under mild conditions. *Green Chemistry* **2017**, *19*, 5708–5713.
- (204) Kusmus, D. *Practical Training Internship Report as Part of MSc*; Report; Vrije Universiteit, 2014.
- (205) Merbouh, J. M. B.; Nabyl Preparation of 4-acetylamino-2,2,6,6-tetramethylpiperidine-1-oxoammonium tetrafluoroborate, and the oxidation of geraniol to gerianal. *Organic Syntheses* **2005**, *82*, 80.
- (206) Sharma, A.; Gamre, S.; Roy, S.; Goswami, D.; Chattopadhyay, A.; Chattopadhyay, S. A convenient asymmetric synthesis of the octalactin lactone. *Tetrahedron Letters* **2008**, *49*, 3902–3905.
- (207) Brown, D. G. et al. Discovery of Spirofused Piperazine and Diazepane Amides as Selective Histamine-3 Antagonists with in Vivo Efficacy in a Mouse Model of Cognition. *Journal of Medicinal Chemistry* **2014**, *57*, 733–758.
- (208) Lucio Anelli, P.; Biffi, C.; Montanari, F.; Quici, S. Fast and selective oxidation of primary alcohols to aldehydes or to carboxylic acids and of secondary alcohols to ketones mediated by oxoammonium salts under two-phase conditions. *Journal of Organic Chemistry* **1987**, *52*, 2559–2562.
- (209) Dendele, N.; Bisaro, F.; Gaumont, A.-C.; Perrio, S.; Richards, C. J. Synthesis of a [2.2]paracyclophane based planar chiral palladacycle by a highly selective

- kinetic resolution/C-H activation reaction. *Chemical Communications* **2012**, *48*, 1991–1993.
- (210) Wiberg, K. B.; Stewart, R. The Mechanisms of Permanganate Oxidation. I. The Oxidation of Some Aromatic Aldehydes¹. *Journal of the American Chemical Society* **1955**, *77*, 1786–1795.
- (211) Ruhoff, J. R. n-Heptanoic acid. *Organic Syntheses* **1936**, *16*.
- (212) Báthori, N. B.; Jacobs, A.; Mei, M.; Nassimbeni, L. R. Resolution of malic acid by (+)-cinchonine and (–)-cinchonidine. *Canadian Journal of Chemistry* **2015**, *93*, 858–863.
- (213) Allgeier, H.; Siegel, M. G.; Helgeson, R. C.; Schmidt, E.; Cram, D. J. Macro rings. XLVII. Syntheses and spectral properties of heteroannularly disubstituted [2.2]paracyclophanes. *Journal of the American Chemical Society* **1975**, *97*, 3782–3789.
- (214) Takada, Y.; Tsuchiya, K.; Takahashi, S.; Mori, N. Novel transannular reactions in the acid hydrolysis of diazotized syn- and anti-4-amino[2.2](1,4)naphthalenoparacyclophanes. *Journal of the Chemical Society, Perkin Transactions 2* **1990**, 2141–2145.
- (215) Jayasundera, K. P.; Engels, T. G. W.; Lun, D. J.; Mungalpara, M. N.; Plieger, P. G.; Rowlands, G. J. The synthesis of planar chiral pseudo-gem aminophosphine pre-ligands based on [2.2]paracyclophane. *Organic & Biomolecular Chemistry* **2017**, *15*, 8975–8984.
- (216) Roche, A. J.; Dolbier, W. R. Electrophilic Substitution of 1,1,2,2,9,9,10,10-Octafluoro[2.2]paracyclophane. *Journal of Organic Chemistry* **1999**, *64*, 9137–9143.
- (217) Gauthier, D.; Dodd, R. H.; Dauban, P. Regioselective access to substituted oxindoles via rhodium-catalyzed carbene C–H insertion. *Tetrahedron* **2009**, *65*, 8542–8555.
- (218) Setamdideh, D.; Khezri, B. Rapid and Efficient Reduction of Nitroarenes to Their Corresponding Amines with Promotion of NaBH₄/NiCl₂·6H₂O System in Aqueous CH₃CN. *Asian Journal of Chemistry* **2010**, *22*, 5575.
- (219) Gowda, D. C.; Gowda, S. Formic acid with 10selective reduction of aromatic nitro compounds. *Indian Journal of Chemistry - Section B* **2000**, *09*, 709–711.

- (220) Dong, J.; Jin, B.; Sun, P. Palladium-Catalyzed Direct Ortho-Nitration of Azoarenes Using NO₂ as Nitro Source. *Organic Letters* **2014**, *16*, 4540–4542.
- (221) Wiesner, M.; Revell, J. D.; Wennemers, H. Tripeptides as Efficient Asymmetric Catalysts for 1,4-Addition Reactions of Aldehydes to Nitroolefins—A Rational Approach. *Angewandte Chemie International Edition* **2008**, *47*, 1871–1874.
- (222) Pearson, A. J.; Panda, S. N-Prolinylanthranilic acid derivatives as bifunctional organocatalysts for asymmetric aldol reactions. *Tetrahedron* **2011**, *67*, 3969–3975.
- (223) Moriyama, K.; Sugiue, T.; Saito, Y.; Katsuta, S.; Togo, H. 2,6-Bis(amido)benzoic Acid with Internal Hydrogen Bond as Brønsted Acid Catalyst for Friedel–Crafts Reaction of Indoles. *Advanced Synthesis & Catalysis* **2015**, *357*, 2143–2149.
- (224) Sheehan, J. C.; Hess, G. P. A New Method of Forming Peptide Bonds. *Journal of the American Chemical Society* **1955**, *77*, 1067–1068.
- (225) Rebek, J.; Feitler, D. Mechanism of the carbodiimide reaction. II. Peptide synthesis on the solid phase. *Journal of the American Chemical Society* **1974**, *96*, 1606–1607.
- (226) Benoiton, N. L.; Chen, F. M. F. 2-Alkoxy-5(4H)-oxazolones from N-alkoxy-carbonylamino acids and their implication in carbodiimide-mediated reactions in peptide synthesis. *Canadian Journal of Chemistry* **1981**, *59*, 384–389.
- (227) Montalbetti, C. A. G. N.; Falque, V. Amide bond formation and peptide coupling. *Tetrahedron* **2005**, *61*, 10827–10852.
- (228) Carpino, L. A. 1-Hydroxy-7-azabenzotriazole. An efficient peptide coupling additive. *Journal of the American Chemical Society* **1993**, *115*, 4397–4398.
- (229) Albericio, F.; Bofill, J. M.; El-Faham, A.; Kates, S. A. Use of Onium Salt-Based Coupling Reagents in Peptide Synthesis¹. *Journal of Organic Chemistry* **1998**, *63*, 9678–9683.
- (230) Xu, C.-P.; Luo, S.-P.; Wang, A.-E.; Huang, P.-Q. Complexity generation by chemical synthesis: a five-step synthesis of (-)-chaetominine from l-tryptophan and its biosynthetic implications. *Organic & Biomolecular Chemistry* **2014**, *12*, 2859–2863.
- (231) Vaughan, J. R.; Osato, R. L. Preparation of Peptides Using Mixed Carboxylic Acid Anhydrides. *Journal of the American Chemical Society* **1951**, *73*, 5553–5555.

- (232) Anderson, G. W.; Zimmerman, J. E.; Callahan, F. M. Reinvestigation of the mixed carbonic anhydride method of peptide synthesis. *Journal of the American Chemical Society* **1967**, *89*, 5012–5017.
- (233) Evindar, G.; Batey, R. A. Parallel Synthesis of a Library of Benzoxazoles and Benzothiazoles Using Ligand-Accelerated Copper-Catalyzed Cyclizations of ortho-Halobenzanilides. *Journal of Organic Chemistry* **2006**, *71*, 1802–1808.
- (234) Hoffmann, R.; Woodward, R. B. Orbital Symmetries and endo-exo Relationships in Concerted Cycloaddition Reactions. *Journal of the American Chemical Society* **1965**, *87*, 4388–4389.
- (235) Arrieta, A.; Cossío, F. P.; Lecea, B. Direct Evaluation of Secondary Orbital Interactions in the Diels-Alder Reaction between Cyclopentadiene and Maleic Anhydride. *Journal of Organic Chemistry* **2001**, *66*, 6178–6180.
- (236) Paul, R.; Anderson, G. W. N,N'-Carbonyldiimidazole, a New Peptide Forming Reagent¹. *Journal of the American Chemical Society* **1960**, *82*, 4596–4600.
- (237) Anderson, J. C.; Ford, J. G.; Whiting, M. Chirality transfer in the aza-[2,3]-Wittig sigmatropic rearrangement. *Organic & Biomolecular Chemistry* **2005**, *3*, 3734–3748.
- (238) Paul, R.; Anderson, G. W. N,N'-Carbonyldiimidazole in Peptide Synthesis. III.1 A Synthesis of Isoleucine-5 Angiotensin II Amide-I. *Journal of Organic Chemistry* **1962**, *27*, 2094–2099.
- (239) Bodanszky, M, *Principles of Peptide Synthesis*, 2nd ed.; Springer-Verlag: Berlin, 1993.
- (240) Carpino, L. A. Methyl ester nonequivalence in the ¹H NMR spectra of diastereomeric dipeptide esters incorporating N-terminal .alpha.-phenylglycine units. *Journal of Organic Chemistry* **1988**, *53*, 875–878.
- (241) Stokes, B. J.; Vogel, C. V.; Urnezis, L. K.; Pan, M.; Driver, T. G. Intramolecular Fe(II)-Catalyzed N-O or N-N Bond Formation from Aryl Azides. *Organic Letters* **2010**, *12*, 2884–2887.
- (242) Anderson, G. W.; Zimmerman, J. E.; Callahan, F. M. The Use of Esters of N-Hydroxysuccinimide in Peptide Synthesis. *Journal of the American Chemical Society* **1964**, *86*, 1839–1842.

- (243) Chen, F.; Huang, S.; Zhang, H.; Liu, F.; Peng, Y. Proline-based dipeptides with two amide units as organocatalyst for the asymmetric aldol reaction of cyclohexanone with aldehydes. *Tetrahedron* **2008**, *64*, 9585–9591.
- (244) Ashworth, I. W.; Cox, B. G.; Meyrick, B. Kinetics and Mechanism of N-Boc Cleavage: Evidence of a Second-Order Dependence upon Acid Concentration. *Journal of Organic Chemistry* **2010**, *75*, 8117–8125.
- (245) Lavrado, J.; Cabal, G. G.; Prudêncio, M.; Mota, M. M.; Gut, J.; Rosenthal, P. J.; Díaz, C.; Guedes, R. C.; dos Santos, D. J. V. A.; Bichenkova, E.; Douglas, K. T.; Moreira, R.; Paulo, A. Incorporation of Basic Side Chains into Cryptolepine Scaffold: Structure-Antimalarial Activity Relationships and Mechanistic Studies. *Journal of Medicinal Chemistry* **2011**, *54*, 734–750.
- (246) Xie, H.; Ng, D.; Savinov, S. N.; Dey, B.; Kwong, P. D.; Wyatt, R.; Smith, A. B.; Hendrickson, W. A. Structure-Activity Relationships in the Binding of Chemically Derivatized CD4 to gp120 from Human Immunodeficiency Virus. *Journal of Medicinal Chemistry* **2007**, *50*, 4898–4908.
- (247) Clayden, J.; Greeves, N.; Warren, S.; Wothers, P., *Organic Chemistry*; Oxford University Press: 2000.
- (248) Staudinger, H.; Meyer, J. Über neue organische Phosphorverbindungen III. Phosphinmethylderivate und Phosphinimine. *Helvetica Chimica Acta* **1919**, *2*, 635–646.
- (249) Subrayan, R. P.; Rasmussen, P. G. High nitrogen chemistry: Synthesis and properties of N,N-bis(4,5-dicyano-1-methyl-2-imidazolyl)cyanamide and N,N,N',N',N'',N''-hexakis(4,5-dicyano-1-methyl-2-imidazolyl)melamine. *Tetrahedron* **1999**, *55*, 353–358.
- (250) Shalev, D. E.; Chiacchiera, S. M.; Radkowsky, A. E.; Kosower, E. M. Sequence of Reactant Combination Alters the Course of the Staudinger Reaction of Azides with Acyl Derivatives. Bimanes. 30. *Journal of Organic Chemistry* **1996**, *61*, 1689–1701.
- (251) Saxon, E.; Luchansky, S. J.; Hang, H. C.; Yu, C.; Lee, S. C.; Bertozzi, C. R. Investigating Cellular Metabolism of Synthetic Azidosugars with the Staudinger Ligation. *Journal of the American Chemical Society* **2002**, *124*, 14893–14902.

- (252) Tahara, Y.-k.; Ito, M.; Kanyiva, K. S.; Shibata, T. Total Synthesis of cis-Clavicipitic Acid from Asparagine via Ir-Catalyzed CH bond Activation as a Key Step. *Chemistry – A European Journal* **2015**, *21*, 11340–11343.
- (253) Xie, H.; Ng, D.; Savinov, S. N.; Dey, B.; Kwong, P. D.; Wyatt, R.; Smith, A. B.; Hendrickson, W. A. Structure-Activity Relationships in the Binding of Chemically Derivatized CD4 to gp120 from Human Immunodeficiency Virus. *Journal of Medicinal Chemistry* **2007**, *50*, 4898–4908.
- (254) Duschmalé, J.; Wennemers, H. Adapting to Substrate Challenges: Peptides as Catalysts for Conjugate Addition Reactions of Aldehydes to α,β -Disubstituted Nitroolefins. *Chemistry – A European Journal* **2012**, *18*, 1111–1120.
- (255) Seebach, D.; Goliński, J. Synthesis of Open-Chain 2,3-Disubstituted 4-nitroketones by Diastereoselective Michael-addition of (E)-Enamines to (E)-Nitroolefins. A topological rule for C, C-bond forming processes between prochiral centres. Preliminary communication. *Helvetica Chimica Acta* **1981**, *64*, 1413–1423.
- (256) Wiesner, M.; Revell, J. D.; Wennemers, H. Tripeptides as Efficient Asymmetric Catalysts for 1,4-Addition Reactions of Aldehydes to Nitroolefins—A Rational Approach. *Angewandte Chemie International Edition* **2008**, *47*, 1871–1874.
- (257) Kumar, T. P.; Sattar, M. A.; Prasad, S. S.; Haribabu, K.; Reddy, C. S. Enantioselective Michael addition of aldehydes to nitroolefins catalyzed by pyrrolidine-HOBt. *Tetrahedron: Asymmetry* **2017**, *28*, 401–409.
- (258) Hu, X.; Wei, Y.-F.; Wu, N.; Jiang, Z.; Liu, C.; Luo, R.-S. Indolinol-catalyzed asymmetric Michael reaction of aldehydes to nitroalkenes in brine. *Tetrahedron: Asymmetry* **2016**, *27*, 420–427.
- (259) Wang, Y.; Li, D.; Lin, J.; Wei, K. Organocatalytic asymmetric Michael addition of aldehydes and ketones to nitroalkenes catalyzed by adamantoyl l-prolinamide. *RSC Advances* **2015**, *5*, 5863–5874.
- (260) Kumar, T. P. Asymmetric Michael addition of aldehydes to nitroolefins catalyzed by a pyrrolidine-pyrazole. *Tetrahedron: Asymmetry* **2014**, *25*, 1286–1291.
- (261) Wang, Y.; Ji, S.; Wei, K.; Lin, J. Epiandrosterone-derived prolinamide as an efficient asymmetric catalyst for Michael addition reactions of aldehydes to nitroalkenes. *RSC Advances* **2014**, *4*, 30850–30856.

- (262) Ghosh, S. K.; Qiao, Y.; Ni, B.; Headley, A. D. Asymmetric Michael reactions catalyzed by a highly efficient and recyclable quaternary ammonium ionic liquid-supported organocatalyst in aqueous media. *Organic & Biomolecular Chemistry* **2013**, *11*, 1801–1804.
- (263) Choudary, B. M.; Rajasekhar, C. V.; Gopi Krishna, G.; Rajender Reddy, K. L-Proline-Catalyzed Michael Addition of Aldehydes and Unmodified Ketones to Nitro Olefins Accelerated by Et₃N. *Synthetic Communications* **2007**, *37*, 91–98.
- (264) Mandal, T.; Zhao, C.-G. Modularly Designed Organocatalytic Assemblies for Direct Nitro-Michael Addition Reactions. *Angewandte Chemie International Edition* **2008**, *47*, 7714–7717.
- (265) Wang, W.-H.; Abe, T.; Wang, X.-B.; Kodama, K.; Hirose, T.; Zhang, G.-Y. Self-assembled proline-amino thioureas as efficient organocatalysts for the asymmetric Michael addition of aldehydes to nitroolefins. *Tetrahedron: Asymmetry* **2010**, *21*, 2925–2933.
- (266) Szcześniak, P.; Staszewska-Krajewska, O.; Furman, B.; Młynarski, J. Asymmetric Synthesis of Cyclic Nitrones via Organocatalytic Michael Addition of Aldehydes to Nitroolefins and Subsequent Reductive Cyclization. *Chemistry-Select* **2017**, *2*, 2670–2676.
- (267) Burés, J.; Armstrong, A.; Blackmond, D. G. Curtin–Hammett Paradigm for Stereocontrol in Organocatalysis by Diarylprolinol Ether Catalysts. *Journal of the American Chemical Society* **2012**, *134*, 6741–6750.
- (268) Schnitzer, T.; Budinská, A.; Wennemers, H. Organocatalysed conjugate addition reactions of aldehydes to nitroolefins with anti selectivity. *Nature Catalysis* **2020**, *3*, 143–147.
- (269) Li, P.; Xu, J.-C. 1-Ethyl 2-Halopyridinium Salts, Highly Efficient Coupling Reagents for Hindered Peptide Synthesis both in Solution and the Solid-Phase. *Tetrahedron* **2000**, *56*, 8119–8131.
- (270) Neumann, K. T.; Donslund, A. S.; Andersen, T. L.; Nielsen, D. U.; Skrydstrup, T. Synthesis of Aliphatic Carboxamides Mediated by Nickel NN₂-Pincer Complexes and Adaptation to Carbon-Isotope Labeling. *Chemistry – A European Journal* **2018**, *24*, 14946–14949.

- (271) Denmark, S. E.; Burk, M. T. Lewis base catalysis of bromo- and iodolactonization, and cycloetherification. *Proceedings of the National Academy of Sciences* **2010**, *107*, 20655.
- (272) Liu, X.; An, R.; Zhang, X.; Luo, J.; Zhao, X. Enantioselective Trifluoromethylthiolating Lactonization Catalyzed by an Indane-Based Chiral Sulfide. *Angewandte Chemie International Edition* **2016**, *55*, 5846–5850.
- (273) Nishiyori, R.; Tsuchihashi, A.; Mochizuki, A.; Kaneko, K.; Yamanaka, M.; Shirakawa, S. Design of Chiral Bifunctional Dialkyl Sulfide Catalysts for Regio-, Diastereo-, and Enantioselective Bromolactonization. *Chemistry – A European Journal* **2018**, *24*, 16747–16752.
- (274) Ke, Z.; Tan, C. K.; Liu, Y.; Lee, K. G. Z.; Yeung, Y.-Y. Catalytic and enantioselective bromoetherification of olefinic 1,3-diols: mechanistic insight. *Tetrahedron* **2016**, *72*, 2683–2689.
- (275) Hibert, M.; Solladie, G. Substituent effect during the synthesis of substituted [2.2] paracyclophane by photoextrusion of carbon dioxide from a cyclic diester. *Journal of Organic Chemistry* **1980**, *45*, 4496–4498.
- (276) Zhou, Z.; He, X. Rapid microwave-promoted solvent-free synthesis of hypervalent iodine reagents. *Journal of Chemical Research* **2009**, *2009*, 30–31.
- (277) Cipiciani, A.; Fringuelli, F.; Mancini, V.; Piermatti, O.; Pizzo, F.; Ruzziconi, R. Synthesis of Chiral (R)-4-Hydroxy- and (R)-4-Halogeno[2.2]paracyclophanes and Group Polarizability. Optical Rotation Relationship. *Journal of Organic Chemistry* **1997**, *62*, 3744–3747.
- (278) Das, A. K.; Bose, P. P.; Drew, M. G. B.; Banerjee, A. The role of protecting groups in the formation of organogels through a nano-fibrillar network formed by self-assembling terminally protected tripeptides. *Tetrahedron* **2007**, *63*, 7432–7442.
- (279) Song, C.; Tapaneeyakorn, S.; Murphy, A. C.; Butts, C.; Watts, A.; Willis, C. L. Enantioselective Syntheses of α -Fmoc-Pbf-[2-¹³C]-l-arginine and Fmoc-[1,3-¹³C₂]-l-proline and Incorporation into the Neurotensin Receptor 1 Ligand, NT8-13. *Journal of Organic Chemistry* **2009**, *74*, 8980–8987.
- (280) Sakaguchi, H.; Tokuyama, H.; Fukuyama, T. Stereocontrolled Total Synthesis of (-)-Kainic Acid. *Organic Letters* **2007**, *9*, 1635–1638.

- (281) Batsanov, A. S.; Georgiou, I.; Girling, P. R.; Pommier, L.; Shen, H. C.; Whiting, A. Asymmetric Synthesis and Application of Homologous Pyrroline-2-alkylboronic Acids: Identification of the B–N Distance for Eliciting Bifunctional Catalysis of an Asymmetric Aldol Reaction. *Asian Journal of Organic Chemistry* **2014**, *3*, 470–479.
- (282) Inoue, T.; Ito, K.; Tozaka, T.; Hatakeyama, S.; Tanaka, N.; Nakamura, K. T.; Yoshimoto, T. Novel inhibitor for prolyl aminopeptidase from *Serratia marcescens* and studies on the mechanism of substrate recognition of the enzyme using the inhibitor. *Archives of Biochemistry and Biophysics* **2003**, *416*, 147–154.
- (283) Choi, H.-D.; Seo, P.-J.; Son, B.-W.; Kang, B.-W. Synthesis of 5-chloro-3-[4-(3-diethylaminopropoxy) benzoyl]-2-(4-methoxyphenyl) benzofuran as a β -amyloid aggregation Inhibitor. *Archives of Pharmaceutical Research* **2003**, *26*, 985–989.
- (284) Xu, D.-Z.; Liu, Y.; Shi, S.; Wang, Y. Chiral quaternary alkylammonium ionic liquid [Pro-dabco][BF₄]: as a recyclable and highly efficient organocatalyst for asymmetric Michael addition reactions. *Tetrahedron: Asymmetry* **2010**, *21*, 2530–2534.
- (285) Betancort, J. M.; Barbas, C. F. Catalytic Direct Asymmetric Michael Reactions: Taming Naked Aldehyde Donors. *Organic Letters* **2001**, *3*, 3737–3740.